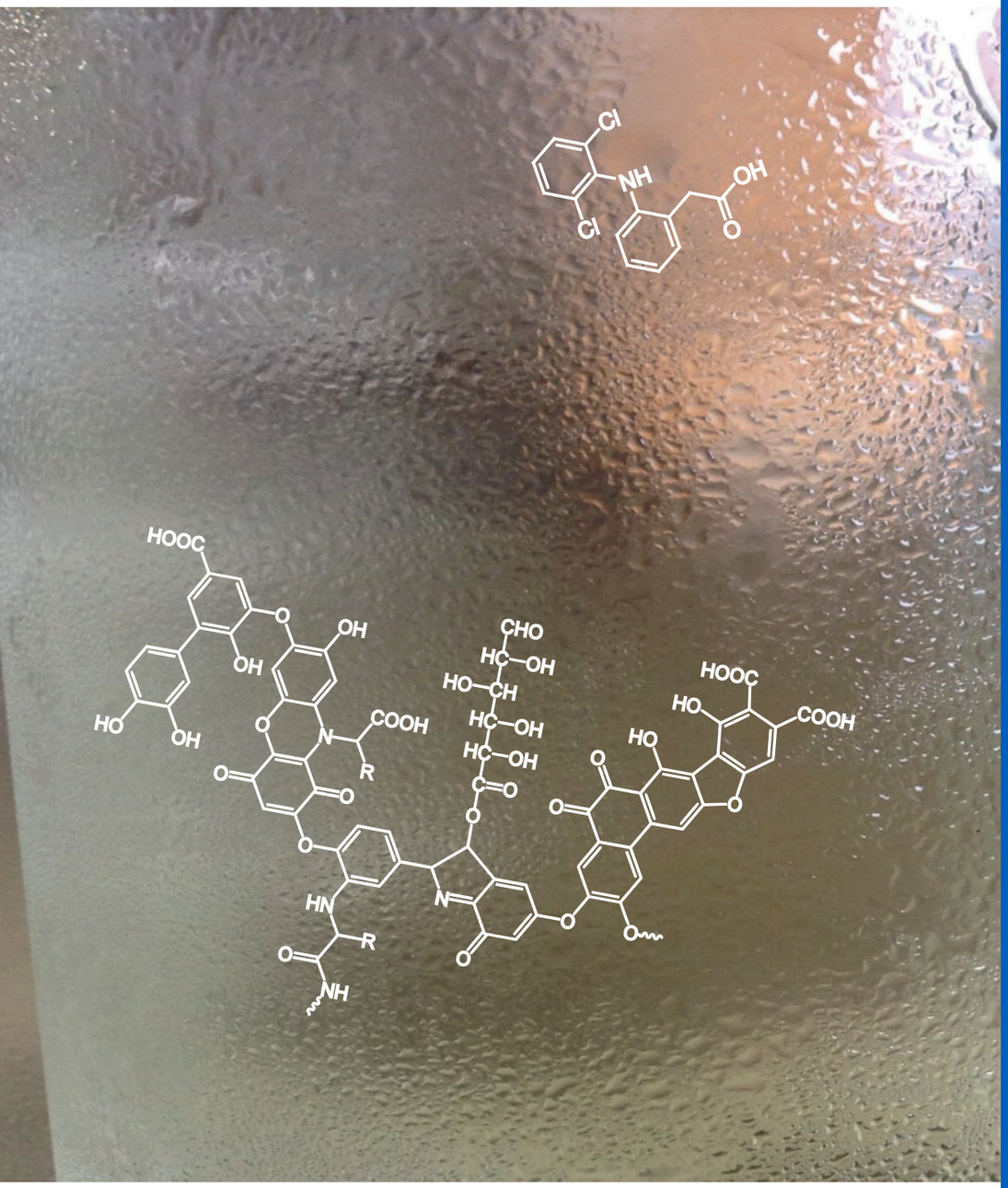

ISBN 978-9-4635705-7-2

Surrogate-based online monitoring and control framework for trace organic contaminant removal during ozonation of secondary wastewater effluent: *from lab-scale to practical application*

ing. Michael Chys

2017

FACULTY OF
BIOSCIENCE ENGINEERING

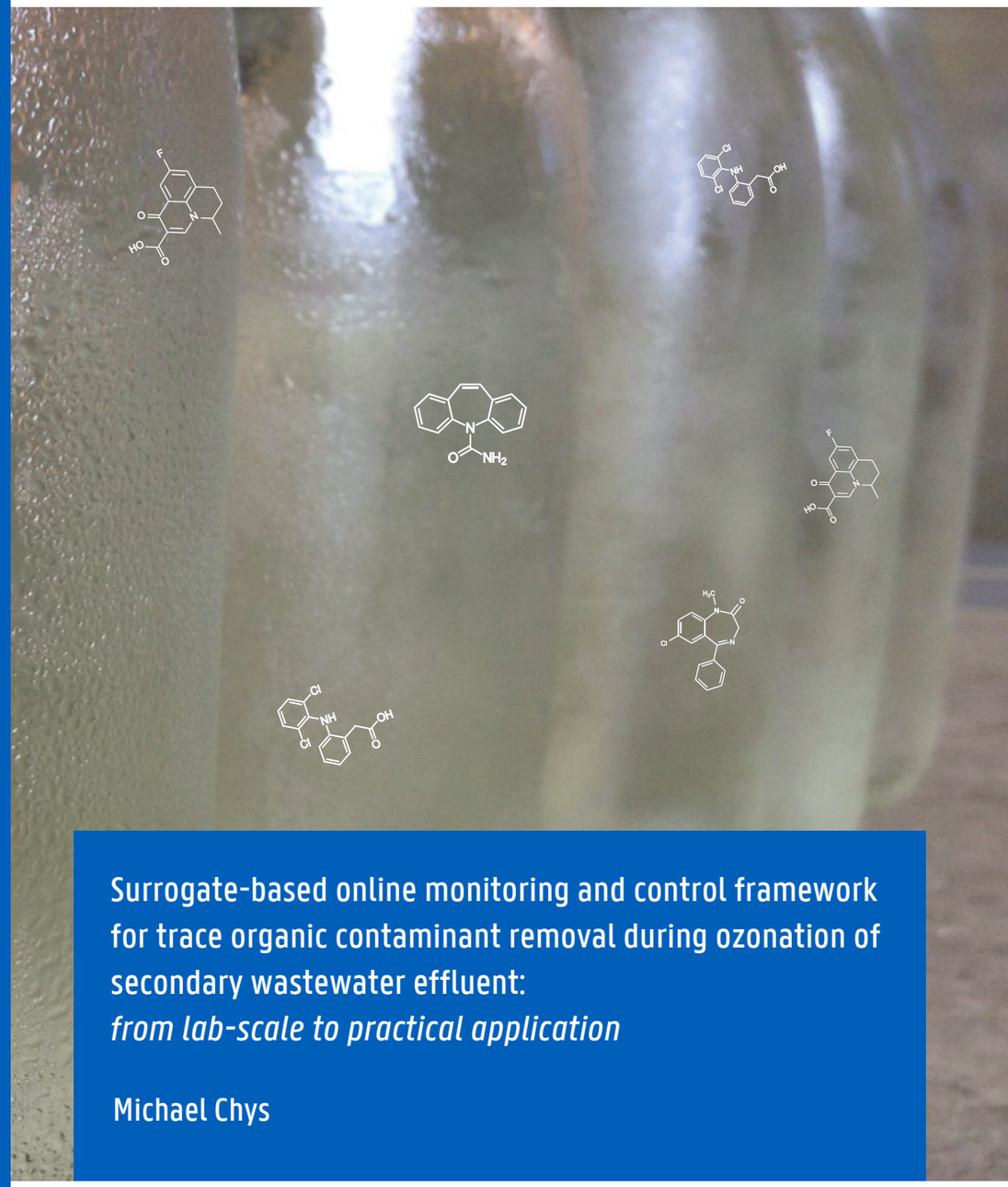

Surrogate-based online monitoring and control framework for trace organic contaminant removal during ozonation of secondary wastewater effluent: *from lab-scale to practical application*

Michael Chys

GHENT
UNIVERSITY

It's all about finding the calm in the chaos.

(D. Karan)

Supervisors

Prof. dr. ir. Stijn Van Hulle

Research Group LIWET – Laboratory for Industrial Water and Ecotechnology

Department of Industrial Biological Sciences

Faculty of Bioscience Engineering, Ghent University – Campus Kortrijk

Prof. dr. ir. Kristof Demeestere

Research Group EnVOC – Environmental Organic Chemistry and Technology

Department of Sustainable Organic Chemistry and Technology

Faculty of Bioscience Engineering, Ghent University

Prof. dr. ir. Ingmar Nopens

BIOMATH - Department of Mathematical Modelling, Statistics and Bioinformatics

Faculty of Bioscience Engineering, Ghent University

Dr. ing. Wim Audenaert

BIOMATH - Department of Mathematical Modelling, Statistics and Bioinformatics /

CMET - Center for Microbial Ecology and Technology

Faculty of Bioscience Engineering, Ghent University

AM-TEAM

Chair of the examination committee

Prof. dr. ir. Paul Van Der Meeren

Department of Applied Analytical and Physical Chemistry

Faculty of Bioscience Engineering, Ghent University

Board of examiners

Prof. dr. Paolo Roccaro (Universita degli Studi di Catania, Italy)

Dr. ir. Achim Ried (Xylem Services GmbH, Germany)

Prof. dr. ir. Arne Verliefde (Ghent University)

Dr. ing. Youri Amerlinck (Ghent University)

Dean of the faculty of Bioscience Engineering, Ghent University

Prof. dr. ir. Marc Van Meirvenne

Rector of Ghent University

Prof. dr. ir. Rik Van de Walle

Surrogate-based online monitoring and control framework for trace organic contaminant removal during ozonation of secondary wastewater effluent

from lab-scale to practical application

ing. Michael Chys

Thesis submitted in fulfilment of the requirements for the degree of Doctor (PhD) in Applied Biological Sciences

Dutch translation of the title:

Surrogaat gebaseerde online opvolging en controle raamwerk voor het verwijderen van organische sporencontaminanten gedurende ozonisatie van secundair afvalwatereffluent: van laboschaal tot praktische toepassing

Cover:

Glass bottles of freshly sampled ozonated effluent, taken from a cooled autosampler, with structural formulas of pharmaceuticals and humic acid.

Please refer to this work as follows:

Chys, M. (2017) Surrogate-based online monitoring and control framework for trace organic contaminant removal during ozonation of secondary wastewater effluent: from lab-scale to practical application. PhD dissertation, Ghent University, Belgium

ISBN: 978-94-6357-057-2

Woord vooraf

'Michael, wat denk je erover om te doctoreren?', dat kreeg ik te horen na één van mijn laatste mondelinge examens. Ik wist eigenlijk nog niet goed wat ik zou doen na 4 jaar te studeren aan '*de PIH*' (toen reeds HOWEST GKG) en begon er toen pas concreet over na te denken. Ik had ondertussen al even kunnen proeven van het academische wereldje na een half jaar masterthesissen in Denemarken en wou er dus onmiddellijk aan beginnen. Nu was er enkel nog funding nodig om vier jaar te kunnen overbruggen. Enkele projecten werden aangevraagd, ik werkte ondertussen aan wat kleinere projecten eerst bij Bruno en daarna ook bij de LED water samen met een heleboel bedrijven. Alvast bedankt aan Vlakwa en Veerle voor de fijne samenwerkingen! Een tweetal jaren waren reeds voorbij toen ik bij de integratie in UGent als academiserings-assistent met een gerust gevoel kon verder werken aan dit doctoraat. Stijn, bedankt om reeds zeer vroeg iets in mij te zien, mij altijd veel vertrouwen te schenken en te steunen, ook al viel de aanvraag van een IWT-beurs al eens tegen. Je gaf me de kans (en hier en daar wat budgetjes) om aan een uitdagend onderzoek te werken met heel veel vrijheid. Zo kon ik op verschillende mooie locaties mijn onderzoek gaan voorstellen en met veel anderen samenwerken, ook al moest ik mij 'opofferen' om hiervoor tot Montréal of Las Vegas te trekken.

Dit werk is uiteindelijk enkel tot stand gekomen door de samenwerking met en tussen mijn (vier) promoteren. Hoewel ik meestal een kleine verbazing zag in de mensen hun ogen toen ik mijn aantal promotoren vermelde heb ik dit nooit zo ervaren. Kristof, Wim en Ingmar ook jullie bedankt voor de steun en vertrouwen die jullie schonken. Kristof, bedankt voor jou toewijding en de drang om telkens een mooie taart af te leveren, met kers! Jij zorgde ervoor dat ik zeker ook de fijne puntjes niet uit het oog verloor. Wim, jij legde een uitstekende basis voor mijn doctoraat waarop ik kon verder werken en, samen met jouw onmeetbaar enthousiasme, zorgde dit ervoor dat ik mij bij de ozon verslaafden kan rekenen. Weinig is beter dan de geur van verse ozon bij het ontkrieken van de dag. Onze gezamenlijke interesse in efficiëntie, en het gebruik van verschillende tools, zorgde voor heel wat bijkomende gedachten wisselingen naast het doctoraat, al dan niet met een *'pichet'* in de hand. Vergeet ook niet dat Canada niet is opgenomen in een gps met BENELUX-kaarten. Ingmar, ook bedankt om telkens betrokken te blijven en steeds met een nuchtere blik mijn onderzoek te bekijken. Ook al waren er soms periodes dat we elkaar minder horen of zagen, toch gaf je altijd die opmerking die mee hielp de kers op de taart te plaatsen. Je steun en kansen die je mij en andere jonge mensen o.a. gaf bij BIWA zal ik niet vergeten.

Verder dien ik nog heel veel andere personen te bedanken die direct of indirect een bijdrage leverden aan dit werk. Leendert, jij gaf mij alle info die je maar kon geven om me op weg te helpen met de SPE's om alle micropolluent analyses tot een goed einde te brengen. Mijn poging om het record per dag telkens te verbeteren leverde me jammer genoeg wel een blessure op. Lies, ik kon altijd erop vertrouwen dat mijn analyses perfect werden uitgevoerd. Ik kwam met plezier langs bij jullie! Ook bedankt aan Ipalle, Aquafin en Xylem voor de samenwerking bij de piloot experimenten en andere staalnames op hun zuiveringsstations. *Merci beaucoup aux opérateurs de Ipalle de me permettre sur leurs stations de traitement.* Erik en collega's, bedankt om mij te ontvangen in jullie onderzoekshal te Aartselaar. Ook bedankt aan Marjoleine en Adrien voor de medewerking en jullie steun zodat ik mijn onderzoek werkelijk kon toepassen! *Achim, Harald, Arne and Uli, also a big thanks to all of you for the input during discussions, to support us with an online sensor (and a 2nd flow-through cell) and the help with the economic calculations, which are an important part in this complete work.*

Terugkijkend op al het experimentele werk bevat in dit doctoraat, en veel rondrijden in heel Vlaanderen, werd heel wat samen uitgevoerd met thesisstudenten. Zonder jullie en de vele analyses zou ik geen uitgebreide dataset hebben zoals nu het geval is. Emma, Chantal, Sabine, Michael en Jan, jullie werk heeft van allen een belangrijk stukje bijgedragen tot deze thesis. Ik hoop dat ook jullie trots zijn op het werk die jullie uitvoerden ook al vergde dit soms UV-VIS spectra opnemen tot sluitingstijd of doorwerken tijdens de zomerperiode. Ook bedankt aan alle andere thesisstudenten die ik begeleide, andere projecten of samenwerkingen buiten het thema van mijn doctoraat. Dit zorgde voor een welgekomen afwisseling en zorgde ervoor dat ik mij ook eens kon verdiepen in andere zaken. Ook geef ik graag een woordje aan de YWP's die de BENELUX-conferenties toch wel lichtjes legendarisch maakten. Grote feestjes, kleine oogjes, uitwisseling van toponderzoek en een fantastisch team. Dit smaakt naar meer over twee jaar!

Natuurlijk kan ik ook niet anders dan een woordje te richten naar alle Kortrijk collega's. Ik kwam op mijn eerste dagen wat onzeker toe maar al snel zorgden de collega's voor een aangename sfeer en kon ik altijd terecht bij iedereen wanneer nodig. Nele, Evelyne, Stijn junior, jullie waren een fijne (letterlijk en figuurlijk) dichte collega. Bedankt om soms mijn gezever te aanhoren, ideeën uit te wisselen en de sfeer in de bureau toch net iets aangenamer te maken! Nele, hopelijk beleef je nog steeds veel plezier aan je nieuwe uitdaging en jouw gezinnetje. Evelyne, nog veel ontdekkingsplezier waar je ook naar toe gaat. Stijn, zorg goed voor onze komende generaties en vergeet ze zeker de ozon 'cuteness factor' niet aan te leren! Ann D., Pascal, Joël, Yannick, ook bedankt aan jullie om mij toe te laten in het chemie team. Ann V., bedankt om er steeds voor te zorgen dat mijn soms vele bestellingen snel geleverd konden worden. Isabel, je hielp mij altijd

weer met de lach toen ik langskwam met SAP problemen of andere vragen. Ook alle andere collega's hartelijk dank voor uiteenlopende zaken zoals hulp in het labo maar zeker de frisse streekbiertjes bij een mooie gelegenheid.

Een doctoraat is een lang proces die niet mogelijk is zonder steun buiten het werk en onderzoek. Daarom een welgemeende dankjewel aan mijn familie en vrienden voor verschillende zaken en interesse die jullie toonden, ook al was het misschien niet altijd makkelijk om nu te weten wat ik exact aan het doen was. Papa en mama, bedankt om mij altijd onvoorwaardelijk te steunen en talrijke kansen te geven. Zonder dit zou ik niet zijn wie en waar ik nu ben. Rik en Ilse, betere schoonouders kan ik mij niet wensen en ik ben ook altijd meer dan welkom bij jullie. Ook jullie bedankt voor de steun die ik steeds kreeg.

Fie'tje, als laatste maar belangrijkste wil ik jou bedanken. Jij doet me lachen en maakt me gelukkig. Na meer dan 12 jaar steun jij me nog iedere dag en ook tijdens deze laatste eindspurt deed je alles om het mij zo goed mogelijk te maken. Ondertussen zijn we getrouwd en bouwen we letterlijk aan ons verder leven. Het is meer dan de moeite waard!

Kortrijk, December 2017

Michael Chys

Summary

Municipal water resource recovery facilities (WRRFs), previously known as wastewater treatment plants (WWTPs), are a major pathway through which trace organic contaminants (TrOCs) enter the aquatic environment. The accumulation of these TrOCs (in the environment) and the increased use of reclaimed wastewater may trigger unwanted ecological effects or pose a risk to human health. To protect the aquatic environment and strongly driven by (pending) legislation, operators of WRRFs are preparing for plant upgrades with advanced treatment technologies to reduce the TrOC discharge. One of the most promising technologies is the use of ozonation as a tertiary treatment prior to discharge, as ozone itself will react with TrOCs and will lead to the generation of unselective and highly oxidative hydroxyl radicals (HO•). This technology has been successfully tested, its efficiency in TrOC abatement has been proven, and it is for example one of the selected technologies currently being implemented in Switzerland as well as in other countries (e.g. Germany, France, United States, etc.). The wide application of ozonation on WRRFs is however challenged by the unavailability of an online control framework that ensures efficient TrOC abatement and minimizes the by-product formation potential at the lowest possible costs. Conventional ozonation control strategies based on e.g. the measurement of dissolved ozone concentrations is not possible due to the presence of high concentrations of (fast reacting) organic matter and TrOCs can not be measured in real-time.

Surrogate-based methods using online measurable parameters such as e.g. the UV absorbance at 254 nm or fluorescence have been investigated, and linear correlation models have been developed. A wide overview of currently existing correlation models is given in Chapter 1 together with a summary of current and upcoming legislation, (planned) full-scale installations and their applied control strategies. The three most important control strategies, i.e. flow proportional, load proportional and differential control of the ozone dose, are described in view of their applicability under variable full-scale conditions. Based on this literature review, it was concluded that current surrogate correlation models are lacking kinetic information related to ongoing reactions. A more generical framework is needed which can be applied (i) for numerous TrOCs that are currently known or that might be detected in future and (ii) at different treatment sites. Therefore, in this dissertation, the main goal was to develop, calibrate and validate a surrogate-based correlation model in view of variable effluent conditions, ensuring an easily applicable and reliable control framework. Increasing the current scientific knowledge, and the

understanding of practical applicability and economical implications were the main routes to meet this goal. These objectives are clearly stated in Chapter 2.

To increase the understanding of effluent variability, water quality was assessed at 15 different sampling locations at different Belgian WRRFs (Chapter 3). A broad range of values was noticed for most characteristics although little differences could be noticed for spectral measurements (e.g. UVA_{254} or fluorescence) among the different locations. The limited amount of observed outliers are clearly site or event dependent. A lower variability (for spectral measurements) will make it easier to develop and apply a control framework based on these spectral measurements. On the other hand, significant variations among the different plants (especially smaller sized plants) could be noticed related to conventional water quality parameters such as alkalinity (correlated with the electrical conductivity) and pH which are known to have an influence on the ozonation process. The effluent matrix reactivity is therefore a major point of attention that needs to be considered when developing a generical and effective control framework.

New correlation models based on UVA_{254} and fluorescence surrogate parameters and considering kinetic information, are presented in Chapter 4. Overall, abatement patterns of TrOCs (ΔTrOCs) having different reactivity towards ozone showed to represent an inflected shape, related to the decrease of both surrogates, that will be of importance for WRRF operators. Both UVA_{254} and fluorescence surrogates can be used to control ΔTrOC, although fluorescence measurements indicate a slightly better reproducibility and an enlarged control range. A generical framework relating these surrogates and ongoing chemical kinetics is put forward to construct correlations for any compound with known apparent second order reaction rate constants towards ozone ($k_{O3,TrOC}$). Mainly, two different reaction phases are defined for which a separate linear correlation was obtained. This model framework was validated at lab- and pilot-scale as described in Chapter 5. The inflected correlation model between ΔTrOCs and the surrogates predicts the removal of TrOCs (based on statistical evidence) solely using the 2nd order reaction rate constant with ozone ($k_{O3,TrOC}$) and in a more adequate manner than similar models using a single linear correlation over the entire removal range. This allows the use of this new model for current and future TrOCs under investigation which is highly interesting when imposed discharge limits might include more and other TrOCs in future. The use of UVA_{254} might be preferable at this point for online monitoring of TrOC abatement as the model showed a good predictive power (based on statistical evidence and visual confirmation), and reliable online sensors are commercially available. On the other hand, parallel factor analysis of the 3D fluorescence spectra enables monitoring of multiple types of organic matter with a different reactivity behavior towards ozone

and HO•, and might even increase the predictive power given by a general lower degree of scattering. This is of importance when developing kinetic modelling frameworks and for achieving a better understanding of the occurring changes of organic matter during ozonation. Fluorescence might, due to its higher sensitivity compared to UV-VIS, also become more valuable for drinking water treatment where organic matter levels are lower, especially after oxidative or other treatment.

The ΔUVA_{254}-based surrogate model was further implemented in an online control framework on pilot-scale to control the ozone dose during continuous operation (Chapter 6). A one sensor approach was used although a differential control strategy (based on ΔUVA_{254}) was applied. The practical implications of online spectral sensors and the effect of effluent dynamics in terms of load and composition (i.e. reactivity) was assessed in relation with the applied control strategies. The use of one sensor to measure the effluent characteristics both before and after ozonation resulted in a good working system, reduced costs and could slightly reduce the effect of fouling on the measurements. Nevertheless, the need for cleaning was clearly indicated and the use of ultrasonic cleaning resulted in significantly less fouling. The variable effluent reactivity towards ozone seemed more influential than the effluent load. The use of ΔUVA_{254} as control parameter ensured the supply of the required ozone doses during varying water quality and weather conditions, and at a lower operational cost than other more commonly control strategies. This ensures the desired TrOC abatement, but also minimizes ozone overdosing and the potential risk of by-product formation. The use of flow or load proportional control strategies were clearly not able to cope with the dynamic ozone demand of the effluent. However, the additional response time of using ΔUVA_{254} might be a disadvantage, which opens perspectives for the combination with load-based approaches (i.e. O_3:DOC ratio based control) and the construction of a combined feedback-feedforward system. Further research can be done on full-scale installations to elaborate more on this new control concept.

As a first step for further investigation in the future, ozonation coupled with three (biological) filtration technologies have been evaluated in different combinations as tertiary treatment for WRRF effluents (Chapter 7). Ozonation resulted in a 90% removal of the total amount of quantified TrOCs with, however, a limited increase of the unselective toxicity. Slow sand filtration (SSF) following ozonation showed to be the only technology able to reduce the unselective toxicity to the same level as before ozonation based on the used toxicity test. Based on other reports, also BAC might be an appropriate post-treatment. Further research is however needed in this specific area of expertise. In view of process control, the innovative correlation

models developed for the monitoring and control of TrOC removal during ozonation, were verified for their applicability during ozonation in combination with TF (trickling filtration), biological activated carbon (BAC) or SSF. Particularly for the poorly ozone reactive TrOCs, statistically significant models were obtained that correlate TrOC abatement and ΔUVA_{254}, demonstrating the applicability of the control strategy for the complete tertiary treatment train.

Finally, the main potential for surrogate parameters, i.e. controlling the ozone dose effectively in terms of TrOC abatement and costs, was achieved by developing new correlation models. Further potential for this kind of measurements can be seen as incorporation in a (semi-)kinetic model that can be used for both design and control purposes, also in less heavily loaded water applications. This is more elaborated on in Chapter 8, in which an overall discussion of the results of this dissertation is given, also laying out still existing research gaps and potential future research.

Samenvatting

Huishoudelijke waterherwinningsfaciliteiten (ofwel Water Resource Recovery Facilities, WRRFs), eerder gekend als afvalwaterbehandelingsinstallaties, zijn een belangrijke bron langs waar organische sporenelementen (ofwel Trace Organic Contaminants, TrOCs) het aquatische milieu binnen dringen. De accumulatie van deze TrOCs (in het milieu) en het verhoogde gebruik van herwonnen afvalwater kunnen ongewenste ecologische effecten veroorzaken of een gevaar voor de gezondheid van de mens vormen. Om het aquatische milieu te beschermen, en sterk gedreven door (opkomende) wetgeving, bereiden WRRF-exploitanten zich voor op de uitbreiding van hun huidige installaties met geavanceerde behandelingstechnologieën, zodanig de lozing van TrOCs te verminderen. Een van de meest belovende technologieën is het gebruik van ozonisatie als tertiaire behandeling net voor het lozen van het gezuiverde afvalwater aangezien de ozon zal reageren met de TrOCs en leidt tot de generatie van niet-selectieve maar zeer oxidatieve hydroxyl radicalen (HO•). Deze technologie is succesvol uitgetest en zijn efficiëntie om TrOCs te verwijderen is bewezen. Het is bijvoorbeeld een van de geselecteerde technologieën die momenteel geïmplementeerd worden in o.a. Zwitserland maar ook Duitsland, Frankrijk, Verenigde Staten, etc. De brede toepassing van ozonisatie op WRRFs wordt echter uitgedaagd door de afwezigheid van een online controleraamwerk dat een efficiënte TrOC reductie garandeert en het potentieel om (toxische) bijproducten te vormen minimaliseert tegen de laagst mogelijke kostprijs. Conventionele controle strategieën gebaseerd op o.a. de meting van opgeloste ozonconcentraties kan niet worden toegepast door de aanwezigheid van hoge concentraties (snel reagerend) organisch materiaal en TrOC kunnen niet online worden opgemeten.

Surrogaat gebaseerde methoden die gebruik maken van online opmeetbare parameters, zoals bv. de UV absorbantie bij 254 nm of fluorescentie zijn reeds onderzocht en lineaire correlatiemodellen werden ontwikkeld. Een breed overzicht van de bestaande correlatiemodellen is weergegeven in hoofdstuk 1 samen met een samenvatting van de huidige en toekomstige wetgeving, (geplande) volle-schaal installaties, en hun toegepaste controle strategieën. De toepasbaarheid van de drie belangrijkste controle strategieën (debiet proportioneel, belading proportioneel en differentieel) van de ozon dosis worden beschreven rekening houdend met variabele en volle-schaal omstandigheden. Op basis van dit literatuuronderzoek werd geconcludeerd dat kinetische informatie in verband met aangaande reacties ontbreken bij de huidige surrogaat gebaseerde correlatiemodellen. Er is een meer generisch kader nodig dat

toegepast kan worden voor (i) een breed gamma TrOCs die zowel gekend zijn of die in de toekomst kunnen gedetecteerd worden en (ii) verschillende installaties en locaties. Daarop gebaseerd was het hoofddoel in dit proefschrift het ontwikkelen, kalibreren en valideren van een surrogaat gebaseerd correlatiemodel, gemakkelijk toepasbaar bij variabele effluent condities, en waarbij een betrouwbare controle kan worden gewaarborgd. Het vergroten van de huidige wetenschappelijke kennis en het begrijpen van praktische en economische implicaties waren de belangrijkste in acht genomen zaken om dit doel te bereiken. Deze doelstellingen staan duidelijk beschreven in hoofdstuk 2.

Om meer kennis te verwerven omtrent de effluent variabiliteit is de waterkwaliteit opgevolgd op 15 verschillende locaties bij verschillende Belgische WRRFs (hoofdstuk 3). Een grote variabiliteit van de meeste karakteristieken werd waargenomen hoewel weinig verschillen werden waargenomen voor spectrale metingen (bv. UVA_{254} of fluorescentie) tussen de verschillende locaties. De beperkte hoeveelheid waargenomen afwijkingen zijn duidelijk afhankelijk van de staalname locatie of gebeurtenis. Een lagere variabiliteit (voor spectrale metingen) maakt het makkelijker om een controleraamwerk te ontwikkelen en toe te passen op basis van deze metingen. Anderzijds kunnen significante variaties tussen verschillende (vooral kleinere) WRRFs worden opgemerkt, gerelateerd met conventionele waterkwaliteitsparameters zoals alkaliniteit (gecorreleerd met de elektrische geleidbaarheid) en pH die gekend zijn een invloed te hebben op het ozonisatieproces. De effluentmatrix reactiviteit is daarom een belangrijk aandachtspunt waarmee rekening moet worden gehouden bij het ontwikkelen van een generiek en effectief controleraamwerk.

Nieuwe correlatiemodellen gebaseerd op UVA_{254} en fluorescentie surrogaatparameters, met in acht name van kinetische informatie, zijn gegeven in hoofdstuk 4. Algemeen hebben de verwijderingspatronen van TrOCs (ΔTrOCs) met een verschillende ozonreactiviteit, in relatie tot de afname van beide surrogaten, een krommende correlatie aangetoond wat van belang is voor WRRF-operatoren. Zowel UVA_{254} als fluorescentie surrogaten kunnen gebruikt worden om ΔTrOCs te controleren, hoewel fluorescentiemetingen een iets betere reproduceerbaarheid en een groter controlebereik vertonen. Een generiek raamwerk die zowel surrogaten als aangaande kinetische reacties relateren wordt voorgesteld zodanig correlaties te construeren voor elke component met gekende schijnbare tweede orde reactiesnelheidsconstante voor ozon ($k_{O3,TrOC}$). Hoofdzakelijk worden twee verschillende reactiefasen gedefinieerd waarvoor een aparte lineaire correlatie werd verkregen. Dit modelraamwerk werd gevalideerd op labo- en pilootschaal zoals beschreven in hoofdstuk 5. Het twee-delig correlatiemodel tussen ΔTrOCs en de surrogaten

voorspelt de verwijdering van TrOCs (gebaseerd op statistisch bewijs) door alleengebruik te maken van $k_{O3,TrOC}$ en op een meer adequate manier dan vergelijkbare modellen met een enkele lineaire correlatie over het ganse verwijderbereik. Dit maakt het gebruik van dit nieuwe model mogelijk voor huidige en toekomstige TrOCs (die onderzocht worden) wat zeer interessant is aangezien meer en meer TrOCs kunnen opgenomen worden in toekomstige lozingslimieten. Het gebruik van UVA_{254} kan op dit moment de voorkeur genieten voor de online opvolging van ΔTrOCs, gezien het model een goede voorspellende kracht heeft (op basis van statisch bewijs en visuele bevestiging), en betrouwbare online sensoren in de handel verkrijgbaar zijn. Anderzijds maakte parallelle factor analyse van 3D fluorescentie spectra het mogelijk om verschillende soorten organische componenten, met elk een eigen reactiviteit ten opzichte van ozon en HO•, op te volgen en de voorspellende kracht te vergroten door een algemeen lagere spreiding van de meetgegevens. Dit is van belang bij het ontwikkelen van kinetische modellen en voor het bekomen van betere inzichten in de aangaande veranderingen van het organisch materiaal tijdens ozonisatie. Fluorescentie kan, door de hogere gevoeligheid ten opzichte van UV-VIS, ook waardevol zijn voor drinkwaterbehandeling vooral na oxidatieve of andere behandelingen, waar een lagere aanwezigheid is van organische stoffen.

Het ΔUVA_{254}-gebaseerde surrogaatmodel werd verder geïmplementeerd in een online control raamwerk op pilootschaal zodanig de ozondosis continue te controleren (hoofdstuk 6). Een één sensor aanpak werd gehanteerd hoewel een differentiële controlestrategie (gebaseerd op ΔUVA_{254}) werd toegepast. De praktische implicaties van online spectrale sensoren en het effect van effluentdynamiek (zowel belasting als samenstelling/reactiviteit) werd beoordeeld, afhankelijk van de toegepaste controlestrategieën. Het gebruik van één sensor voor het opmeten van de effluent karakteristieken zowel voor als na ozonisatie resulteerde in een goed werkend systeem, verminderde kosten en een verlaagd effect van verontreinigingen op de metingen. Niettemin is het nog steeds noodzakelijk de spectrale sensor schoon te maken al leidde een ultrasone reiniging tot aanzienlijk minder vervuilingen. De variabele effluentreactiviteit ten opzichte van ozon leek een grotere invloed te hebben dan de belasting. Het gebruik van ΔUVA_{254} als controleparameter zorgde voor de toevoer van de vereiste ozondosis tijdens variërende waterkwaliteit en weersomstandigheden, en tegen een lagere operationele kost dan andere, algemenere strategieën. Dit zorgt voor de gewenste TrOC reductie, maar minimaliseert ook ozon overdosering en het mogelijke risico op het vormen van (toxische) bijproducten. Het gebruik van debiets- of belading proportionele controle strategieën was duidelijk niet in staat om te voldoen aan de dynamische ozonvraag van het effluent. De extra responstijd bij het gebruik van ΔUVA_{254} kan echter een nadeel zijn. Dit vormt mogelijks perspectieven voor een gecombineerde benadering met belading

proportionele strategieën (bv. O_3:DOC ratio) en de ontwikkeling van een gecombineerd feedback-feedforward systeem. Verder onderzoek kan uitgevoerd worden op volle-schaal installaties om dit nieuwe controle concept verder uit te werken.

Als een eerste stap voor verder toekomstig onderzoek werd ozonisatie gekoppeld met drie (biologische) filtratietechnieken en geëvalueerd in verschillende combinaties als tertiaire behandeling voor WRRF-effluent (hoofdstuk 7). Ozonisatie resulteerde in 90% verwijdering van de totale hoeveelheid gekwantificeerde TrOCs met enkel een beperkte toename van niet-selectieve toxiciteit. Langzame zandfiltratie na ozonisatie bleek de enige techniek die de niet-selectieve toxiciteit kon verminderen tot hetzelfde niveau als voor ozonisatie gebasseerd op de gebruikte toxiciteitstest. Beschikbaar onderzoek wijst echter ook biologische actieve kool aan als bruikbare techniek. Verder onderzoek is echter nodig in dit specifiek onderzoeksgebied. Procescontrole in acht nemend, werden de ontwikkelde correlatiemodellen voor de opvolging en controle van ΔTrOCs tijdens ozonisatie toegepast en geverifieerd bij een combinatie van druppelfiltratie, biologische actieve kool of langzame zandfiltratie na ozonisatie. Specifiek voor de slecht ozon reactieve TrOCs werden statisch significante modellen verkregen die ΔTrOCs en ΔUVA_{254} correleren. De toepasbaarheid van de controlestrategie voor de volledige tertiaire behandelingstrein werd zo aangetoond.

Tenslotte kan gesteld worden dat het belangrijkste potentieel voor surrogaatparameters, d.w.z. het effectief controleren van de ozondosis in termen van TrOC afname en kosten, bereikt werd door het ontwikkelen van nieuwe correlatiemodellen. Verdere mogelijkheden voor dit soort metingen zijn o.a. het inwerken in een (semi-)kinetisch model dat zowel voor ontwerp- als controledoeleinden kan gebruikt worden, ook bij minder zwaar beladen water(zuiverings)toepassingen. Dit wordt verder uitgewerkt in hoofdstuk 8 waarin een algemene discussie over de resultaten van dit proefschrift wordt gegeven alsook nog bestaande toekomstige onderzoeksmogelijkheden.

Acknowledgements

Ghent University is acknowledged for the PhD grant of Michael Chys and for funding the automated SPE equipment (Special Research Fund - 01B07512). The financial support (AUGE/11/016) from the Hercules Foundation of the Flemish Government is acknowledged for the UHPLC-Q-Exactive™ mass spectrometry equipment.

Aquafin NV provided finances and help during sampling, analysis, construction and operation of the ozone pilot which is greatly appreciated. WEDECO and WTW (both brands of Xylem inc.) provided a full-spectral online UV-VIS sensor and helped in bringing the pilot experiments to a good end.

Ipalle and Aquafin allowed us to sample their WRRF plants which was a great help to this dissertation. This project was initiated within the LED H2O project which belongs to the LED network (www.lednetwerk.be) and is financially supported by the Flemish Knowledge Center Water (Vlakwa vzw).

Table of contents

List of abbreviations

λ	wavelength
(3D) EEM	(three-dimensional) excitation-emission matrix
AC	activated carbon
ACA	aldehydes and carboxylic acids
AOC	assimilable organic carbon
AOP	advanced oxidation process
a_{p1}	slope of ΔTrOC vs. ΔS during reaction phase 1
a_{p2}	Slope of ΔTrOC vs ΔS during reaction phase 2
AWT	advanced water treatment
BAC	biological activated carbon filtration
bDOC	biodegradable dissolved organic carbon
BEAR	Best Elimination, Analysis and monitoRing
BOD_5	biological oxygen demand (measured during 5 days)
BV	bed volume
CAPEX	capital expenditure
CAS	conventional activated sludge
CCβ	detection capability of TrOC analysis
CDPH	California department of public health
CECs	contaminants of emerging concern
CFD	computational fluid dynamics
COD	chemical oxygen demand
$color_i$	absorption coefficient within the visible range with *i* related to the wavelength
CT	dissolved ozone concentration (C) in time (T)
CW	constructed wetland
DOC	dissolved organic carbon
DOC_{eq}	dissolved organic carbon equivalent (determined based on UVA_{254})
E1	estrone
E2	17 beta-estradiol
EBCT	empty-bed contact time
EC	electrical conductivity
EDC	electron donating capacity

EE2	17 alpha-ethinylestradiol
EfOM	effluent organic matter
EQS	environmental quality standards
ERM	electron rich moieties
EU	European Union
FB-FF	feedback-feedforward
F_{max}	intensity value at peak wavelengths of a defined PARAFAC component
GAC	granular activated carbon
HESI-II	heated electrospray ionization
HO•	hydroxyl radicals
HPLC	high performance liquid chromatography
HPLC-DAD	high performance liquid chromatography with a diode array detector
HRT	hydraulic retention time
I	inflection point
I.E.	inhabitant equivalent
IOD	instantaneous ozone demand
IPR	indirect potable reuse
I_x	intensity values at peak wavelengths of a defined region within EEM fluorescence spectra
k	second order reaction rate constant
$k_{HO•,TrOC}$	second order reaction rate constant with hydroxyl radicals
KMO	Kaiser-Meyer-Olkom criterion
$k_{O3,TrOC}$	apparent second order reaction rate constant with ozone
K_{ow}	octanol/water partition coefficient
lab	laboratory
LCA	life cycle assessment
LC-MS	liquid chromatography with mass spectrometry
LED	light-emitting diodes
LOESS	Local regrESSion
LOX	liquid oxygen
MAE	mean absolute error
MeOH	methanol
n	number of samples
NDIR	non-dispersive infrared

NDMA	N-nitrosodimethylamine
n_{max}	maximum number of samples
NOM	natural organic matter
NPDES	national pollution discharge elimination system
NWRI	national water research institute
OPEX	operational expenditure
ORP	oxidation-reduction potential
PAC	powdered activated carbon
PARAFAC	parallel factor analysis
PC	principal component
PCA	principal component analysis
pCBA	para-chlorobenzoic acid
PD	photodiode
pKa	acid dissociation constant
PS	priority substances
Q	flow rate
QSAR	quantitative structure activity relationships
R_{ct}	ratio of the HO• exposure to the O_3 exposure
Ref.	reference
RO	reversed osmosis
RU	Raman units
SF	sand filtration
SIRA	strategic innovation and research agenda
SPE	solid phase extraction
SSF	slow sand filtration
SUVA	specific UV absorbance at 254 nm
T	temperature
T&O	taste and odor
TF	total fluorescence
TF	trickling filtration
TIC	Theil's inequality coefficient
TN	total nitrogen
TOC	total organic carbon
TOD	transferred ozone dose
TOTEX	total expenditure

TrOC	trace organic contaminant
UF	ultra filtration
UHPLC-HRMS	ultra high performance liquid chromatography with high resolution mass spectrometry
USA	United States of America
UV	ultra violet
$UVA_{254,eff}$	UVA_{254} signal measured in secondary effluent before ozonation
$UVA_{254,lab}$	laboratory measurement of UVA_{254}
$UVA_{254,O3}$	UVA_{254} signal measured in tertiary effluent after ozonation
UVA_i	absorption coefficient within the UV range, with *i* related to the wavelength
UV-VIS	UV-visible
WFD	water framework directive
WRP	water reuse plant
WRRF	water resource recovery facility
WssTP	water supply and sanitation technology platform
WWTP	wastewater treatment plant
y_i	predicted data
$y_{m,i}$	measured data
ΔS	decrease of a surrogate measurement

Chapter 1

Introduction and literature review

This chapter has been redrafted from:

Chys, M., Audenaert, W., Nopens, I., Demeestere, K. & Van Hulle, S.W.H. Current status and needs for online control of tertiary ozonation, *in preparation*.

1 Introduction

World population is projected to increase to around 9.7 billion individuals by 2050, compared to 7.3 billion in 2015, of which 66% is estimated to be living in urban areas which poses a serious burden on water resources.[1,2] Conventional resources such as ground water should be protected to avoid depletion and a subsequent shift towards a higher degree of surface water use or reused wastewater is needed and expected.[3,4] Indirect potable reuse through e.g. managed aquifer recharge with reclaimed water has already been recognized as a promising strategy and is already been implemented in a few cases.[5] The presence of residual contaminants may, however, have adverse effects on human health. Trace organic contaminants (TrOCs), also known as contaminants of emerging concern (CECs) including (residuals of) pharmaceuticals, personal care products, pesticides, hormones, illicit drugs or other stimulants, have been detected and quantified in the environment.[6–9] TrOCs such as pharmaceuticals may trigger adverse effects on aquatic organisms (e.g. bacterial resistance, chronic toxicity, endocrine disruption and feminization of fish), even at very low concentrations (ng L^{-1} to μg L^{-1} level).[10–15] Increased use of reclaimed wastewater e.g. for crop irrigation might expose human individuals to xenobiotics (incl. pharmaceuticals) through different pathways (Figure 1.1).[16,17] Especially for reuse purposes, several questions are still unanswered such as potential uptake and accumulation of antibiotics or pesticides by plants and crops, as a direct route towards human consumption.[18] Rousis et al.[19] estimated a current exposure or intake of 26 to 227 μg per day per inhabitant for several pesticides for people living in European cities (e.g. Brussels, Copenhagen, Zurich, Milan). In addition, the discharge of pharmaceuticals towards surface waters in the Netherlands was roughly estimated between 1 to 10 g per day per inhabitant originating from Water Resource Recovery Facility (WRRF) effluents, up to a potential 140 tons per year as stated by the Dutch government.[20,21]

To avoid increased exposure towards human individuals (and the aquatic environment), significant investments in infrastructure and the need for innovative technologies are stressed by several advisory bodies such as the WssTP (Water Supply and Sanitation Technology Platform, initiated by the European Commission in 2004). The Strategic Innovation and Research Agenda (SIRA) of the WssTP aims for a future-proof model for an European water-smart society to ensure high levels of health protection and affordability of water sources.[3] One of the key components is the development of advanced water treatment solutions to achieve good status of European water bodies. Next to the need for increased monitoring of water bodies and

discharged (treated) wastewaters, redesigning current infrastructure is one of the main aspects and is aimed for by 2030.

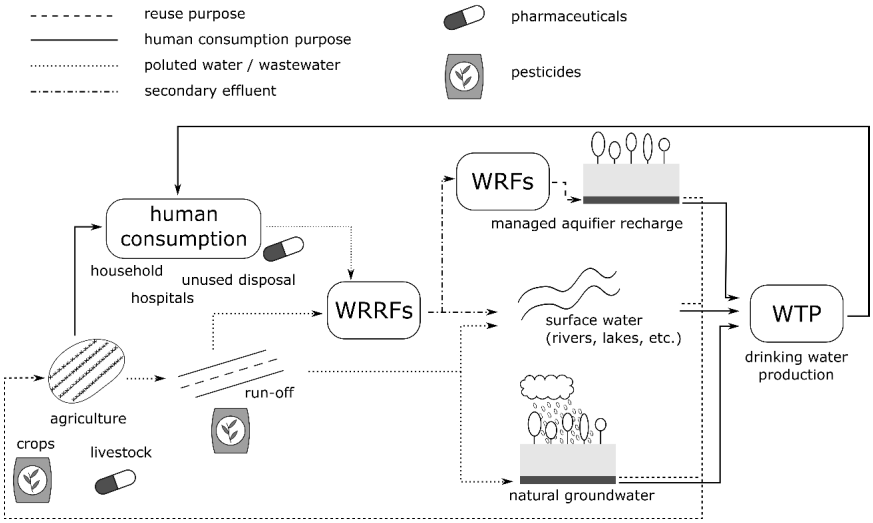

Figure 1.1: Simplified overview of forms and pathways of pharmaceuticals and pesticides, from entering the water cycle until reaching the aquatic ecolife or human consumption. The point-of-entry of pharmaceuticals and/or pesticides is indicated although residues retain present depending on uptake of crops or humans, treatment technology, etc. in the different steps of the complete cycle.

The dedication to protect the aquatic ecosystem and drinking water resources, supported by pending (European) legislation and an increased public awareness, are driving municipal wastewater treatment plants (WWTPs) to upgrade their current treatment installations with advanced technologies to remove TrOCs from their effluents.[22,23] Municipal WWTPs, or also referred to as WRRFs, have been identified as one of the major pathways through which those micropollutants (TrOCs) enter the aquatic environment.[24,25] TrOCs are entering WRRFs through excretion by human individuals, direct disposal, (road) run-off, etc. which results in general concentrations in the influent between 0.1 - 10 μg L^{-1} with in specific cases extreme concentrations in the high μg L^{-1} levels.[7] In Belgium, TrOCs entering WRRFs originating from households accounted for 92% of the total amount.[25] Potential solutions are being offered to prevent TrOCs entering the WRRFs such as e.g. selective collection of wastewaters. The largest source of TrOCs - therapeutic drug use of humans - is however impossible to completely

eliminate as recognized by different governmental bodies.[9,26] This lead recently to increased funding for additional treatment at WRRFs.[27,28] Conventionally designed WRRFs are only to a limited extent capable of removing TrOCs (1 to 2 orders of magnitude) with most still present in the effluent between 0.001 - 1 μg L^{-1}, and some cases over 1 μg L^{-1}.[6,7,29,30] With the potential presence of more than 80 000 individual chemicals in these effluents,[31] treatment upgrades are essential to protect the aquatic environment and potential drinking water resources of humans and animal wildlife.

Several tertiary treatment technologies (e.g. ozonation, activated carbon filtration, membrane filtration, etc.) are capable to cope with and remove these emerging contaminants prior to discharge.[32] Especially ozonation and activated carbon are put forward as major solutions to reduce the discharge levels of TrOCs in receiving water bodies originating from WRRFs, and are evaluated in Table 1.1.[32–35] Both are currently being implemented in Switzerland (strongly driven by regulation) as well as in other countries.[22,28] The choice for one or the other is seen as mainly case or site depending but it can be stated that activated carbon will mainly induce a higher cost and space requirement compared to ozonation.[36] An LCA study performed within the framework of the NEPTUNE-project (a EU FP6 project) recommended ozonation (combined with post sand filtration) as most optimal solution for TrOC abatement, considering the environmental sustainability compared to powdered activated carbon (PAC, combined with post sand filtration).[37,38] Although it was also stressed that this was only a first rough estimate, and more data is needed to expand that study, the high production cost of PAC is considered as a serious burden.

Ozonation shows very fast reactions when applied to secondary effluents from WRRFs as they contain a significant amount of effluent organic matter (EfOM). A broad range of TrOCs are removed due to both direct ozone reactions and the generation of the unselective and highly oxidative hydroxyl radicals (HO•), formed by reaction of ozone with EfOM or through the autocatalytic reaction chain.[39] Single ozonation is therefore essentially considered as an AOP (advanced oxidation process).[40] As ozone is conventionally applied in ranges from 1 to 15 mg L^{-1} (mostly around 0.5-1.0 g O_3 g^{-1} DOC (=Dissolved Organic Carbon)) for tertiary treatment,[41] intermediate and oxidation products can be formed by reaction with the TrOCs. Most of the formed oxidation products are however, mainly formed during reaction with the bulk organic matter or other constituents present in the water matrix. Bromate and N-nitrosodimethylamine (NDMA) are two examples of potentially carcinogenic, harmful but easily biodegradable by-products formed during effluent ozonation.[42,43] Their formation depends strongly on the applied

ozone dose and the water matrix composition.[44,45] This disadvantage of ozonation has been widely recognized and e.g. the Swiss water protection act of March 2014 already specifies the use of a polishing step such as slow sand filtration to eliminate biodegradable oxidation products.[28] Biological filtration processes are getting the advantage over other more energy intensive processes able to cope with e.g. NDMA formation such as UV photolysis.[42]

Table 1.1: Comparison of ozone and activated carbon treatment as the most relevant tertiary treatment technologies for TrOC abatement (adapted from Mielcke and Ried[46], supplemented based on refs.[32,41,47,48]).

	Ozone treatment	**Activated carbon (AC)**
Effectiveness	High	High
Interferences	Suspended solids, high organic loads	Suspended solids, high organic loads
Operational and investment costs	Acceptable, depending on WRRF scale (from 0.02 to 0.18 € m^{-3} for O_3(-SF))	Acceptable, depending on WRRF scale (from < 0.12 to 0.25 € m^{-3} for PAC-SF (or UF))
Performance	Highly depending on feed-water quality, TrOC specific reactivity, reactions depending on presence of electron-rich moieties	Highly depending on feed-water quality, TrOC specific affinity, removal depending on presence of hydrophobic or positively charged compounds
Transformation by-products	Relevant, originating from TrOCs, EfOM and e.g. bromide (bromate)	None or less relevant compared to ozone treatment
Process controlling	Basic control available, reliable dose control for TrOC abatement under development	Undefined, monitoring of TrOC abatement is under development, advances in control are limited (mainly based on bed volume and flow rate)
Environmental issues	Degradation or transformation of TrOCs	Adsorption of TrOCs, recycling and/or disposal of AC/sludge

Although ozonation and its (number of) applications are only recently ascending when it comes to the tertiary treatment of municipal wastewater for the removal of TrOCs (also see section 4.1), full-scale applications exist already from the early 1900's for drinking water disinfection.[49,50] The

use of ozone in drinking water applications is already established for over a century mostly aiming for disinfection, seen most important in the past.[49] Some installations are however used for oxidation of recalcitrant organic contaminants and 45 years ago, applications were reported for the tertiary treatment of municipal wastewater. After initial interest, applications declined due to a high number of operational and maintenance problems. Renewed interest is noticed since the 1990's due to an increased degree of innovation and experience, (slightly) growing until today.[51] More details of current full-scale applications is included in section 4.1. Other applications can be found in the treatment of swimming pool and cooling water, air treatment, medicinal therapy, the agricultural, food and electronic industry, etc.[52]

Ozonation has its proven capabilities in different fields of application and though interest is growing, a complete break-through for TrOC abatement from WRRF effluents is still hampered by a lack of clearly defined control targets and mechanisms. Rapid development of ozone processes at WRRFs, and the design and operation of these processes, is affected by two main knowledge gaps:[48,53–55] (i) the need to predict the scavenging rate from the effluent organic matter (EfOM) and formation of transformation products using suitable surrogates and, (ii) an increased understanding to design processes and apply appropriate control strategies. Furthermore, the composition of effluent can be highly dynamic and depends after all on the source of the wastewater and involves both organic and inorganic substances.[56–62] A schematic overview of different effluent constituents is given in Figure 1.2 and is further elaborated on in Chapter 3. Different control mechanisms and approaches exist for secondary effluent ozonation, whether or not adapted from other water treatment fields such as drinking water applications. Although it seems logical to use similar ozone dose control approaches, secondary effluent is characterized with large amounts of EfOM which leads to a fast ozone consumption and a near unity ratio between the consumed and transferred ozone dose (TOD) within seconds to maximally a few minutes. This in contrast to drinking water in which the (immediate) consumed ozone dose is lower, and control relies frequently on a certain remaining ozone concentration at the outlet of the ozonation reactor.

To provide a reliable control framework, there is the basic need to reach a certain defined target. The current lack of these target definitions is difficult for plant operators to identify the appropriate ozone dose. Although legislation for TrOC abatement is up-coming, a clear definition of the target to be reached is needed but is currently lacking due to limited knowledge about toxicological implications of (mixtures of) TrOCs. Raising concerns for by-product formation and a potential associated toxicity can also not be avoided. One of the main aspects

given in the remainder of this chapter is a concise overview of current and up-coming legislation, their limits that will influence the control targets, and the differences that might exist between different countries. Frequent TrOC monitoring is however difficult. The use of the available analytical equipment such as ultra-high performance liquid or gas chromatography coupled with (multiple) mass spectrometry detectors is capable of providing detailed information on the presence and quantity of TrOCs, but these methods are time, cost and labor intensive. Therefore, readily available, online, and significantly less expensive measurement technologies are needed for both process monitoring and ozone dose control.

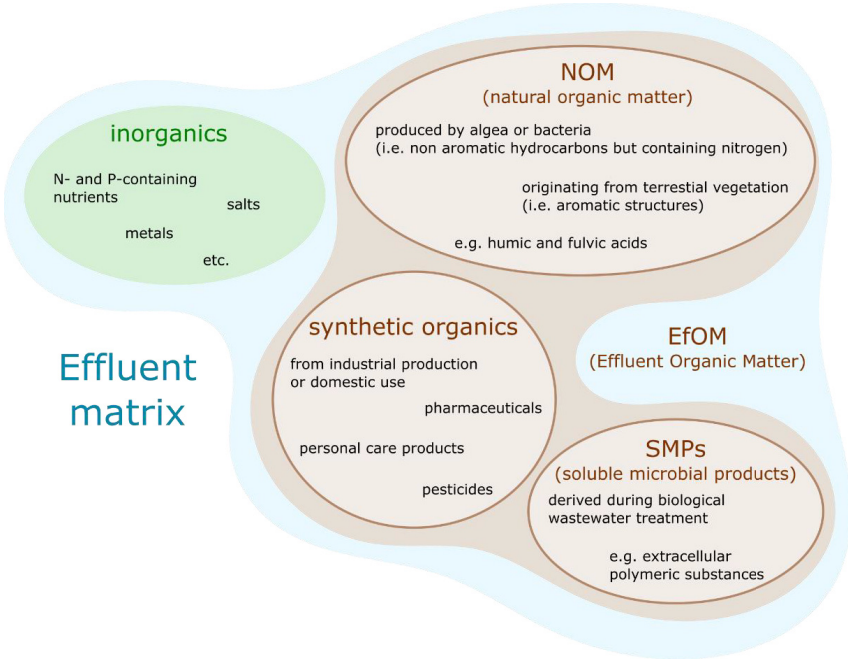

Figure 1.2: Schematic representation of the effluent composition (i.e. matrix) and the different possible constituents.

Finally, it can be stated that this review brings together the current state-of-the-art of indicators and surrogates to use, (potential) control strategies and, implications and difficulties that occur during tertiary ozonation of WRRF effluents in view of TrOC abatement. The ozonation of secondary effluent with the aim of TrOC abatement, and the control of this process, needs to

cope with different challenges. As an example, effluents can be highly dynamic in time and the ozone demand might vary. Controlling the ozone dose is at first aiming to reach its target but secondly, it needs to be considered if the strategy results in cost savings and avoids the increase of overall complexity (e.g. increased maintenance or human intervention). The review provided, therefore contains an assessment of different indicators and surrogates that could be used. As previously mentioned, different full-scale installations already exist for disinfection but also some for the abatement of TrOCs. An overview is made including the currently applied control strategies. Advantages and disadvantages are consequently listed and compared with different possible control strategies that can be applied.

2 Control targets: definition and driving forces

Upgrading of conventional WRRFs is mainly done after regulation is imposed (e.g. the Swiss situation, section 2.1), supported by a scientific and technological basis. Next to current gaps in chemical and technical knowledge (as already mentioned in section 1), the lack of specific regulatory values (highly related to toxicological knowledge)[10] hampers process design of ozonation (or other post-treatment) processes. In Europe, (upcoming) effluent regulation on TrOCs is the main driver of advanced wastewater treatment. In the United States, the number of applications is also limited but, in contrast to Europe, disinfection is the main goal of ozonation and only a few plants use ozone for (proactive) protection of surface waters/water sources against TrOC exposure (see overview of plants in section 4.1, Table 1.8 and refs.[22,48,49]).

In any case, a TrOC abatement strategy to protect the aquatic environment needs the development and implementation of sound monitoring and evaluation tools.[28] This to pursue effective advanced treatment of discharged effluents, going hand-in-hand with imposed legislation.

2.1 Regulatory trends and background

The situation on TrOC abatement regulation in Europe (and more specifically the European Union containing 28 member countries) is briefly explained in view of defining specific targets

for (online) control strategies of tertiary ozonation processes. Starting from Audenaert et al.[22], a comparison is made with Switzerland, as a non EU-member ahead with developing and implementing concrete legislation and guidelines, and the current situation in the United States of America (USA). Table 1.2 gives a brief overview of the (current) regulation in those three regions. Online monitoring of TrOC abatement is still under development for all, and it is mentioned if indicator compounds (given in section 2.2) have been defined for process performance assessment.

Table 1.2: Comparison of the status of TrOC (abatement) regulation in the European Union (EU), Switzerland and the United States of America (not considering disinfection applications, adapted from Audenaert et al.[22])

	EU 	**Switzerland** 	**USA** 
Specific TrOC regulation	Under development, some WRRFs take proactive measures	In place	In place for water reuse schemes, some WRRFs take proactive measures
Indicator compounds	Under development, sometimes locally defined (e.g. France)	Defined	Defined for water reuse
Criteria	Based on concentration (EQS)[a] (defined for surface waters)	Based on removal (%) (defined for WRRF effluents based on size)	Based on removal (log) (defined for water reuse)
Preferred treatment technology	O_3 or P/GAC, followed by SF or UF	O_3 or P/GAC, followed by SF or UF	UF/RO + oxidation (water reuse)

[a] EQS = Environmental Quality Standards

Due to recent developments in environmental legislation (in Europe, e.g. EU and Switzerland), many WRRFs will be equipped with advanced treatment steps (especially ozonation). These new regulations will control the discharge of TrOCs into the natural environment. Switzerland is the first country that enforced TrOC control on a national scale. In the EU, priority pollutants were defined, but regulatory developments are slower and currently still in a drafting phase. Monitoring data on certain compounds (defined on a 'watch list') will be collected throughout the EU before further actions will be taken. In the United States, some WRRFs were proactively equipped with advanced treatment steps but as in the EU, control at the point source is not enforced by law. Regulation of TrOCs in the USA is especially important for water reuse projects.

Further data on the occurrence and fate of TrOCs will and has to be collected in the near future. This is essential for the development of effective and accepted regulation. In parallel, online monitoring frameworks (e.g. based on spectral measurements) have to be further established to continuously assess plant performance in terms of TrOC abatement. These tools will also be useful for the control of those plants (i.e. optimal ozone dosing). Different legislative frameworks (regionally dependent) are being put in place, each having a distinctly defined indicator method or target compound(s). This is summarized in Table 1.3 containing different examples. Further discussion and details on (imposed) discharge limits or removal is given in section 2.2.

To date, limited full-scale plants make use of online monitoring of TrOC removal as the scientific basis for this was only established during the last 10 years (the first paper on that specific topic was published in 2007).[63] Online monitoring of process performance is under full development and will most likely be applied on larger scale in the near future. In Europe (incl. Switzerland), ozone and/or (powdered/granular) activated carbon are the preferential technologies for TrOC abatement, while in the USA often membrane filtration (i.e. to reduce organics and enhance increase ozone efficiency) is used in combination with an (advanced) oxidation process. However, Table 1.2 has to be interpreted with care as the design of treatment trains is highly dependent on the treatment goal. While in the USA TrOCs are mainly removed in water reuse schemes, the advanced European plants discharge their effluents into the environment. This explains why treatment trains are composed differently.[22]

Table 1.3: Indicator compounds for TrOCs (and applied criteria) defined by different regions, each having their own purpose as discussed within the text. They are grouped according to their reactivity towards ozone and HO•, based on Gerrity et al.[64] TrOCs adopted by the EU, Switzerland or CDPH are indicated by an 'X' or their respective classification. Guideline values of NWRI are given if available.

	Group	$k_{O3,TrOC,pH=7}$ (M^{-1} s^{-1})	$k_{HO•,TrOC}$ (10^9 M^{-1} s^{-1})	EU[a]	Switzerland	NWRI[b] classification	CDPH[c] classification
References	64	39,64–66	39,64–67	23,68	28	22,69	40,64,70
Bisphenol A	I	7×10^5	10				A
Carbamazepine	I	3×10^5	9		X	10 µg L^{-1}	C
Diclofenac	I	1×10^6	8	X	X		D
Estrone (E1)	I	1.8×10^6	n.a.	(X)[e]		320 ng L^{-1}	A
17 beta-estradiol (E2)	I	1.7×10^6	n.a.	X			A
Ethinylestradiol (EE2)	I	1.7×10^6	9.8	X			A
Naproxen	I	2×10^5	10				E
Sulfamethoxazole	I	3×10^6	6		X		B
Triclosan	I	4×10^7	10			2 100 µg L^{-1}	A
Trimethoprim	I	3×10^5	7				D
Atenolol	II	2×10^3	8			4 µg L^{-1}	D
Benzotriazole	II	135	11		X		D
Gemfibrozil	II	5×10^4	10				F
Metoprolol	II	2×10^3	7.3				D
Mecoprop	II	111	n.a.		X		E
DEET	III	<10	5			200 µg L^{-1}	G
Ibuprofen	III	10	7				G
pCBA	III	<0.1	5				G
Phenytoin	III	<10	6				G
Primidone	III	1	7			10 µg L^{-1}	G
1,4-Dioxane	IV	<1	3				Alternative criterion (0.5-log removal)
Atrazine	IV	6	3				D
Iopromide	IV	0.8	3.3				H
Meprobamate	IV	<1	4			200 µg L^{-1}	H
Musk Ketone	V	<1	0.2				I
TCEP[d]	V	<1	0.6			5 µg L^{-1}	H
Cotinine	n.a.	n.a.	n.a.			1 µg L^{-1}	D
Sucralose	n.a.	n.a.	n.a.			150 ng L^{-1}	n.a.

[a] referring to recommended TrOCs to be included but not yet on the 'priority list'; [b] National Water Research Institute; [c] California Department of Public Health (letter codes are explained in section 2.2); [d] tris(2-chloroethyl) phosphate; [e] included in an updated watch list, indicated as an example; n.a. = not available.

2.2 Regulatory defined and upcoming control targets

The EU puts in place a broad range of environmental legislation. The EU Water Framework Directive (WFD)[71] sets out "strategies against pollution of water" and is one of the most important pieces of the EU environmental legislation. It states that all EU inland and coastal waters had to achieve "good status" by 2015, which means that Environmental Quality Standards (EQS) had to be met. EQS for 33 priority substances (PS) and 8 other pollutants (including industrial chemicals, plant protection products and metals/metal compounds; in absolute concentrations) in surface waters were defined.[72] By an adaption of the WFD, EQS for 15 new substances were proposed of which for the first time, three pharmaceuticals were mentioned: 17 alpha-ethinylestradiol (EE2), 17 beta-estradiol (E2) and diclofenac.[68] Some concerns were raised by the European utilities related to increased costs for treatment and monitoring as a result of this decision. Questions raised as (i) not enough data is available related to the environmental impact of pharmaceuticals (and their treatment, e.g. potential toxic by-products formation) and (ii) in the state-of-art of analytically measuring E2 and EE2, the EQS was 20-100 times more stringent than the ongoing detection limits.[73] Finally, the pharmaceuticals were not included in the updated list and hence, not directly regulated.[74] Nevertheless, they are added to a 'watch list' of 10 (groups of) substances for which monitoring data had to be gathered throughout the EU (to be established by 14 September 2014). Next to the aforementioned pharmaceuticals, the watch list was supplemented with estrone (E1), antibiotics, pesticides, a UV filter and an antioxidant commonly used as food additive promoted by their frequent occurrence in the environment and/or the inefficiency of conventional WRRFs to remove such compounds.[23] The collected data will be used as a support during the periodic review of the list of PS in view of its future extension while a max. 4 years monitoring period is applied.[74] As an example, and even long before the establishement of the watch list, France already conducted a national monitoring campaign in which data (for plant dependent substances) was collected at 170 WRRFs, started in 2002 (http://www.ineris.fr/rsde/).[22]

As a European country, but acting independently of the EU member states, Switzerland established an innovative regulatory framework to protect the environment and water resources, based on Swiss research projects conducted between 2002 and 2010. Risks inherent to endocrine disrupting compounds and the development of strategies to cope with them were established on a solid scientific basis. TrOCs of interest have been defined, considering detection methods, quantified loads, working mechanisms and adverse effects on ecosystems.[75,76] A set of indicator

compounds is proposed for which 80% removal is required. No discharge limits in the form of absolute concentrations were applied. The currently proposed indicator compounds (sulfamethoxazole (antibiotic), diclofenac (pain killer), mecoprop (herbicide), benzotriazole (corrosion inhibitor) and carbamazepine (anti-epileptic)) are a good representation of the wide variety of TrOCs present in (Swiss) wastewater and are measurable with a single analytical method.[28] Three types of WRRFs to be upgraded with an advanced treatment step (ozonation or powdered activated carbon adsorption) during a 25 year-time period (2016-2040) were defined, treating combined 50% of the Swiss wastewater: (i) large sized (> 80 000 I.E.) as a general large load reduction to surface waters, (ii) medium sized (> 24 000 I.E.) to specifically protect sensitive or drinking water sources, and (iii) small sized (> 8 000 I.E.) with a dilution at discharge less than 1/10 as an environmental protection barrier. The Swiss Government will subsidize the projects by 75% based on the polluter-pays principle. Total costs are approximated at 1.2 billion Swiss Francs (1.1 billion EUR or 1.25 billion USD).[77]

In the United States, WRRF effluent discharge is regulated by permits from the National Pollution Discharge Elimination System (NPDES).[49] TrOCs are not regulated, as only basic contaminants (such as nutrients) are covered by the NPDES permits. Although water reuse and wastewater treatment (final discharge) are different concepts, it is worth mentioning that for (in)direct potable reuse schemes some guidelines or regulations on TrOCs do exist. The National Water Research Institute (NWRI) published a report on public health criteria for direct potable reuse systems in which some guideline values are given for some useful indicator substances (Table 1.3).[69] Additionally, some States have specific regulations. For example the California Department of Public Health (CDPH) defined advanced treatment criteria for groundwater replenishment systems. This implies that e.g. oxidation processes must achieve optimal removal of indicator compounds. Different compound classes (nine in total, based on the (difference in) chemical structure of TrOCs) were defined of which at least one indicator compound per class should be chosen to assess the system performance. They are listed as follows: A) Hydroxy Aromatic, B) Amino/Acylamino, C) Nonaromatic with carbon double bonds, D) Deprotonated Amine, E) Alkoxy Polyaromatic, F) Alkoxy Aromatic, G) Alkyl Aromatic, H) Saturated Aliphatic and I) Nitro Aromatic. Examples are given in Table 1.3. Removal of at least 0.3 (A-G) - 0.5 (H-I) log (50 - 69%, depending on the class given between brackets) should be achieved. It was stated that an online surrogate measurement, reflecting – possibly through continuous monitoring – the removal of at least 5 indicator compounds (out of those nine classes) should be applied.[70]

2.3 Oxidation transformation products

One of the main drawbacks of the ozonation process is the potential formation of toxic by-products or transformation products because of its reaction with TrOCs and/or EfOM. Degradation by ozonation will increase the total amount of aldehydes, carboxylic acids, and other easily assimilable organic carbon (AOC).[78] Currently, most effects are widely unknown and investigation of this aspect requires significant elaboration. In comparison with e.g. hypochlorite, smaller concentrations of halogenated by-products (e.g. trihalomethanes, haloacetic acids, etc.) are formed.[79,80] Ozonation has shown to lead to the production of mutagenic compounds such as nitrosamines (e.g. NDMA) and various efforts have been made to identify those.[33,42,81–86] Various classes of amine compounds such as dimethylamine or compounds with a N,N-dimethylamino group only pose a problem at high concentrations (molar yield < 5%), e.g. industrial wastewater containing amine-based dyes.[16,87,88] Other N,N-dimethylamino compounds (e.g. connected to sulfamide, hydrazine, hydrazides, and carbazides, molar yields up to 94%) or amine-based polymers used for sludge or water treatment were also appointed as potential percursors.[42,84–86,89–91] Formation of NDMA is therefore clearly marked as a wastewater dependent problem and hence, the exact precursors are not completely known. The other well-known example is the oxidation of bromide towards the potential carcinogenic bromate or other bromine containing organic compounds (e.g. bromoform),[44,92–94] of which the formation reactions are largely known and extensively described by e.g. Von Gunten.[44]

Optimal ozone dosing is required to lower the extent of by-product formation. The formation of bromate or NDMA has been associated with EfOM but has also been indicated to be WRRF specific.[78,95–97] The formation will depend on different factors such as (i) presence or absence of specific precursor ions and moieties and (ii) the reactivity (i.e. composition) of the total effluent matrix. The formation has been generally associated with high ozone dosages exceeding effluent specific threshold values because of the reaction with the available EfOM.[42,44,45,78] A low HO• exposure (i.e. the presence or concentration of HO• in time) was associated with low ozone doses due to high availability of electron rich moieties, rapidly reacting with ozone.[98] Additionally, the increased formation of transformation products has been attributed to an increased HO• exposure, indicated by a higher AOC (5-52%), aldehyde (31-47%) and carboxylic acid (12-43%) formation if H_2O_2 was added to the ozonation process.[78] An example is given in Figure 1.3 showing a clear lag-phase before any formation of bromate could be noticed.[99]

The current dissertation focuses specifically on control strategies and methods for the online control and monitoring of TrOC abatement during ozonation. Optimizing the ozone dose (and cost) to have an efficient TrOC abatement, it can be assumed that by-product formation will be minimized when the ozone dose is kept as low as possible although previous factors (i.e. presence of precursors and effluent matrix reactivity) will play a major role. Hence, the issue of potential toxic by-product formation is briefly introduced and might be linked to this research in future.

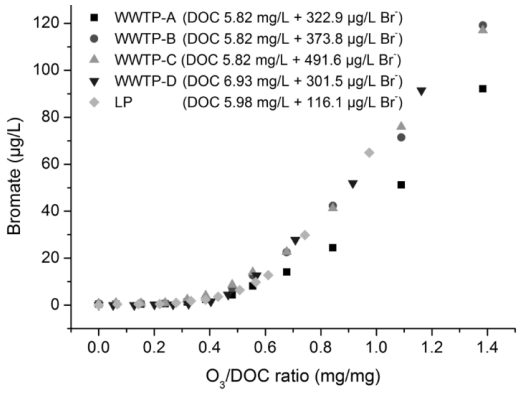

Figure 1.3: Bromate formation in µg/L as a function of O_3:DOC ratio showing a clear lag-phase before the formation of bromate can be noticed, adapted from Li et al.[99] The different colored markers indicate different water matrices and initial bromide concentrations.

3 Performance control and assessment tools: indicators and surrogates

The main challenge for a broad application and dose control of tertiary wastewater ozonation depends largely on two main aspects:[98] (i) the wide range of structural diverse TrOCs in terms of reactivity (given as apparent second order reaction rate constants with ozone ($k_{O3,TrOC}$) or hydroxyl radicals, HO• ($k_{HO•,TrOC}$)), sorption, biodegradability, etc. and, (ii) the EfOM dynamics in terms of load and composition (i.e. the scavenging capacity). Secondary treated wastewater effluent contains numerous TrOCs (as discussed in section 1) but it is unworkable to follow-up all (measurable) TrOCs (potentially more than 80 000)[31] to assess the performance of the ozonation process. Consequently, some indicator compounds should be identified and monitored, as cited

previously (see section 2.2), which represent a broad range of TrOCs and that can be easily measured. The removal of an indicator component will give an idea of the removal of structurally similar TrOCs.[40,64,98] Analytical TrOC determination has shown to quantify TrOCs down to ng L^{-1} concentrations and is therefore critical for the assessment of the ozonation process.[40] Although this way of TrOC determination will remain of main importance for i.a. regulatory purposes, measurement of trace levels is highly time consuming, labor- and cost intensive.[100] This makes it inapplicable for online monitoring or control of the ozonation process.

Readily available measurements are therefore needed to control the ozone dose. The water flow rate, and the ozone gas concentration in both the feed- and off-gas are good candidates for controlling the exact ozone dose. Alternative measurements are however needed to control the TrOC abatement by ozone. The ozone dose and contact time have been identified as key parameters in defining HO• exposure, influencing the formation of potential toxic by-products.[101,102] Additionally, an online monitoring framework will reduce the need of frequent monitoring of indicator compounds.[40] Control mechanisms adopted from drinking water applications have proven to be unsuccessful. The use of CT is well established in drinking water applications and describes the decrease of dissolved ozone concentration (C) in time (T). This surrogate has limited capabilities during treated wastewater oxidation as residual ozone is only measured at high doses.[103] TrOC oxidation will however persist although no CT can be determined. Next to the increased dosing costs, residual ozone concentrations in wastewater applications have also been associated with the formation of bromate.[63]

The need for easily measurable surrogate parameters is therefore required to monitor and control TrOC abatement and support engineering purposes. Surrogate measurements, as a means of predicting the behavior of difficult-to-measure contaminants, are well established among researchers with respect to water quality parameters (e.g. turbidity, COD). In contrast, it has not been adopted widely by researchers studying (the removal of) TrOCs.[40] For example turbidity as a surrogate for pathogens has already been well established[40] and also the O_3:DOC ratio, ΔUVA_{254} or ΔTF (total fluorescence) are seen as alternatives of the CT approach for the follow up of microbial inactivation.[104] In accordance, surrogate measurements for the effluent organic matter (EfOM), such as the measurement of the UV-absorbance at 254 nm (UVA_{254}), color or fluorescence are being proposed and used as alternative.

3.1 Indicators of TrOC presence and/or abatement

Although indicator compounds already reduce the analytical work load significantly, they are not able to serve as online monitoring or control of the applied ozone dosages. However, it enables to construct surrogate models that can be used online and are representative for a wide range of TrOCs. Indicators should be representative for a broad range of TrOCs and are selected based on treatment persistence, environmental (i.e. presence, toxicity) and societal (i.e. still in use or already forbidden for use, e.g. some pesticides) relevance, chemical structure (i.e. reactivity for O_3 and/or HO•) and ease of analysis.[40,64,82,103,105] Especially for its application with tertiary ozonation, compounds have been grouped based on their observed removal efficiency.[40] It is assumed that indicator compounds within these groups are a good representation of other compounds with a similar structure. An initial method to develop and apply an indicator framework is given by Dickenson et al.[40] who based the selection of indicator compounds on an occurrence study and some pilot-scale experiments. TrOCs stated as "good" or "intermediate" removable are included as indicator compounds. However, TrOCs with lower ozone reactivity are of most interest as these mainly react through indirect reaction pathways (HO•). Some indicators for the most ozone-recalcitrant TrOCs are pCBA, ibuprofen and iopromide,[106] and should therefore also be included.

This indicator framework was further elaborated on by several authors, putting the use of different groups forward (up to 5).[64,98] Each group is defined by specific second order reaction rates for both direct (ozone, $k_{O3,TrOC}$) or indirect (HO•, $k_{HO•,TrOC}$) reactions. Selecting one (or more) compounds of each group gives a list of ≥ 5 indicators that need to be monitored, representative for other compounds within the same groups. These groups are defined by Lee et al.[98] and Gerrity et al.[64], and are given in Table 1.4. Some removal efficiencies of different TrOCs of each group are summarized in Table 1.5 originating from different studies, applying different ozone doses.

Clear differences are noticeable among the different groups as the lowest dose (0.33 g O_3 g^{-1} DOC) already results in TrOC abatement below detection limits in practically all cases for high ozone reactive TrOCs (group I). A decreasing reactivity towards ozone or HO• logically results in lower removal efficiencies and, consequently, higher ozone doses are needed to achieve a minimum of 80% removal: 0.5-1.0 g O_3 g^{-1} DOC for group II and III, and > 1.0 g O_3 g^{-1} DOC for the most recalcitrant TrOCs (IV and V), not even going above 25% ΔTrOC for TCEP. More examples of different TrOCs in each group are given in Table 1.3. It is remarkable that current

indicator compounds of interest (European Union) or even adopted in a currently imposed regulatory framework (Switzerland) do not contain any TrOC that react poorly with ozone ($k_{O3,TrOC}$ < 10 M^{-1} s^{-1}). For the EU, only three pharmaceuticals/hormones were of initial interest that all react highly with ozone ($k_{O3,TrOC}$ > 10^5 M^{-1} s^{-1}). TrOCs that react poorly with ozone should also be adopted, ensuring a broad representative framework. The establishment of a watch list of TrOC compounds (section 2.2) does however contain TrOCs showing refractory behavior to ozone (e.g. 2-ethylhexyl-4-methoxycinnamate, a UV filter) although this was no criteria to include those compounds into the watch list.[23] Studies including those compounds were noticed to be limited, hence a lack of knowledge exists regarding the removal in real scenarios. Recent developments also unraveled some limitations of such group-based classification - although providing insightful classification for TrOC abatement - as even this might not result in sufficient distinction among different reactivities, especially at low ozone doses for TrOCs reacting mainly through indirect ozone reactions.[54]

Table 1.4: Different groups of TrOCs defined by specific second order reaction rates for both direct (ozone, $k_{O3,TrOC}$) or indirect (HO•, $k_{HO•,TrOC}$) reactions, adapted from Lee et al.[98] and Gerrity et al.[64]

Group	**Description**	$k_{O3,TrOC,pH7}$ **criteria** (M^{-1} s^{-1})	$k_{HO•,TrOC}$ **criteria** (10^9 M^{-1} s^{-1})
I	high reactivity with both ozone and HO•	≥ 10^5	≥ 5
II	moderate reactivity with ozone and high reactivity with HO•	< 10^5 and ≥ 10	≥ 5
III	low reactivity with ozone and high reactivity with HO•	< 10	≥ 5
IV	low reactivity with ozone and moderate reactivity with HO•	< 10	< 5 and ≥ 1
V	low reactivity with both ozone and HO•	< 10	< 1

Table 1.5: Abatement of TrOCs obtained in different studies in perspective of added ozone dosages (mg L^{-1} and/or g O_3 g^{-1} DOC) and grouped based on the reactivity of TrOCs with ozone and HO•. Abatement (%) above 90% (or below the detection limit), between 50 and 90%, and below 50% are indicated in green, orange or blue respectively.

O_3 dose	mg L^{-1}	2.1	2.2	2.1	3.6	3.3	3.9	4.4	4.4	4.1	5.1	n.a.	4.8	4.9	7.1	7.3	8.7
	g O_3 g^{-1} DOC	0.33	0.36	0.40	0.56	0.62	0.66	0.72	0.72	0.91	0.97	0.6-1	1	1.00	1.11	1.49	1.78
ΔUVA_{254}	%	n.a.	23	n.a.	n.a.	n.a.	35	n.a.	n.a.	n.a.	42	n.a.	49	n.a.	n.a.	n.a.	n.a.
Ref.		107	108	33	107	33	108	109	109	33	108	103	64	107	107	107	107
Group[64]	**TrOCs**	**Abatement (%)**															
I	Carbamazepine	>99	>94	99	>99	99	>94	n.a.	>99	99	>92	>90	>95	>99	>99	>99	>99
I	Diclofenac	>99	>99	99	>99	99	>98	>94	93	99	>99	>90	>47	>98	>98	>98	>98
I	Sulfamethoxazole	93	n.a.	87	>99	96	n.a.	>99	>99	96	n.a.	>90	>99	>99	>99	>99	>99
I	Naproxen	>96	n.a.	98	>96	85	n.a.	>99	98	88	n.a.	>90	>4	>92	>66	>92	>92
I	Trimethoprim	>99	n.a.	97	>99	95	n.a.	>92	>99	94	n.a.	n.a.	>52	>97	>97	>97	>97
II	Mecoprop	n.a.	35	45	n.a.	68	74	n.a.	n.a.	64	>89	n.a.	n.a.	n.a.	n.a.	n.a.	n.a.
II	Metoprolol	n.a.	47	61	n.a.	88	>74	n.a.	n.a.	95	>78	>90	n.a.	n.a.	n.a.	n.a.	n.a.
III	Ibuprofen	<1	n.a.	88	>82	n.a.	n.a.	>99	n.a.	n.a.	n.a.	>90	n.a.	>94	>24	>94	>94
IV	Iopromide	14	n.a.	25	40	24	n.a.	n.a.	n.a.	42	n.a.	50-90	n.a.	73	91	91	>95
IV	Meprobamate	31	n.a.	n.a.	41	n.a.	n.a.	n.a.	n.a.	n.a.	n.a.	50-90	69	58	>98	81	87
V	TCEP	18	n.a.	n.a.	<1	n.a.	n.a.	n.a.	n.a.	n.a.	n.a.	<25	17	<1	17	6	10

n.a. = not available

It should be noted that actual indicators that need to be monitored will likely be imposed by legislative means. As described in section 2.2, Switzerland already defined a list of five compounds, and the USA (California specifically) has a classification of compounds based on functional sites that need to be removed to a certain extent in case of groundwater replenishment. The latter might seem more of interest stating previous observations with respect to the insufficient uniform representation of the Swiss indicator compounds. A major drawback of this approach is that structural differences between similar TrOCs exist and other dominant reactions might occur. Some compounds have multiple sites to be attacked by ozone; therefore are equivocal to classify.[54]

3.2 Surrogates for TrOC abatement

Surrogates for the follow-up of TrOC abatement by tertiary ozonation have to meet two main criteria:[40] (i) they need to be quantifiable parameters that serve as a performance measure of treatment processes related to the removal or abatement of specific contaminants and, (ii) they should be a means to assess the water quality without conducting tedious TrOC analysis.

EfOM has been addressed as (one of) the main influencers of the ozonation process.[110] The organic matrix indirectly gives rise to HO• production besides directly consuming a significant fraction of the ozone.[111,112] Significantly impacted by direct ozone and hydroxyl radical (HO•) reactions, different measurement methods have gained attention in characterizing the EfOM to follow-up the ongoing processes. Oxidant induced changes of EfOM can provide more rapid information on oxidant exposure, and hence TrOC removal. The exact relation between both will however remain dependent on the (variation of) reactivity of the complete effluent matrix. EfOM characterization can easily be performed by (online measurable) spectral surrogates, correlating well to ozone dose and TrOC removal, such as UV absorption at 254 nm (UVA_{254}),[40,63,64,82,100,103,113,114] $color_{436}$,[103,115] total fluorescence (TF)[64] and dissolved organic carbon (DOC).[33,98,115]

3.2.1 Dissolved Organic Carbon (DOC)

The total or dissolved organic carbon (TOC or DOC) content is typically used as a surrogate in different drinking water processes to indicate the total amount of dissolved organic matter (or EfOM in this case).[116] TOC/DOC is measured offline, semi-online (e.g. through catalytic oxidation and NDIR (non-dispersive infrared) detection on samples taken automatically at fixed time intervals)[117] or online as it is spectrally deducible from a UV-VIS spectrum (using a multi-wavelength approach) although some site specific calibration adjustments might be needed.[118] Ozonation at realistic ozone doses for the degradation of TrOCs (near 1 g O_3 g^{-1} DOC) mainly results in transformation of the EfOM (up to more than 90% of electron rich moieties) and no actual mineralization.[40,41,98] As such, only very limited DOC removal is expected. The percentage removal of DOC is therefore not usable as an indicator for TrOC abatement with ozone.

Normalizing the ozone dose to the effluent DOC (g O_3 g^{-1} DOC) is often used as an operating parameter to compare different waters with varying quality.[33,39,45,55,98,119–121] It is mainly assumed that identical O_3:DOC ratios will yield similar ozone and HO• exposures if the EfOM characteristics are similar.[98] The elimination of different TrOCs will be comparable in this scenario when having (practically) the same $k_{O3,TrOC}$ and $k_{HO•,TrOC}$. In a thorough screening of 10 different WRRF effluents, Lee et al.[98] noticed more or less similar TrOC abatement for those with similar $k_{O3,TrOC}$ and $k_{HO•,TrOC}$, with the exception of two effluents. Already accounting for the presence of nitrite (NO_2^--N), these effluents consumed more ozone resulting in lower TrOC abatement for the same O_3:DOC ratio attributed to the increased presence of electron-rich moieties. This variability in effluent characteristics consequently leads to a varying initial ozone dose threshold in which a negligible amount of HO• is formed.[98,121] The use of an O_3:DOC ratio in these cases might therefore result in an incorrect prediction of TrOC abatement.

3.2.2 UV-Visible absorbance

The UV absorbance at a wavelength of 254 nm (UVA_{254}) has received by far the most attention for its potential use to control the ozone dose.[40,53,64,82,100,103,113,115,122] Especially longer wavelengths (λ between 240 and 320 nm) are affected during ozonation although a general decrease is observed for the complete UV-VIS spectrum.[100] Out of this complete spectrum, UVA_{254} is widely known as a representation for conjugated moieties containing aromatic and double carbon bond

structures.[40,114] The presence of these moieties is responsible for high UV-absorption but also for the typical yellowish color of WRRF effluent, commonly represented at 436 nm.[123] These electron rich moieties are highly susceptible for direct ozone attacks and, therefore, the decrease of UVA_{254} (ΔUVA_{254}) is connected with the oxidation of these components present in the EfOM.[103,124] Electron poor moieties, non-aromatic or other ozone resistant moieties, can also be indirectly correlated by ΔUVA_{254} given the generation or presence of HO• during EfOM oxidation. Differential absorbance has therefore been recognized as a valuable measurement of the EfOM during ozonation processes.[100] Another use of this surrogate is its normalization according to the DOC concentration, known as the specific UV absorbance at 254 nm (SUVA). The SUVA (L mg^{-1} C m^{-1}) has a strong linear correlation with the percentage of aromaticity in organic components as shown by Weishaar et al.[124] (R^2 = 0.97, n = 13), confirming its ability to act as a surrogate for (the aromaticity of) EfOM during the ozonation process.

Ozonation will result in EfOM transformations along with the degradation of TrOCs leading to an overall absorbance decrease. Changes in UVA_{254} are therefore indirectly correlated with the applied ozone dosages while TrOC degradation depends on its reactivity with ozone and hydroxyl radicals.[100,115] The use of the relative decrease of UVA_{254} (ΔUVA_{254}) was first proposed by Buffle et al.[121] to determine the ozone exposure in wastewater applications after observing a first-order kinetic relationship.[64] ΔUVA_{254} has mostly been used in a linear relationship (eq. 1.1) to describe the removal of TrOC indicator compounds during ozonation, mentioned for the first time by Bahr et al.[63] and further elaborated on by several others.[40,64,82,103,113,125] Bahr et al.[63] chose to draw the linear correlations through the origin, thus without considering an intercept (*b*). Wert et al.[103] and others[40,64] concluded that this approach is especially inapplicable for slower reacting TrOCs ($k_{O3,TrOC} < 10^3$ M^{-1} s^{-1}) as correlations only started from 15% ΔUVA_{254}, and an intercept should always be considered. It was also concluded for the first time that these correlations are consistent for different wastewater effluents, which is an important aspect that must be retained in further adaptations of these correlation models.[103]

Table 1.6 provides an overview of available linear correlations in literature according to eq. 1.1 with *a* as the slope and *b* as the intercept, available for the monitoring of ΔTrOCs in relation to ΔUVA_{254}. Figure 1.4 displays six selected TrOCs with differing $k_{O3,TrOC}$ and $k_{HO•,TrOC}$ for which multiple authors constructed a linear correlation.

$$\Delta TrOC = a \times \Delta UVA_{254} + b \qquad \text{eq. 1.1}$$

Table 1.6: Compilation of single linear correlations available in literature describing the relation between ΔUVA_{254} and $\Delta TrOCs$. The slope (a), intercept (b) and the coefficient of determination (R^2) are given if mentioned in the respective literature sources. The unavailability of data is marked by "-".

	$k_{O3,TrOC,pH=7}$ (M^{-1} s^{-1})	$k_{HO•,TrOC}$ (10^9 M^{-1} s^{-1})	Ref.	**Wert et al.**[103] (n = 8 - 26)			**Bahr et al.**[63] (n = 5 - 9)			**Gerrity et al.**[64] (n = 40-124)			**Dickenson et al.**[40,a] (n = 4)			**Pisarenko et al.**[82] (n = 3 - 5)		
				a	b	R^2	a	b	R^2	a	b	R^2	a	b	R^2	a	b	R^2
1,4-Dioxane	< 1	3	[64]	-	-	-	-	-	-	1.57	-18	0.69	-	-	-	-	-	-
Atenolol	2×10^3	8	[64]	2.1	-7.2	0.91	-	-		2.37	-4	0.79	-	-	-	-	-	-
Atrazine	6	3	[64]	-	-	-	-	-	-	1.79	-21	0.76	-	-	-	-	-	-
Bezafibrate	5.9×10^2	7.4	[63]	-	-	-	1.7	0	0.94	-	-	-	-	-	-	-	-	-
Carbamazepine	3×10^5	8.8	[63]	2.5	14.3	0.73	3.7	0	0.85	-	-	-	-	-	-	5.79	-28.7	0.834
Clofibric acid	< 20	4.7	[63]	-	-	-	1.4	0	0.95	-	-	-	-	-	-	-	-	-
DEET	< 10	5	[64]	-	-	-	-	-	-	1.59	-2	0.67	2.38	-23.28	0.99	2.00	-18.80	0.99
Diclofenac	1×10^6	7.5	[63]	-	-	-	4.4	0	0.49	-	-	-	-	-	-	-	-	-
Dilantin	-	-	-	2.08	-30.5	0.89	-	-		-	-	-	2.52	-26.11	0.98	-	-	-
Estrone	1.8×10^6	-	[39]	-	-	-	3.5	0	0.71	-	-	-	-	-	-	-	-	-
Gemfibrozil	5×10^4	10	[64]	-	-	-	-	-	-	1.8	31	0.62	-	-	-	-	-	-
Ibuprofen	10	7	[64]	-	-	-	1.6	0	0.97	1.62	5	0.64	-	-	-	-	-	-
Iohexol	1.4	2.8	[63]	-	-	-	0.7	0	0.56	-	-	-	-	-	-	-	-	-
Iopamidol	-	-	-	-	-	-	0.9	0	0.76	-	-	-	-	-	-	-	-	-
Iopromide	0.5	3.1	[63]	1.45	-10.0	0.95	1	0	0.81	-	-	-	2.78	-67.96	0.88	-	-	-
Ketoprofen	-	-	-	-	-	-	1.5	0	0.89	-	-	-	-	-	-	-	-	-
Meprobamate	< 1	4	[64]	1.92	-35.1	0.89	-	-		1.87	-16	0.64	2.35	-40.73	0.95	1.87	-16.70	0.97
Naproxen	2×10^5	9.6	[63]	-	-	-	3.2	0	0.39	-	-	-	-	-	-	-	-	-
pCBA	< 0.1	5	[64]	1.95	-30.2	0.81	-	-		1.31	3	0.48	-	-	-	-	-	-
Phenazone	-	-	-	-	-	-	2.1	0	0.88	-	-	-	-	-	-	-	-	-
Phenytoin	< 10	6	[64]	-	-	-	-	-	-	1.72	2	0.6	-	-	-	2.33	-14.9	0.993
Primidone	1	7	[64]	2.22	-39	0.92	-	-		1.54	-1	0.65	-	-	-	2.3	-22.5	1
Sulfamethoxazole	2.5×10^6	5.5	[82]	-	-	-	-	-	-	-	-	-	-	-	-	4.93	-18.3	0.79
TCEP	< 1	0.6	[64]	-	-	-	-	-	-	0.57	-7	0.56	-	-	-	0.51	-5.9	0.954
Trimethoprim	2.7×10^5	6.9	[82]	-	-	-	-	-	-	-	-	-	-	-	-	3.97	12.4	0.778

[a] graphically derived from the given data points

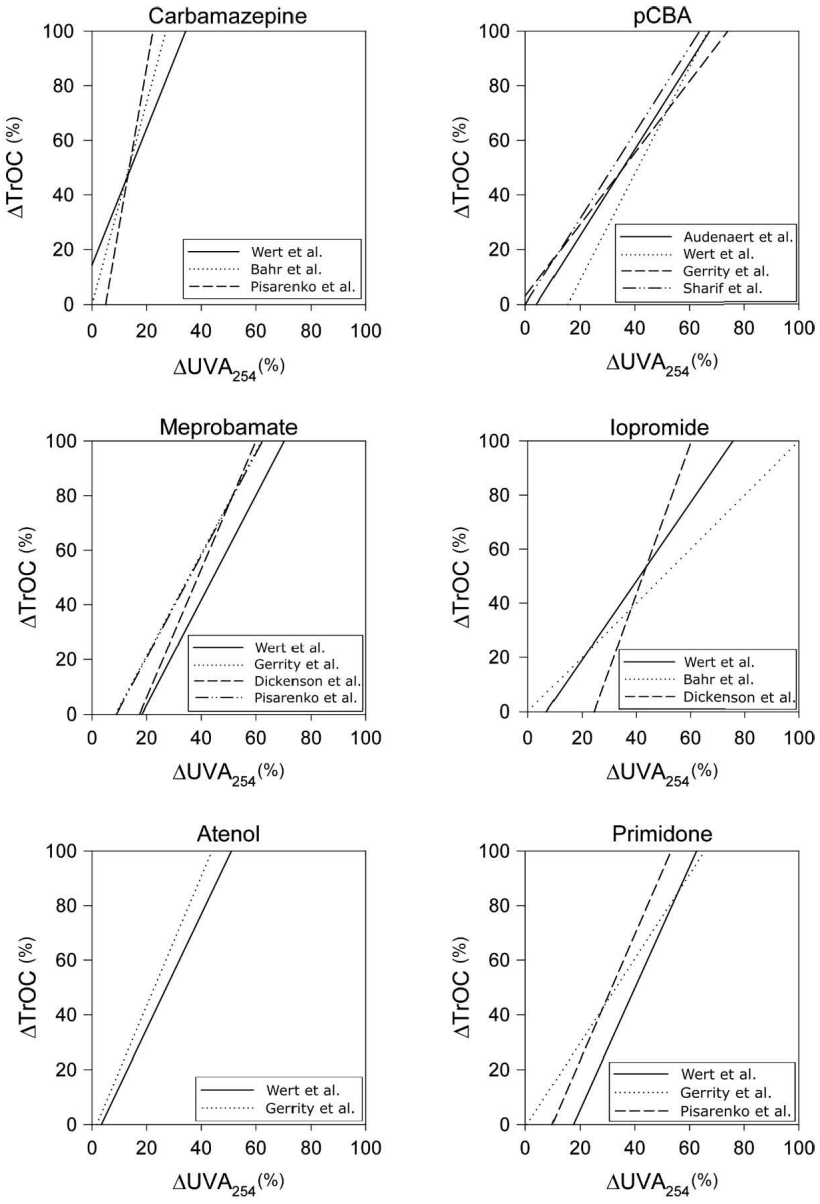

Figure 1.4: Comparison of single linear correlations between six different TrOCs (ΔTrOC) and the decrease of UVA_{254} (ΔUVA_{254}) during ozonation. Single correlations are obtained from literature and are given in Table 1.6

In addition, Audenaert et al.[113] ($\Delta TrOC = 1.58 \times \Delta UVA_{254} - 6.46$, $R^2 = 0.94$, n = 12) and Sharif et al.[115] ($\Delta TrOC = 1.57 \times \Delta UVA_{254}$; derived from the given relationships of the O_3 consumption with ΔUVA_{254} and ΔpCBA) established a correlation specifically for pCBA.

Linear correlations are constructed for a wide range of TrOCs as depicted in Table 1.6. Good ($k_{O3,TrOC} \approx 10^4$-10^6 M^{-1} s^{-1}, e.g. diclofenac and carbamazepine) and medium ($k_{O3,TrOC} \approx 10^1$-10^4 M^{-1} s^{-1}, e.g. atenol and bezafibrate) ozone reactive TrOCs but also ozone recalcitrant TrOCs ($k_{O3,TrOC} < 10^1$ M^{-1} s^{-1}, e.g. pCBA and iopromide) are well correlated, referring to the potential of ΔUVA_{254} for the follow-up of TrOCs also mainly reacting with HO•. Correlations for the same TrOCs are however clearly different depending on the considered study, as also visually depicted by a few examples in Figure 1.4. Good agreement with practically identical correlations is seen for e.g. atenol while already some clear differences can be noticed for others (e.g. carbamazepine, meprobamate, primidone, pCBA) and large deviations are noticed for iopromide. It appears that especially TrOCs with a low $k_{O3,TrOC}$ (< 10 M^{-1} s^{-1}), depending on the HO• generation by ozone reactions with the EfOM, are affected resulting in deviating correlations. High variations are also noticed for the slope and especially intercept values as given in Table 1.6. Experiments resulting in these correlations have been performed by different authors using effluents with varying water quality known to influence ongoing reactions. During ozonation, the initial phase (low ΔUVA_{254}) is characterized with high direct ozone reactions and therefore, TrOCs reacting through indirect reaction pathways are less affected at that time.[126,127] Partially destroyed UV absorbing DOM moieties during this initial phase become recalcitrant to ozone but not to HO•.[53] Enhanced ozonation will increase the HO• generation, ΔUVA_{254}, and logically the removal of ozone recalcitrant TrOCs. Further investigation of these linear correlations and the data used to construct those indicated a more convex curved behavior (of the data) pronounced especially for low ozone reactive TrOCs,[100] leading to deviations between measured and predicted values.[33]

It is clear from literature that these single linear correlations are insufficiently accounting for TrOC specific properties (e.g. $k_{O3,TrOC}$). Additionally, a compilation of existing correlations (Table 1.6) is only specifically applicable for 25 different TrOCs and can be used indicatively for TrOCs exhibiting similar reactive behavior. If compared to the potential presence of more than 80 000 compounds (see section 1), it seems only to be effective for approximately 0.03% of those. It should however be stated that probably compounds will be present with a similar reactive behavior. As described in section 2.2, no clear legislative discharge limits are defined and the list of TrOCs to control is still under development. Therefore, the need exists for a generically applicable, easily and widely adaptable control framework. A first approach is presented by

Nanaboina and Korshin[100] developing a semi-empirical correlation between ΔUVA_{254} and ΔTrOCs, hypothesizing that the general EfOM composition consists of three different moieties with respect to affinity with ozone and HO• (two reacting differently with ozone and HO•, and one as inert chromophores). This resulted in an "S-shaped" correlation (Figure 1.5), especially for low ozone reactive TrOCs (e.g. pCBA, gemfibrozil, etc.), defined by an initial slope ($S_{initial}$) and the ΔUVA_{254} corresponding to 50% ΔTrOC $(\Delta A/A_0)_{50\%}$. As the R_{ct} (i.e. the ratio of HO• exposure over the O_3 exposure)[128] was assumed constant within this approach (only one effluent investigated), further elaboration will be necessary to confirm this for multiple WRRFs. Similar inflected correlations were noticed during the research within this dissertation, and are extensively discussed in the upcoming Chapters.

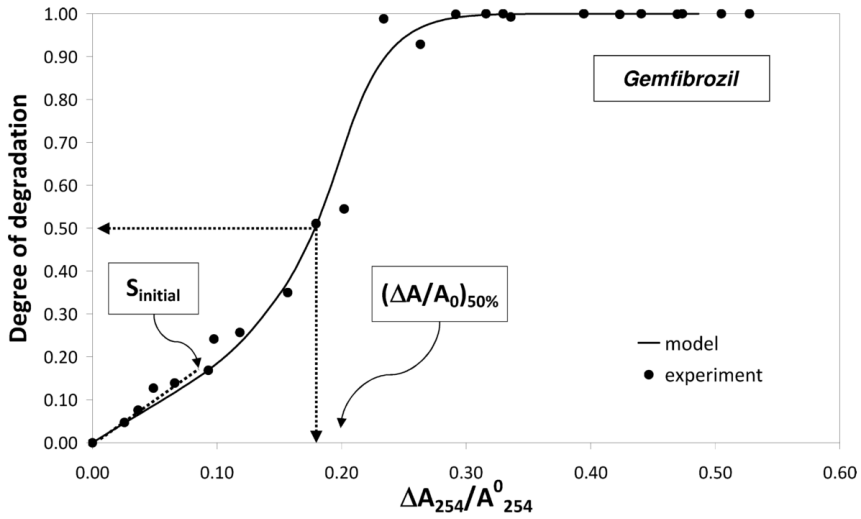

Figure 1.5: Correlation between the relative changes of absorbance and degradation of gemfibrozil, indicative for the approach used by and adapted from Nanaboina and Korshin.[100]

Other UV-Visible (UV-VIS) derived parameters are e.g. the absorbance at 436 nm (representative for the true color)[55,100] or the TOC/DOC content. $Color_{436}$ is often used in wastewater applications as an alternative measure for the presence of chromophoric EfOM.[103] Although it is not a direct measure for target compounds such as e.g. aromatics, color removal has been (non-linearly) correlated with the removal of TrOCs.[103] Its wide applicability is however hampered since at low ozone dosages (< 0.2 g O_3 g^{-1} DOC), high decreases of up to 60% of the absorbance

at 436 nm can already be noticed.[63] Ozone dosages > 0.5 g O_3 g^{-1} DOC are difficult to be monitored as color is practically completely eliminated.[63] This shows only limited advantage for the online control of the ozone dose and the associated TrOC removal, as it has previously been mentioned that most recalcitrant TrOCs are eliminated within the range of 0.5 – 1.0 g O_3 g^{-1} DOC.

3.2.3 Fluorescence

Fluorescence spectroscopy is 10 to 1000 times more sensitive than UV-VIS absorption measurements. More than UV-VIS, fluorescence is able to distinguish different chromophores.[129] Its principle is based on light absorbing and exciting fluorophores. Emission wavelengths are fluorophore dependent which results in a three dimensional (3D) excitation-emission matrix (EEM) in which different groups can be distinguished, related to e.g. humic acid-like, fulvic acid-like or protein-like components.[129–131] 3D EEM spectroscopy has gained significant attention for its use during oxidative treatment processes as it basically provides a fingerprint of the (Ef)OM present.[120] As this method consists of synchronous emission and excitation spectroscopy scans, it results in a large amount of measured fluorescence intensities and data points.[129,131–133] Different interpretation approaches therefore exist to either reduce the amount of data points in one (or more) specific parameters or ratio's, or to extract specific information related to one or more groups of components.[129] EEM spectroscopy has already been widely used to follow-up these type of component groups in different water applications. A summarizing overview of these groups is given in Figure 1.6, obtained during investigation of different spring and cave waters.[131] For example, humic acid related to a marine environment (salt water) originating from algal production could be distinguished within a EEM (peak M, Figure 1.6).[129]

It should be noted that also 3D fluorescence spectroscopy can be used to estimate the DOC as even better correlations could be obtained compared to the relation with UVA_{254} or multi-wavelength UV-VIS approaches, attributed to its ability of estimating the molecular distribution of the DOC.[134] Highly particulate media did however show to attenuate the fluorescence signal and further investigation would be needed.[135] Fluorescence spectroscopy can also be used in a differential approach similar to ΔUVA_{254} (see section 3.2.2) to follow-up TrOC abatement during ozonation. Although significantly less investigated, Gerrity et al.[64] and Pisarenko et al.[82] showed the use of the relative decrease of total fluorescence (TF, integrated total area of the 3D EEM) as

a surrogate for the complete organic matrix. Compared to UVA_{254}, TF has the advantage of containing significantly more spectral information from several groups of components.

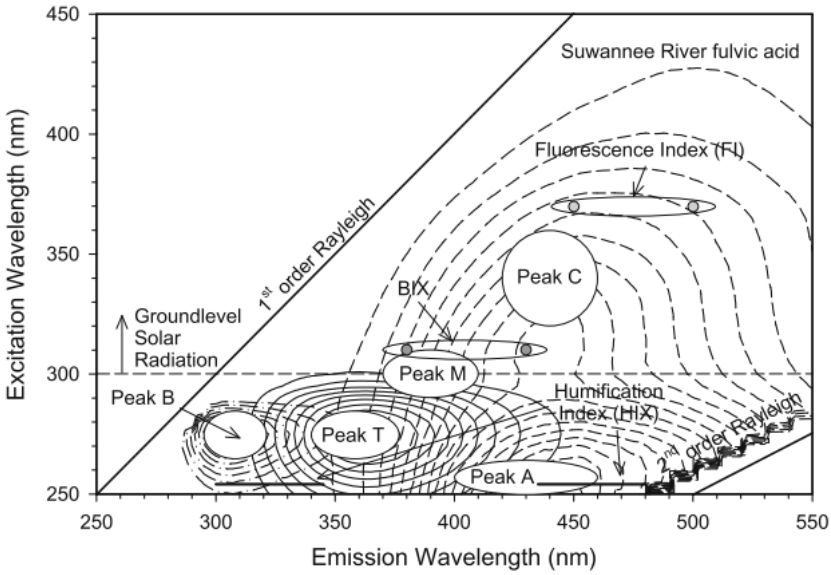

Figure 1.6: General representation of a 3D EEM obtained from cave and spring water characterization.[131]

A frequently, quantitative method for EEM interpretation is given by Chen et al.[133], defining five specific regions representing simple aromatics (regions I and II), fulvic acid-like components (III), soluble microbial byproducts or SMPs (IV), and humic acid-like components (V). This method has already been successfully applied to detect and follow-up these components in WRRFs.[136] An overview of located regions in EEMs is given in Figure 1.7. Oxidative treatment as ozonation will decrease the intensity of these peaks according to their reactivity towards ozone and HO• although also the formation of new moieties has been detected. Newly formed peaks are mostly related to groups containing electron drawing aromatic moieties.[129,132]

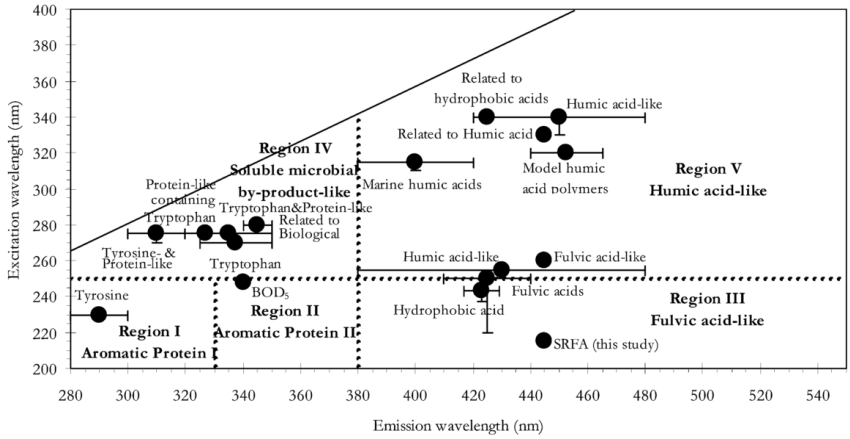

Figure 1.7: Location of EEM peaks based on literature reports and defined excitation and emission wavelength boundaries for five regions gathered by Chen et al.[133]

Linear correlations were constructed for a wide range of TrOCs as depicted in Table 1.7, similar to eq. 1.1. Figure 1.8 displays four selected TrOCs with differing $k_{O3,TrOC}$ and $k_{HO^{\bullet},TrOC}$ for which multiple authors constructed a linear correlation. Agreement of correlations between different authors clearly depends on the TrOC investigated, in large similarity to previous observations with ΔUVA_{254}. Good agreement with practically identical correlations is seen for e.g. meprobamate while already some clear differences are noticed for others (e.g. carbamazepine, primidone, TCEP). Although the use of fluorescence is generally promoted to be more sensitive compared to UV-VIS derived parameters (Gerrity et al.[64] was not able to establish correlations for ΔUVA_{254} and TrOCs with $k_{O3,TrOC} > 10^5$ M^{-1} s^{-1}), no clear advantage in terms of reproducibility is noticed at first sight comparing the correlations from Figure 1.4 and Figure 1.8.

For now, TF is being put forward but its determination depends strongly on the boundaries (range of excitation and emission wavelengths) of the measured 3D EEM. Commercial availability of online sensors is also more limited compared to UV-VIS although some sensors are available with specific wavelengths.[64] Regional integration of the EEMs is therefore needed to use this surrogate in practice and was shown to be correlated with ΔTrOCs in a similar (S-shaped) approach as Nanaboina & Korshin[100] previously reported for ΔUVA_{254}.[137] The further usage of fluorescence as a surrogate should therefore be investigated and a fixed methodology should be determined to establish generically applicable correlations.

Table 1.7: Compilation of single linear correlations available in literature describing the relation between ΔTF and ΔTrOCs. The slope (a), intercept (b) and the coefficient of determination (R^2) are given if mentioned in the respective literature sources. The unavailability of data is marked by "-".

	$k_{O3,TrOC,pH=7}$ (M^{-1} s^{-1})	$k_{HO•,TrOC}$ (10^9 M^{-1} s^{-1})	Ref.	Gerrity et al.[64] (n = 26 - 104)			Pisarenko et al.[82] (n = 3 - 5)		
				a	b	R^2	a	b	R^2
1,4-Dioxane	<1	3	[64]	1.29	-57	0.70	-	-	-
Atenolol	2×10^3	8	[64]	1.55	-33	0.83	-	-	-
Atrazine	6	3	[64]	1.46	-61	0.80	-	-	-
Bisphenol A	7×10^5	10	[64]	1.33	22	0.56	-	-	-
Carbamazepine	3×10^5	9	[64]	1.72	-3	0.53	1.93	18.6	0.974
DEET	<10	5	[64]	1.07	-24	0.76	-	-	-
Diclofenac	1×10^6	8	[64]	1.48	12	0.56	-	-	-
Gemfibrozil	5×10^4	10	[64]	1.32	0	0.77	-	-	-
Ibuprofen	10	7	[64]	1.15	-20	0.77	-	-	-
Meprobamate	<1	4	[64]	1.53	-59	0.82	1.22	-36.8	0.91
Naproxen	2×10^5	10	[64]	1.74	-4	0.55	-	-	-
pCBA	<0.1	5	[64]	0.86	-15	0.54	-	-	-
Phenytoin	<10	6	[64]	1.16	-22	0.66	1.54	-41.5	0.965
Primidone	1	7	[64]	1.05	-22	0.74	1.82	-70.6	0.971
Sulfamethoxazole	3×10^6	6	[64]	1.66	-6	0.54	1.5	23.7	0.97
TCEP	<1	0.6	[64]	0.44	-19	0.56	0.37	-9	0.904
Triclosan	4×10^7	10	[64]	1.00	-41	0.57	-	-	-
Trimethoprim	3×10^5	7	[64]	1.60	4	0.50	1.39	43.4	0.992

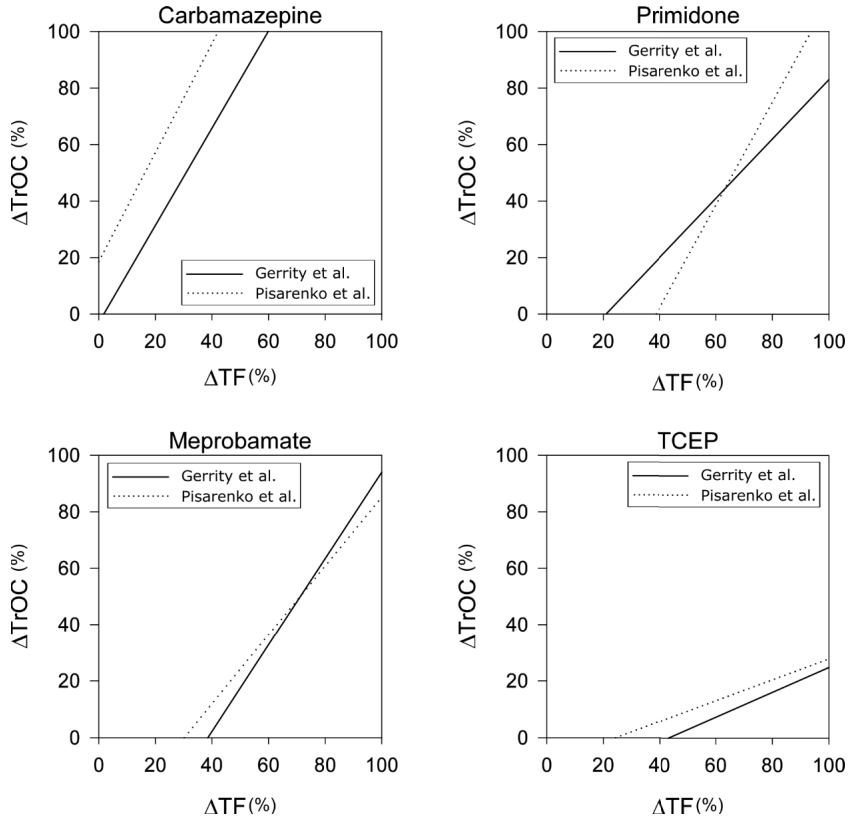

Figure 1.8: Comparison of single linear correlations between four different TrOCs (ΔTrOC) and the decrease of TF (ΔTF) during ozonation. Single correlations are obtained from literature and are given in

4 Control strategies

For the successful application of an ozone system in a WRRF, four crucial elements have to be considered which will in turn also determine the cost and treatment efficiency:[41] (i) the ozone demand of the secondary effluent (often determined on lab- (or pilot-)scale) which determines the required range of ozone dose , (ii) the required ozone capacity, obtained by multiplying the ozone dose by the effluent flow rate, (iii) the different elements of an ozone unit (e.g. air or liquid oxygen (LOX) supply, ozone generator, reaction chamber, cooling and off-gas handling) , and (iv) the control of the process, preferably by online measurements. In this dissertation, (i) and (iv) are of importance in which especially the ozone demand of the secondary effluent will be influenced by varying conditions (e.g. in water quality), and in its turn will have an effect on the applied control strategy.

Several readily available (and basic) measurements are in place to allow a stable process control such as the water flow rate, ozone concentration in both feed and off gas, gas flow rate and ozone concentration in the effluent after ozonation and can be used to determine the transferred ozone dose (TOD).[41] Different indicators (e.g. dissolved O_3, the R_{ct} concept (i.e. assuming a certain ratio of the HO• exposure over the O_3 exposure)) for the control of the ozone dose based on those measurements can however not be applied due to the high ozone demand. Alternative measurement strategies exist and were described in section 3.2.

In the following sections, an overview is given of current ozone applications of which the different applied or investigated control strategies are further discussed, identifying their basic working principle and comparing their (dis)advantages.

4.1 Current full-scale ozone applications and practice

As mentioned in the introduction of this literature review (section 1), the number of WRRFs applying ozonation as a tertiary treatment technology is increasing. It was estimated by a survey in 2004 that only nine ozone installations were present in the European, African, Asian and Australasian region at municipal WRRFs used for final discharge or (small scale) water reuse.[51] In agreement, also only nine installations were operational in the USA in 2010.[49] During subsequent years, applications have significantly grown and more are expected to be constructed in the

coming years and decades, mainly driven by the need for TrOC abatement. Current full-scale applications including their applied ozone dose control strategy are listed in Table 1.8. For some older installations, any information on the use of a specific control strategy is lacking in available literature. It can therefore be assumed that these are operating at a fixed ozone dosing (mg O_3 L^{-1}) determined on prior (expert) knowledge and potentially adjusted with some (frequently) taken offline measurements. The older plants are mainly situated in the USA or Japan and are aiming towards disinfection, color removal and/or resolving taste and odor (T&O) problems in general. Applications are noticed for both final discharge and water reuse purposes, although in a lower extent (see Table 1.8). Ozone dosing is mainly based on expert knowledge and might be manually adjusted using an offline measurement to comply with imposed disinfection criteria.[138]

The amount of applications with respect to final discharge is growing (mainly for TrOC abatement) and more investigation is directed towards a more (cost) effective control of the ozone dosage. For example some recent plants in Germany, France and Switzerland are using (or investigating) alternative dosing strategies based on online measureable surrogate parameters in line with those presented in section 3.2. Plants are already in place and fully operational in Switzerland (Dübendorf and Oberwynental) and Germany (Bad Sassendorf, Schwerte and Duisburg-Vierlinden). In addition, 14 full-scale installations (11 in Switserland and 3 in Germany) are currently under construction or planned in order to reduce TrOC discharge.[139] Especially Switzerland is taking the lead as large investments and (pilot) projects are in progress to decide on the best applicable technology for each WRRF that needs to be upgraded under the Water Protection Act (see also section 2.2).[76] Remarkable is the continuous application of a post biological treatment step (mainly (biological) sand filtration), as depicted by Table 1.8, in order to counter the potential mitigation of (toxic) by-products of the ozonation process.

With respect to the abatement of TrOCs for final discharge of WRRF effluents, projects are expected to increase even more, also in other countries. France has already two plants (Sophia Antipols and St. Pourçain-sur-Sioule) and Sweden has constructed its first full-scale installation (Linköping). Also in North-America, applications will increase with already planned installations in Monterey, California (USA) and the (until now) largest plant in Montreal, Québec (Canada) treating effluent at a capacity of 4 150 000 m^3 day^{-1} in 2020.

Table 1.8: Overview of current (and under construction) full-scale applications and ozone dose control for advanced wastewater treatment. Adapted and completed from Audenaert et al.[22,48] (table displayed on three consecutive pages)

WRRF and/or location[a]	**Year (of installation)**	**Application**	**Target**	**Capacity (m^3 day^{-1})**	**Ozone dose (mg O_3 L^{-1})**	**Control strategy**
St. Pourçain-sur-Sioule, France[140]	n.a.	Final discharge (incl. post SF)	TrOC abatement	2 160	6-12	Main: Flow Optional: - UVA254 load - ΔUVA_{254} (%) - residual O_3 in gas
Kisshoin Treatment Plant, Kyoto, Japan[141]	n.a.	Final discharge	Color removal COD reduction Disinfection	120 000	max. 20	n.a.
Ariake AWTP, Tokyo, Japan[142]	n.a.	Final discharge (incl. chlorination & microfiltration) Water reuse (lavatory flushing and irrigation)	T&O[d] Disinfection	n.a.	n.a.	n.a.
Tamagawa Joryu Plant, Tokyo, Japan[141]	n.a.	Final discharge (incl. post AC)	Disinfection T&O[d]	43 000	5-10	n.a.
Wastewater reclamation plant, Beijing, China[143]	n.a.	Final discharge	n.a.	800 000	5	n.a.
Mahoning County, Ohio, USA[49,138]	1995	Final discharge	Disinfection	36 400	n.a.	n.a.
South Caboolture AWTP, Queensland, Australia[10,144]	1999	Water reuse (non-potable), 3-steps	Disinfection TrOC abatement	10 000	9 (2+5+2)	n.a.
Shibaura AWTP, Tokyo, Japan[142]	2004	Final discharge (incl. chlorination & microfiltration) Water reuse (lavatory flushing and irrigation)	T&O[d] Disinfection	4 300	n.a.	n.a.
Konantyubu, Japan[141]	2005	Final discharge (incl. post BAC)	Organic oxidation	6 500	n.a.	n.a.
F. Wayne Hill WRP, Gwinnett County, Georgia, USA[49,138,145]	2003 (refurbished 2006)	Water reuse (surface water injection for IPR)	Disinfection (two-stage)	275 000	7.4	n.a.

WRRF and/or location[a]	Year (of installation)	Application	Target	Capacity (m^3 day^{-1})	Ozone dose (mg O_3 L^{-1})	Control strategy
Frankfort, Kentucky, USA[49,138]	1980 (refurbished 2007)	Final discharge	Disinfection Color removal	18 200	1.5	n.a.
Fred Hervey WRP El Paso, Texas, USA[49,138]	1985 (refurbished 2008)	Water reuse (irrigation, industrial cooling water, aquifer injection for IPR)	Disinfection	57 000	4.3	n.a.
Bad Sassendorf, Germany[146]	2009	Final discharge (incl. post polishing pond)	TrOC abatement	7 200-15 600	5-15	Flow UVA_{254} load
Belmont, Indiana, USA[49]	2010	Final Discharge	Disinfection	n.a.	6	n.a.
Southport, Indiana, USA[49]	2010	Final Discharge	Disinfection	n.a.	6	n.a.
Schwerte WRRF, Germany[147]	2010	Final discharge (recirculation to nitrification or post PAC)	TrOC abatement (Perfluorinated surfactants)	25 920	2-7	Flow
Southwest Treatment Plant, Springfield, Missouri, USA[49,138]	1978 (refurbished 2011)	Final discharge	Disinfection Color removal	480 000	3.2	n.a.
Duisburg-Vierlinden, Germany[148]	2011	Final discharge (incl. post biological fluidized bed)	TrOC abatement	9 600	n.a.	Flow DOC load[c]
Sophia Antipols, France[147,149]	2012	Final discharge (incl. post biofilter)	Disinfection TrOC abatement	6 800	5 (0.5 g O_3 g^{-1} DOC)	Flow
EC Little Water Recycling Facility, El Segundo, California, USA[138]	2013	n.a.	Pre-membrane oxidation	140 000	16	n.a.
Scottsdale AWT, City of Scottdale, Arizona, USA[138]	2013	n.a.	T&O[d]	140 000	n.a.	n.a.
Bernières-sur-Mer, France[22]	2014	Final discharge	Disinfection	n.a.	n.a.	n.a.
Neugut, Dübendorf Switzerland[150]	2014	Final discharge (incl. post-SF)	80% ΔTrOC (over full treatment train)	6 000-57 000	1.6–2.7 (0.33–0.5 g O_3 g^{-1} DOC)	ΔUVA_{254} (%) (BEAR-strategy[b])
Reinach, Oberwynental, Switzerland[139]	2016	Final discharge (incl. post-SF)	TrOC abatement	n.a.	n.a.	n.a.
La Prairie, Québec, Canada[138]	2016	Final discharge	Disinfection	90 000	4.5	n.a.
Clark County Water Reclamation Districts Las Vegas, Nevada, USA[49,138,151]	2006 (refurbished 2017)	Water reuse (surface water injection for IPR)	Disinfection (two-stage)	275 000	16	n.a.

WRRF and/or location[a]	Year (of installation)	Application	Target	Capacity (m^3 day^{-1})	Ozone dose (mg O_3 L^{-1})	Control strategy
Linköping, Sweden[152,153]	2017	Final discharge Post-denitrification	TrOC abatement	n.a.	n.a.	n.a.
Advanced Water treatment Facility, Monterey RWPCA, California, USA[138]	Planned for 2018	Final discharge	TrOC abatement	32 000	14.9	n.a.
Advanced WRRF Montreal, Québec, Canada[138]	Planned for 2020	Final discharge	Disinfection TrOC abatement	4 150 000	16.4	n.a.

[a] references given as superscript

[b] ARA Neugut developed their own control strategy based on ΔUVA_{254} spectral measurements, which was called the 'BEAR'-strategy (= Best Elimination, Analysis and monitoRing)

[c] an applied ozone dosage relative to the DOC content (g O_3 g^{-1} DOC)

[d] T&O = taste and odor

n.a. = not available

In line with these evolutions, the further increasing need for upgrades to comply with (upcoming) regulations but also some concerns related to (cost) effectiveness induced several studies developing or testing appropriate control strategies. Only four full-scale installations investigated the application of alternative control strategies (i.e. compared to traditional approaches such as a residual O_3 or a flow proportional strategy). In France (St. Pourçain-sur-Sioule), Germany (Bad Sassendorf and Duisburg-Vierlinden) and Switzerland (Dübendorf) spectral measurements were used. Although TrOC abatement was the goal in each of the cases, no details were given in literature or reports of the implemented control strategy and its correlation with TrOC abatement. Most likely, experience and knowledge obtained during pilot-scale testing or initial full-scale testing is used to determine the set-points. The plant in Dübendorf (Switzerland) has however developed its own control strategy based on ΔUVA_{254} spectral measurements ('BEAR'-strategy = Best Elimination, Analysis and monitoRing), aiming at 80% TrOC removal of selected indicator components.[154,155] This strategy will be explained in more detail in section 4.4.

Further discussion of these control concepts tested or applied at full-scale (Table 1.8) and pilot-scale (Table 1.9) installations is elaborated in the following sections (4.2 to 4.4). Summarized, three main control concepts are noticeable: (i) flow proportional, (ii) load proportional and (iii) differential surrogate control.

4.2 Flow proportional

Flow proportional ozone dosing is probably the most basic ozone dosing strategy, mainly based on operator knowledge and dosing experiments, setting a fixed ozone dose (in mg O_3 L^{-1}) proportional to the flow rate of the incoming effluent. Dilution due to varying weather conditions, sudden changes in concentrations of (in)organic constituents due to malfunctions, etc. might, however, influence the variability of the secondary effluent. Several examples demonstrate that variable effluent composition and reactivity need to be accounted for. The studies performed by Nanaboina & Korshin[100] and Audenaert et al.[113] showed different behavior of the differential absorbance spectra under ozonation showing varying reactivity of the EfOM. Additionally, the presence of other scavengers influences ongoing reactions. In the case of Lee et al.,[98] bicarbonate was responsible for ± 20% of the total HO• consumption. Also the reactivity towards EfOM was hypothesized to be variable by a factor of 3 to 5.[156] As one of the results, poor correlations with the ozone dose and abatement of TrOCs (e.g. pCBA) has been experienced unless corrections for the presence of specific constituents were made (e.g. NO_2^--N and NH_4^+-N (ammonium)).[115]

Table 1.9: Pilot-scale applications and ozone dose control for advanced wastewater treatment (table displayed on two consecutive pages)

WRRF and/or location[a]	**Years (of operation)**	**Application**	**Target**	**Capacity (m^3 day^{-1})**	**Ozone dose (mg O_3 L^{-1})**	**Control strategy**
Tucson, Arizona, USA[64]	n.a.	Final discharge	TrOC abatement	57.6	0-9 (0-1.5 g O_3 g^{-1} DOC)	Flow Monitoring of O_3:DOC and ΔUVA_{254} (%)
Reno, Nevada, USA[64,120]	n.a.	Final discharge (incl. post BAC)	Disinfection TrOC abatement	57.6	5 (0.5 g O_3 g^{-1} DOC) incl. 1.0 molar H_2O_2:O_3	Flow Monitoring of O_3:DOC and ΔUVA_{254} (%)
City of Las Vegas, Nevada, USA[64,82]	n.a.	Final discharge	Disinfection TrOC abatement	57.6	0-10 (0-2.0 g O_3 g^{-1} DOC)	Flow Monitoring of O_3:DOC and ΔUVA_{254} (%)
Eawag WRRF, Switzerland[114]	n.a.	Final discharge	TrOC abatement	0.72	0.1-0.9 g O_3 g^{-1} DOC	DOC load[c] Monitoring of ΔUVA_{254} (%)
Vienna, Austria[157]	n.a.	Final discharge	TrOC abatement	792-864	0.6-1.5 g O_3 g^{-1} DOC	1st DOC load 2nd residual O_3 liquid (0.1 mg L^{-1})
Berlin, Germany[158]	n.a.	Final discharge (incl. post coagulation and SF)	TrOC abatement P-removal	108-360	0.2-1.05 g O_3 g^{-1} DOC	ΔUVA_{254} (%)
Paderborn-Sande, Germany[159]	n.a.	Final discharge (incl. post-SF)	TrOC abatement	n.a.	2-10	Flow
Vienna, Austria[135]	n.a. (finished)	Final discharge (incl. post biofiltration)	TrOC abatement	n.a.	0.7 g O_3 g^{-1} DOC (standard operation)	Main: DOC load Others tested (ΔUVA_{254}, Fluorescence)
Little Rive Pollution Control Plant (LRPCP), Windsor, Ontario, Canada[109]	n.a.	Final discharge	TrOC abatement	5.76	2.8-4.4 (0.46-0.72 g O_3 g^{-1} DOC)	Flow
Berlin-Ruhleben, Germany[63]	2004-2005	Final discharge	disinfection TrOC abatement	48	2-14	Flow Monitoring of O3:DOC and ΔUVA_{254} (%)

WRRF and/or location[a]	Years (of operation)	Application	Target	Capacity (m^3 day^{-1})	Ozone dose (mg O_3 L^{-1})	Control strategy
Wüeri, Regensdorf, Switzerland[33,160]	2007-2008 (full current testing)	Final discharge (incl. post-SF)	TrOC abatement	10 500 (max. rain flow 21,600)	2-10[160] 1.6-5.3[33]	Flow DOC load (0.36-1.16 g O_3 g^{-1} DOC)
Vidy, Lausanne, Switzerland[32,161]	2009-2010	Final discharge (incl. post-SF)	TrOC abatement	8 640	n.a.	DOC load (0.6-1.0 g O_3 g^{-1} DOC) 0.1 mg L^{-1} Residual O_3
Gelsenkirchen, Germany[147]	2008-2012	Final discharge (incl. post SF)	TrOC abatement	150	5-10	Flow
Gothenburg, Sweden[d,162]	2014	Final discharge	TrOC abatement	n.a.	3-10	Main: Flow DOC load
Rosenbergsau, Switzerland[108]	2015 (March-June)	Final discharge	TrOC abatement	15.6-31.2	2.0-5.6	DOC load ΔUVA_{254} (%)
Dinslaken, Germany[163]	2015 (aug.)-2017	Final discharge (incl. post-SF)	TrOC abatement	190	20	Flow
Aachen Soers, Germany[164]	2017	Final discharge (incl. post-SF)	TrOC abatement Toxicity reduction	n.a.	n.a.	n.a.

[a] references given as superscript

[b] ARA Neugut developed their own control strategy based on ΔUVA_{254} spectral measurements and was called the 'BEAR'-strategy (= Best Elimination, Analysis and monitoRing)

[c] an applied ozone dosage relative to the DOC content (O_3 g^{-1} DOC)

[d] the main experiments were conducted in Gothenburg, Sweden although 9 other plants in Sweden were also included in the study

n.a. = not available

The reactivity of ozone towards the complete effluent matrix has a direct impact on the efficiency of the consumed ozone. An increasing fraction of highly ozone reactive species will result in more direct ozone reactions before indirect reactions can take place, especially influencing poorly ozone reactive TrOCs.[156] Especially the presence of NO_2^--N, and to a lesser extent NH_4^+-N, has a large influence as these exhibit high reactivity towards ozone and HO• (Table 1.10).[115] This dynamic behavior of the effluent water quality has however led to the need of other and better control strategies, considering also the incoming concentration and composition of the organic load (EfOM) or other inorganic constituents (e.g. NO_2^--N, NH_4^+-N, etc.). Different reaction kinetics with ozone and HO• are given in Table 1.10 for the most probable inorganic compounds.

Table 1.10: Oxidation kinetics of the most probable inorganic compounds with ozone and HO radicals at ambient temperature, based on Von Gunten[165]

Compound	k_{O3} **(M^{-1} s^{-1})**	$k_{HO•}$ **(M^{-1} s^{-1})**
Nitrite (NO_2^-)	3.7×10^5	6×10^9
Ammonia/-ium (NH_3/NH_4^+)	20/0	9.7×10^7 [a]
Bromide (Br^-)	160	1.1×10^9
Sulfide (H_2S/S^{2-})	$3\times10^4/3\times10^9$	$1.5\times10^{10}/9\times10^9$
Manganese (Mn(II))	1.5×10^3	2.6×10^7
Iron (Fe(II))	8.2×10^5	3.5×10^8
Carbonates (CO_3^{2-}/HCO_3^-)	n.a.	10^6-10^8

[a] rate constant for NH_3, n.a. = not available

4.3 Load proportional

A load proportional ozone dosing strategy is based on an (online) measurement (representative for the load or its concentration e.g. DOC, UVA_{254}, etc. in the water) and its ratio with the amount of ozone dosed. Related to this measurement, more information is given in section 3.2 (and its subsections). As can be derived from Table 1.8 and Table 1.9, this strategy is certainly gaining more interest for pilot- and full-scale installations. This strategy has for example been applied at the WRRF in Bad Sassendorf, controlled based on the set-point of the specific ozone

dose with DOC (O_3:DOC ratio) measured before ozonation. Online UVA_{254} measurements and their correlation with DOC were used to approximate the DOC.[144]

UVA_{254} is historically the first proxy of the total/dissolved organic carbon content.[166,167] More recently, other strong correlations were derived between multiple wavelengths (e.g. 254 and 350 nm).[168] Carter et al.[169] calibrated a two component model (270 and 350 nm) with one component representing aromatic chromophores and the other representing (weakly) hydrophilic substances, as single wavelength approaches showed some limitations.[170] Indeed, single wavelength determination of DOC has already been associated with lack of robustness. Although single wavelength approaches are operating adequately within one plant, location or type of wastewater, a two wavelength approach is beneficial for more variable applications.[169] Even better results are obtained with multiple wavelength approaches, even in less complex matrices such as drinking water.[157,171] As mentioned in section 3.2.3, also fluorescence measurements were successfully applied to estimate the DOC content in the KOMOZAK-project with more accurate predictions compared to UV derived DOC estimations.[135]

The O_3:DOC ratio has been correlated with the abatement of several TrOCs but several issues are however still in place, hampering an efficient process control. Varying observations are noticed as e.g. El-taliawy et al.[162] had a good working O_3:DOC strategy for an effluent flow up to three times the dry weather flow. Varying weather behavior can however lead to a variable effluent matrix composition and reactivity. Schaar et al.[157] noticed a residual ozone concentration at intermediate ozone doses (i.e. 0.7 g O_3 g^{-1} DOC) when rain events occurred. Nevertheless, it has been shown that this drawback can be countered (partially) by implementing some safety factors (e.g. dissolved ozone measurement) that become active during rain events.[144] Lee et al.[98] on the other hand noticed clear influences on the correlations due to an increase of the NO_2^--N concentration. This increase of IOD (instantaneous ozone demand) affected the lag in HO• production and therefore hampered the removal of low ozone reactive TrOCs. Several reports[45,98,172] investigated the relation of water quality and kinetics in terms of removal efficiency based on the ozone and HO• exposure and the affinity of TrOCs towards those oxidants. Comparing these different studies, some deviations in EfOM reactivity and TrOC abatement were noticed, indicating the presence of other factors affecting the removal efficiency that are likely more pronounced during full-scale operation.[162] It is noteworthy that most studies mentioned were performed under a controlled environment at lab-scale.

4.4 Differential control

Differential control of the ozone dose is based on the differential ratio of measurements performed before and after ozonation. The set-point of such control is based on a (percentage) decrease of a parameter, measured before and after treatment. Especially UVA_{254} and fluorescence measurements are indicated as very promising, as discussed in sections 3.2.2 and 3.2.3. Currently, spectral sensors are commercially available to measure the UV-VIS spectrum or UVA_{254} specifically online and are mainly making use of mercury or xenon lamps as a light source. Recent advancements are however capable to reduce costs and size of these commercial sensors by making use of UV light-emitting diodes (LED) and photodiode (PD) technology.[122,173–175] In order to avoid nitrate (NO_3^--N) interference at lower wavelengths, the use of an online LED sensor at 280 nm (reflecting similar DOM species as 254 nm) was successful in controlling TrOC abatement during ozonation applying similar correlation models as exhibited in section 3.2.2.[122] As mentioned, little studies apply online fluorescence as it is relatively expensive and a lot of data processing is needed. Nevertheless, studies are being conducted that develop online LED based fluorescence sensors, although some offline calibration is still required.[122] Currently, few pilot- and full-scale applications used ΔUVA_{254} (see Table 1.8 and Table 1.9) but significant research is done to also put the use of fluorescence measurements in practice.

As an example, the plant in Dübendorf, Switzerland has developed its own control strategy based on ΔUVA_{254} spectral measurements, resulting in a more or less constant TrOC removal of 80-84% (of a set of selected indicator components).[150,154] The difference between the measured ΔUVA_{254} and the set-point are the main input to a calculating algorithm determining the needed ozone dose (mg L^{-1}). This in contrast to previous mentioned approaches (see section 3.2.2) making a direct correlation between ΔUVA_{254} and ΔTrOCs. Although limited information is shared related to this algorithm (e.g. no relation is specified between ΔUVA_{254} and the ozone dose), it can be stated that, accounting for the effluent flow rate, the generation of ozone is adjusted. This BEAR (Best Elimination, Analysis and monitoRing) measurement principle is given in Figure 1.9.

In association, also Stapf et al.[158] recently demonstrated ΔUVA_{254} successfully on pilot-scale, in order to evaluate its behavior under real life conditions. During a NO_2^--N spike, the control strategy rapidly detected the decreased ΔUVA_{254} and the ozone dosage was increased in accordance. The ΔUVA_{254} strategy was clearly able to control the ozone dose as it (i) detected changes in ozone demand (e.g. the NO_2^--N spike), (ii) estimated the TrOC abatement and, (iii)

acted as a safeguard of a properly working ozonation unit. During operation, no dissolved ozone could be measured in the effluent after ozonation.[158] Ozone is known to absorb in the region near 254 nm and might thus have adverse effects on the measured UVA_{254} signal. Normally, complete reaction can be expected but the chance still remains under certain circumstances (e.g. anomalies, highly ozone recalcitrant organics). Potential safeguards such as a dissolved ozone or redox sensor (i.e. ORP, under exploited although requiring less maintenance and calibration), or using a fixed bed catalyst in the sampling stream (e.g. anthracite, activated carbon or manganese dioxide) to remove any residual ozone can be implemented to protect the control strategy.[176]

Implementing an additional measurement after ozonation induces an additional delay of the measurement due the hydraulic residence time (HRT) of the ozone unit. HRT of typical full-scale units go up to 10-15 minutes. Nevertheless, the effect for secondary effluent ozonation can be seen minimal as previous research noticed almost steady-state behavior of UVA_{254} or DOC during the day.[63] Also in current pilot-scale studies, little problems were noticed.[158]

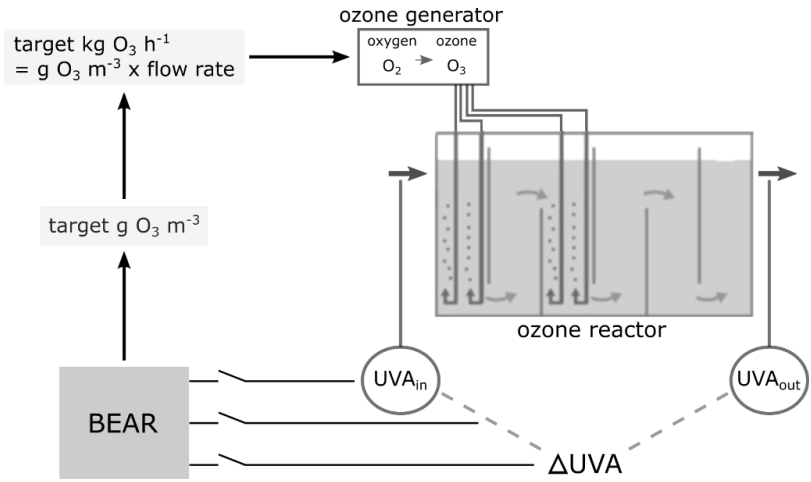

Figure 1.9: Principle of the BEAR-strategy for the control of the ozone dosage at the WRRF of Dübendorf, Switzerland. Adapted and translated from Schachtler and Hubaux[150]

5 Discussion and further needs

Several legislative and scientific factors (e.g. the need to enhance ecolife quality in surface water or to reduce the presence of TrOCs in water reuse schemes) are stressing the need for a more intensive treatment of discharged wastewater. Ozonation has shown to be a promising technology to degrade TrOCs in an efficient way. Nevertheless, the increased interest of ozonation for treating a water matrix with the presence of high concentrations of organic matter (EfOM) or other (e.g. nitrogen) constituents has shown that conventional control tools are hampered by serious drawbacks. New approaches and online measureable parameters are needed to allow for an online control, limiting the need for expensive and time consuming determination of TrOC concentrations. Especially the differential UVA_{254} during ozonation seems to offer a powerful, robust and straightforward tool that can easily be incorporated in full-scale installations.[64] Also UV derived parameters such as DOC or fluorescence measurement showed great potential. UV-visible or fluorescence based surrogate parameters are of main interest and have been correlated with the abatement of TrOCs. More recently, also other surrogates have appeared such as the electron donating capacity (EDC)[53] or NO_3^--N formation[177] but these still need further investigation to use them in an online control framework.

Although different (single) correlation models are available for a selection of indicator compounds with different reactivity, some drawbacks still exist. Some differences exist between indicator compounds mentioned in different regulatory frameworks (Table 1.3) and those for which correlations have been developed (Table 1.6 and Table 1.7). Additionally, current regression models are not representative for physical and chemical phenomena. Therefore, the need exists for a generically applicable, easily and widely adaptable control framework. Nanaboina and Korshin[100] and Liu et al.[137] have for example already developed semi-empirical models between the decrease of surrogates (UVA_{254} or fluorescence) and ΔTrOCs although these models still contain TrOC specific parameters or parameters depending on the effluent water quality characteristics that need to be experimentally determined. EfOM has been addressed as one of the main influencers of the ozonation process.[110] Besides consuming a significant fraction of the ozone, the organic matrix also indirectly gives rise to HO• production.[111,112] Especially low ozone reactive TrOCs are affected as it seems that the HO• generation (and hence the TrOC abatement) result in a curved relationship with ΔUVA_{254} (or ΔTF), not described by single regression models. The use of fluorescence is still in its infancy but its higher maximum percentage reduction due to ozonation than UVA_{254}, known to have a high amount of inert

absorbance, might have potential for a greater control range.[54] First results are pointing towards a higher consistency and increased sensitivity.[82,101]

Online sensors for UVA_{254}, DOC or fluorescence are available, although reliable fluorescence devices are still less commercialized. LED based sensors are gaining interest although sometimes, some frequent offline calibration is needed with standardized solutions.[122] Currently, TF (total fluorescence) is mainly investigated but might be too general and different oxidant induced changes might be missed. Future developments should ascertain if the presence of different classes of fluorescent compounds has a big advantage over absorbance spectra.[101] Although correlation models for the control of TrOC abatement still need some refinement, some pilot- (and full-)scale testing has been done comparing different control strategies. The main strategies can be seen as (i) flow proportional, (ii) load proportional or (iii) differential based control strategies. The (dis)advantages of these three strategies are laid out in Table 1.11 and are graphically represented in Figure 1.10. The use of online sensors during long-term operation however has its implications and current pilot-scale experiments already revealed some practical issues. These spectral sensors are requiring regular maintenance and are influenced by scaling or biological fouling of the analyzer.[64] It is therefore of high importance to assess the practical implications and define their impact on the operation of the ozonation process.

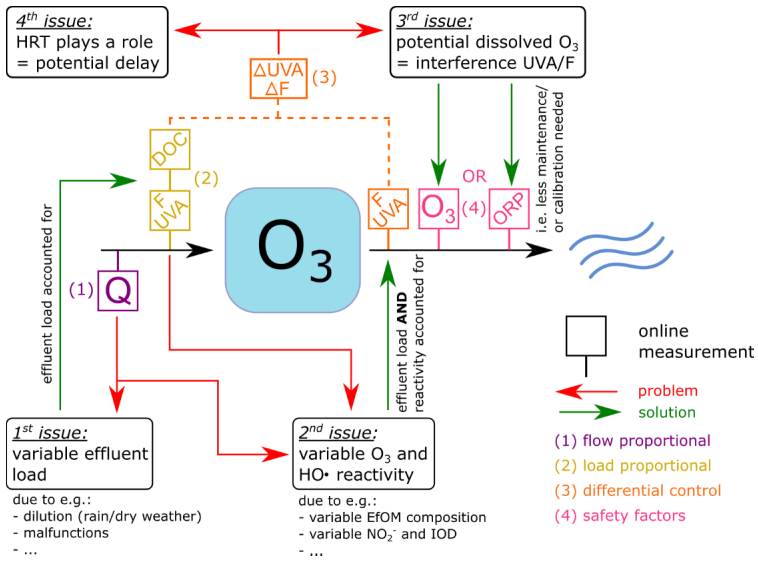

Figure 1.10: Summary of ozone dose control strategies with different complexity, associated issues and their online measurements.

Table 1.11: Pros and cons of the different control strategies based on the literature review

	Advantages	Disadvantages
Flow proportional	- Easily implementable using existing infrastructure - Flow measurement well established - No sensor (re)calibration needed	- Not accounting for variable effluent load (concentration) - Not accounting for variable effluent reactivity (EfOM properties and e.g. NO_2^-) - High chance for ineffective O_3 dosing and TrOC abatement - No prediction of TrOC abatement
Load proportional	- Online measurements commercially available - Accounting for variable effluent load - Prediction of TrOC abatement - No delay, direct control action possible	- Not accounting for effluent reactivity (EfOM properties and e.g. NO_2^-) - ΔTrOC prediction not generically applicable
Differential	- Online measurements commercially available - Accounting for variable effluent load - Accounting for variable effluent reactivity (EfOM properties and e.g. NO_2^-) - Prediction of TrOC abatement - ΔTrOC prediction generically applicable if appropriate correlation models are used - Accurate TrOC abatement and O_3 dosing - Safety assurance after ozonation (i.e. feedback of occurring effluent changes)	- Two sensors needed, or switching mechanism if usage of one sensor - Influence of residual ozone - Potential effect of delay due to HRT

Based on previous discussion, the main conclusions and further needs can be summarized as follows:

(i) Conventional control strategies, wether adopted or not from drinking water applications, are hampered by serious drawbacks;

(ii) Surrogate correlation models based on DOC or (differential) UVA_{254} or fluorescence surrogates show great potential as it is easily correlated with ΔTrOCs, although fluorescence contains multi-dimensional data that can be further explored;

(iii) Correlation models are defined, although needing some refinement as current (single) correlation models are not representing physical and chemical phenomena;

(iv) Practical implications are insufficiently addressed applying different control strategies (i.e. flow proportional, load proportional or differential control) during current studies

(v) Limited studies address the effect of effluent variability on the online control of the ozone dose, especially on pilot- or full-scale installations, and more investigation to assess real effluent dynamics in terms of reactivity towards ozone is needed.

Increasing this current knowledge is however essential to make online control widely applicable for different treatment sites. Moreover, real applications will depend on the economic viability. Some economic assessment studies and cost calculations have been conducted (in which energy price played the most important role)[178,179] but **to date, and to the best of the author's knowledge, no studies have been performed accounting for the cost implications (and potential savings or additional expenses) applying different control strategies.**

Chapter 2

Objectives and outline

1 General aim and specific objectives

Ozonation as a barrier for TrOCs entering the aquatic environment through WRRFs has definitely proven its capabilities. Currently applied ozone dosing control strategies, i.e. mostly flow, and in some cases load-proportional, mostly result in sub-optimal operation. Optimal ozone dosing, accounting for plant dynamics, is of high importance to

(i) lower operational costs;
(ii) guarantee consistent TrOC abatement;
(iii) minimize by-product formation.

with (i) and (iii) currently being the major factors slowing down full-scale application of the ozonation technology, the relevance of this PhD research becomes clear. Offline monitoring is time, cost and labor intensive as discussed in Chapter 1. In literature, surrogate-based models have been proposed which correlate the abatement of TrOCs with the decrease of surrogates such as UVA_{254} or fluorescence (see Chapter 1 section 3.2). Although these models were applied on different investigation scales (lab-, pilot- and full-scale), multiple limitations still exist:

(i) How TrOC specific properties (e.g. $k_{O3,TrOC}$) are influencing the shape (linearity) of these correlations is one of the major issues, as they are not representing chemical phenomena taking place. The production of HO• will clearly have a greater influence on the removal of TrOCs with a lower affinity for direct ozone reactions. Modelling strategies applying more kinetic based approaches already noticed significant deviations between measured and predicted removal for the more recalcitrant TrOCs;[45]
(ii) Extensive validation in real-life situations is lacking;
(iii) The impact of such control strategies on operational costs and other operational aspects were not studied;
(iv) Additionally, much information is present, but often (parts of) fluorescence spectra (socalled Excitation Emission Matrices or EEMs) are used as such, without any statistical processing or without any relation to underlying groups of chemical compound.

To ensure the successful application of such surrogate correlation models, (i) the models should be made generic applicable by adding mechanistic knowledge, (ii) extensive validation in real-life situations should be performed, (iii) together with assessment of practical aspects (e.g. sensor matintenance) and (iv) economics (e.g. savings related to better ozone dosing). Correlation models are after all mostly constructed in a controlled (laboratory) environment which also does not account for technical issues such as drift and fouling of sensors and the associated need for technical interventions (e.g. cleaning the sensors). Large amounts of technical interventions can make the process more expensive and less reliable. Pilot- and full-scale studies examining online surrogate correlation models are still rather scarce and more knowledge is needed to run these control approaches over longer time. Furthermore, secondary effluents contain numerous constituents which presence or concentration might vary in time under influence of weather conditions, diurnal patterns, operational implications, etc. More insights in these dynamics are therefore of great importance and the influence of weather conditions is largely unknown.

The main goal of a control strategy or model is to ensure TrOC abatement targets are efficiently reached at the lowest cost, with the lowest risk for the formation of potentially toxic by-products, and reliably applicable during long term operation under real-life conditions at different plants. Therefore the main objective of this dissertation can be outlined as follows:

To develop, calibrate and validate a surrogate-based correlation model under variable effluent conditions in order to establish a generically applicable and reliable control framework.

Followed by more specific aims necessary to reach the main goal:

(i) to obtain a better understanding of the relation between surrogate measurements (UV-VIS and fluorescence) and TrOC abatement by ozonation;

(ii) to gain insights and increase knowledge related to the effluent dynamics in terms of load (i.e. concentration) and composition (i.e. reactivity);

(iii) to demonstrate the applicability of the developed model and to assess potential practical implications using online spectral sensors on pilot-scale;

(iv) to evaluate potential economic implications in terms of operational cost savings in comparison with other available control strategies;

(v) to provide a list of considerations and guidelines to consider for final full-scale implementation of an online control strategy, and highlight existing knowledge gaps for future investigation.

2 Outline

A schematic overview of the outline of this dissertation is given in Figure 2.1, showing the different research chapters and their relation towards each other (indicated by arrows). As described, the aim of this work was to develop a surrogate-based correlation model and to scale this up towards a practical application. Consequently, the conducted research is basically performed both at lab and on pilot-scale, indicated in respectively green and blue in Figure 2.1.

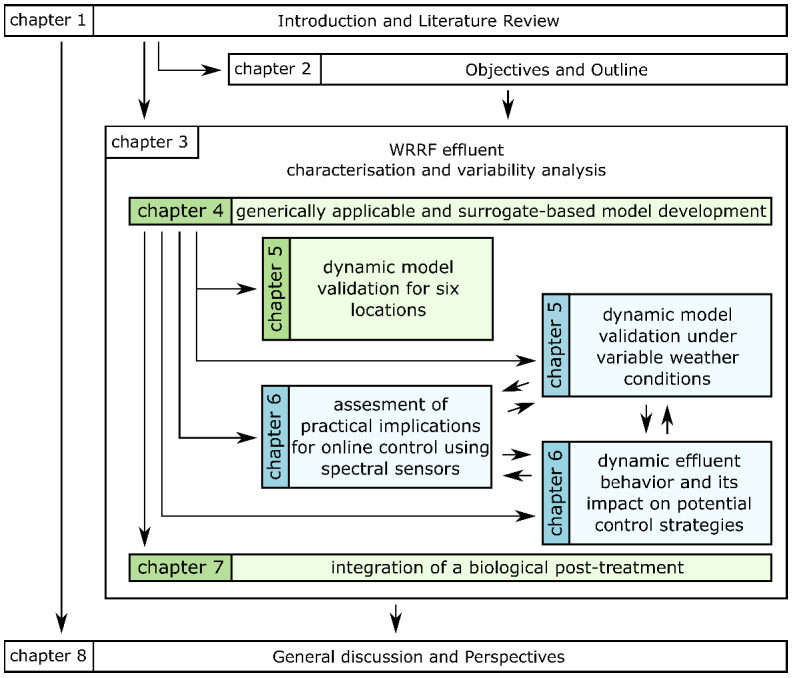

Figure 2.1: Schematic outline of this dissertation. Work performed at lab- and pilot-scale is respectively indicated in green and blue.

Chapter 1 contains a literature review and already stated the current status of and needs for online control of tertiary ozonation. After introducing the topic and its context of this dissertation, the status and role of legislation were discussed. Furthermore, possible indicator approaches and surrogates (correlation models) were listed and described. Finally, the current status of full-scale installations applying tertiary ozonation and some pilot-scale installations applying different control strategies were given and discussed. An outline of the further needs concludes the chapter. **Chapter 2** builds on this and states the aims and general objective, and contains a summarized outline of this work.

Chapter 3 summarizes effluent characterization performed at 15 different sampling locations. This information was used to have an idea of the effluent water quality variability in Belgium. Next to a list of standard water quality parameters, TrOCs and spectral measurements were considered. Principle Component Analysis (PCA) was used to reduce the available information and define the characteristic parameters to consider during model development.

Chapter 4 presents the research aiming at a better understanding of the relation between surrogate measurements (UV-VIS and fluorescence) and TrOC abatement by ozonation. Starting from lab-scale experiments, improved correlation models were developed taking into account the role of different oxidative species, i.e. O_3 and HO•. Generically applicable models were constructed for a broad range of TrOCs, i.e. independently of those used during calibration of the model in the current work. Furthermore, the possibilities of PARAFAC (PARAllel FACtor analysis) to help elucidate the kinetics of derived fluorescence signals was investigated.

Chapter 5 provides validation of the correlation models developed in **Chapter 4**, to prove that a robust and reliable control framework was developed. Validation was done for different types of municipal wastewater on lab-sale. Own results were compared to literature. Moreover, the validation was extended with a data set, obtained from pilot-scale experiments.

Chapter 6 discusses a pilot-scale application of the developed correlation models in which two different spectral sensors were compared - including required maintenance and control – in a single sensor system. Furthermore, the effluent variability in terms of concentration and composition was addressed comparing three possible control strategies in terms of operational costs and efficiency of TrOC abatement. The findings from pilot-scale experimentation were extrapolated to account for a full-scale WRRF and therefore, presents a complete picture of the operational expenses and potential savings.

Chapter 7 describes different post-ozonation treatment technologies, based on filtration and biological processes, and their efficiency for TrOC abatement and to limit (or reduce) toxicity. This chapter concludes with the assessment of the developed UVA_{254} based correlation model when such post-treatment is included in this framework.

Chapter 8 finally concludes this dissertation with an overall discussion of the main findings in previous chapters. Some perspectives are also included to provide a basis for future research.

Chapter 3

Municipal wastewater effluent characterization and variability analysis in view of tertiary ozonation: the situation in Belgium

This chapter has been redrafted from:

Chys, M., Demeestere, K., Nopens, I., Audenaert, W.T.M. & Van Hulle, S.W.H. Municipal wastewater effluent characterization and variability analysis in view of tertiary ozonation: the situation in Belgium, *submitted*.

1 Introduction

The presence of TrOCs in municipal wastewater effluents pose an environmental burden on receiving water bodies as residual pharmaceuticals, personal care products, hormones etc. may trigger unwanted ecological effects.[10,11] Tertiary treatment technologies as an additional step to remove these contaminants before discharge are currently under development. One of these most promising technologies is the application of ozonation prior to discharge.[32] Although ozonation has been successfully tested to remove these TrOCs, the implementation of this technology and its overall efficiency on a broad scale might depend on effluent characteristics, which can differ between different WRRFs. The composition of effluent depends after all on the source of the wastewater and involves both organic and inorganic substances. The effluent organic matter (EfOM) is composed of recalcitrant natural organic matter (NOM) (humic and fulvic acids), synthetic organic (micro)pollutants created during domestic applications, and soluble microbial products like extracellular polymeric substances produced during biological wastewater treatment (also see Figure 1.2).[180] Also micro-organisms can be counted as organic consituents, although these will only be minorly relevant compared to the higher concentrations of previous stated compounds. Similar to organic compounds, inorganic compounds are influenced by the preceding secondary (and biological) treatment step and originate from several chemical compounds, some containing nitrogen and phosphorous. Influents of WRRFs are known to be highly influenced by a diurnal pattern but also by fluctuating weather conditions. Large rain fall events will dilute the wastewater. Although these received wastewaters are intensively treated in conventional WRRFs and buffering occurs (especially in larger plants), the effluent quality will logically depend on the influent and its variations. Therefore, it is important to know the composition of secondary effluent to understand the possible reactions and interactions between organic and inorganic compounds present in the water matrix during ozonation.[62]

A tertiary ozonation process and the occurring reactions themselves will be influenced by the presence of most impurities. The main parameters affecting the stability of ozone are chemical and physical water characteristics such as temperature, pH, EfOM content and composition, alkalinity scavengers like carbonate and bicarbonate, and also the presence of highly ozone reactive inorganic constituents (e.g. NO_2^--N). For example, alkalinity scavengers will compete with other constituents for the available ozone given their high reactivity ($k_{O3} \approx 10^6$-10^8 M^{-1} s^{-1}).[181]

Other parameters such as the water turbidity and ammonia will have similar effects on the oxidation efficiency.

The major sink for oxidants such as ozone is considered to be the presence of EfOM. Ozone is dosed to remove targeted TrOCs but those are only present in minor concentrations (ng L^{-1} to µg L^{-1} levels) compared to the organic matter (mg L^{-1} levels). The EfOM concentration levels are mostly expressed by parameters such as COD or DOC content, but also by general spectral measurements such as the UV absorbance at 254 nm (UVA_{254}) or the total fluorescence response (as discussed in Chapter 1). Nevertheless, not only the amount but also the composition will play a major role.[55] For example, the instantaneous ozone demand (IOD) gives an idea of the amount of highly ozone reactive species. This influences ongoing reactions, as e.g. Buffle et al.[126] could observe high transient HO• concentrations related to a first initial phase with fast ozone reactions. Additionally, also spectral measurements such as specific regions within a fluorescence 3D Excitation-Emission matrix (EEM) have been associated with different types of organic matter, showing distinct behavior and properties.[133,136] Additional to the potential varying effect of (in)organic constituents on the ozonation process, spectral measurements have been put forward as online measurable to control the ozone dose for TrOC removal purposes as discussed in Chapter 1 (Section 3).[63,64,103] Logically as main input parameters, the variability of these characteristics in time and among different WRRFs is of high importance to implement a generically applicable control framework for ozone dose and TrOC removal control.

This chapter aims therefore at investigating the variability of both conventional physical-chemical water quality parameters as also others such as spectral measurements or ozone specific parameters (e.g. IOD) between different WRRF locations and over time (± 1 year). In view of a potential tertiary ozonation step it is important to develop a better understanding of the effluent characteristics that need to be dealt with, to know if relations can be derived between different parameters and if variations between plants or in time can be demonstrated on a statistically founded basis by using principal component analysis. Finally, advice should be provided on the usability of spectral measurements in a generical control framework as well as to identify which effluent characteristics are identified to vary significantly and need to be accounted for during ozone dose control.

2 Materials and Methods

2.1 Experimental set-up and sampling procedure

Secondary effluent was collected from 13 WRRFs located in different regions of Belgium with an I.E. (Inhabitant Equivalent) ranging from 500 to 116 100 (and operated by Aquafin NV or Ipalle). These WRRFs, and their specific effluents, have been selected based on their location, receiving water (i.e. influent), and configuration of the WRRFs installation (i.e. size and type of (biological) wastewater treatment). A detailed and schematic overview of the selected WRRFs is respectively given in Table 3.1 and Figure 3.1, containing details of the treatment train preceding each sampling location. Two WRRFs contained a tertiary treatment, i.e. a constructed wetland (CW) and a sand filtration (SF), and samples were taken also before and after this tertiary treatment, bringing the total of sampling locations at 15. All 15 locations were sampled at least three times during different sampling campaigns over ± 10 months. The WRRFs of Aartselaar and Harelbeke, respectively locations 11 and 15, were sampled more frequently (respectively 3 consequtive months and during a little less than 1.5 years) to also include long time variations.

During one year, a total of 273 samples (both grab and composite) were taken and analyzed for several physical-chemical characteristics (e.g. alkalinity, COD, pH, NO_2^--N, etc.), UV-Visible spectra and fluorescence. Sampling of secondary effluents is less sensitive to the sampling strategy (e.g. compared to WRRF influents) due to the buffering of the complete WRRF treatment.[182] The combined planning of grab and composite samples ensured representative samples retaining the variability of the effluent.[183,184] Samples were stored at 4 °C or analyzed immediately if possible. Samples for TrOC analysis were taken during a period of 2 years for the Harelbeke plant (7 samples) and 2 months for the Aartselaar plant (47 samples).

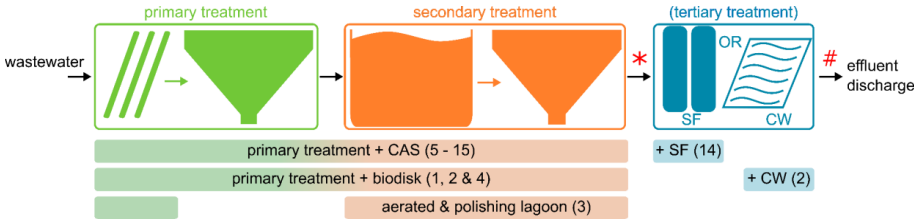

Figure 3.1: Simplified schematic configuration of the WRRFs treatment trains, preceding the sampled locations during this study. The colored bars indicate the applied treatment at the specific sampling locations and the numbers are given between brackets, referring to Table 3.1. Point of sampling is indicated with an asterisks (*) for locations 1, 3-13 and 15, and a number sign (#) for locations 2 and 14.

Table 3.1: Overview of selected WRRFs and the associated sampling locations after secondary (or tertiary) treatment

Nr.	WRRF location	I.E.	Type of receiving wastewater (influent)	(Secondary or tertiary) treatment technology	Size category[a]
1	Kruiseke	500	100% municipal wastewater	Biodisk + settler	Cat. 3
2				Biodisk + settler + constructed wetland	
3	Mont-Saint-Aubert	600	100% municipal wastewater	Aerated and polishing lagoon	
4	Oedeghnien	730	100% municipal wastewater	Biodisk + settler	
5	Heule	14 000	± 100% municipal wastewater[b]	CAS[c]	
6	Péruwelz	14 000	mainly municipal wastewater	CAS[c]	
7	Ath	22 000	mainly municipal wastewater	CAS[c]	
8	Ingelmunster	35 000	municipal and industrial wastewater (from food industry = good biological degradation)	CAS[c]	Cat. 2
9	Comines-Warneton	40 000	mainly municipal wastewater (50% from Belgium, 50% from France)	CAS[c]	
10	Froyennes	50 000	mainly municipal wastewater	CAS[c]	
11	Aartselaar	54 000	municipal and industrial wastewater (from food industry = good biological degradation)	CAS[c]	
12	Menen	66 000	mainly municipal wastewater (70% from Belgium, 30% from France)	CAS[c]	
13	Waregem	80 000	municipal and industrial wastewater (from textile industry = difficult to degrade biologically)	CAS[c]	Cat. 1
14				CAS[c] + sand filtration	
15	Harelbeke	116 100	mainly municipal wastewater (low degree of industrial wastewater)	CAS[c]	

[a] size category determined by the inhabitant equivalent of each plant: large (I.E. > 80 000, cat. 1), medium (I.E. = 24 000 – 80 000, cat. 2) and small (I.E. < 24 000, cat. 3) sized plants

[b] receiving wastewater can be highly diluted e.g. due to a large share of receiving rain water

[c] CAS = conventional activated sludge

2.2 Analytical methods

Nitrite (NO_2^--N), nitrate (NO_3^--N), ammonium (NH_4^+-N) and COD were determined spectrophotometrically using Hach-Lange cuvettes and a DR2800 spectrophotometer (Hach-Lange, Belgium). Alkalinity (as mg L^{-1} $CaCO_3$) was determined according to standard methods.[185] Turbidity was measured with a portable Hi 98703 (Hanna Instruments, USA). Conductivity (EC) and pH were registered by a multi-meter (HQ30D or HQ40D, Hach Belgium).

The instantaneous ozone demand (IOD), defining the rapid ozone consumption within 5 seconds after dosing, was determined based on Hoigné and Bader[186] and Roustan et al.[187] The IOD was determined after spiking ozone to the effluent and allowing a reaction time of 5 seconds. All measurements were performed in triplicate and samples were continuously mixed at ± 300 rpm. 25 mL of effluent was spiked with 2.5 or 5.0 mL of an ozone stock solution to result in an overdose of ozone depending on the effluents ozone demand. To prepare this stock solution, demineralized water (ice-cooled, 250-500 mL) was purged by an ozone/oxygen gas mixture (300 mL min^{-1}) using an oxygen-fed ozone generator (up to 8 g O_3 h^{-1}, COM-AD-02, Anseros GmbH, Germany) achieving approximately 90 mg O_3 L^{-1} in the stock solution. The reaction between EfOM and ozone was stopped after 5 seconds by adding an indigo solution (1 mM potassium indigotrisulfonate in 20 mM H_3PO_4) that immediately reacts with any remaining ozone. Sufficient mixing and fast ozone reactions will take place within this time interval.[98] Although fast ozone reactions can take place within milliseconds, this time-interval allowed a good estimation of the IOD at a practically feasible level. Determination of the ozone concentration in the stock solution and in the spiked effluent after 5 seconds was achieved based on the indigo method, established by Bader and Hoigné.[188] Phosphate buffer (pH = 2) was added to ensure the stability of the indigo concentration in the solution. The difference in indigo absorption before and after 5 seconds of reaction (taking dilution into account) can be established as the IOD.

2.3 TrOC analysis

Samples for TrOC analyses (all pharmaceuticals) were stored in precleaned glass bottles at -20 °C in the dark, prior to analysis (within less than 1 month) or at 4 °C if analysis took place within 48 hours. Before storage, samples were filtered using a glass microfiber filter (1.0 μm, class GF/B,

Whatmann). Furthermore, Na_2EDTA (1 g L^{-1}) was added and samples were acidified to a pH of 3 with formic acid (LC-MS grade). After storage, samples were brought back to a pH of 7.0 ± 0.1 with 5 M NaOH and 10% formic acid, followed by filtration through a nylon filter (0.45 µm, Whatmann). TrOCs were then isolated and concentrated with solid-phase extraction (SPE) using Oasis HLB 6cc cartridges by loading 100 mL (or 200 mL to increase the concentration factor in certain cases) of each sample onto the cartridge after conditioning with HPLC-grade methanol and HPLC-grade water. Analyses were performed on the extract after washing with 6 mL HPLC-grade water, elution with 5 mL of HPLC-grade methanol (or 5 mL of 1:1 MeOH:Acetone) and reconstitution in 1 mL MeOH:H_2O (10:90) containing 0.1% (v/v) formic acid and 0.1 g L^{-1} $Na_2EDTA.2H_2O$. The instrumental analyses were performed by injecting 10 µL in an UHPLC-HRMS benchtop Q-Exactive™ Orbitrap (Thermo-Fisher Scientific, USA) equipped with a reversed phase column (Hypersil Gold column, 1.9 µm particle diameter, 2.1×50 mm), a heated electrospray ionization (HESI-II) source (working in positive ionization mode) and operated in full scan (150-500 m/z). The analytical recovery during the entire analysis (SPE and UHPLC-HRMS) was determined for each measurement sequence. More details on the analytical methodology for the complete list of 40 measureable TrOCs is provided by Vergeynst et al.[189], including the detection limits - equivalent to the definition of the detection capability (*CCβ*) as defined by the EU Commission Decision 2002/657/EC. This list is reduced in this work based on the analytical recovery (min. 20% required) during SPE and instrumental analyses, variability of analytical efficiency (i.e. reproducibility during peak integration, mass error < 4 ppm, error on retention time < 15%) , and frequency of detection in all samples (min. 20% required).

2.4 Spectral measurements

UV-Visible (UV-VIS) and fluorescence measurements were done on samples without any filtration to keep the sample as close as possible to the real-scale conditions. UV-VIS absorption data were obtained using a Shimadzu UV-1601 or UV-1800 spectrophotometer. Spectra were taken between 200 and 800 nm with 0.5 nm increments using 1 cm quartz-cuvettes. The notation of the absorption coefficient (m^{-1}) is given as UVA_i or $color_i$ with *i* related to the wavelength, e.g. 254 nm (UVA_{254}) or 436 nm ($color_{436}$). A few specific wavelengths (i.e. 210, 220, 254, 310 and 436 nm) have been selected for further use based on their relevance and their previous usage in literature.[190] Nitrogen species such as NO_3^--N and NO_2^--N are known to absorb below 250 nm and are showing maximum absorbance values around 220 and 210 nm respectively, although

specific determination of both might vary in literature.[118] The organic matrix is systematically represented by the absorbance at 254 nm (aromatic and double-bond moieties),[40,114] 310 nm (often used as a general representation of the (natural) organic matter)[191] and 436 nm (color).[55,100]

Fluorescence EEMs were obtained using 1 cm quartz-cuvettes and a Shimadzu RF-5301 Fluorimeter. Dilution was performed if UVA_{254} was above 0.3 cm^{-1} or when fluorescence measurements exceeded the maximal measurable intensity.[192–194] Fluorescence intensities were measured at excitation wavelengths of 220-450 nm in 5 nm increments, and emission wavelengths of 280-600 nm in 1 nm increments. Excitation and emission slit widths were set at 5 nm, and a response time of 0.25 s was utilized. Raman scans of demineralized water were obtained at an excitation wavelength of 350 nm over an emission wavelength range of 365-450 nm in 0.2 nm increments, for the calculation of the Raman peak. The area of the Raman peak was used to normalize the fluorescence intensity of all spectra, finally expressed as RU (Raman units).[195,196] The spectra were accounted for the applied dilution factor during measurement before any further data processing. The 3D EEM was further used to derive several variables such as the total fluorescence (TF), determined by integration of the volume under the whole EEM. Different regions within the EEMs have been associated with different types of organic matter and properties, as defined by Chen et al.[133] and modified further by other authors, e.g. Sgroi et al.[136] Five different regions were used representing aromatic proteins, tyrosine-like substances (I_1), aromatic proteins, tryptophan-like substances (I_2), fulvic-like and humic-like substances (I_3), microbial byproducts, proteins, tryptophan-like substances and biopolymers (I_4) and humic-like substances (I_5). These different regions are typical EEM peaks present in wastewater matrices (see also Figure 1.6 and Figure 1.7 from Chapter 1).[136] Details on the range of excitation and emission wavelength, associated with these regions, are given in Table 3.2.

Table 3.2: Fluorescence regions and their excitation-emission wavelength boundaries.[133] The fluorescence intensity used for further analyses was determined at the peak wavelength, similar to Sgroi et al.[136]

Variable	Excitation wavelengths (nm)		Emmision wavelengths (nm)	
	Region boundary	Peak wavelength	Region boundary	Peak wavelength
I_1	220-250	225	250-320	290
I_2	220-250	225	320-390	340
I_3	220-300	245	390-580	440
I_4	250-300	275	250-390	345
I_5	250-580	345	300-450	440

2.5 Data analysis

Principal Component Analysis (PCA) is used as a pattern recognition method, aiming to reduce the large number of variables into a smaller number of principal components (PCs) or representative variables.[197] To reduce the contribution of variables with minor significance and increase the ease of interpretation, varimax normalized rotation was carried out.[198] The extracted number of PCs is defined by using the Kaiser criterion,[199] retaining only PCs with Eigenvalues greater than unity and analyzing the scree plot (see section 3.3). SPSS statistics 24 was used to perform all statistical analysis (www.spss.com).

3 Results and Discussion

3.1 Effluent water quality

3.1.1 Physical-chemical water characteristics

An overview of all effluent characteristics determining the physical-chemical water quality is given in Figure 3.2, showing distinct variations for most parameters. Variable results are seen especially for alkalinity (between 84 and 384 mg $CaCO_3$ L^{-1}), NO_3^--N (between 1.13 and 19.0 mg N L^{-1}), EC (between 396 and 1347 µS cm^{-1}), COD (between 5.8 and 84.6 mg O_2 L^{-1}), IOD (between 2.9 and 16.0 mg O_3 L^{-1}) and a few of the spectral measurements (e.g. UVA_{210}, UVA_{220}, UVA_{254} and I_2) with for example UVA_{210} and UVA_{254} between 66.7 - 395 m^{-1} and 9.0 - 63.9 m^{-1} respectively. These can all (except NO_3^--N) be considered to influence ongoing reactions during tertiary ozonation.[165] All characteristics have been analyzed , resulting in 273 samples during a time frame of a little under 1.5 years at 15 different sampling locations. Logically, this results in varying observations as effluent (and its quality) is susceptible to operational deviations (e.g. malfunctions) and variations in receiving influent of the WRRF due to e.g. weather conditions, diurnal patterns, etc. but also the location as some WRRFs are receiving specific industrial wastewater.

Having an in-depth look focusing on the samples for all 15 locations combined (without the additional taken samples for location 11 and 15), alkalinity (Figure 3.3a) and IOD (Figure 3.3c) are showing respectively a little (only location 1 and 2 for alkalinity) to no clear specific

dependence on the sampling locations (in contrast to COD, UVA_{254} and TF, Figure 3.3b,d,e) and are highly variable within one plant. The significant lower alkalinity values at location 1 and 2 (both originating from the WRRF of Kruiseke) are presumable related with the very small size of the WRRF, and hence its higher susceptibility to fluctuations (i.e. weather conditions, flow or constituents) in the receiving municipal wastewater.

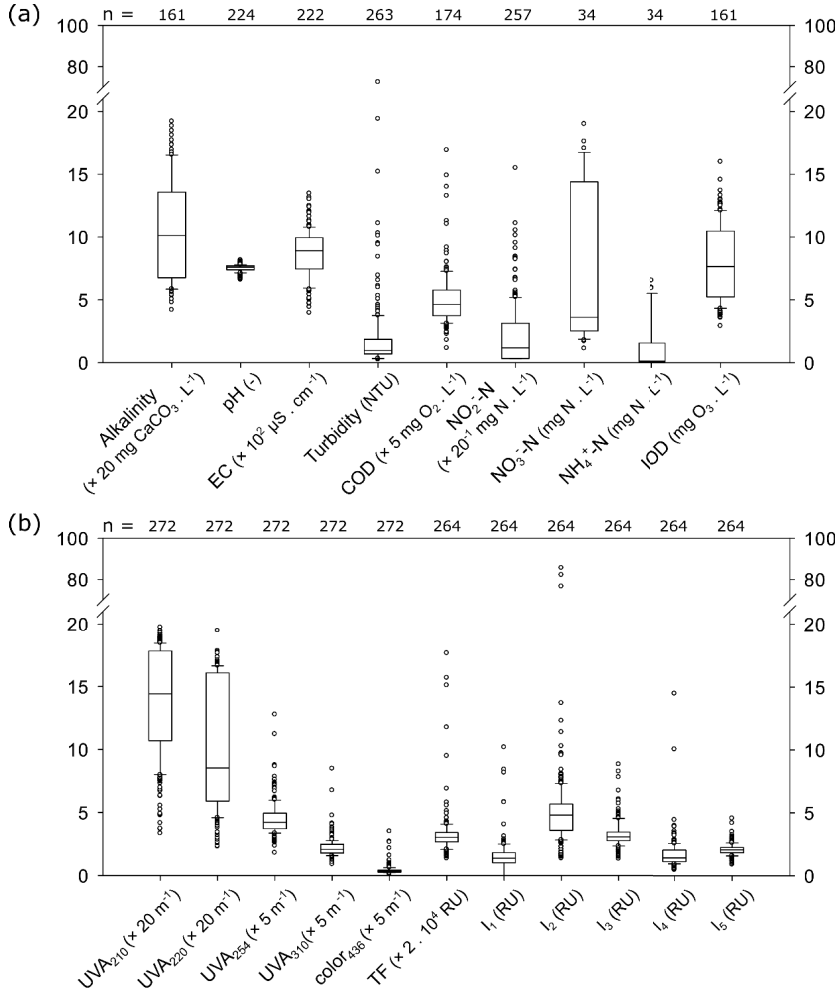

Figure 3.2: Water quality of all effluent samples presenting both (a) conventional physical-chemical characteristics and (b) spectral measurements, analyzed for all 15 sampling locations. The whiskers of the boxplots indicate the 10th and 90th percentile of the data distribution, while the white dots are the outliers considering all measured data.

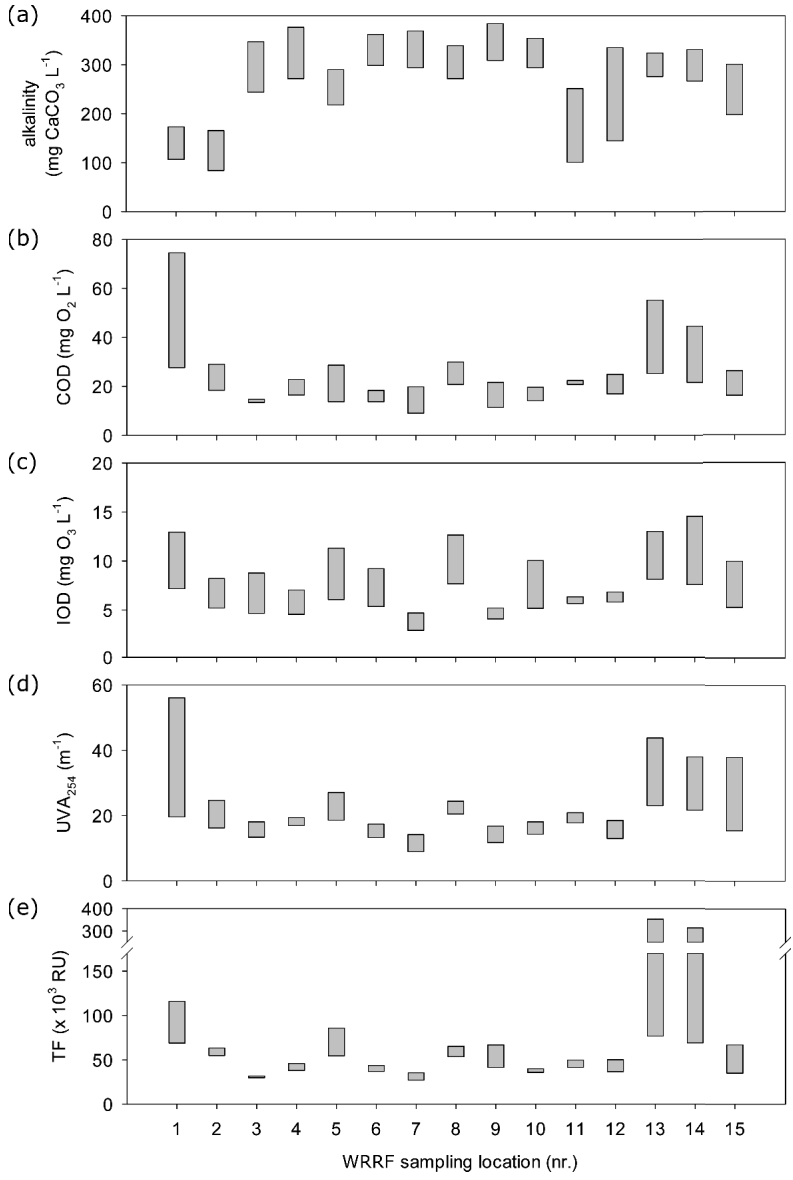

Figure 3.3: Selected physical-chemical water quality characteristics of effluent samples taken during three sampling campaigns of which all samples within one campaign were taken within similar time intervals. The characteristics are depicted as (a) alkalinity, (b) COD, (c) IOD, (d) UVA_{254} and (e) TF. WRRF sampling location numbers are referring to Table 3.1. Grey bars are indicating the maximal and minimal measured values.

The large variations of IOD (Figure 3.2a), up to a factor of 5 between the minimal and maximal measured values, have great impact on a potential tertiary ozonation step. IOD is representative for the amount of ozone susceptible moieties and low (high) values are indicative for a decreased (increased) need of unselective oxidant species to react with the other, ozone recalcitrant moieties. Additionally, the initial phase of fast ozone reactions has been related to very high observed transient HO• concentrations, playing an essential role during the oxidation processes.[126] Logically, variations in the IOD are an indication of the HO• formation potential, influencing consecutive reactions with less ozone reactive moieties.

A few remarkable outlier measurements are noticed for turbidity and fluorescence measurements (TF, I_2, I_4). Short-term large increases of turbidity are not illogical considering the possibility of flushing out more suspended particles (e.g. sludge) from the settler succeeding biological treatment. The specific data-points from Figure 3.2 (high values of turbidity) could be allocated to sampling location 1 and 11, respectively originating from the smallest WRRF before passing through a constructed wetland (CW) and one of the largest plants but sampled at a time with increased flow (i.e. first flush), as a presumable consequence of abnormalities in the settler. Outliers for turbidity can thus be attributed to specific events, whereas the high variability in fluorescence response (specifically for TF, I_2 and I_4) are clearly plant specific. Figure 3.3e shows, for each sampling location individually, the TF for samples taken at similar moments. The response from locations 13 and 14 (both WRRF of Waregem, respectively before and after a tertiary sand filtration) is clearly remarkable with a difference up to 3 to 13 times comparing respectively with the minimum and maximum values of the other plants. Although these locations (i.e. 13 and 14) show comparable values with other locations concerning characteristics such as alkalinity (see Figure 3.3a), pH (little variation in general, see Figure 3.2), turbidity, etc. relatively high values are also noticed for COD and UVA_{254} (Figure 3.3b-d). The increased TF is mainly caused by I_2 and I_4, both remarkably higher compared to I_1, I_3 and I_5, and both representing regions within the EEMs that contain tryptophan-like substances (in contrast to I_1, I_3 and I_5). The increased response for I_2 and I_4, and the presumable increased presence of tryptophan-like substances, is clearly specific for these locations.

Both UVA_{254} (Figure 3.3d) and COD (Figure 3.3b) are showing a similar pattern of which the larger values noticed at locations 1, 13 and 14 can be associated with the previous mentioned abnormalities (location 1) and the increased presence of tryptophan-like substances and substances having a significant degree of aromaticity (associated with the increased values of e.g. I_1 and I_2, representing aromatic proteins and tryptophan-like substances, in location 13 and 14).

Locations 13 and 14 are following conventional activated sludge treatment of a WRRF receiving a share of industrial textile wastewater mixed with the municipal wastewater, unique among the selected WRRFs (Table 3.1). Textile wastewater is known to contain a significant amount of dyes which retain some absorption[39] and are traditionally difficult to be removed during secondary (biological) wastewater treatment. Additionally, previous research indicated highly increased intensity values during fluorescence measurements associated with these kind of substances.[200] Dyes consisting of aromatic, heterocyclic and nitrogen containing moieties such as azobenzene or triazines typically show a low reactivity towards ozone and consequently a very low yield for O_3 consumption.[39,200,201] Despite the higher values of general EfOM parameters such as UVA_{254} (Figure 3.3d), TF (Figure 3.3e) and COD (Figure 3.3b), no remarkable increase of IOD (Figure 3.3c) was noticed, supporting the hypothesis of an increased amount of ozone recalcitrant moieties. As such, the presence of these kind of substances in the effluent poses a challenge for consecutive ozonation because of the presence of these rather case-specific substances.

3.1.2 TrOC concentrations

54 samples were analyzed for 40 TrOCs (all pharmaceuticals) of which 22 TrOCs are retained for discussion and displayed in Figure 3.4. Some basic characteristics of these TrOCs are summarized in Table 3.3 in view of tertiary ozonation. Although samples were taken at two different WRRF sampling locations (and almost 2 years difference), i.e. location 11 (n_{max} = 47) and 15 (n_{max} = 7), no clear component specific differences or variations are noticed. TrOCs were overall detected ranging from 1 ng L^{-1} to > 2 µg L^{-1}. Interpreting all data as a whole and as given in Figure 3.4, it is noticed that for 21 of the 22 individual TrOCs, the measured concentrations are within a relatively small range (i.e. order of magnitude). This is especially the case for TrOCs having an average concentration of 10 ng L^{-1} or above. A high variation (3 orders of magnitude) is only noticed for sulfamethazine (i.e. an antibiotic used to treat infections as e.g. bronchitis) which presence might depend on specific periods of increased illness among the population. Diclofenac was consistently detected at the highest concentrations (on average 928 ng L^{-1}; variation over a factor of 5.3). TrOCs quantified at high concentrations such as carbamazepine and venlafaxine showed even lower differences between the minimum and maximum values, i.e. within a factor of respectively 3.5 and 4.1. This indicates a more or less consistent discharge of TrOCs in the receiving water bodies and might also pose an advantage when applying TrOC monitoring or control strategies based on the relative decrease of TrOC levels in the effluent.

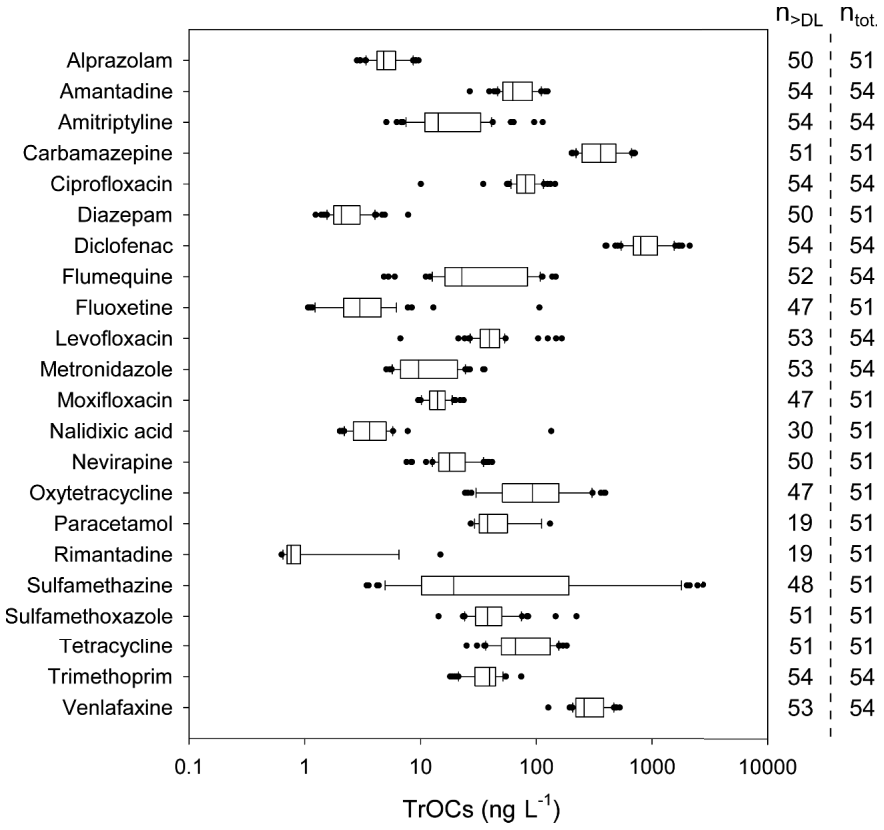

Figure 3.4: Concentration levels (ng L^{-1}) of 22 TrOCs, quantfied (> DL) in minimum 20% of all samples. The whiskers of the boxplots indicate the 10th and 90th percentile of the data distribution, while the black dots are the outliers considering all measured data. The quantification frequency is indicated on the right indicating the total number of samples in which the TrOC was measured ($n_{tot.}$) and the number of samples above the detection limit ($n_{>DL}$).

Table 3.3: Overview of quantified TrOCs and literature data on the apparent 2nd order reaction rate constants for ozone ($k_{O3,TrOC}$) and HO ($k_{HO•,TrOC}$), if available.

TrOCs	Type	$Log\ K_{ow}$[202,c]	$k_{O3,TrOC,pH7}$ ($M^{-1}\ s^{-1}$)	$k_{HO•,TrOC}$ ($10^9\ M^{-1}\ s^{-1}$)	Ref.
Alprazolam	Antianxiety	2.12	< 1	n.a.	[b]
Amantadine	Antiviral Antiparkinsonian	2.3	8	n.a.	[a]
Amitriptyline	Antidepressant	4.9	2.5×10^3	10.3	[203,204]
Carbamazepine	Antiepileptic	2.45	3×10^5	8.8	[39,64]
Ciprofloxacin	Antibiotic	2.3	1.9×10^4	4.1	[111,205]
Diazepam	Antianxiety	2.82	< 1	7.2	[66]
Diclofenac	Anti-inflammatory drug	4.0	1×10^6	7.5	[66]
Flumequine	Antibiotic	1.7	6	8.26	[206,a]
Fluoxetine	Antidepressant	n.a.	n.a.	n.a.	
Levofloxacin	Antibiotic	0.35	6×10^4	5.2	[207]
Metronidazole	Antibiotic	-0.1	< 1	6.2	[65]
Moxifloxacin	Antibiotic	0.95	n.a.	n.a.	
Nalidixic acid	Antibiotic	1.41	n.a.	n.a.	
Nevirapine	Antiretroviral	3.89	n.a.	n.a.	
Oxytetracycline	Antibiotic	-0.90	n.a.	n.a.	
Paracetamol	Painkiller	0.46	n.a.	n.a.	
Rimantadine	Antiviral	3.34	n.a.	n.a.	
Sulfamethazine	Antibiotic	0.14	n.a.	n.a.	
Sulfamethoxazole	Antibiotic	0.89	5.5×10^5	5.5	[65]
Tetracycline	Antibiotic	-1.37	1.9×10^6	n.a.	[39,208]
Trimethoprim	Antibiotic	0.79	2.7×10^5	6.9	[111]
Venlafaxine	Antidepressant	2.8	8.5×10^3	8.15	[65,209]

[a] $k_{O3,TrOC}$ values based on experimental observations and the developed correlation model in Chapter 4

[b] $k_{O3,TrOC}$ assumed to be the same as for diazepam due to its similarities in structure (and experimental observations in Chapter 5)

[c] K_{ow} = octanol-water partition coefficient. Seen as one of the indicators of the sorption potential on e.g. sludge particles.

n.a. = not available in literature

3.2 Correlation between characteristic parameters

Potential correlations between different physical-chemical water characteristics are determined according to the correlation matrix displayed in Table 3.4. All characteristics, and their correlations, can be roughly summarized in three main groups - keeping the goal of tertiary ozonation in mind - which are (i) mainly influenced by the secondary biological treatment such as the nitrogen containing species (NO_2^--N, NO_3^--N, NH_4^+-N) and organic loads, (ii) indicative for the load in the effluent such as EC or alkalinity (some depending partially on the biological treatment), and (iii) representing the organic matrix in its whole (e.g. TF, COD) or specific (groups of) moieties such as UV-VIS or fluorescence spectral measurements. These three groups are introduced to facilitate the discussion.

Remaining concentrations of NO_2^--N, NO_3^--N and NH_4^+-N have a good correlation with each other, up to the 0.01 significance level. Most WRRF sampling locations were preceded with a biological treatment (i.e. activated sludge) in several different configurations (see Table 3.1). Nitrification is transforming NH_4^+-N species into NO_2^--N and NO_3^--N. Denitrification will further proceed by transforming NO_3^--N to N_2 with NO_2^--N being an intermediate product of this complete reaction.[210] It is therefore logical that the presence of one of these constituents correlates with the removal (or production) of another. The presence of NO_2^--N can for example be a sign of ineffective biological treatment (nitrification-denitrification) as it is aimed to transform all nitrogen to N_2 gas.[211] Furthermore, also spectral measurements such as UVA_{210} and UVA_{220} show an excellent correlation (Pearson coefficients up to more than 0.9 at the 0.01 significance level) with these nitrogen-containing species (especially NO_3^--N). The UV absorbance at 210 or 220 nm have been recognized as indicators for nitrogen-containing species such as NO_2^--N or NO_3^--N respectively as both show clear absorbance maxima around these wavelengths.[118,190] However, specific determination of both can be influenced by each other and by other constituents absorbing around these wavelengths (e.g. a large variety of organic moieties such as humic acids), indicated by the correlation (Pearson coefficient 0.20-0.27 with NO_2^--N) with UVA_{254}, UVA_{310} and $color_{436}$ at the 0.01 confidence level. This probably contributes to the low correspondence of NO_2^--N and UVA_{210} (or UVA_{220}) in Table 3.4. All NO_2^--N measurements (n = 198) were below 1 mg N L^{-1} (indicating a good removal during biological treatment), in contrast to NO_3^--N (up to 19.0 mg N L^{-1}) and other UV absorbing constituents that might be present (e.g. organics, see Figure 3.2). To ensure a reliable and trustworthy correlation between nitrogen-containing species and UV-VIS measurement, the need for multivariate data analysis (e.g. principle component analysis or partial least square regression) is recognized.[118]

Table 3.4: Correlation matrix of the physical-chemical effluent characteristics (given as letters A to T) with indication of the Pearson coefficient. One or two asterisks (*) are marking the significant correlations at the 0.05 and 0.01 level (2-tailed) respectively (also indicated as light or dark grey shaded). The strongest correlations (Pearson coefficient ≥ |0.75| and < |0.75| but ≥ |0.50|) are respectively indicated in green and yellow (all at the 0.01 confidence level except NO_2^--N vs NO_3^--N).The physical-chemical variables are: alkalinity (A, mg $CaCO_3$ L^{-1}), pH (B), EC (C, µS cm^{-1}), turbidity (D, NTU), COD (E, mg O_2 L^{-1}), NO_2^--N, NO_3^--N and NH_4^+-N (F-H, mg N L^{-1}), IOD (I, mg O_3 L^{-1}), UVA_{210}, UVA_{220}, UVA_{254}, UVA_{310} and $color_{436}$ (J-N, m^{-1}), TF and $I_{1\text{-}5}$ (O-T, RU).

		A	B	C	D	E	F	G	H	I	J	K	L	M	N	O	P	Q	R	S	T
Alkalinity	A	1	-	-	-	-	-	-	-	-	-	-	-	-	-	-	-	-	-	-	-
pH	B	-.23**	1	-	-	-	-	-	-	-	-	-	-	-	-	-	-	-	-	-	-
EC	C	.68**	-.21**	1	-	-	-	-	-	-	-	-	-	-	-	-	-	-	-	-	-
Turbidity	D	0.09	-0.09	-0.07	1	-	-	-	-	-	-	-	-	-	-	-	-	-	-	-	-
COD	E	0.02	-0.11	0.07	.64**	1	-	-	-	-	-	-	-	-	-	-	-	-	-	-	-
NO_2^--N	F	-0.05	0.02	-0.1	.20**	.37**	1	-	-	-	-	-	-	-	-	-	-	-	-	-	-
NO_3^--N	G	-.74**	0.03	-0.16	-.63**	-.77**	-.50*	1	-	-	-	-	-	-	-	-	-	-	-	-	-
NH_4^+-N	H	-0.06	.80**	-.45*	0.33	.53**	.64**	-.42*	1	-	-	-	-	-	-	-	-	-	-	-	-
IOD	I	.23**	0.05	.25**	.28**	.59**	.24**	-.84**	.39*	1	-	-	-	-	-	-	-	-	-	-	-
UVA_{210}	J	-.55**	.26**	-.37**	-.13*	0.01	-0.01	.94**	-0.12	-.33**	1	-	-	-	-	-	-	-	-	-	-
UVA_{220}	K	-.62**	.27**	-.29**	-0.1	-0.02	-0.11	.98**	-0.32	-.43**	.91**	1	-	-	-	-	-	-	-	-	-
UVA_{254}	L	0.05	-0.01	.15*	.48**	.75**	.22**	-.54**	.75**	.67**	-.15*	-.23**	1	-	-	-	-	-	-	-	-
UVA_{310}	M	0.05	-0.02	.14*	.65**	.79**	.20**	-.49**	.68**	.59**	-.12*	-.17**	.95**	1	-	-	-	-	-	-	-
$color_{436}$	N	0.07	-0.07	0	.78**	.75**	.27**	-.64**	.74**	.39**	-.13*	-.15*	.68**	.84**	1	-	-	-	-	-	-
TF	O	.16*	-0.12	.32**	0.05	.49**	-0.09	0.13	0.3	.40**	-0.09	-0.1	.58**	.49**	.24**	1	-	-	-	-	-
I_1	P	-.19*	-0.1	0.08	.12*	.38**	0.06	0.22	0.25	0.12	.15*	.18**	.21**	.24**	.25**	.16**	1	-	-	-	-
I_2	Q	.21**	-.15*	.33**	0.03	.42**	-0.05	.48**	-0.14	.30**	-0.1	-0.09	.39**	.35**	.17**	.94**	0.08	1	-	-	-
I_3	R	0.05	0.01	.25**	-0.03	.43**	-0.1	-0.1	.56**	.48**	-0.09	-.13*	.71**	.54**	.18**	.82**	0.01	.63**	1	-	-
I_4	S	.26**	-.18**	.35**	0.07	.42**	-0.04	-.77**	.59**	.33**	-.19**	-.19**	.42**	.37**	.20**	.94**	0	.98**	.65**	1	-
I_5	T	0.09	-0.03	.35**	0.07	.39**	-0.13	-.38*	0.02	.46**	-.20**	-.22**	.67**	.57**	.32**	.42**	.20**	.17**	.69**	.21**	1

Additionally, also the alkalinity is partially depending on the biological treatment and some correlation can be noticed with a few previous discussed characteristcs (e.g. NO_3^--N, UVA_{210}, UVA_{220}). The presence of CO_3^{2-} (and HCO_3^-) will act as an important scavenger for hydroxyl radicals (HO•) with reaction rates in the order of 10^6-10^8 M^{-1} s^{-1} and, therefore, increasing the ozone demand of the wastewater.[181] As mainly occurring as a HO• scavenger, little effect can be expected on the IOD (direct ozone reactions) hence their low correlation (Pearson coefficient 0.23).

Water characteristics being indicative for the effluent loads such as alkalinity and EC exhibit a good correlation with each other (Pearson coefficient of 0.68, 0.01 level, n = 147). Both characteristics are determined by the presence of ions within the water. Alkalinity is greatly affected by the biological treatment process and roughly refers to the bases that can be converted to uncharged species by acidification. It should be mentioned however that EC is (especially more than alkalinity) representative for all ions present and not as a sole representation for the alkalinity levels. Dilution of an effluent will have its effect on both parameters. An additional benefit of such a correlation is that EC is easily measured online while alkalinity determination requires sampling and offline analyses in the lab. Therefore, such a correlation poses a potential indirect online follow-up of the alkalinity, known to influence ozone reactions.[165] Nevertheless, further investigations will be necessary to develop this kind of soft sensor as there is currently no indication to be plant independent, hence posessing great enhancement potential.

A large share of the observed correlations are related in one or another way with the organic matrix present in the effluent. COD as a surrogate for the full (chemically oxidizing) organic matrix shows good correlations with IOD and all spectral measurements, all significant at the 0.01 level, with the exception of UVA_{210} and UVA_{220} (both previously related to NO_3^--N). More specifically, UVA_{254} (as also UVA_{310} and $color_{436}$) are showing the best correlation with COD (Pearson coefficient 0.75 or above). This is in line with previous research which has led to the availability of sensors enabling the online follow-up of the COD.[190] IOD, as a representation of the highly ozone reactive species, is also correlated with COD although to a slightly lesser extent (Pearson coefficient 0.59). The IOD will thus clearly be influenced by the organic matrix although no ideal correlation exists and the preceding biological treatment, hence its correlation with e.g. NO_3^--N (Pearson coefficient 0.84). This means that next to the amount of organics present, the composition of it (more specifically the share of highly reactive moieties) and the presence of other reactive constituents (e.g. NO_2^--N) will have an influence. The IOD is furthermore correlated to a similar extent with UVA_{254} (Pearson coefficient 0.67), which is known

to be greatly influenced by (electron rich) aromatic and saturated moieties absorbing at this wavelength.[212]

The fluorescence derived parameters are representing the organic matrix and, hence, their good correlations with others such as UVA_{254}, COD, etc. as depicted in Table 3.4. Nevertheless, while no clear differences are noticed between the UV-VIS derived parameters (with the exception of UVA_{210} and UVA_{220}), I_1 is giving clearly different relationships compared to TF and $I_{2\text{-}5}$. In addition to previous observations, I_2 and I_4 are strongly correlated with each other as both are representative for tryptophan-like substances. Similarly, also I_3 and I_5 are showing some correlative behavior as both are (partially) representing humic acids-like substances, and are both having the highest correlations to IOD and UVA_{254} (Pearson coefficient 0.46-0.71) compared to I_1,I_2 and I_4 (Pearson coefficient $\leq$ 0.42 for all, see Table 3.4). I_1, representing aromatic proteins and tyrosine-like substances, is in contrast to other derived parameters clearly not correlated with the IOD. This might suggest that this surrogate measurement is an indicator for the amount of recalcitrant moieties within the EfOM. It is hypothesized that it can be used to follow-up ozone recalcitrant organics, which is of high interest in order to have a good insight of the complete ongoing reactions process. Although aromatic moieties (e.g. susceptible to ozone) are showing intensities in these regions, other lower reactive species might also be present at these wavelengths. Further investigation (e.g. kinetic degradation experiments) is however required to confirm previous findings. To focus more in-to detail on specific moieties, e.g. PARAFAC can be used to deconvolute the EEMs. The application of PARAFAC is fully described in Chapter 4.

3.3 Principle component analysis in view of the control of a tertiary ozonation step

The resulting rotated principle component (PC) matrix is presented in Table 3.5. It was decided to use these four PCs, with each an Eigenvalue significantly larger than 1 (= Kaiser criterion), for further analysis.[199] This decision is supported by a total explained variance of 74.9% and the fact that the scree plot contains a clear inflection point when retaining these four components. The Kaiser-Meyer-Olkom (KMO) criterion for sampling adequacy (KMO = 0.67 > 0.5) is fulfilled, and also the Barlett's test of sphericity ($\chi^2(153) \approx 3017.5$; $p = 0.00 < 0.05$) indicated sufficient correlation between items to perform PCA.[213] All variables given in Table 3.4 are included in this analysis if more than 100 measurements could be attributed. This excluded the limited data available on NO_3^--N (n = 34) and NH_4^+-N (n = 28).

Table 3.5: The resulting rotated principle component (PC) matrix with the indication of Eigenvalues and explained variance (%)

	PC1	**PC2**	**PC3**	**PC4**
Eigenvalue	4.50	4.26	2.71	2.01
% of explained variance	25.0	23.7	15.1	11.1
$Color_{436}$ (m^{-1})	0.91	0.00	0.09	-0.03
UVA_{310} (m^{-1})	0.91	0.29	0.11	0.01
Turbidity (NTU)	0.85	-0.16	-0.04	-0.06
COD (mg O_2 L^{-1})	0.83	0.32	0.18	-0.07
UVA_{254} (m^{-1})	0.83	0.45	0.08	-0.02
IOD (mg O_3 L^{-1})	0.55	0.41	-0.23	-0.20
I_5 (RU)	0.44	0.31	-0.03	0.36
TF (RU)	0.19	0.96	0.05	0.16
I_2 (RU)	0.10	0.94	0.02	0.15
I_4 (RU)	0.11	0.93	-0.07	0.15
I_3 (RU)	0.23	0.91	-0.07	0.10
UVA_{220} (m^{-1})	0.01	-0.01	0.95	-0.15
UVA_{210} (m^{-1})	-0.08	0.00	0.86	-0.24
I_1 (RU)	0.29	-0.05	0.79	0.17
EC (µS cm^{-1})	-0.04	0.27	-0.14	0.81
pH (-)	-0.06	0.00	-0.02	-0.68
Alkalinity (mg $CaCO_3$ L^{-1})	-0.05	0.01	-0.54	0.56
NO_2^--N (mg N L^{-1})	0.24	-0.15	0.09	-0.45

The first and second PC are respectively explaining 25.0% and 23.7% of the total variance and contain most of the information on measurements related to the organic matrix (Table 3.5). PC1 describes most information from COD, IOD, turbidity and UV-VIS measurements, such as UVA_{254} and UVA_{310}. PC2 retains most information obtained from fluorescence derived measurements with the clear exception of I_1, previously defined to have a distinct behavior. The third and fourth PC are more related towards conventional physical-chemical water characteristics. PC3 described most information from I_1 (representing potential ozone refractory organics), UVA_{210} and UVA_{220} (related with inorganic nitrogen-containing species after biological treatment). PC4 is clearly a representation of the basic water quality mainly containing information on pH, EC, alkalinity and NO_2^--N.

In Figure 3.5, the score plots of the four PCs is given comparing PC1 with PC2 (Figure 3.5a), and PC3 with PC4 (Figure 3.5b). Other combinations of PCs in score plots does not give any additional (visual) information and are therefore not given. PC1 and PC2 are in large quantity situated around the zero point, indicating no large variations within these PCs. Nevertheless, some outlier values are noticed which can be attributed to some disturbance - by e.g. particles or due to analytical anomalies - in the measurements (PC1, from e.g. sampling locations 1 and 11) and the increased fluorescence response noticed in sampling locations 13 and 14 (PC2). It is noted that both of these observations have been mentioned previously, when describing the individual characteristics of the different sampling locations. Both PC1 and PC2 are mainly describing variations in the spectral measurements. A low variability of spectral measurements as input to a control framework reduces the chance on errors and will make it easier to develop such framework. Nevertheless, outlier values were noticed which still need to be accounted for and will require extensive validation of a surrogate-based correlation model during long-term operation and for different WRRFs.

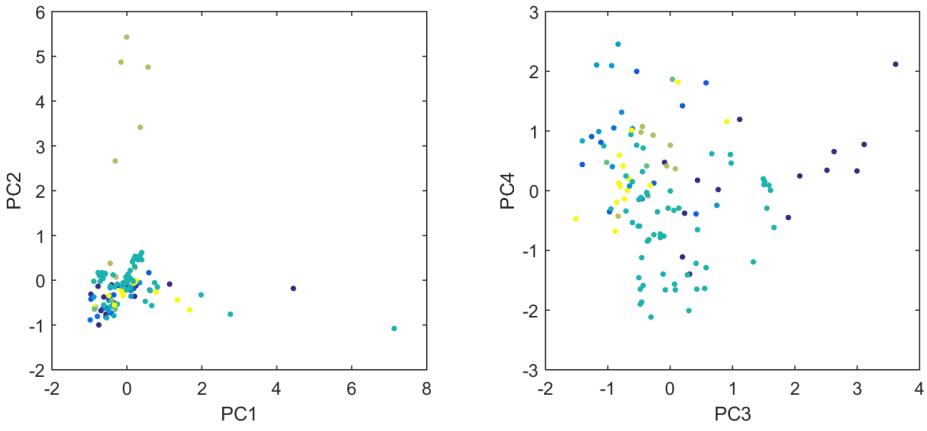

Figure 3.5: Score plots of the PCA analysis with all physical-chemical water characteristics giving (a) PC1 vs. PC2 and (b) PC3 vs PC4. The data is color coded based on WRRF size (I.E.) ranging from dark blue (smallest = 500 I.E.) to yellow (largest = 110 000 I.E.)

PC3 and PC4 are exhibiting a much higher degree of variation. If the plant size is accounted for, most variation in measurements is attributed with decreasing WRRF size. The larger plants exhibit much less variability, presumably a consequence of the large buffering capacity of such a plant. The smaller a WRRF, the more direct influence will be noticed of abnormalities in the process operation or in variations of the receiving influent. Variations of PC3 can be due to anomalies in the biological treatment and will directly influence the ozonation process when e.g. an increase of NO_2^--N occurs. On the other hand, the presence of I_1, describing low ozone reactive substances, will increase the need for indirect ozone reactions and therefore the (increased) generation of HO•. PC4, containing e.g. information related to alkalinity and pH, will have its direct influence on the ozonation process. Where alkalinity will more act as an inhibitor of the ozonation process, an elevated (decreased) pH will lead to an elevated (decreased) production of HO•. This greatly influences the chain reactions or autocatalytic decomposition of ozone, according to known radical chain reactions pathways.[112,165]

4 Conclusion

WRRFs and their (secondary) effluents were meticulously selected, totaling 15 different locations in Belgium. General water quality variability has been assessed in view of a tertiary ozonation step. Spectral measurements such as UV-VIS or fluorescence are put forward as input for an online control framework and showed limited variations among the different plants. Although slight differences could be noticed comparing the raw measurements between the different WRRFs, totaling in a broad range of observed values for each spectral parameter, the general variability was rather low. The limited amount of observed outliers are clearly site or event dependent. A lower variability will make it easier to develop and apply a control framework based on these spectral measurements. The low variability over a total of 15 sampling locations suggests that such a control framework has the potential to be generically applicable. In addition, also variations in TrOC concentration levels seemed to be small, given that the presence of most individual compounds remained in the same order of magnitude over multiple sampling events at two different WRRFs. This poses an advantage when applying TrOC monitoring or control strategies based on the relative decrease of TrOC levels in the effluent.

On the other hand, significant variations among the different plants (especially smaller sized plants) could be noticed related to conventional water quality parameters such as alkalinity

(correlated with the electrical conductivity) and pH which are known to have an influence on the ozonation process. In addition, similar observations were made for less ozone reactive substances (tyrosine-like compounds) based on fluorescence measurements (I_1), defined on their complete lack of correlation with the IOD. These variations clearly need to be accounted for during ozone dose control although no good reliable correlation could be obtained between most water quality parameters (e.g. alkalinity, IOD, etc.) and the spectral measurements. Therefore, no assessment of most water quality parameters is possible and the overall reactivity of the organic matrix is a major attention point that needs to be implemented in a generical and effective control framework.

Chapter 4

Development of novel surrogate-based correlation models in view of real-time control of ozonation of secondary treated municipal wastewater

This chapter has been redrafted from:

Chys, M., Audenaert, W.T.M., Deniere, E., Mortier, S.T.F.C, Van Langenhove, H., Nopens, I., Demeestere, K. & Van Hulle, S.W.H. Surrogate-based correlation models in view of real-time control of ozonation of secondary treated municipal wastewater: model development and validation, *Environ. Sci. Technol.*, accepted. DOI: 10.1021/acs.est.7b04905.

1 Introduction

Municipal wastewater treatment plants have been identified as a major pathway through which trace organic contaminants (TrOCs) enter the aquatic environment.[24] TrOCs such as pharmaceuticals may trigger unwanted ecological effects (e.g. bacterial resistance, chronic toxicity, endocrine disruption and feminization of fish).[10,11] Additionally, increased use of reclaimed wastewater e.g. for crop irrigation might expose human individuals to xenobiotics (incl. pharmaceuticals).[16,17] Driven by pending (European) legislation[22,23] and/or as a precaution to protect the aquatic environment and drinking water sources, operators of (municipal) wastewater treatment plants (WRRFs) are preparing for plant upgrades with advanced technologies to remove these micropollutants from secondary effluents. Tertiary treatment technologies (e.g. ozonation, activated carbon filtration, membrane filtration, etc.) have been tested to remove these emerging contaminants prior to discharge.[32] Ozonation was successfully tested at lab-, pilot- and full-scale, and is therefore one of the major technologies currently being implemented in Switzerland (strongly driven by regulation) but also in other countries.[22,28] At ozone dosages up to 1 g O_3 g^{-1} DOC (dissolved organic carbon), the parent TrOCs can be removed above 80 % or even below detection limits for components with $k_{O3,TrOC} > 10$ M^{-1} s^{-1}.[98]

Although ozonation has its proven capabilities in different fields of application, currently applied control strategies for ozone dosage (e.g. flow-based) result in sub-optimal operation. Not only the effluent flow rate, but also the composition and hence the ozone demand of secondary effluent, are highly dynamic in time. Optimal ozone dosing is required to lower operational costs and to minimize the extent of by-product formation. The formation of bromate or N-nitrosodimethylamine (NDMA), both potentially carcinogenic, has been associated with the ozonation of effluent organic matter (EfOM) when exceeding effluent specific threshold values, mostly at high ozone dosages.[42,44,45] However, frequent TrOC monitoring is difficult as this requires advanced analyses that are time, cost and labor intensive. Therefore, readily available, online, and significant less expensive surrogate measurement technologies are needed for both process monitoring and ozone dose control. EfOM has been addressed as one of the main influencers of the ozonation process.[110] Besides consuming a significant fraction of the ozone, the organic matrix also indirectly gives rise to HO• production.[111,112] As the EfOM is significantly impacted by direct ozone and hydroxyl radical (HO•) reactions and can be easily characterized using (online) measurement methods, oxidant induced changes of EfOM can provide more rapid information on oxidant exposure, and hence TrOC removal. The following EfOM related

measurements have shown to correlate well to ozone dose and TrOC removal: dissolved organic carbon (DOC)[33,98,115], UV absorption at 254 nm (UVA_{254})[40,63,64,82,100,103,113,114] and total fluorescence (TF)[64].

So far, mostly linear relationships are considered which only appear to produce a good correlation for TrOCs having a high reactivity with ozone as discussed in Chapter 1 (i.e. mainly O_3 rather than HO• is responsible for their degradation). Often moderate or poor linear correlations are achieved between the decrease of the measured surrogate parameter (mostly ΔUVA_{254}) and the removal of ozone-recalcitrant TrOCs.[98,127] This might lead to an over or under prediction of the actual TrOC removal, which results in respectively an actual TrOC removal not meeting the imposed discharge limits or an overdose of ozone, associated with higher economical costs and possible more pronounced by-product formation. Components with a low reactivity towards ozone ($k_{O3,TrOC} < 10\ M^{-1}\ s^{-1}$) show a more convex curved behavior with only limited degradation in ΔUVA_{254} ranges below 20%.[100,127] In literature, it is insufficiently addressed how the TrOC specific properties (e.g. $k_{O3,TrOC}$) are influencing the linearity of these correlations. The production of HO• will clearly have a larger influence on the removal of TrOCs with a lower affinity for direct ozone reactions. Modelling strategies applying more kinetic based approaches noticed significant deviations between measured and predicted removal for the more recalcitrant TrOCs.[33] Hereby, the production of HO• has been indicated to be highly depending on the organic matrix. More recently, Chon et al.[53] indicated a shift in electron donating capacity of the EfOM when increasing the ozone dose, influencing the relation between ΔTrOCs and ΔUVA_{254}. Especially lower ozone reactive species showed no significant removal within a first phase of reaction. It is known that ozone decrease follows pseudo first order kinetics after an initial, fast reaction phase.[126] Consequently, this shift in reaction pathways is likely to influence the used correlation models. Further elaboration, with the aim of providing generical models independent of TrOCs and effluent samples used during development is now needed.

Recently, the use of fluorescence spectroscopy has gained a lot of interest.[64,82] Compared to a single-wavelength UV absorption approach, more differentiated spectral information (e.g. related to the underlying chemical moieties) can be extracted from these type of measurements. Due to its added value of providing a more detailed view of the entire (effluent) organic matrix, significant research has been performed in the last years for a broad range of applications. Empirical correlations have been developed for differential total fluorescence (ΔTF) related to the oxidation of a wide range of TrOCs.[64] Although much information is present, often (parts of) fluorescence spectra (so called Excitation Emission Matrices or EEMs) are used as such, without

any statistical processing or without any relation to underlying groups of chemical compounds. An overall decrease of EfOM with a certain fluorescence intensity can be expected during ozonation, although the rates of transformation may differ among different major groups of components (i.e. humic and fulvic acid-like, soluble microbial products).[133] These different reaction rates might be studied by distinguishing the component specific zones within the EEMs. In this respect, statistical methods are useful. For example, PARAFAC (parallel-factorial analysis) has been applied to monitor natural water quality,[192] and also to monitor and control different stages of wastewater treatment.[136,214] Although, PARAFAC analysis is a multi-way method that requires model development, a certain number of samples and several minutes of instrumental measurement, it allows to define the interesting wavelengths within complex EEMs. In view of online monitoring and ozone dose control, only the defined wavelength combinations can then be used together with the developed method, to significantly reduce the needed measuring time.

Given the limitations of the current (linear) surrogate models, and the possibility to use different spectral measurements, the aim of this study was to develop improved correlation models based on UVA_{254} and fluorescence for 9 TrOCs having a wide range of ozone reactivity ($k_{O3,TrOC}$ from < 1 to 10^6 M^{-1} s^{-1}) and for a broad range of ozone doses (up to ± 2 g O_3 g^{-1} DOC_{eq}). The shape of the correlations was studied to gain in depth process understanding and to provide generical knowledge that can be used to construct correlations for any compound for which $k_{O3,TrOC}$ and $k_{HO\bullet,TrOC}$ are known. Consequently, a framework to develop empirical correlations for a wide range of TrOCs is put forward. Although empirical correlations are extremely valuable for online process monitoring and control of TrOC removal, alternative models are needed to use in the early development and engineering stage of ozone reactors. Therefore, fluorescence data were thoroughly statistically processed (using PARAFAC) prior to use in those models to unravel multiple groups of components in the effluent matrix with a different reactivity towards ozone and HO•.

2 Materials and Methods

2.1 Standards and reagents

All chemicals used were of analytical grade with a purity of at least 98%. Nine TrOCs (all pharmaceuticals) have been selected based on their ozone reactivity, environmental relevance, and occurrence in WRRF effluents. Individual stock solutions, stored at -18°C in the dark, were made at 1 g L^{-1} in deionized water (0.5 g L^{-1} for trimethoprim), and used for preparing diluted mixtures. To increase the solubility, related standards were used (e.g. sodium diclofenac) or NaOH/HCl was added to the stock solutions. Consequently, all standards were soluble at this concentration as this was also an additional criteria to select these nine TrOCs.

The studied TrOCs can be classified in three groups according to their secondary reaction rates with ozone at a pH of 7 as follows: diclofenac, trimethoprim and levofloxacin (group I, $k_{O3,TrOC} > 5\times10^4$ M^{-1} s^{-1}); amitriptyline, ciprofloxacin and venlafaxine (group II, 5×10^4 M^{-1} $s^{-1} > k_{O3,TrOC} > 10$ M^{-1} s^{-1}); and amantadine, flumequine and metronidazole (group III, $k_{O3,TrOC} < 10$ M^{-1} s^{-1}). This classification is rather arbitrary and – like in other studies[40,65,215] – mainly aimed to facilitate the discussion. It is the individual apparent second order reaction rate constants ($k_{O3,TrOC}$) of each compound that will be of most importance in developing the correlation model framework within this work. Details on TrOC specific $k_{O3,TrOC}$ and $k_{HO\bullet,TrOC}$ are given in Chapter 3 (Table 3.3). Further details are also included related to the TrOCs polarity (log K_{ow}), one of the indicators of its potential sorption on e.g. sludge particles.

2.2 Experimental procedures

Secondary effluent samples were collected from a conventional activated sludge treatment of the municipal WRRF in Harelbeke, Belgium (116,100 I.E., Aquafin NV). Three grab sampling campaigns were performed at different times (further denoted as effluent 1, 2 and 3 – effluent 3 was used to verify conclusions drawn based on effluent 1 and 2). Clear differences in effluent characteristics (e.g. COD, NO_2^--N, …) were noticed when rain fall occurred before sampling (24 and 72 hours), resulting in a natural dilution of the (treated) wastewater. Further details about the amount of rain fall before sampling and information on the effluent characteristics can be found in Table 4.1.

Table 4.1: Characteristics of the sampled effluents (determined on samples without dilution; '… ± …' indicates the average and standard deviation on triplicate measurements). Details of analytical measurement methods are given in section 2.3 or in Chapter 3 (sections 2.2 and 2.4).

Effluent number	**1**	**2**	**3**
Rain fall[a] 24 hours before sampling (L m^{-2})	0.00	0.00	1.66
Rain fall[a] 72 hours before sampling (L m^{-2})	0.00	1.30	1.66
Alkalinity (mg $CaCO_3$ L^{-1})	212 ± 6	238 ± 6	264 ± 10
NH_4^+-N (mg N L^{-1})	0.157 ± 0.002	0.488 ± 0.004	0.207 ± 0.003
NO_3^--N (mg N L^{-1})	5.09 ± 0.03	2.49 ± 0.08	3.15 ± 0.03
NO_2^--N (mg N L^{-1})	0.246 ± 0.001	0.110 ± 0.001	0.084 ± 0.002
COD (mg O_2 L^{-1})	24.4 ± 0.9	27.9 ± 1.1	37.2 ± 0.7
DOCeq[b] (mg C L^{-1})	9.9	11.2	13.1
pH	7.32	7.58	7.39
Conductivity (µS cm^{-1})	935	920	905
Turbidity (NTU)	1.54	2.85	11.1
UVA_{254} (m^{-1})	19.6	22.1	25.8
IOD (mg O_3 L^{-1})	10.2 ± 0.1	12.8 ± 0.3	12.6 ± 0.3
IOD, NO_2^--N corrected (mg O_3 L^{-1})	9.4 ± 0.1	12.4 ± 0.3	12.3 ± 0.3
HO• exposure[c] (during IOD) (M.s)	1.64×10^{-10}	1.22×10^{-10}	1.24×10^{-10}

[a] rain fall provided by the monitoring station of the Flemish government (Zwevegem, www.waterinfo.be)

[b] DOC values based on the relationship with UVA_{254} and previous experiences with effluent water from the same WRRF (DOC_{eq} (mg C L^{-1}) = UVA_{254} (m^{-1}) × 1.97^{-1})[113]

[c] HO• exposure (M.s) is explained in section 2.3.[39]

Ozonation experiments were conducted in batch mode using 1 L glass reactors at room temperature and a mechanical mixer at a speed of 200 rpm (Janke & Kunkel GmbH & Co.KG, Germany). Effluent was spiked with a mixed stock solution of the selected TrOCs up to a concentration of 10 µg L^{-1} (effluent 1) and 1 µg L^{-1} (effluent 2 and 3) for each compound, to take possible effects of concentration levels into account. The spiked effluent was treated with ozone up to 17.3 mg L^{-1} (or a specific dose up to ± 2 g O_3 g^{-1} DOC_{eq}) by adding specific amounts of a

freshly prepared ozone stock solution. The stock solution was prepared by purging (ice-cooled) distilled water with an ozone/oxygen gas mixture (300 mL min^{-1}) using an oxygen-fed ozone generator (up to 8 g O_3 h^{-1}, COM-AD-02, Anseros GmbH, Germany) achieving approximately 90 mg O_3 L^{-1} in the stock solution. After ozone addition and complete reaction (30 min), distilled water was added to bring the volume of the effluent sample to 800 mL, obtaining equal dilution independent of the volume of ozone stock added (i.e. dilution < 20 %). Ozone concentrations in the stock solution were measured based on the indigo method of Bader & Hoigné.[188] The samples were analyzed for surrogate parameters and TrOCs, after storage for maximum 3 weeks at 4°C and -20°C, respectively.

2.3 Analytical methods

Details related to TrOC analysis, determination of general parameters (e.g. alkalinity, NO_2^--N, COD, EC, pH, etc.), spectral measurements (UV-VIS and 3D EEMs) and IOD, defining the rapid ozone consumption within 5 seconds after dosing, is given in sections 2.2 to 2.4 of Chapter 3. HO• exposure was determined using both pCBA (during effluent characterization) or metronidazole (during model development) as probe components due to their low $k_{O3,TrOC}$ (pCBA: < 0.1 M^{-1} s^{-1}; metronidazole: < 1 M^{-1} s^{-1})[39,65] and their high $k_{HO•,TrOC}$ (pCBA: 5.0×10^9 M^{-1} s^{-1}; metronidazole: = 6.2×10^9 M^{-1} s^{-1}).[39,65]

HO• exposures are often determined using pCBA (para-chlorobenzoic acid) as a probe compound due to its specific reaction affinity towards ozone and HO•.[216] Due to its low apparent 2nd order reaction rate constant with ozone ($k_{O3,pCBA}$ < 0.1 M^{-1} s^{-1}) and its high reaction rate with HO• ($k_{HO•,pCBA}$ = 5.0×10^9 M^{-1} s^{-1}),[39] it can be assumed that removal of pCBA is mainly due to reactions with HO• and only a negligible contribution of direct ozone reactions is assumed. Similar properties can be attributed to the pharmaceutical metronidazole (MNZ, see Table 3.3), which is part of the nine selected TrOCs within the performed batch experiments. Therefore, metronidazole can be used as an alternative of pCBA as a probe compound to estimate the HO• exposure. The calculation of HO• exposure is consequently governed by eq. 4.1.

$$HO\bullet\ exposure = \int HO\bullet .dt = \frac{ln([MNZ]_0 - [MNZ])}{k_{HO•,MNZ}} \qquad \text{eq.4.1}$$

where $[MNZ]_0$ is the initial concentration before ozone dosing and [MNZ] the concentration of metronidazole after reaction (30 min). The 2nd order rate constant with HO• is given by $k_{HO\bullet,pCBA}$ (see Table 3.3). The HO• exposure related to the IOD was determined separately and batch wise using pCBA (see eq. 4.2) as a probe compound.

$$HO\bullet\ exposure = \int HO\bullet .dt = \frac{ln([pCBA]_0 - [pCBA])}{k_{HO\bullet,pCBA}} \quad \text{eq.4.2}$$

The HO• was determined after spiking ozone to the effluent and allowing a reaction time of 5 seconds. All measurements were performed in triplicate and samples were continuously mixed at ± 300 rpm. 25 mL of effluent was spiked with 30 µL of a pCBA solution up to a concentration of 100 µg L^{-1}. Furthermore, 5.0 mL of the ozone stock solution was added. The reaction between EfOM and ozone was stopped after 5 sec by adding 1 mL of a 2.16 g L^{-1} $NaNO_2$ solution that immediately reacts with any remaining ozone. Remaining pCBA concentrations were determined by HPLC-DAD (Agilent 1100 series, USA). The stationary phase consisted of a C-18 reversed phase column (Alltima, Alltech), with 1 mL min^{-1} of eluent consisting of acetonitrile:water (50:50) adjusted to pH 2 with phosphoric acid.[216]

2.4 PARAFAC analysis

Fluorescence spectral corrections and PARAFAC analysis were performed by adapting the drEEM® toolbox in Matlab.[195] Correction of fluorescence EEMs was undertaken to minimize bias due to sample and instrumental related variability. Raw spectral data were blank corrected and sample specific matrices of correction factors for inner filter effects were applied, calculated based on UV absorbance spectra. Normalization to RU was performed afterwards and Rayleigh-Tyndell and Raman scatter lines were removed for quantitative analysis and to allow EEMs to be displayed uniformly. All samples were used for subsequent PARAFAC analysis and for integration to determine the total fluorescence (TF) of each sample.

Fluorescence intensities below an excitation wavelength of 225 nm and an emission wavelength of 281 nm were excluded from all EEMs for PARAFAC analysis based on leverage plots. Outlier samples were excluded based on outlier tests (i.e. examining the structure in the error residuals)

and leverage plots. A non-negativity constraint and random initialization were applied for the models. A model with four components could be identified (Figure 4.1). All components could be associated with different types of chemical groups with specific properties according to Chen et al.[133] Split-half analysis was performed for validation of this model using following settings: four alternating determined splits, three runs per model of two combined splits and a 10^{-10} convergence criteria. The results of this validation step (i.e. comparison of different model loadings) is given in Appendix A. Intensity values at peak wavelengths of the defined PARAFAC components are expressed as F_{max}1, 2, 3 and 4 (in RU).

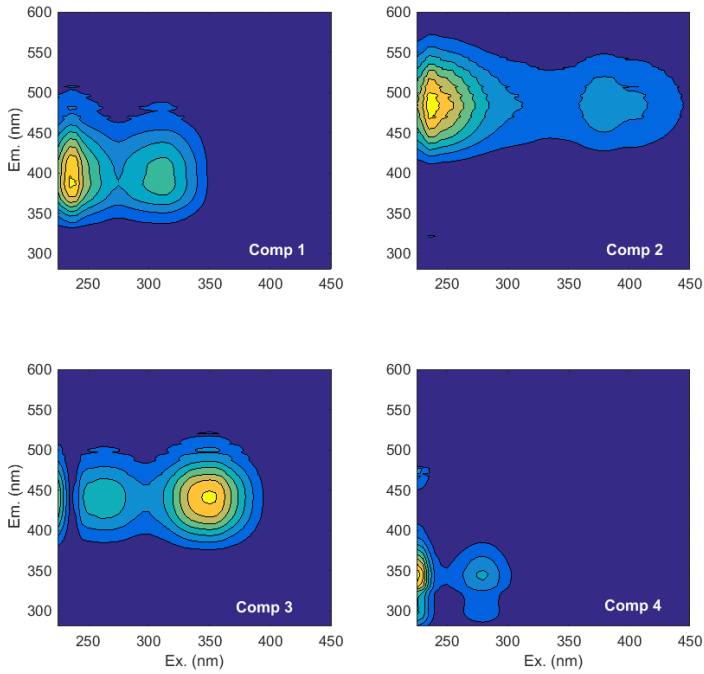

Figure 4.1: Visualized location of the defined PARAFAC components within the EEMs.

The development of a PARAFAC model requires significant computational power and is time consuming, making it impossible to perform online for control applications. After successfully constructing the PARAFAC model (as is the case in this Chapter), this model can be applied to other measurements without any additional model construction or development necessary (as is done in Chapter 5). Associated chemical groups and/or properties have been assigned to the

different components using peak allocation and the wavelengths defined by the PARAFAC model. The research from Chen et al.[133] and Ishii and Boyer[214] – and the presented graphs and tables associating the wavelengths of the 3D EEM spectrum with different chemical groups and properties – has been compared to the detected PARAFAC components in the this study. The result of this is summarized in Table 4.2.

Table 4.2: Peak wavelengths and chemical groups/properties associated with the defined components during PARAFAC analysis of all EEMs.

PARAFAC component	**Peak wavelengths (nm)**		**Associated chemical groups/properties** (based on [133,214])
	Ex.	Em.	
1	235 310	385	Fulvic acids Less hydrophobic
2	235 380	487	Fulvic acids Hydrophobic Larger[b] molecular size
3	260 350	440	Humic acids Hydrophobic Large molecular size
4	225[a] 280	345	Trypthophan and protein-like Small molecular size

[a] peak at edge of EEM during PARAFAC analysis

[b] compared to PARAFAC component 1 and based on components exhibiting similar intensities around the same excitation and emission wavelengths in literature[214]

Component 1 (Ex. 235 & 310 nm; Em. 385 nm) and 2 (Ex. 235 & 380 nm; Em. 487 nm) both represent fulvic acid-like moieties based on prior studies defining the region of intensities related to specific chemical moieties.[133] Component 2 is expected to consist of hydrophobic compounds whereas component 1 is probably less hydrophobic with a smaller molecular size. Ishii & Boyer [214] also showed, indicated by the shorter excitation and emission peak wavelengths, a positive association between compounds in the former region and a smaller molecular size. Component 3 (Ex. 260 & 350 nm; Em. 440 nm) is affiliated with humic acid-like moieties, hydrophobic in nature, and a rather large molecular size (indicated by higher peak wavelengths). Tryptophan and protein-like compounds with a rather small molecular size exhibit fluorescence intensity in the

region of component 4 (Ex. 225 & 280 nm; Em. 345 nm).[133] More information on the location of the defined fluorescence components is given in. Although the main goal of this manuscript is to develop a reliable framework of correlation models rather than to define specific regions in EEM spectra, these peak allocations provide supporting information for data interpretation.

3 Results and Discussion

3.1 Surrogate correlation patterns of TrOCs

The abatement pattern of each TrOC was related to changes in UVA_{254}, TF and F_{max}1-4. Figure 4.2 to Figure 4.7 shows the percentage of elimination of each TrOC in relation with the decrease of UVA_{254}, TF and the PARAFAC components (F_{max}1, 2, 3 and 4), respectively. The TrOC abatement and the decrease of each surrogate in relation to the added ozone dose (in g O_3 g^{-1} DOC_{eq}) is given in Appendix B (Figure B.1 and Figure B.2). Group I compounds (diclofenac, levofloxacin and trimethoprim) with the highest $k_{O3,TrOC}$ showed complete removal at 25% ΔUVA_{254}, 52% ΔTF, 54% ΔF_{max}1, 37% ΔF_{max}2, 61-65% ΔF_{max}3 and 51% ΔF_{max}4. Group II compounds (amitriptyline, ciprofloxacin and venlafaxine) only showed complete removal starting from 29-33% ΔUVA_{254}, 56-66% ΔTF, 60-70% ΔF_{max}1, 42-54% ΔF_{max}2, 68-73% ΔF_{max}3 and 57-70% ΔF_{max}4. Amantadine, flumequine and metronidazole (Group III) were not completely removed at the observed maximal ΔUVA_{254} (47%), ΔTF (81%), ΔF_{max}1 (84%), ΔF_{max}2 (70%), ΔF_{max}3 (83%) and ΔF_{max}4 (90%). It should, however, be stated that the data related with F_{max}4 were highly scattered (hence its 4th rank during PARAFAC analysis) which makes it hard to draw strong conclusions from this surrogate parameter. Nevertheless, other F_{max} parameters showed clear abatement patterns with only limited scattering.

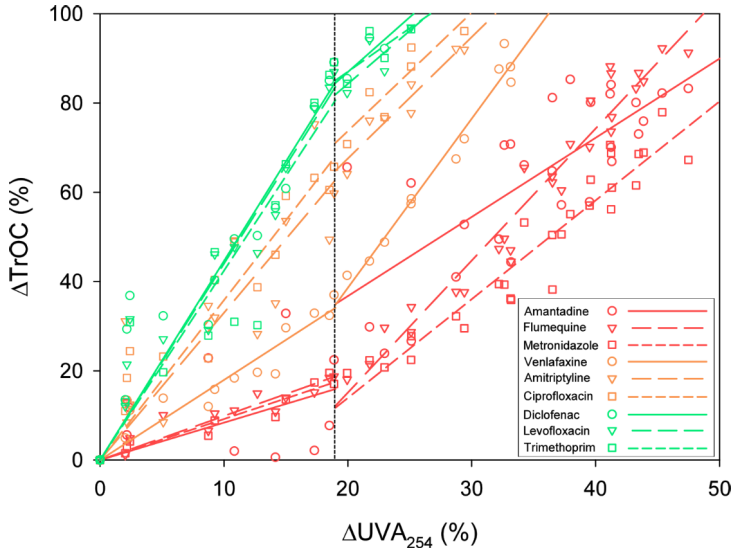

Figure 4.2: Abatement pattern of TrOCs in relation to ΔUVA_{254}, divided in two phases related to the main occurring mechanisms (dotted line indicates the inflection point).

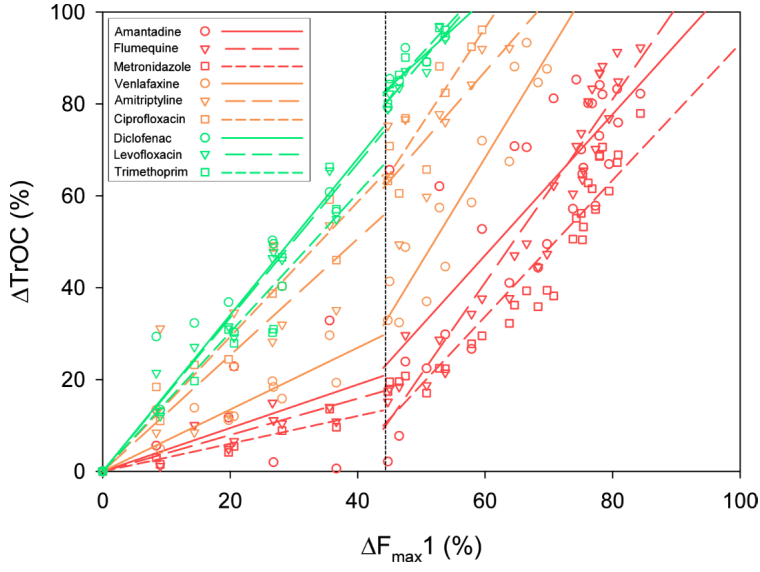

Figure 4.3: Abatement pattern of TrOCs in relation to $\Delta F_{max}1$, divided in two phases related to the main occurring mechanisms (dotted line indicates the inflection point).

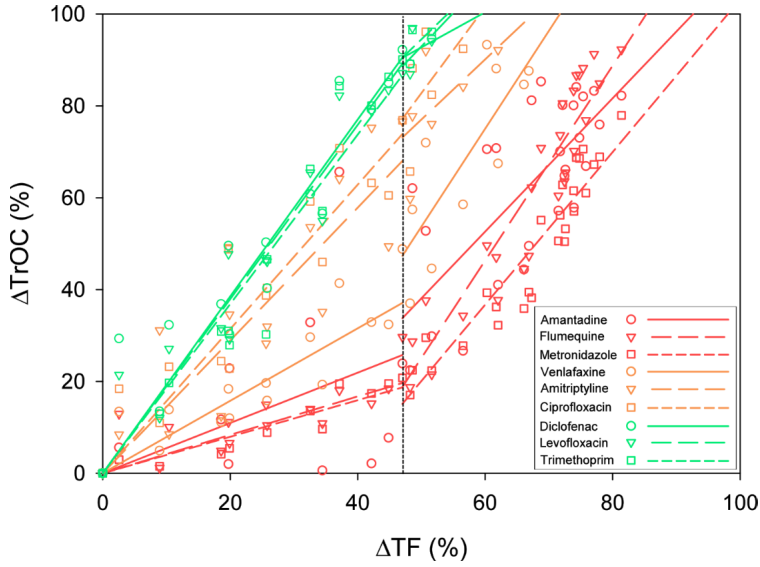

Figure 4.4: Abatement pattern of TrOCs in relation to ΔTF, divided in two phases related to the main occurring mechanisms (dotted line indicates the inflection point).

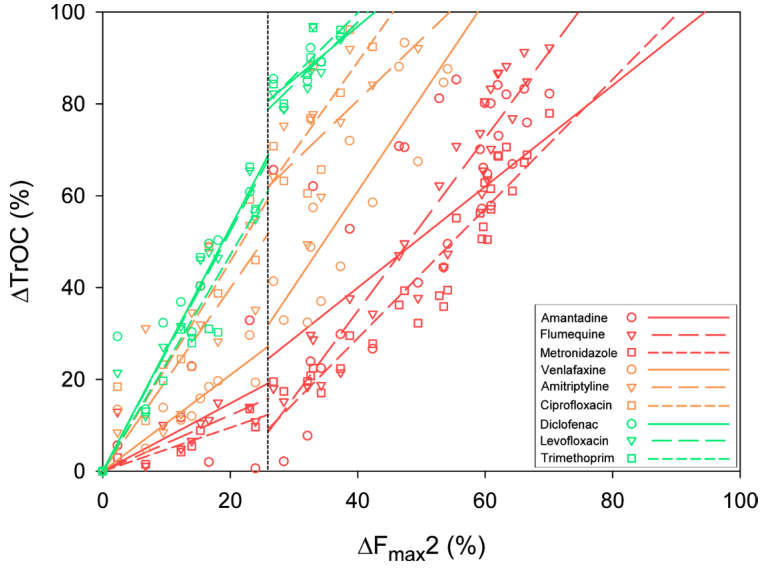

Figure 4.5: Abatement pattern of TrOCs in relation to $\Delta F_{max}2$, divided in two phases related to the main occurring mechanisms (dotted line indicates the inflection point).

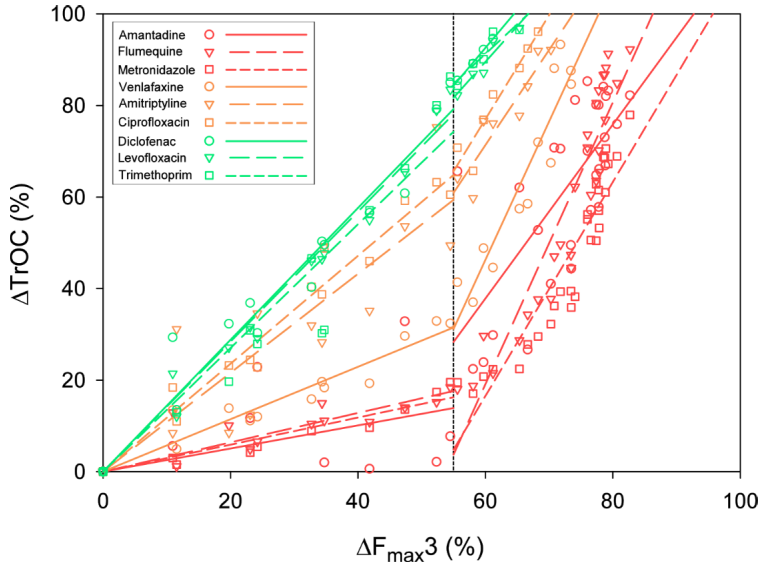

Figure 4.6: Abatement pattern of TrOCs in relation to $\Delta F_{max}3$, divided in two phases related to the main occurring mechanisms (dotted line indicates the inflection point).

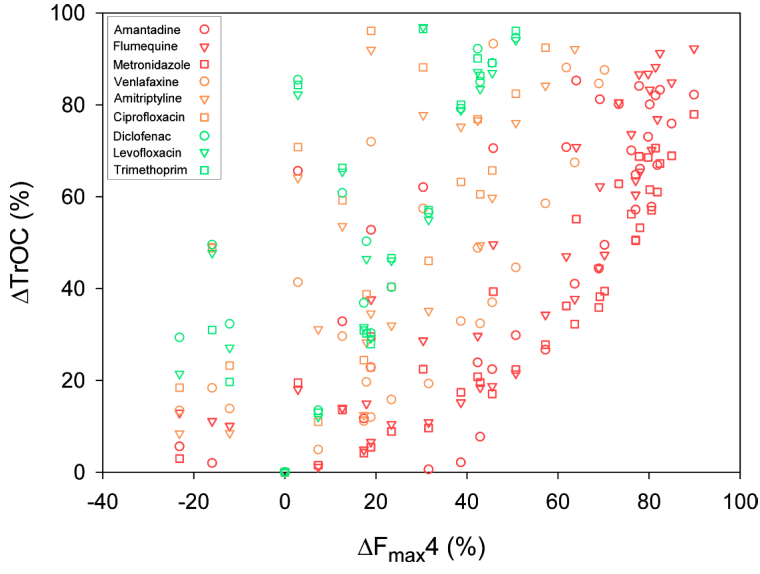

Figure 4.7: Abatement pattern of TrOCs in relation to $\Delta F_{max}4$.

3.1.1 TrOC abatement related to ΔUVA_{254}

A linear relationship, as assumed by most authors[40,63,64,82,100,103,113,114], was not able to describe in a representative way the observed trend over the full ΔUVA_{254} and $\Delta TrOC$ range in Figure 4.2, especially for the group III compounds. The shape of the curves is more complex and can be related to the main occurring reaction mechanisms. At low ozone doses, and corresponding low ΔUVA_{254}, removal of pollutants and EfOM is mainly due to direct ozone reactions. This is supported by the relatively high values for rapid ozone consumption, often referred to as "instantaneous" ozone demand, which were between 7.7 and 10 mg O_3 L^{-1} for the studied effluents (considering dilution during experimentation and a NO_2^--N correction). Systematically increasing the ozone dose (and consequently higher ΔUVA_{254}) results in a significant increased removal of the pharmaceuticals within group III, while the removal of group I compounds slightly levelled off as function of ΔUVA_{254}. Overall, two main hypotheses are put forward to explain the observed phenomena: (i) transformation of the organic matrix leads to products with higher HO• production yields, as proposed by Audenaert et al.[113] and Lee et al.[98], and/or (ii) after an initial reaction phase with fast direct ozone reactions, residual dissolved ozone starts occurring that can react further with hydroxyl ions, forming HO• or other oxidative radicals (autocatalytic decomposition).[112] It is clear that HO• production relies on a complex mechanism that is significantly affected by oxidant induced changes of the EfOM properties.[126] During the initial phase, where most reactive moieties react with ozone, very high transient HO• concentrations have been observed, hereby playing an essential role during the oxidation processes.[126] For example, HO• exposure of all effluents, measured during IOD determination, amounted on average $(1.37 \pm 0.24)\times10^{-10}$ M.s, i.e. 56% of the maximum obtained HO• exposure during all experiments (see further, Figure 4.13). It was assumed by Audenaert et al.[113] that the degree of hydroxylation when ozonation proceeds might increase. New electron rich moieties (e.g. phenolic compounds) may be formed which may lead to a higher HO• production.[55,126] Additionally, prolonged ozonation results in a residual concentration of dissolved ozone, and ozone decomposition can be assumed to be further controlled by a radical chain reaction and not by its direct reaction with moieties present in the EfOM. This is in contrast with the initial phase in which chain reactions or autocatalytic decomposition seem not to play a key role.[121] Such radical chain reactions are extensively described elsewhere.[112,165]

Based on the reactions discussed above, the entire range of ΔUVA_{254} can be divided into two sections (Figure 4.2). In phase 1, transformation of target compounds and EfOM is dominated

by rapid ozone reactions. Starting phase 2, highly ozone reactive compounds have already been degraded and indirect (less selective) HO• radicals dominate the reaction pathways. For both phases and for each TrOC, a distinct linear relationship could be obtained between ΔTrOC and ΔUVA_{254}. No intercept was considered for the first part as it was not statistically significant ($p > 0.05$ for all nine TrOCs separately). The location of the inflection point (19% ΔUVA_{254}) was determined minimizing the standard error between the predicted values (based on the two part linear function) and the experimental data points. From a methodological point of view, a more detailed approach compared to most already published studies (as listed during the introduction e.g.[40,63,64,103]) was used, as up to 20 data points/measurements are taken into consideration within a range from 0 to 47% ΔUVA_{254} for each experiment.

Relating the slope of phase 1 (a_{p1}, obtained from Figure 4.2) to $k_{O3,TrOC}$ showed a logarithmic relation with a good fit ($R^2 = 0.77$, n = 7, Figure 4.8a). Therefore, a linear regression has been performed according to eq. 4.3. Logically, ozone-based degradation of TrOCs in a near neutral pH environment strongly depends on $k_{O3,TrOC}$.[98] Zimmerman et al. [45] already suggested that mostly a correlation between the removal of the component and the $k_{O3,TrOC}$ occurs. Lee et al.[65] observed similar TrOC abatement in different WRRF effluents when normalizing the applied ozone dose to the initial DOC. Consequently, the relationship as presented in Figure 4.8a (and eq. 4.3 with regression coefficients m and b (i.e. intercept)) allows to estimate other correlations (between ΔTrOC and ΔUVA_{254}) for TrOCs not selected in this study, if $k_{O3,TrOC}$ is known (i.e. a generical applicable correlation model is put forward).

The correlation in phase 2 of Figure 4.2 shows no dependency on the $k_{O3,TrOC}$ (Figure 4.8b). In addition, no statistical difference was noticed between the average slopes of each TrOCs group, with an overall averaged slope of 2.54 ± 0.60 (n = 9). This supports the hypothesis that, independent of the affinity of each TrOC towards ozone, unselective reactions with HO• play a more prominent role in phase 2. In contrast to the $k_{O3,TrOC}$ of the nine TrOCs (differences with several orders of magnitudes), the $k_{HO•,TrOC}$ has a much smaller variation (all in the same order of magnitude, see Table 3.3). Consequently, it is difficult to make a strong correlation between the $k_{HO•,TrOC}$ and slope in phase 2.

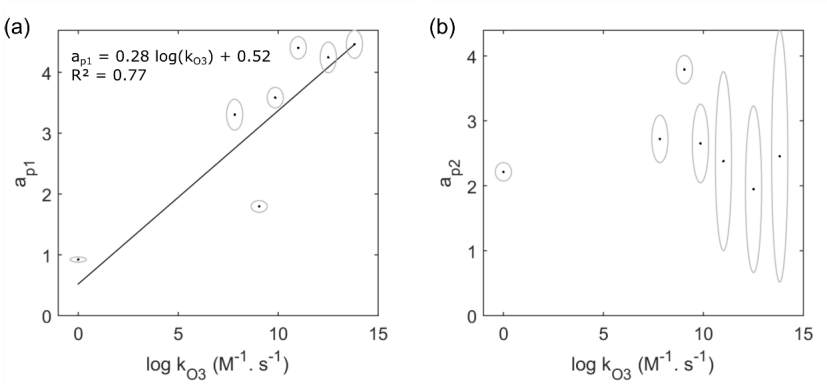

Figure 4.8**:** Relationship between the TrOC $k_{O3,TrOC}$ (see Table 3.3) and the slope of (a) the first phase and (b) the second phase linear correlations between ΔTrOC and ΔUVA_{254}. Data points are given from left to right for metronidazole, amitriptyline, venlafaxine, ciprofloxacin, levofloxacin, trimethoprim and diclofenac (in order of increasing $k_{O3,TrOC}$). The error on a_{p1}, a_{p2} and $k_{O3,TrOC}$ is indicatively shown by a circle around the data point.

The given approach is somewhat in line with recent available literature also including a two phase relation between ΔTrOCs and ΔUVA_{254} (or ΔTF), confirming the need of considering multiple phases in the correlation model of this work. Park et al.[54] used a kinetic approach by including also the R_d constant and empirically determined parameters, attributing the contribution of ozone and HO• during two reaction phases. This approach is highly interesting establishing operational control points and helps to determine regulatory and performance requirements. Also Nanaboina and Korshin[100] used a kinetic approach including empirically determined parameters (i.e. water or TrOC specific) to correlate ΔTrOCs and ΔUVA_{254}. However, the currently considered fixed empirical parameters are depending on a varying water quality (or are TrOC specific) and therefore some additional offline work still needs to be done. For online control, the empirical correlation model of the current work seems advantageous although both are of value for full-scale applications.

The above observations taken into account, the abatement of every possible target TrOC can be predicted using eq. 4.4 ($\Delta S \leq I$) and eq. 4.5 ($\Delta S \geq I$), with ΔS the decrease of the surrogate measurement (e.g. ΔUVA_{254}) and I the inflection point (solely depending on the surrogate e.g. 19 % ΔUVA_{254}) between both correlations. The shape of the entire curve, including the two phases, will be determined by the ratio of the $k_{O3,TrOC}$ versus the $k_{HO\bullet,TrOC}$ of the TrOC, as is exemplified by the different curve shapes of compounds belonging to the defined groups in this study. This

prediction allows for online monitoring if combined with eq. 4.3. Non-continuous correlations were used for curve fitting to handle both phases separately and to be able to interpret the relations during each phase independently. Correlations for the TrOCs (excluding amantadine) showed minor changes (< 7% for ΔUVA_{254}) near the intersection or inflection point, resulting in almost equality of both curves for most TrOCs at the inflection point. The deviation of amantadine had to deal with a lot of scattering, especially in the low ΔUVA_{254} region. This component was consequently not used further for the regression between the slope of phase 1 and the $k_{O3,TrOC}$.

$$a_{p1} = m \times \log(k_{O3,TrOC}) + b \qquad \text{eq. 4.3}$$

$$\Delta TrOC_{0 \rightarrow inflection} = a_{p1} \times \Delta S \qquad \text{eq. 4.4}$$

$$\Delta TrOC_{inflection \rightarrow \ldots} = a_{p1} \times I + a_{p2} \times (\Delta S - I) \qquad \text{eq. 4.5}$$

Of course, there is some uncertainty on both a_{p1} and $k_{O3,TrOC}$, which has been experimentally determined during previous curve fitting (a_{p1}) or which has been based on a conventional order of error that is often seen for reaction rate constants (i.e. 50% for $k_{O3,TrOC}$). These uncertainties might explain the outlier value of venlafaxine (Figure 4.8a). Noteworthy is that $k_{O3,TrOC}$ values (at pH 7) should be used with caution. Uncertainties thereon should always be considered as actual values that can be strongly influenced by experimental errors or by even slight changes in conditions (such as pH) due to alterations in speciation (neutral/charged).[111] Also the presence of large molecular structures, e.g. humic acid-like moieties, having low dissociation rates can affect species speciation having pK_a values close to near neutral pH (i.e. the natural effluent pH). These uncertainties have been taken into account for the determination of both m and b (and the error thereon) in the linear regression (eq. 4.3) by using the technology proposed by York et al.[217] Using a sampling technology, the uncertainty on the model predictions of ΔTrOC can be determined accordingly. This analysis has been done for a sample size of 10 000 using Sobol sampling.[218] The model parameters included in the analysis and their uncertainty are also listed in Table 4.3. Finally, the 95% confidence interval is determined as demonstrated in Figure 4.9 for ΔUVA_{254}. Further elaboration is given during the model validation described in Chapter 5.

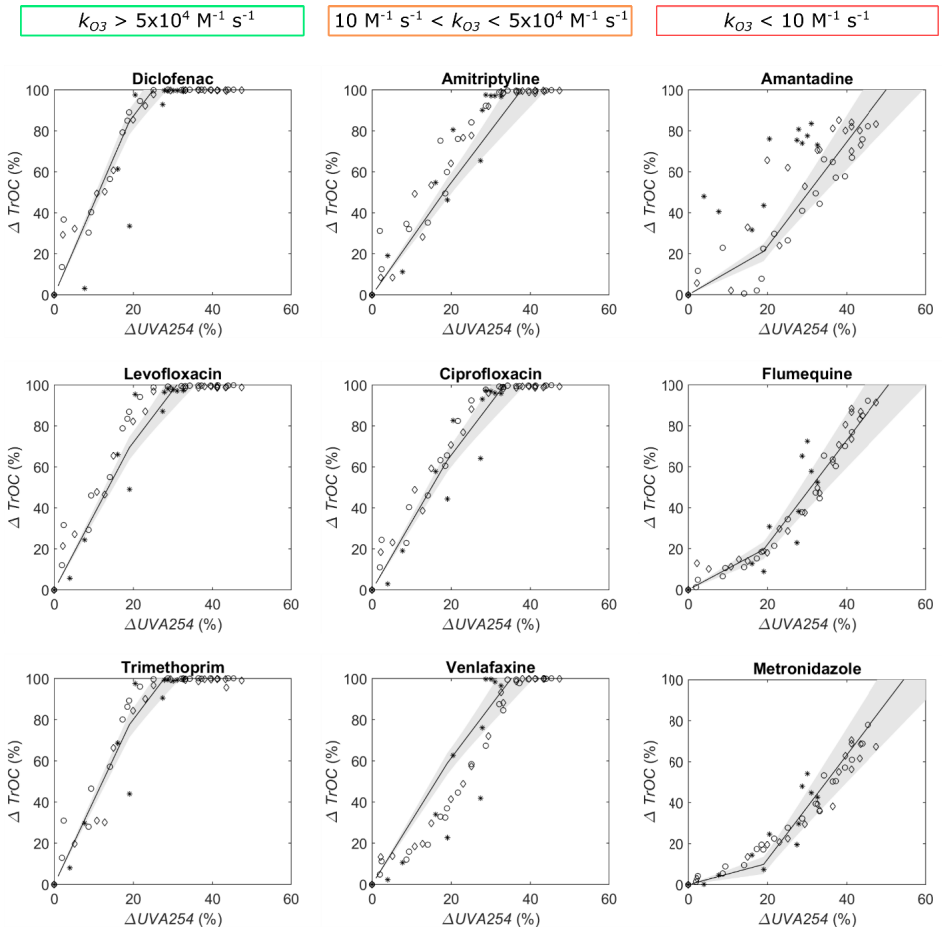

Figure 4.9: Abatement pattern for each individual TrOC in relation with ΔUVA_{254}. Data are obtained from measurements on effluent 1 (○), 2 (◊) and 3 (*). Correlations are drawn based on the developed model and the $k_{O3,TrOC}$ given in Table 3.3. The grey areas are indicating the 95% confidence interval of the calculated correlation.

3.1.2 TrOC abatement related to fluorescence based surrogates

The relationship between ΔTrOC and both ΔTF and ΔF_{max}1-3 could be described in a similar way as for ΔUVA_{254}. Surrogates including the largest share of the EEMs, and therefore containing the most spectral information (i.e. representing absorbance or intensities for a broader range of chemical moieties) showed a higher maximal removal (ΔTF = 81%, $\Delta F_{max}1$ = 84%, $\Delta F_{max}2$ = 70% and $\Delta F_{max}3$ = 83%; Figure 4.2 to Figure 4.7) than UVA_{254} (47%). Nevertheless, it is clear that each defined fluorescent component exhibits a mutually different behavior during the oxidation processes. A higher decrease of fluorescence intensity was observed before reaching the inflection point, compared to UVA_{254}. Inflection of the curves was only established at 55% $\Delta F_{max}3$ and at 47% ΔTF, 44% $\Delta F_{max}1$ and 26% $\Delta F_{max}2$. The data related to $F_{max}4$ (containing the least amount of spectral information, given its 4th rank) were highly scattered. $F_{max}4$ was not further considered as no significant correlations were found, most likely due to the limited amount of effluent samples used for building the correlations and the high variability in $F_{max}4$ data.

The relationship between the slope of the linear correlations in phase 1 (through the origin) and the $k_{O3,TrOC}$ showed a logarithmic behavior with a good match (R^2 = 0.75 - 0.76, n = 7, Figure 4.10a and Figure 4.11a,c,e). As already noticed for UVA_{254}, the slope of the correlation in phase 2 showed no dependency on the $k_{O3,TrOC}$ (Figure 4.10b and Figure 4.11b,d,f) and the average of the slopes of each TrOC group was found to be not statistically different (Table 4.3). This confirms the results obtained with UVA_{254} and shows that abatement predictions of TrOCs can be done using similar equations as eq. 4.3-4.5 for fluorescence surrogates. In association, the 95% confidence interval is determined as demonstrated in Figure 4.12 ($\Delta F_{max}1$) and in Appendix B (ΔTF and $\Delta F_{max}2$-3). Further elaboration is given during the model validation described in Chapter 5.

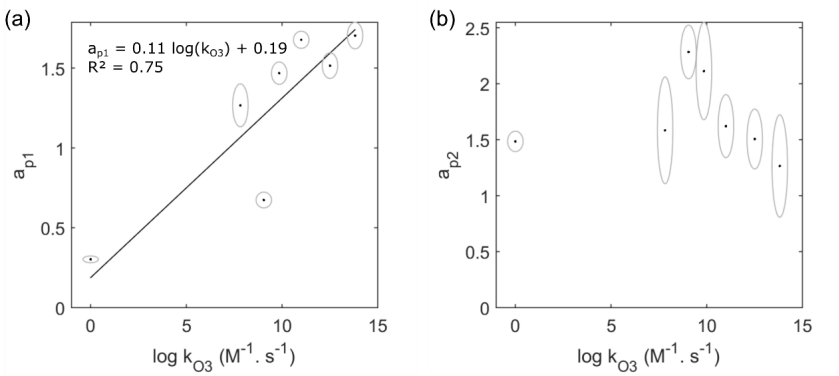

Figure 4.10**:** Relationship between the TrOC $k_{O3,TrOC}$ (see Table 3.3) and the slope of (a) the first phase and (b) the second phase linear correlations between ΔTrOC and $\Delta F_{max}1$. Data points are given from left to right for metronidazole, amitriptyline, venlafaxine, ciprofloxacin, levofloxacin, trimethoprim and diclofenac (in order of increasing $k_{O3,TrOC}$). The error on a_{p1}, a_{p2} and $k_{O3,TrOC}$ is indicatively shown by a circle around the data point.

Table 4.3: Slopes of the correlations between the removal of TrOCs and decrease in surrogate measurements (a_{p1} represents the slope of the first phase, based on the apparent second order reaction rate constant with ozone ($k_{O3,TrOC}$); a_{p2} represents the slope of the second phase; and the percentage decrease of the surrogate at the inflection point between both phases is given by I, %).

Surrogate	I (%)	$a_{p1} = m \times \log(k_{O3,TrOC}) + b$ ($k_{O3,TrOC}$ dependent)		a_{p2} ($k_{O3,TrOC}$ independent)
		m	b	
ΔUVA_{254}	19	0.28 ± 0.02	0.52 ± 0.13	2.54 ± 0.60
$\Delta F_{max}1$	44	0.11 ± 0.01	0.19 ± 0.05	1.71 ± 0.34
$\Delta F_{max}2$	26	0.16 ± 0.01	0.36 ± 0.08	1.54 ± 0.33
$\Delta F_{max}3$	55	0.10 ± 0.01	0.08 ± 0.05	2.13 ± 0.62
ΔTF	47	0.12 ± 0.01	0.30 ± 0.05	1.57 ± 0.44

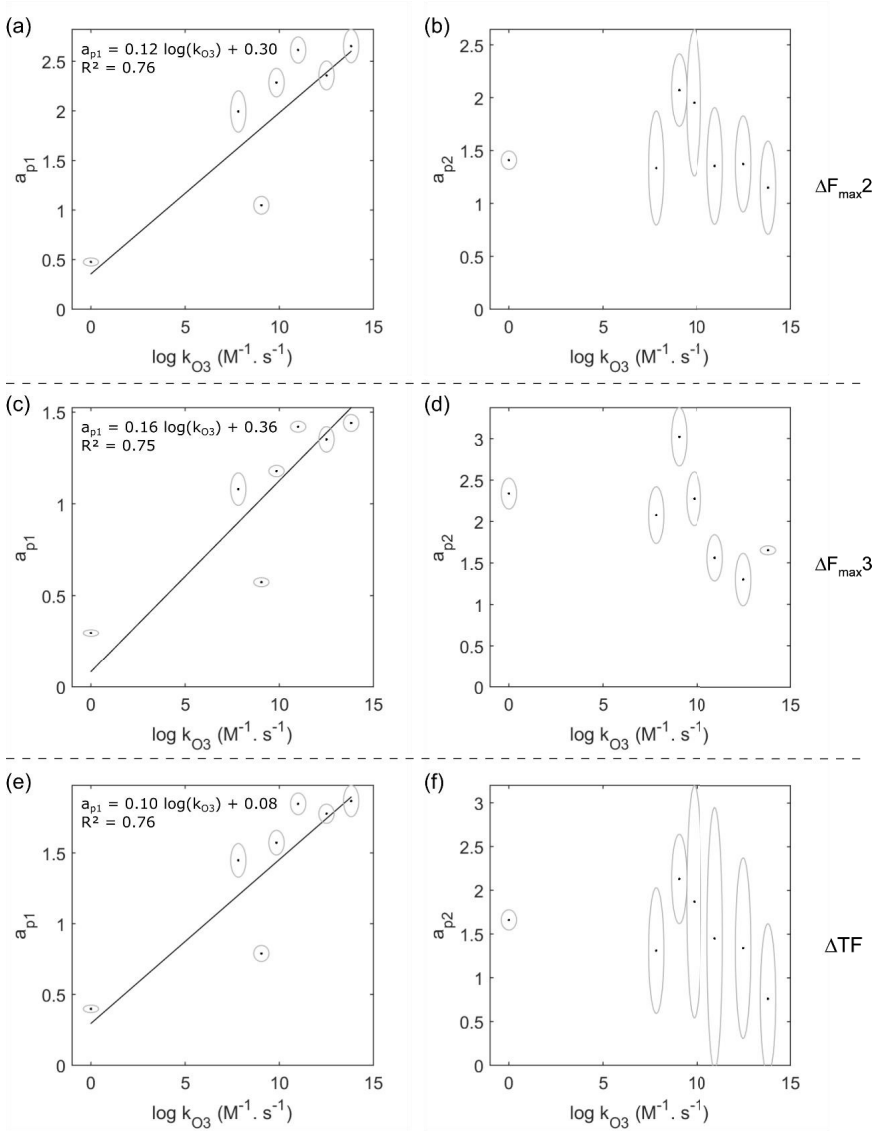

Figure 4.11**:** Relationship between the TrOC $k_{O3,TrOC}$ (see SI-Table 1) and the slope of the linear correlation between ΔTrOC and $\Delta F_{max}2$ (a-b), $\Delta F_{max}3$ (c-d) or ΔTF (e-f),. (a, c, e) represent the region related to reaction phase 1, while (b, d, f) represent the region related to the reaction phase 2. Data points are given from left to right for metronidazole, amitriptyline, venlafaxine, ciprofloxacin, levofloxacin, trimethoprim and diclofenac (in order of increasing $k_{O3,TrOC}$). The error on a_{p1}, a_{p2} and $k_{O3,TrOC}$ is indicatively shown by a circle around the data point.

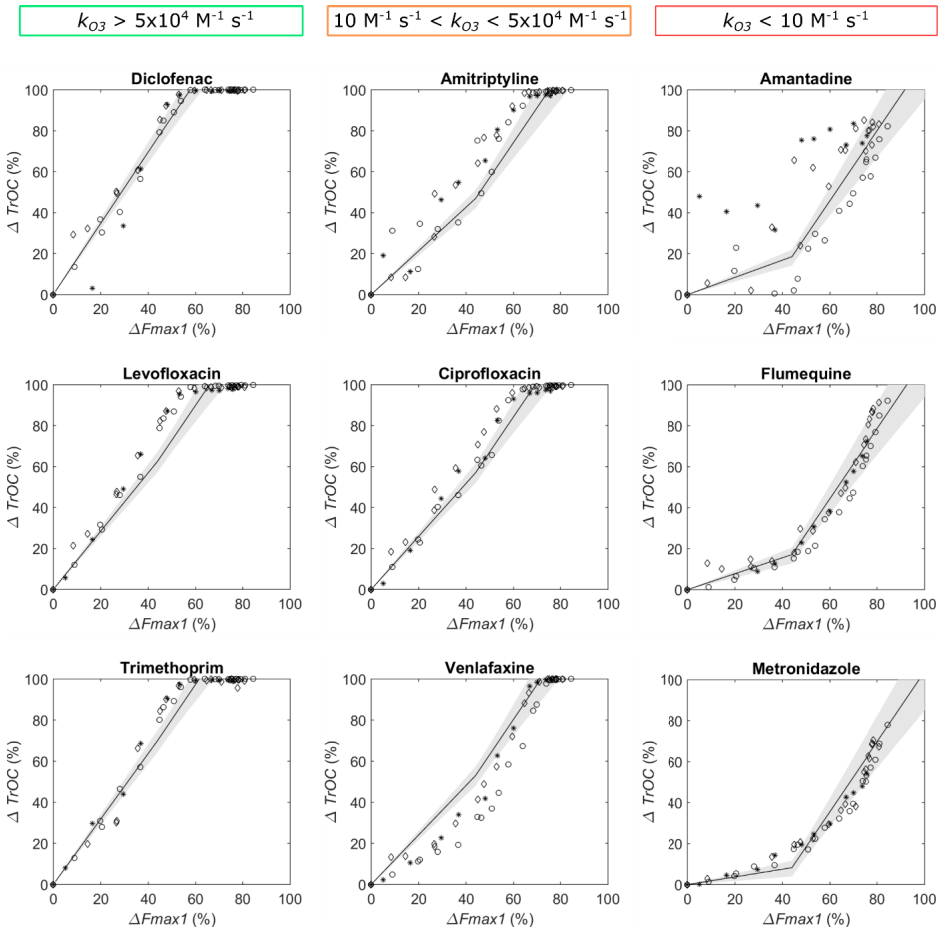

Figure 4.12: Abatement pattern for each individual TrOC in relation with $\Delta F_{max}1$. Data are obtained from measurements on effluent 1 (○), 2 (◊) and 3 (*). Correlations are drawn based on the developed model and the $k_{O3,TrOC}$ given in Table 3.3. The grey areas are indicating the 95% confidence interval of the calculated correlation.

3.1.3 Verification of the applicability of the surrogate-based correlation models

The developed correlations based on UVA_{254} and fluorescence surrogates were applied on an independent set of data (effluent 3) and were able to describe ΔTrOC with a good agreement between predicted and measured values. This is confirmed by Theil's inequality coefficient (TIC)[219] being all below 0.3 (the cut-off value), indicating a good agreement. The goodness-of-fit

between predicted and measured values can be quantified by calculating the TIC and is expressed by eq.4.6, where y_i represents the predicted data points and $y_{m,i}$ representing the measured data points.

$$TIC = \frac{\sqrt{\sum_i (y_i - y_{m,i})^2}}{\sqrt{\sum_i y_i^2} + \sqrt{\sum_i y_{m,i}^2}} \quad \text{eq. 4.6}$$

Although some variation on the individual data points is noticed compared to the developed correlations, they are mostly near the 95% confidence interval of the model (Figure 4.9, Figure 4.12 and Figure B.3-Figure B.5). This is particularly true when using fluorescence measurements (TF and F_{max}1-3, Figure 4.12 and Figure B.3-Figure B.5), being a careful indication of a potentially more robust relationship between ΔTrOC and the decrease of fluorescence compared to the use of UVA_{254}. The higher turbidity of effluent 3 indicates the presence of a larger amount of solids, compared to effluents 1 and 2 used for model development. This might have affected the ozonation process and/or the spectroscopic measurements (i.e. the increased degree of scattering for effluent 3). Zucker et al.[220] already clearly showed an under-prediction of TrOC degradation using relationships based on e.g. O_3:DOC ratios, which was attributed to the presence of solids. Zimmerman et al.[45] observed an over-prediction of TrOCs oxidation in a full-scale installation when applying a semi-empirical model in which the presence of solids was not accounted for. Although not investigated in detail within this study, the model compounds within this study reflect a wide range in log K_{ow} values (see Table 3.3) and suspended solids might be responsible for their sorption.[220]

The different plots in Figure 4.2 to Figure 4.7 also indicate that a certain background level of UVA_{254} or fluorescence intensity might be considered when controlling the ozone dose for ΔTrOCs. Mainly for TrOCs belonging to group III, their concentration is still significantly reducing, even if the further decrease in surrogate is very limited. This is exemplified by an almost vertical increase of the relationships depicted in the Figures. Comparable findings by Nöthe et al.[55] indicate that a maximal decrease of UVA_{254} and fluorescence should be considered. In this context, van der Helm[221] also hypothesized a stable background UVA_{254} level after completion of the ozonation process, which they incorporated within a model for drinking water applications. After removing a certain amount of organic matter, it seems that further ozonation and thus

changes in the matrix composition do not lead to significant changes of UVA_{254} or other surrogate measurements (also noticeable in Figure B.2). Potentially, the first stage of oxidation results in a significant reduction of absorbance or fluorescence related to the breakdown of complex organic matter and to simultaneous reduction of aromaticity, as also observed during chlorination and ozonation of natural organic matter in prior studies.[39,222,223] Also reactions with EfOM species (e.g. aromatics) could generate components (e.g. aldehydes or ketones) that continue to absorb light at wavelengths used in the spectrophotometric measurements.

3.2 HO• exposure

The usefulness of HO• exposure measurements has already been indicated for predicting removal efficiencies of ozone-refractory TrOCs, although requiring measurements of probe compounds like pCBA.[98] The HO• exposure determined in three different effluents at various initial ozone concentrations is plotted in Figure 4.13a and shows a maximum of 2.4×10^{-10} M.s.

The HO• exposure increases exponentially ($R^2 = 0.75$, n = 48) with an increasing ozone dose. The little amount of HO• formed at low ozone doses is presumably due to the ozone consumption by NO_2^--N (calculated to be between 0.2 and 0.7 mg O_3 L^{-1}, Table 4.1; associated with maximum 0.1 g O_3 g^{-1} DOC), and because of the fraction of EfOM that is prone to direct ozone attacks. Although Lee et al.[98] described a linear relation between the specific ozone dose (up to 1.75 g O_3 g^{-1} DOC) and HO• exposure, they also determined a threshold value (varying between 0.06 – 0.24 g O_3 g^{-1} DOC) below which no or little radical production was noticed. The non-linear relationship between HO• exposure and specific ozone dose as observed in Figure 4.13a is likely to be attributed to the availability of data at very low ozone doses (i.e. higher resolution) and the high initial ozone demand of the used effluent samples. An increased number of data consequently results in a more pronounced view on the curve of the relationship. The abatement profile of TrOCs within group III clearly show similarities with the regression in Figure 4.13a. Group III pharmaceuticals only react in a limited extent at low ozone doses. Similar to this research, also Nöthe et al.[55] observed only a significant enhanced removal of ozone refractory components after dosing ± 0.5 g O_3 g^{-1} DOC.

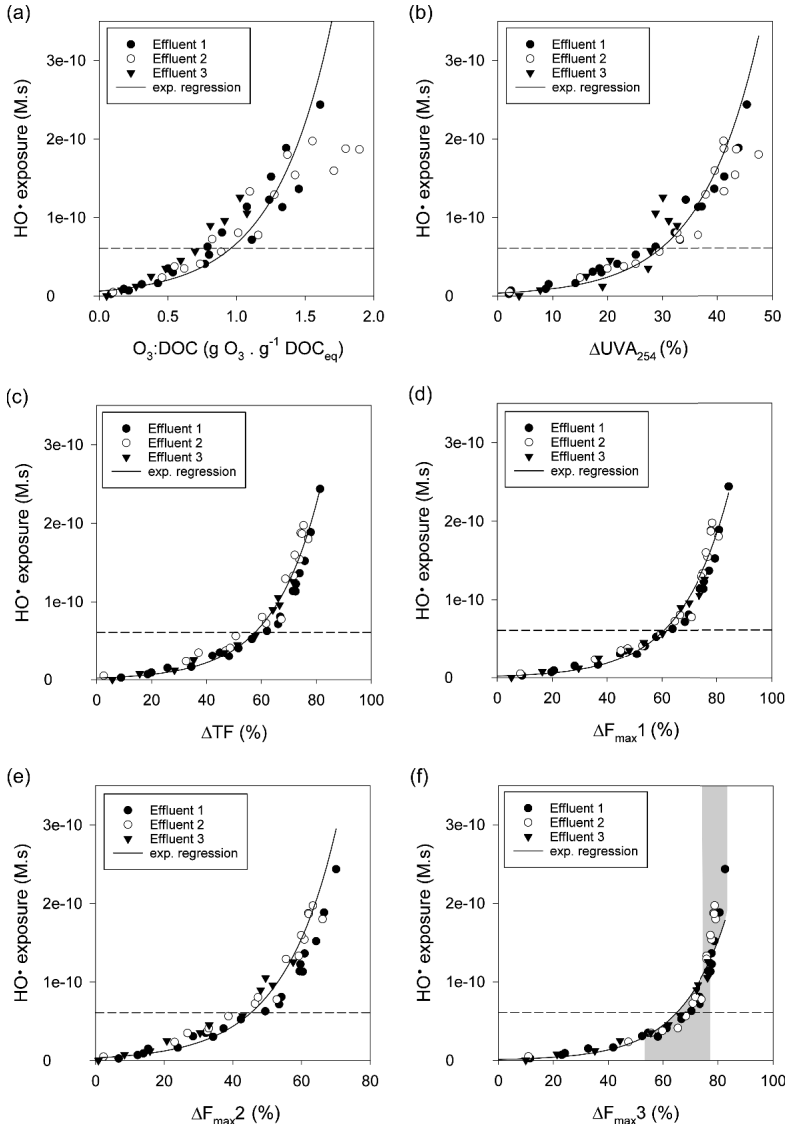

Figure 4.13: HO• exposure determined in three different effluent samples, correlated exponentially with the initial O_3:DOC_{eq} dose (a), ΔUVA_{254} (b), ΔTF (c) and ΔF_{max}1-3 (d-f). Grey shaded areas are added for visual aid in (f) and are referred to in the text. (the dotted line indicates the 25% level of the maximally obtained HO• exposure)

The determined HO• exposures were correlated to the surrogate measurements, as a good agreement (exponential function; n = 48) was found between HO• exposure and ΔUVA_{254} (R^2 = 0.82), ΔTF (R^2 = 0.89), $\Delta F_{max}1$ (R^2 = 0.90), $\Delta F_{max}2$ (R^2 = 0.86) and $\Delta F_{max}3$ (R^2 = 0.90). The correlation between HO• exposure and surrogate measurements as presented in Figure 4.13b-f shows the ability of using UVA_{254} or fluorescence measurements instead, yielding a potential online and direct estimation. Although all surrogate measurements exhibit a similar shape related to HO• exposure, it is noticed that especially $\Delta F_{max}3$ exhibit a more inflected curve with a steeper incline at the higher removal percentages (compared to ΔUVA_{254}, $\Delta F_{max}1$-2 and ΔTF, Figure 4.13b-e) which is not described by the exponential relation (grey shaded in Figure 4.13f). To quantify such differences, the change of ΔUVA_{254}, ΔTF, and $\Delta F_{max}1$-3 for an increase in the HO• exposure from 25% up to 50, 75 and 100% of the maximally obtained HO• exposure during experimentation, is plotted in Figure 4.14. It is clear that a HO• exposure increasing above 25% of its maximum value (arbitrary selected based on observations) has only limited impact on $\Delta F_{max}3$, $\Delta F_{max}1$ and – to a slightly lesser extent – ΔTF, compared to ΔUVA_{254} and $\Delta F_{max}2$. A maximum additional (relative) decrease of 49 and 48% is noticed for respectively ΔUVA_{254} and $\Delta F_{max}2$, while this amounts only 32 and 27% for $\Delta F_{max}1$ and $\Delta F_{max}3$. This underlines a difference in affinity of the different surrogate parameters towards the reactions occurring during the ozonation process. While UVA_{254} and $F_{max}2$ indicate to be mainly associated with reaction pathways induced by both direct and indirect ozone reactions, $F_{max}1$ and $F_{max}3$ are probably dominated by direct ozone reactions instead of indirect (HO•) reactions. A more in-depth kinetic study is recommended to further elucidate these findings. Nevertheless, an explanation can be found also by considering the properties of the different chemical groups showing intensities within the $F_{max}1$ and $F_{max}3$ spectral regions. Both are described as fulvic and humic acid-like matter, respectively, prone to molecular weight changes[224] and – based on the observations of this study – probably with a high degree of aromaticity.[193] Swietlik et al.[224] also concluded that especially hydrophobic acids consisting of C_5-C_9 aliphatic carboxylic acids and humic acids, characterized with a high degree of aromaticity, showed a high reactivity for ozone. Although UVA_{254} is generally known as a parameter to describe aromaticity, it is also known that moieties not reacting well with ozone absorb at this wavelength as well.[221] Organic matter associated with $F_{max}2$ (fulvic acid-like) indicates to be less reactive towards ozone, and is therefore assumed to contain a lower degree of aromaticity.

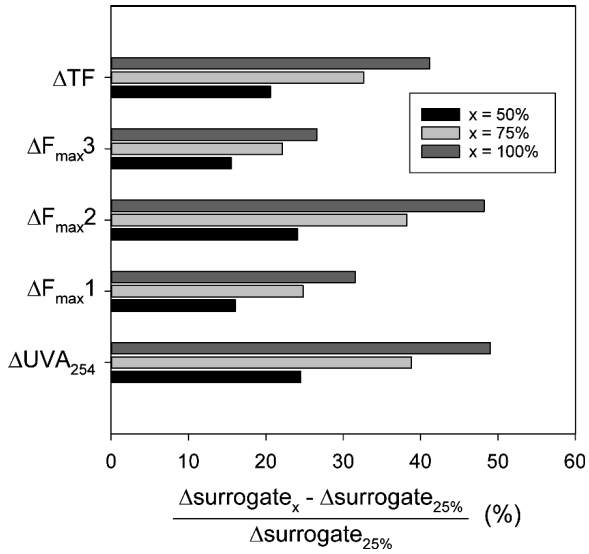

Figure 4.14: Additional relative decrease of ΔUVA_{254} and $\Delta F_{max}1\text{-}3$ ($[\Delta surrogate_x - \Delta surrogate_{25\%}] / \Delta surrogate_{25\%}$) when the HO• exposure increased from 25 to 50, 75 and 100% of its maximum value.

4 Conclusion

A novel, generically applicable correlation model was developed, and calibrated based on UVA_{254} or fluorescence surrogate parameters in which two main reaction phases could be distinguished. After a first initial phase, correlated with the TrOC specific $k_{O3,TrOC}$, a second phase with unselective reactions occurs. Overall, it can be concluded that both UVA_{254} and fluorescence surrogates have their specific benefits. The measurement of ΔUVA_{254} by online sensors has already been established, while online sensors for fluorescence are still under development. Potential benefits of fluorescence measurements involve an improved robustness and the increased control range that can be applied. Further, the higher sensitivity (1-2 orders of magnitude) of fluorescence compared to UV-VIS can be especially of added value in the drinking water field (DOC levels are much lower). While UVA_{254} only decreases up to 47% in the studied range of ozone doses (0 - 2 g O_3 g^{-1} DOC_{eq}, being higher than ozone doses most likely applied on full-scale), TF and F_{max} 1-3 decrease up to 84%. Moreover, PARAFAC analysis of the 3D EEMs enables the monitoring of multiple types of organic matter with a different reactive behavior, providing a better understanding of the occurring changes of organic matter during ozonation.

Chapter 5

Dynamic model validation on lab- and pilot-scale of surrogate-based correlation models

This chapter has been partially redrafted from:

Chys, M., Audenaert, W.T.M., Deniere, E., Mortier, S.T.F.C, Van Langenhove, H., Nopens, I., Demeestere, K. & Van Hulle, S.W.H. Surrogate-based correlation models in view of real-time control of ozonation of secondary treated municipal wastewater: model development and validation, *Environ. Sci. Technol.*, accepted. DOI: 10.1021/acs.est.7b04905.

Chys, M., Audenaert, W.T.M., Vangrinsven, J., Bauwens, M., Mortier, S.T.F.C, Van Langenhove, H., Nopens, I., Demeestere, K. & Van Hulle, S.W.H. Dynamic validation of online applied and surrogate-based models for tertiary ozonation on pilot-scale, *submitted*.

1 Introduction

Ozonation has its proven capabilities for the removal of TrOCs (Trace Organic Contaminants) in secondary municipal wastewater, although currently applied control strategies for ozone dosage result in sub-optimal operation. Control strategies based on online water quality measurements could improve operation, and increase the sustainability and cost-effectiveness of ozonation. Effluent organic matter (EfOM) is easily characterized using (online) spectral measurement methods, and hence the decrease of UV absorption at 254 nm (UVA_{254})[40,63,64,82,100,103,113,114] and fluorescence[64] has been correlated with the removal of TrOCs. So far, mostly linear relationships are considered, showing a good correlation for TrOCs having a high reactivity with ozone (i.e. mainly O_3 and not HO• is responsible for their degradation). Often moderate or poor linear correlations are achieved between the decrease (Δ) of the measured surrogate parameter (mostly UVA_{254}) and the removal of ozone-recalcitrant TrOCs.[127] This might lead to an over- or under-prediction of the actual TrOC removal, resulting in exceeding the imposed discharge limits or an overdose of ozone, associated with higher costs and possibly more pronounced by-product formation. Components with a very low reactivity towards ozone ($k_{O3,TrOC} < 10\ M^{-1}\ s^{-1}$) show a more convex curved behavior (ΔTrOC vs. ΔUVA_{254}) with only limited degradation in very low ΔUVA_{254} ranges (below 20%).[100,127]

Different authors constructed (mostly single) correlation models in several effluents, being applicable for specifically selected TrOCs.[40,63,64,82,100,103,113,114] The novel correlation model developed in Chapter 4 (based on UVA_{254} and fluorescence measurements) was constructed starting from a (semi-)mechanistic point-of-view to allow a more accurate control of the ozone dosing, and to enable also the construction of correlations for other TrOCs – not included in the model development – if their $k_{O3,TrOC}$ is known. Basically two linear functions are used of which the individual slopes are correlated with the prevalent reactions (i.e. first phase is correlated with the apparent second order ozone reaction rate coefficient $k_{O3,TrOC}$; second phase is dominated by HO•-induced reactions and is independent of $k_{O3,TrOC}$). Considering (1) the varying water characteristics of WRRF effluents and thus varying reactivity of the (organic) matrix (as observed during Chapter 3); and (2) the fact that most available $k_{O3,TrOC}$ of TrOCs are determined in 'clean' water (i.e. without competition of a dominant organic matrix), a validation of this model is necessary for TrOCs with a broad range in $k_{O3,TrOC}$ and for a broad range of effluent compositions.

This chapter therefore aims at a thorough validation of the inflected correlation model developed in Chapter 4 to support the hypothesis of its robustness and to provide a framework for online control by WRRF operators. Previously, two different water qualities were used to develop the correlation models with a third data set as verification. More and better diverged effluents (i.e. other WRRFs, more diverse water characteristics) are used here to investigate the broader validity. Previous studies with effluents from different WRRFs in e.g. Switserland[64,114], Germany[63], Belgium[113] (and in Chapter 3) and the USA[40,64,82,100,103,115] indicate large differences in COD (7 - 40 mg O_2 L^{-1}), TOC/DOC (0.9 - 18 mg C L^{-1}), IOD (1.5 – 7 mg O_3 L^{-1}) or UVA_{254} (2.7 - 28 m^{-1}). COD and TOC/DOC are known surrogates for the amount of organic matter, reacting significantly with the dosed ozone and influencing the direct and indirect reaction pathways. The IOD (instantaneous ozone demand; although not really 'instantaneously' reacting, as proven by Buffle et al.[126]) is an indicator for the amount of highly reactive moieties and logically also for the reactivity of the organic matrix. Although UVA_{254} (or other spectral measurements) are the key input for the correlation models, the different variable water characteristics will give a challenge for correlations models to be validated (as discussed in Chapter 3). Likely, variations of those difference water characteristics will influence the reaction pathways of the dosed ozone.

Despite the merits of the single correlation models presented in literature, some limitations still have to be dealt with as mentioned before. Additionally, the validity of those (single) correlation models is mostly visually evaluated and lacks statistical analysis. Consequently, there is a need for a structured method which evaluates and compares the correspondence of measured and predicted ΔTrOCs using different correlation models. This is possible, for example, by using statistical methods (e.g. t-test) or coefficients known to give an indication of the 'goodness-of-fit' between measured and predicted values (e.g. TIC or the Theil's inequality coefficient, and MAE or the Mean Absolute Error).[219]

A thorough validation of the model developed in Chapter 4 is proposed at both lab- and pilot-scale installations, focusing on three particular issues. First, since the ozone-resistant TrOCs are posing the largest challenges for ozone-based TrOC removal, the lab-scale development of the inflected correlation model is validated using a well-known model compound (i.e. pCBA) assumed to be only reacting with HO•.[39] Effluents from different WRRFs with significantly different water characteristics were selected to challenge the model. Second, the correlation model was applied at pilot-scale during long-time operation for monitoring and control purposes. Third, in order to investigate the enhanced predictive power of the constructed model, a statistical comparison (using the TIC, MAE and t-tests) was made with single correlation models

constructed with the same data as for the inflected model, and also with models established in literature. Additionally, the confidence intervals of the correlations for each TrOC were determined.

2 Materials and Methods

2.1 Experimental set-up: lab-scale

Secondary effluent was collected from four municipal WRRFs (selected from those in Chapter 3 (Table 3.1) but all different from the WRRF used for model development in Chapter 4) in different regions of Belgium with I.E. (Inhabitant Equivalent) ranging from 500 to 80 000. These WRRFs, and their specific effluents, have been selected based on receiving water (i.e. influent), configuration of the WRRF installation (i.e. size and type of (biological) wastewater treatment), and preliminary characterization to enable significant differences between the effluents. A detailed overview of the selected WRRFs is given in Table 5.1. Four of six effluent points have been sampled twice except for those at the Waregem WRRF (only once before and after a tertiary sand filtration step) resulting in a total of 10 different effluents.

Ozonation experiments were conducted in batch mode as described in section 2.2 (Chapter 4). Effluent was spiked with a stock solution of pCBA (100 µg L^{-1}) as an ozone resistant probe compound but reacting well with HO• ($k_{O3,pCBA}$ < 0.1 M^{-1} s^{-1}, $k_{HO•,pCBA}$ = 5.0×10^{9} M^{-1} s^{-1}).[39] It could be assumed that, if pCBA is removed to a certain level, other more reactive TrOCs will at least be removed to the same or higher extent. Six different ozone doses, ranging from 0 to 15 mg O_3 L^{-1}, were added to each effluent.

2.2 Experimental set-up: pilot-scale

A modular pilot-scale reactor was installed at the municipal WRRF of Aartselaar, Belgium which has a treatment capacity of 54,000 inhabitant equivalents and is operated by Aquafin NV (for more details see Table 5.1). The WRRF receives a mixture of mainly municipal wastewater and good biologically degradable industrial (i.e. food industry) wastewater and is treated by conventional activated sludge (CAS).

Table 5.1: Overview of the selected WRRFs and the associated sampling locations after secondary (or tertiary) treatment

Study	Nr.	WRRF location	Size category[a]	Abbreviation	I.E.	Type of receiving wastewater (influent)	(Secondary or tertiary) treatment technology
Lab	1	Kruiseke	Cat. 3	KS1	500	100% municipal wastewater	Biodisk + settler
	2			KS2			Biodisk + settler + constructed wetland
	3	Heule	Cat. 3	HL	14 000	± 100% municipal wastewater [b]	CAS
	4	Comines-Warneton	Cat. 2	CW	40 000	mainly municipal wastewater (50% from Belgium, 50% from France)	CAS
	5	Waregem	Cat. 1	WRG1	80 000	municipal and industrial wastewater (from textile industry = difficult to degrade biologically	CAS
	6			WRG2			CAS + sand filtration
Pilot	7	Aartselaar	Cat. 2	ASL	54 000	municipal and industrial wastewater (from food industry = good biological degradation)	CAS

CAS = Conventional Activated Sludge

[a] size category determined by the inhabitant equivalent of each plant: large (I.E. > 80,000, cat. 1), medium (I.E. = 24,000 – 80,000, cat. 2) and small (I.E. < 24,000, cat. 3) sized plants, in according to Table 3.1

[b] receiving wastewater can be highly diluted e.g. due to a large share of receiving rain water

The pilot, of which a schematic overview is given in Figure 5.1, consisted of three tubular reactors of 2 m height (50 mm diameter). Secondary effluent was drawn before the main discharge of the WRRF, buffered (filled continuously, max. 1 to 2 hours residence time) and supplied to the pilot near the top of the first column (up to 600 L/h). The flow rate was manually adjusted using a ball valve and monitored using a magnetic inductive flowmeter (SM6000, ifm, Germany).

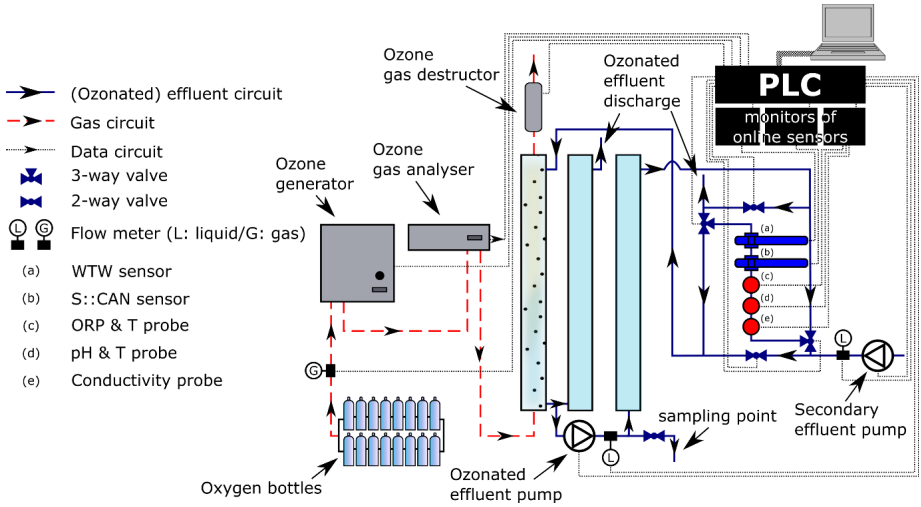

Figure 5.1: Schematic representation of the pilot installation used for ozonation experiments

The pilot was operated in a continuous counter-current flow mode by supplying an O_2/O_3-gas mixture through a bubble diffuser near the bottom of the first column, originating from an oxygen-fed ozone generator (max. 8 g h^{-1}, Modular 8HC, Wedeco, Germany). The ozone gas concentration is monitored by an Anseros ozone analyzer (Ozomat GM-6000-PRO, Germany). The oxygen flow was monitored using a thermal mass flow meter (EL-FlOW®, Bronkhorst, The Netherlands). The first column was followed by another (2^{nd}) column to ensure a stable water level in all columns (i.e. the principle of communicating vessels) while a fixed flow of 350 mL min^{-1} was pumped (qdos60, Watson-Marlow, UK) from the (ozonated) effluent between the first and second column to a third column. This allowed a more extended reaction time if any dissolved ozone would be present after the first column, and kept the total HRT (± 12 min, hydraulic retention time) within the range of current full-scale applications.[45]

For the effluent monitoring before and after ozonation, only one set of sensors was used switching every 15 minutes between both effluents. Conductivity (EC), Oxidation-Reduction potential (ORP), temperature (T) and pH were monitored (SC1000, Hach-Lange GmbH, Germany) as conventional characteristics. Full UV-VIS online spectral sensors were used from S::CAN (spectro::lyser™, Switserland) and WTW (NiCaVis® 705 IQ, Germany). Not considering prior trial runs, continuous experiments have been conducted in a time frame of three months in which the UVA_{254} signal from the S::CAN sensor was used to control the ozone dosage. Different experimental periods were applied in which the set-point of UVA_{254} removal (difference before and after ozone addition) was set at 25% and 40% by controlling the dosed ozone. The WTW sensor was used to monitor the UV-VIS spectrum independently. All data signals from and to sensors, flow meters, valves, etc. were automatically stored and controlled by a PLC (Nextys, Switserland) combined with Tview software (Texas, USA). Extensive detail related to the online measurements is given in Chapter 6.

Samples (grab and composite) were taken to verify the online measurements but also for fluorescence, IOD, alkalinity, and other analysis that only can be performed offline. Specific selected samples were also used for the analysis of TrOCs (see further). Sampling of secondary effluents is less sensitive to the sampling strategy (e.g. compared to WRRF influents) due to the buffering of the complete WRRF treatment.[182] The combined planning of grab and composite samples ensured representative samples retaining the variability of the effluent.[183,184] Especially for regulation purposes, 24 hours composite samples are required although for scientific purposes grab samples or 1 hour composite samples are of high value. Automatic sampling devices (Bühler, Hach-Lange GmbH, Germany), using 1 or 5 L glass containers cooled at 4 °C, were installed to sample effluent before entering the first column and after exiting the third. Sampling intervals were predetermined considering the HRT within the columns.

2.3 Analytical methods

Details related to TrOC analysis, determination of general parameters (e.g. alkalinity, NO_2^--N, COD, EC, pH, etc.), spectral measurements (UV-VIS and 3D EEMs) and IOD, defining the rapid ozone consumption within 5 seconds after dosing, is given in sections 2.2 to 2.4 of Chapter 3. The settings and raw data processing (i.e. Raman normalization, blank and inner filter correction) for fluorescence measurements, or Excitation Emission Matrices' (EEMs), is based

on Murphy et al.[195] and Shutova et al.[196], and is fully described in Chapter 4. HPLC-DAD was used to measure pCBA concentrations (see section 2.3 in Chapter 4).

2.4 Model application and validation

The underlying fluorescence components of the EEMs, associated with different types of chemical groups and their specific properties, could be extracted applying the PARAFAC model established in Chapter 4. Intensity values at peak wavelengths of defined PARAFAC components are expressed as $F_{max}n$ (in Raman Units or RU), with n the number of the defined component.

A framework was developed and calibrated, relating changes in UVA_{254} and fluorescence as surrogate measurements with ongoing reactions during ozonation. The abatement patterns of TrOCs ($k_{O3,TrOC}$ ranging from < 1 to 10^6 M^{-1} s^{-1}) having different reactivity towards ozone showed, in relation to the decrease of UVA_{254} or fluorescence intensity, an 'insect wing' shaped control zone. Two different reaction phases were defined, each of them described by a linear correlation function separated by an inflection point, specific for each surrogate. To allow online process control, the decrease in concentration of every possible TrOC (whether or not used during model development) can be estimated using eq. 5.1 ($\Delta S \leq I$) and 5.2 ($\Delta S \geq I$), with ΔS the decrease of the surrogate measurement (i.e. ΔUVA_{254}, $\Delta F_{max}1$-3 or ΔTF) and I the inflection point (indicating ΔS at which the first phase of reaction ends) between both correlations. The methodology and results regarding the determination of the slopes of the correlation curves before (a_{p1}) and after (a_{p2}) the inflection point and the associated uncertainties are explained in detail in Chapter 4. Correlations have been elaborated only if the TrOC concentration could be measured both in the non-ozonated and ozonated effluent.

$$\Delta TrOC_{0\rightarrow inflection} = a_{p1} \times \Delta S \qquad \text{eq. 5.1}$$

$$\Delta TrOC_{inflection\rightarrow\dots} = a_{p1} \times I + a_{p2} \times (\Delta S - I) \qquad \text{eq. 5.2}$$

The correspondence between measured and predicted data is evaluated using (i) an unpaired t-test of which the null-hypothesis (difference is not significant) is rejected by $p < 0.05$ and can also be used to compare different models if the samples size is equal, (ii) the Theil's inequality

coefficient (TIC) of which a value below 0.3 is commonly seen as an indicator for a good agreement[219] and (iii) a visual inspection to detect outliers or regions with deviations supported with the determination of the MAE (mean absolute error) to highlight differences between measured and predicted data. The discussion of results obtained from the pilot experiment will be divided in (i) TrOCs used for model development and (ii) other TrOCs that could be frequently (i.e. more than 5 times in all samples, n = 43) quantified and of which the $k_{O3,TrOC}$ is known (i.e. 'independent' TrOCs). Additionally, the predictive power of the inflected model will be compared to single correlation models (i) developed with the same data as for the inflected model (see Appendix C for details on equations and slopes) and/or (ii) as given in literature (given in Table 1.6 of Chapter 1)[64,103,113,115] specifically developed for the prediction of pCBA removal (only based on ΔUVA_{254} and on lab-scale). The accuracy of the inflected model in comparison with single correlation models is best exemplified when using UVA_{254} as input for the models, since EEM deduced PARAFAC components are not as widely used in literature for describing correlations with ΔTrOCs. Several authors mention correlations for selected TrOCs while using UVA_{254}, but the number of TrOCs in these studies is limited and often, other TrOCs are considered than those measured during the pilot experiments. The correlation of ΔpCBA with ΔUVA_{254}, on the contrary, is mentioned by multiple authors and forms thus a good basis for comparison.

3 Results and Discussion

3.1 Physical-chemical water characterization

The physical and chemical water characteristics of all effluent streams used during experimentation showed distinct differences as depicted in Figure 5.2. Large differences are seen especially for alkalinity, COD, IOD and the spectral measurements. All these parameters are considered to influence the ongoing reactions during ozonation or to have a direct influence on the correlation models applied for online control.[165] Especially the high variability of UV-VIS and fluorescence measurements, as key input for the correlation models, provides a challenge for the full validation of the developed models. IOD ranged from 3.8 to 16 mg O_3 L^{-1}. Compared to previously used effluents for model development (1 and 2 in Chapter 4, see Figure 5.2) a more extended range is covered in this validation. Consequently, these effluents are considered a good representation for a very broad range of WRRFs and really challenge the developed models.

Difference are also noticed for all characteristics between those used on lab- and pilot-scale. Effluents used on lab-scale, originating from different WRRFs, were clearly more diverse with respect to the UV-VIS and fluorescence spectral measurements. In selecting different WRRFs, the origin of the receiving influent of each plant was taken into consideration. In this respect, especially the WRRF of Waregem is a specific case due to the considerable amount of textile industry wastewater that is mixed with the municipal wastewater as was already noticed during Chapter 3. It is clear from the analyses that this share of textile wastewater has an impact on the UV-VIS response. Textile wastewater is known to contain a significant amount of dyes which retain some absorption[39] and are traditionally difficulty to be removed during secondary (biological) wastewater treatment. Additionally, previous research indicated highly increased intensity values during fluorescence measurements, as also depicted in Figure 5.2.[200]

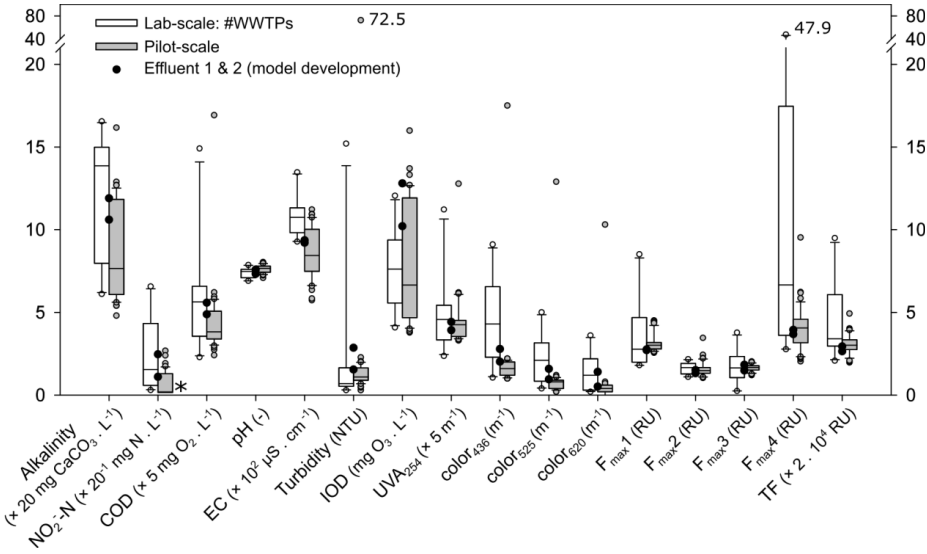

Figure 5.2: Physical-chemical water characteristics of the effluent during lab- (n = 10, white bars) and pilot-scale (n = 43, grey bars) experimentation (laboratory measurements). The black dots (•) indicate the characteristics of the two effluents used in Chapter 4 for the development of the inflected correlation model. An asterisks (*) indicates if values were measured below the detection limit. The whiskers of the boxplots indicate the 10th and 90th percentile of the data distribution, while the white and grey dots are the minimum and maximum of the measured values for all effluent samples during respectively lab- and pilot-scale experiments.

3.2 Model validation by lab-scale experiments: robustness towards different WRRF effluents

3.2.1 Predictability of the inflected correlation model

The inflected correlation model, calibrated in Chapter 4 for UVA_{254}, $F_{max}1$-3 and TF, has been successfully applied to predict the data retrieved by lab-scale ozonation experiments using different WRRF effluents and pCBA as model compound for the most ozone recalcitrant TrOCs. The predicted removal (ΔpCBA) is clearly in correspondence with the measured ΔpCBA, as demonstrated in Figure 5.3a and b for ΔUVA_{254} and $\Delta F_{max}1$, respectively. Considering the total data set (n = 60), the good agreement between measured and predicted values by using ΔUVA_{254} is exemplified by both a t-test (p-value of 0.41) and a TIC value of 0.13. Good results are also obtained when using $\Delta F_{max}1$ as the surrogate (p = 0.44; TIC = 0.14). Visually, a slightly better prediction is observed when using $\Delta F_{max}1$ instead of ΔUVA_{254}, and is confirmed by the MAE being 8.3% ($\Delta F_{max}1$) and 9.2% (ΔUVA_{254}), respectively. The number of experimental data points that are outside the 95% confidence interval of the model is especially lower in the ΔpCBA range above 50%. (4 compared to 9 on a total of 21) in Figure 5.3b than in Figure 5.3a. This is also reflected in the slightly higher p-value obtained by the t-test. The use of other spectral deduced measurements such as $\Delta F_{max}2$-3 or ΔTF were not able to further increase the predictive power (i.e. enhance the results of the t-test, TIC or MAE). For example, the TIC- and MAE-values obtained with $\Delta F_{max}2$ (0.31) and $\Delta F_{max}3$ (0.52) (slightly) exceed the threshold value, while that of ΔTF (0.28) is just below. Also the MAE (15.8-29.2%) was clearly higher, indicating an overall lower agreement in comparison to ΔUVA_{254} and $\Delta F_{max}1$. These observation nicely illustrate the added value of using PARAFAC processing of fluorescence signals (i.e. $F_{max}1$) compared to a general surrogate (ΔTF). This is also graphically clear when considering Figure 5.4.

Detailed p- and TIC-values are summarized in Appendix D, making also a differentiation among the different sampling locations. From this, it becomes clear that the model performance is the weakest for the WRRF effluent of Waregem. This is exemplified by the fact that $\Delta F_{max}2$ – although its overall TIC of 0.31 – shows to be a good predictor for all effluents except that of Waregem (p = 0.064; TIC = 0.75), which can be explained by the significant share of wastewater originating from the textile industry. The dyes consisting of aromatic, heterocyclic and nitrogen containing moieties such as azobenzene or triazines typically show a low reactivity towards ozone and consequently a very low yield for O_3 consumption.[39,200,201] $\Delta F_{max}3$ and ΔTF do not provide a

sufficiently high predictive power for both the effluents of Waregem and Kruiseke, showing that the model could not be validated for these surrogates.

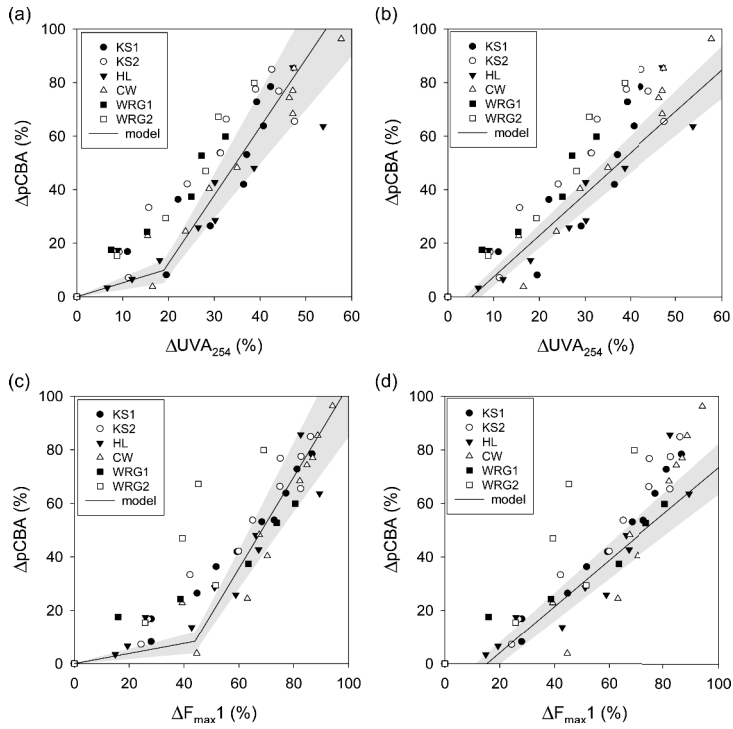

Figure 5.3: Abatement patterns of predicted (full lines) versus measured ΔpCBA (dots) in relation to ΔUVA_{254} or $\Delta F_{max}1$ by applying the inflected model (a and c) and a single correlation model based on own data (b and d). The shaded grey areas indicate the 95% confidence interval of the models. The abbreviations of the WRRFs are explained in Table 5.1.

The highest model robustness is thus obtained with ΔUVA_{254}, $\Delta F_{max}1$ and $\Delta F_{max}2$. Regarding the fluorescence measurements, this is logical since $F_{max}1$ and 2 (both representing different kinds of fulvic acid-like moieties) contain the most amount of spectral information from the EEMs after the PARAFAC analysis (given their 1st and 2nd rank). The presence of moieties showing intensities represented as $F_{max}1$ before ozonation (and also $F_{max}4$, less ozone reactive moieties, indicated in Chapter 4) was clearly higher than those for $F_{max}2$ or 3 (see Appendix E) resulting in a better correspondence after the point of inflection (reaction phase 2 dominated by indirect

(HO•) reactions). UVA_{254} and $F_{max}2$ were indicated in Chapter 4 to be affiliated with reaction pathways dominated by both direct and indirect ozone reactions, giving a representation of all ongoing reactions.

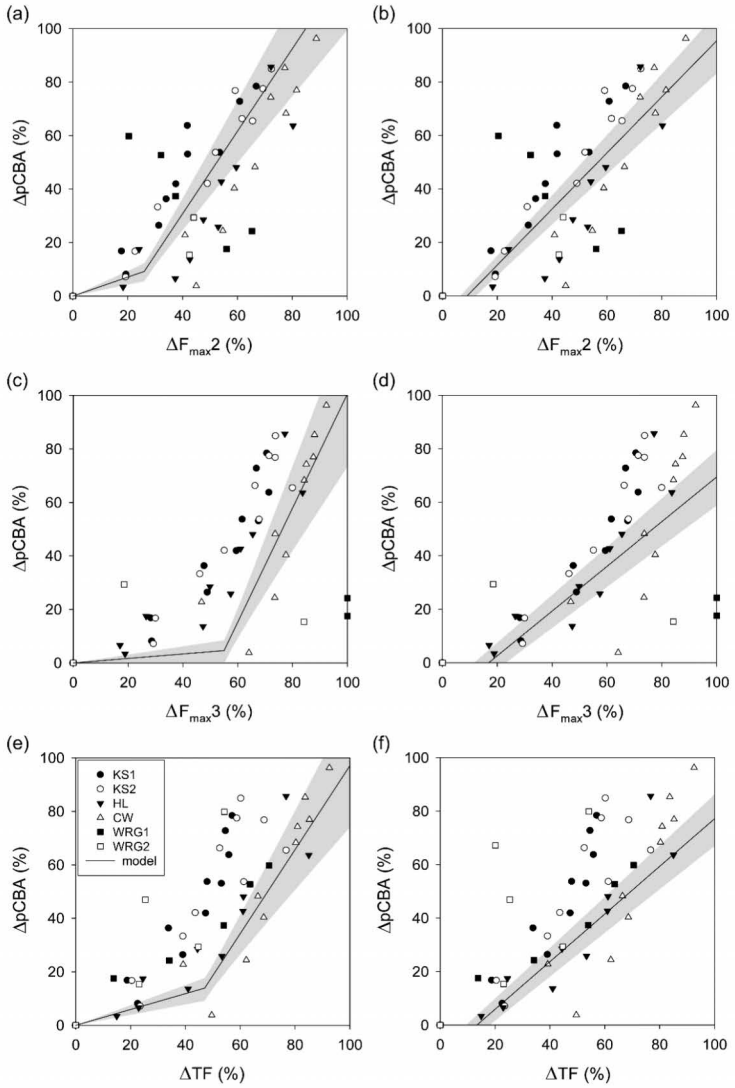

Figure 5.4: Abatement patterns of predicted (full lines) versus measured ΔpCBA (dots) in relation to $\Delta F_{max}1$ (a-b), $\Delta F_{max}2$ (c-d) and ΔTF (e-f) by applying the inflected model (left: a,c,e) and a single correlation model based on own data (right: b,d,f). The shaded grey areas indicate the 95% confidence interval of the models. The abbreviations of the WRRFs are explained in Table 5.1.

3.2.2 Comparison of the inflected and single correlation models

A single correlation model constructed with the same data as used for the development of the inflected model shows a lower predictive power compared to the inflected model, based on the t-test (p = 0.17 versus 0.41), and only limited by the TIC-value (0.14 versus 0.13) and MAE (9.8% versus 9.2%) for ΔUVA_{254}. Several ΔUVA_{254} based single correlation models have been presented in literature, specifically for ΔpCBA. Applying four selected correlations[64,103,113,115], constructed specifically for ΔpCBA, to the experimental data obtained on lab-scale shows TIC-values between 0.11-0.22, thus all below 0.3. The t-test indicates a good predictive power for the correlation from Audenaert et al.[113] (p-value of 0.36), Gerrity et al.[64] (p-value of 0.56) and Sharif et al.[115] (p-value of 0.91), but not for that from Wert et al.[103] (p-value of 0.006). In accordance, the MAE was consistently in line with those observed for the inflected model (7.6-9.2%) with the exception of that from Wert et al.[103] (14.0%). It should be noted in general that the single correlation models of Figure 5.5 were developed and fitted on data specifically for pCBA were the inflected model was constructed using chemical data and is more universal applicable as it is based on the $k_{O3,TrOC}$ of TrOCs.

When looking at the data graphically (Figure 5.3b and Figure 5.5), it becomes clear that ΔUVA_{254} based single correlations do not optimally describe the experimental data in certain ΔUVA_{254} regions. The models by Audenaert et al.[113] (Figure 5.5a) and Gerrity et al.[64] (Figure 5.5d) are showing a slight under-prediction at high ΔUVA_{254} (> 30%), which is also noticed for the own single correlation model (Figure 5.3b). This is also supported by the MAE being higher (between 12.3-14.1%) compared to the inflected model (11.4%). The model based on Sharif et al.[115] (Figure 5.5b) resulted in a slightly lower MAE above 30% ΔUVA_{254} (10.3%). Additionally, the model by Gerrity et al.[64] shows an over-prediction of ΔpCBA for low ΔUVA_{254}. Although MAE values are relatively close to each other, it is visually noticed that all single correlation models are not following the trend of the data, i.e. showing the data point more below the model at low ΔUVA_{254} and above at high ΔUVA_{254}. The model by Wert et al.[103] (Figure 5.5c) shows an under-prediction for the full range of ΔUVA_{254}. This results in additional TrOC removal compared to the desired/predicted ΔTrOC, which might seem an interesting benefit, but will also lead to additional operational costs due to overdosing of ozone.

Focusing on the use of $F_{max}1$, a similar, even more pronounced under-prediction at higher ΔpCBA values (MAE = 11.0% compared to 6.8% if $\Delta F_{max}1 > 50\%$), is observed when using $\Delta F_{max}1$ as the surrogate (Figure 5.3d). This is the important range to reduce pCBA (or other

TrOCs that react slowly with O_3) levels in the secondary effluent. The curving relationship between ΔpCBA and $\Delta F_{max}1$ as experimentally observed is thus better described by the newly developed inflected model (Figure 5.3c) instead of a single correlation model (Figure 5.3d). Whereas 85% of all samples (n = 60) are within a maximum absolute deviation of 20% for the single model (MAE = 9.1%), this increases up to 92% for the inflected model (MAE = 8.3%). This better performance of the latter is also exemplified by the p-value (0.44 versus 0.19). More details concerning the different correlation models and their predictive power are given in Appendix D.

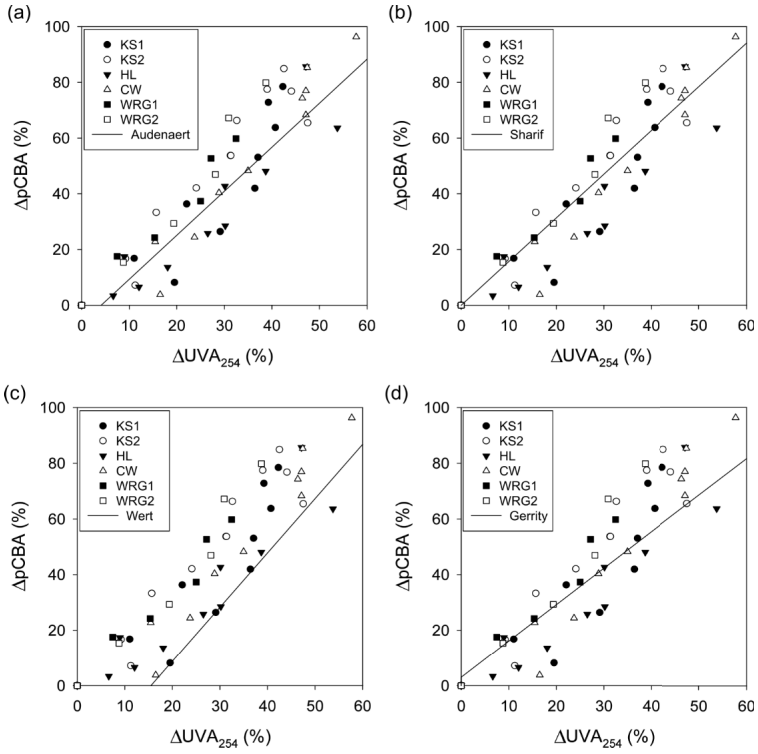

Figure 5.5: Abatement patterns of predicted (full lines) versus measured ΔpCBA (dots) lines) in relation to ΔUVA_{254} by applying the single correlation model described by Audenaert et al.[113] (a), Sharif et al.[115] (b), Wert et al.[103] (c) and Gerrity et al.[64] (d). The abbreviations of the WRRFs are explained in Table 5.1.

3.3 Model validation by pilot-scale experiments: ΔTrOC prediction by $k_{O3,TrOC}$ based surrogate correlations

During pilot-scale ozonation, 13 TrOCs (pharmaceuticals) were selected for the inflected model validation, based on measurable concentration levels in 43 samples before and after ozonation and the availability of the $k_{O3,TrOC}$. More details about the concentration levels and $k_{O3,TrOC}$ is given in Figure 5.6 and Chapter 3 (Table 3.3), respectively.

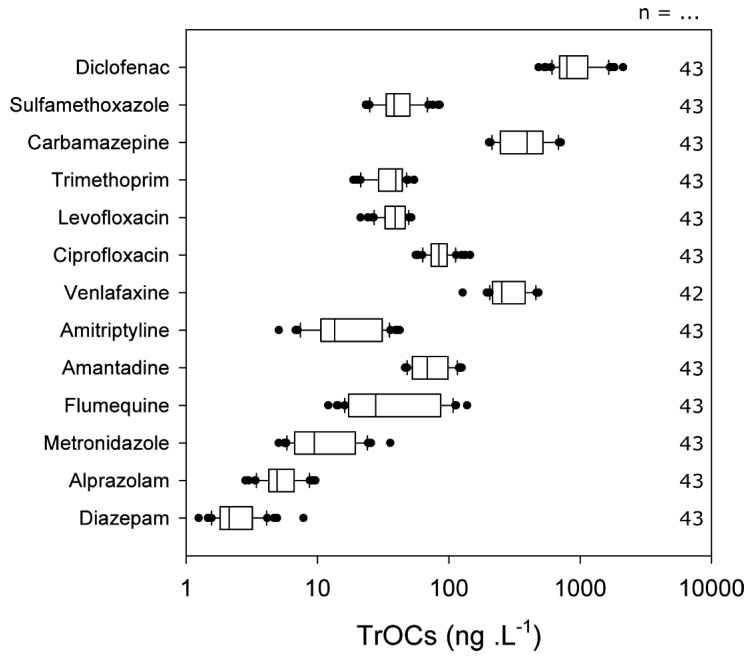

Figure 5.6: Concentrations levels (ng L^{-1}) of the 13 TrOCs in the effluent before ozonation during pilot experimentation at the WRRF of Aartselaar. The quantification frequency of each TrOC is indicated on the right with n_{max} = 43. TrOCs are ranked in order of decreasing $k_{O3,TrOC}$ (see Table 3.3).

As online spectral sensors have been used for monitoring the UV-VIS spectrum before and after ozonation, this UVA_{254} signal was used as input for the correlation model. The use of the online ΔUVA_{254} to monitor the removal of high ozone reactive TrOCs ($k_{O3,TrOC} > 5\times10^4$ M^{-1} s^{-1}; i.e. diclofenac, trimethoprim, levofloxacin) showcases an acceptable predictive power based on a t-

test (p-values between 0.17-0.36) while the TICs (0.10-0.13), MAE (10.6-14.9%) and the graphical representation (Figure 5.7a) indicate a good model performance. Larger discrepancies for specific data points compared to the model are however sometimes noticed, most likely to be attributed on variations in the measurement at these very low ng L^{-1} concentrations, which is the case for high ozone reactive TrOCs (e.g. diclofenac). The MAE remains within acceptable limits, slightly higher than results obtained during the lab-scale validation. For the other TrOCs, having medium ($10\ M^{-1}\ s^{-1} < k_{O3,TrOC} < 5\times10^{4}\ M^{-1}\ s^{-1}$) or low ($k_{O3,TrOC} < 10\ M^{-1}\ s^{-1}$) ozone reactive characteristics, a good agreement between measured and predicted values is clearly obtained, based on t-tests (p-values between 0.28-0.87), TICs (0.09-0.20), MAE (8.0-14.7%) and visual inspection (Figure 5.7b-c). As an independent data set, the model was also applied on four TrOCs different from those used for model development (i.e. alprazolam, carbamazepine, diazepam, sulfamethoxazole). The predictive power is clearly exemplified by statistical evidence although especially good removable TrOCs or those already present in low ng L^{-1} before ozonation are a challenge for the model in the current comparison of Figure 5.7d. Although alprazolam and diazepam (both with $k_{O3,TrOC} < 1$) are present at very low concentrations in the non-ozonated effluents (all < 10 ng L^{-1}), resulting into a more scattered visualization, an acceptable predictive power is exemplified by a t-test (p-values between 0.04-0.72), MAE (8.4-17.7%) and TICs between 0.10-0.28 for alprazolam, carbamazepine and diazepam. Deviations might occur because the TrOC concentration levels are already close to the analytical detection limit which might result in higher uncertainties on the actual measured TrOC levels. Furthermore, deviations seem mostly to result in an under-predication of the TrOC abatement by the model. Although exact prediction is favourable, under-prediction can be seen favourable to over-prediction in oder to achieve (upcoming) discharge limits. For sulfamethoxazole, a $p < 0.05$ indicates a poor model performance, although the TIC (0.17) is far below 0.3. Considering its very high reactivity for ozone ($k_{O3,TrOC} = 5.5\times10^{5}\ M^{-1}\ s^{-1}$), and hence its high removal, the removal of these high ozone reactive TrOCs ranges between 80 and 100% for most samples (due to the applied settings). Considering the uncertainty of $k_{O3,TrOC}$ and the fact that a t-test is based on the average and variance of the removal percentages within the population of samples, this results in a statistical approach which is too strict with low variances for measured and predicted ΔTrOCs (supported by the low TIC). In practice, it should be wise to consider maximum removal rates instead of aiming to achieve 100% as other factors will play a role here (e.g. analytical detection limits). It should also be noted that the ozone dose control will be much more determined by the poor and medium ozone reactive TrOCs rather than by these highly reactive (and easily removable) TrOCs.

It can therefore be concluded that the inflected model, using ΔUVA_{254} as the surrogate parameter, is able to predict ΔTrOC during pilot-scale ozonation if the $k_{O3,TrOC}$ is known. More details on the statistics and graphical representations of the model prediction for the individual compounds are shown in Appendix D and Appendix E.

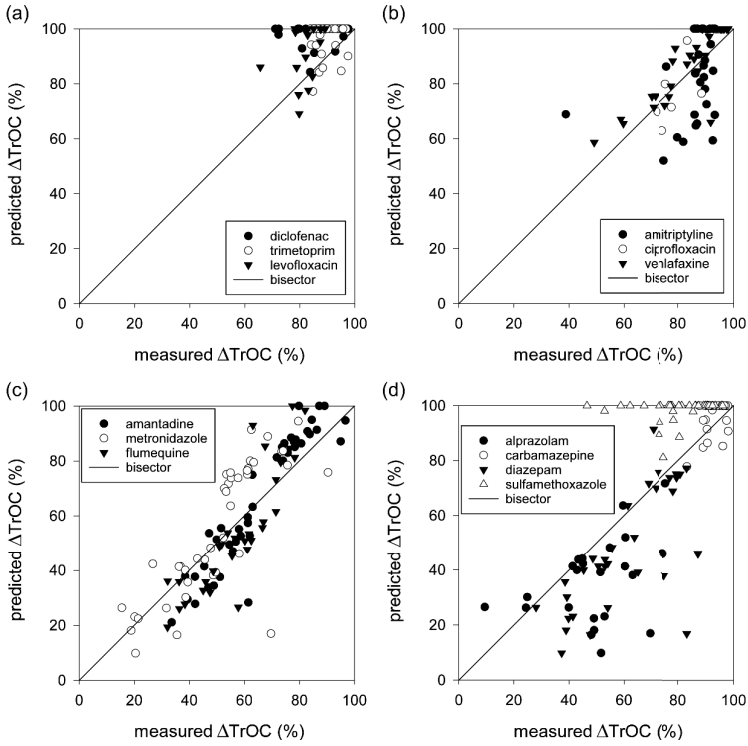

Figure 5.7: Measured and predicted ΔTrOC using the inflected correlation model based on the online ΔUVA_{254} signal. Data are shown separately for TrOCs that were also used during model development and having different reactivity towards ozone: (a) $k_{O3,TrOC} > 5\times10^4$ M^{-1} s^{-1}, (b) 5×10^4 M^{-1} $s^{-1} > k_{O3,TrOC} > 10$ M^{-1} s^{-1}, (c) $k_{O3,TrOC} < 10$ M^{-1} s^{-1}; and (d) for TrOCs not used during model development. (negative values of ΔTrOCs not shown if due to an erroneous measurement of TrOCs or UVA_{254})

Graphs showing the prediction of fluorescence based inflected correlation models are shown in Figure 5.8 ($F_{max}1$) and Appendix E ($F_{max}2$-3, TF, and graphs for individual compounds). Similar statistical results are obtained compared to ΔUVA_{254} (see Appendix D). A visual inspection reveals a better correspondence between predicted and measured values for the poor ozone

reactive TrOCs (especially above 50% ΔTrOC) by $\Delta F_{max}1$, represented by a more uniform spreading of the data points around the bisector than in Figure 5.7c. These TrOCs represent the most difficult ones to be removed by ozonation, and therefore require the highest possible accuracy when optimizing the ozone dosage needed to meet imposed discharge limits.

In line with the results obtained during the lab-scale validation of the inflected model for poor ozone reactive TrOCs (i.e. pCBA, not considering the Waregem samples), the use of $\Delta F_{max}2$ yields more or less similar results after visual inspection compared to $\Delta F_{max}1$ (see statistical parameters in Appendix D and graphs in Appendix E). $F_{max}2$ is a representation for moieties that are reacting both directly and indirectly with ozone, similar to UVA_{254} (see Chapter 4). In contrast to UVA_{254} which represents a broad range of electron-rich moieties, $F_{max}2$ is defined (by PARAFAC analysis) as a group of chemical components with identical reaction characteristics, resulting into less interference of differently reacting moieties.

$F_{max}3$ and TF are clearly not sufficient to use in a framework to predict the removal of TrOCs with varying $k_{O3,TrOC}$. This becomes clear from both the statistical parameters and the graphical representations of the model performance, and agrees with the observations during model development in Chapter 4. Significant models could be obtained, but due to the very high curving behavior of poor ozone reactive TrOCs in relation with $\Delta F_{max}3$ or ΔTF, a poor fit was obtained at higher decreases of $F_{max}3$ and TF. The less predictive power of $F_{max}3$ – although clearly better for highly ozone reactive TrOCs (p-values between 0.14-0.87; TICs between 0.05-0.09; MAE between 8.0-11.5% for pilot experiments), hence the fact of $F_{max}3$ representing humic acids susceptible for mainly direct ozone reactions – can be explained by the fact that $F_{max}3$ contains much less spectral information (3rd rank) compared to $F_{max}1$ and 2. TF, as a representation for the full organic matrix, takes too much variability and information into account which makes it more susceptible for all kinds of interferences.

For at least 9 of the investigated TrOCs, the inflected correlation models using online ΔUVA_{254}, $\Delta F_{max}1$ or $\Delta F_{max}2$ as the surrogate result in a better correspondence (t-tests, TIC results in similar values for all: ΔTIC < 0.03) between predicted and measured ΔTrOCs than the single correlation models (Appendix D and Appendix E). The MAE gave more or less similar results for both types of models using online ΔUVA_{254}, $\Delta F_{max}1$ or $\Delta F_{max}2$, varying between 8.0-19.5%, 5.3-18.4% and 6.0-19.2% (inflected models) and, 5.9-20.1%, 6.3-19.9% and 6.2-21.4% (single correlation models) respectively. The latter are systematically not able to cope with the curving pattern particularly noticed in the removal of poor reactive TrOCs (e.g. amantadine, metronidazole and flumequine) in relation with (in lower extent) ΔUVA_{254} (Figure 5.7c-d vs. Figure E.10c-d) but

especially for $\Delta F_{max}1$ (Figure 5.8c-d vs. Figure E.11c-d), resulting in an under-prediction of ΔTrOCs at higher decreases of UVA_{254} or $F_{max}1$.

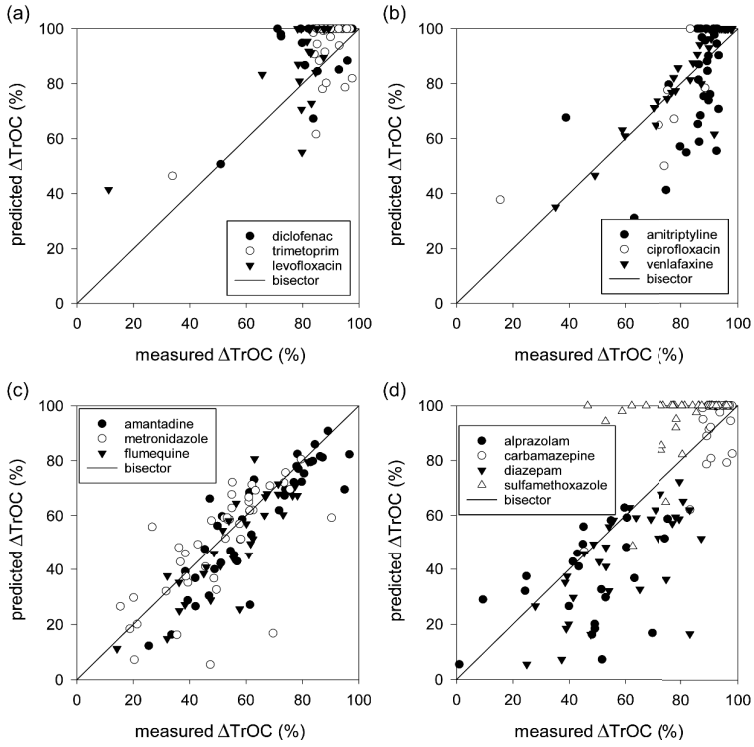

Figure 5.8: Measured and predicted ΔTrOC using the inflected correlation model based on $\Delta F_{max}1$. Data are shown separately for TrOCs that were also used during model development and having different reactivity towards ozone: (a) $k_{O3,TrOC} > 5\times10^4$ M^{-1} s^{-1}, (b) 5×10^4 M^{-1} $s^{-1} > k_{O3,TrOC} > 10$ M^{-1} s^{-1}, (c) $k_{O3,TrOC} < 10$ M^{-1} s^{-1}; and (d) for TrOCs not used during model development. (negative ΔTrOCs not shown if due to an erroneous measurement of TrOCs or $F_{max}1$).

3.4 Considerations for full-scale applications

The TrOC abatement patterns related to the decrease of a certain surrogate are defining the ozone dose control zones that will be of importance for operators of municipal wastewater treatment plants, as discussed in Chapter 4. The inflected correlation models have shown – both during lab- and pilot-scale validation experiments – to predict the removal of TrOCs in an adequate manner, with only the $k_{O3,TrOC}$ of the targeted TrOC needed as input. Although TrOCs

with the highest emerging concern are investigated in literature, thousands of other TrOCs exist and might be present in the effluent of municipal wastewater plants depending on location, type of receiving wastewater, WRRF configuration, etc. Not even considering different legislations for potential imposed discharge regulations, scientific evolutions will most likely lead to the synthesis of new and more different pharmaceuticals, pesticides, etc. which might again end up in the effluent of the WRRFs. The $k_{O3,TrOC}$ of the targeted TrOCs can be a) determined experimentally, b) derived from literature or c) approximated by QSAR (Quantitative Structure-Activity Relationships), reducing the need for extensive experimentation.[225,226] The exact value of $k_{O3,TrOC}$ for a specific TrOC might vary based on the method of determination. As the inflected model is considering the variation of experimental data (used for regression) and the use of varying $k_{O3,TrOC}$, the determination of $k_{O3,TrOC}$ for targeted TrOCs allows a straightforward prediction of the abatement pattern within the 95% confidence interval.

4 Conclusion

Correlation models based on UVA_{254} or fluorescence surrogates have shown to be able to predict ΔTrOC, each having their specific benefits. The measurement of ΔUVA_{254} by using online sensors has already been established, while stable and reliable online sensors for fluorescence are still under development. Therefore, the use of UVA_{254} might be preferable at the current timing for online ΔTrOC monitoring.

Nevertheless, the enhanced data processing of the fluorescence signals, isolating the different intensities associated with moieties reacting similarly to ozone might pose advantages compared to the less selective measurement of UVA_{254} or TF. The validation of the model showed promising potential for future application of fluorescence measurements, processed with the available PARAFAC model. The use of $F_{max}1$ showed generally a slightly more accurate prediction compared to UVA_{254}, and also $F_{max}2$ provided a good estimation of TrOC abatement. The latter surrogate represents moieties with similar reactivity as UVA_{254} but is less influenced by the presence of interfering components in the water matrix. Therefore, $F_{max}1$ and $F_{max}2$ are the fluorescence parameters that are preferred to control the ozone dose for TrOCs abatement. This is particularly the case for poor ozone reactive compounds, which are of the highest interest in controlling the discharge of TrOCs. Nevertheless, $F_{max}3$ which is known to solely react by direct ozone reactions, might give an additional benefit as a good indicator for the behavior of high ozone reactive TrOCs.

Chapter 6

Technical and economical assessment of surrogated-based real-time control and monitoring of secondary effluent ozonation at pilot scale

This chapter has been redrafted from:

Chys, M., Audenaert, W.T.M., Stapel, H., Ried, A., Wieland, A., Weemaes, M., Van Langenhove, H., Nopens, I., Demeestere, K. & Van Hulle, S.W.H. Technical and economical assessment of surrogated-based real-time control and monitoring of secondary effluent ozonation at pilot scale, *submitted*.

1 Introduction

Trace organic contaminants (TrOCs), such as pharmaceuticals, personal care products or pesticides, can be removed by ozonation from municipal wastewater effluent. The ozone dose necessary to remove TrOCs to a specific concentration level not only depends on the reactivity of those TrOCs with ozone (or secondary oxidants such as hydroxyl radicals (HO•)) but also on the presence of effluent organic matter (EfOM) and the associated ozone demand (as discussed in section 4.2 of Chapter 1 and during Chapter 3). Despite the proven capabilities of ozonation, the currently applied doses are (mostly) not flexible enough for the dynamic behavior of the physical-chemical effluent characteristics and, hence, the variable ozone demand of secondary effluent. As an example, applying a flow proportional control approach by dosing a fixed amount of ozone per m^3 of waste water (mostly determined based on user- and/or lab-experience) is not accounting for variations in the effluent matrix unless the fixed dose is altered manually by an operator. Too low ozone doses will lead to a poor TrOC elimination (ΔTrOC), not meeting the targets set (no limits exist yet though, except for Switzerland as discussed in section 2.1 of Chapter 1). Too high ozone doses will result in a higher, unnecessary, economical cost. Additionally, over-dosing of ozone has also been associated with a higher risk of undesired by-product formation such as the potentially carcinogenic N-nitrosodimethylamine (NDMA) and bromate.[42,44,45]

Minimizing both operational costs and by-product formation, two of the main hurdles hindering a fast implementation of the technology, makes real-time control of the ozone dose based on the water quality essential. (Spectral) surrogate measurements have gained significant interest as direct online assessment of TrOC abatement is currently impossible. Dissolved organic carbon,[33,98,115] UV absorption at 254 nm (UVA_{254})[40,63,64,82,100,103,113,114] or fluorescence[64] have been correlated with the removal of TrOCs. Proposed possibilities to control the ozone dose either contain a feedforward or feedback approach. Known feedforward approaches are using the online measurement of either DOC or UVA_{254} of the effluent prior to ozonation.[33,98,115] These measurements will act as an input to a correlation model predicting the TrOC removal related to the ozone dose expressed as e.g. g O_3 g^{-1} DOC (i.e. O_3:DOC ratio), exemplified by Lee et al.[98] Variations of the water quality in terms of concentration levels and properties of EfOM will be taken into account and the ozone dose will be adjusted as such. Alterations in the ozone reactivity of the effluent due to unexpected increases of NO_2^--N or changes within the

composition of the EfOM affecting its reactivity will not be considered using feedforward control.

The use of a feedback control approach (i.e. measurement after treatment) in conjunction with feedforward (i.e. measurement before treatment) takes into account the ozone demand by determining the relative decrease between both (delta, Δ). This decrease in UVA_{254} or fluorescence surrogates (i.e. spectral measurement before and after ozonation) has been correlated well with ΔTrOC for compounds having a broad range of ozone reactivity ($k_{O3,TrOC}$ from < 1 to > 10^6 M^{-1} s^{-1}). Statistical models expressing this correlation based on ΔUVA_{254} have more widely been investigated in literature, but the use of fluorescence has recently gained a lot more attention in the control and monitoring of ΔTrOCs. Chapter 4 showed a large potential for fluorescence surrogate measurement, more specific in assessing ongoing reaction pathways differing between direct and indirect ozone reactions. However, the commercially availability of online UV-VIS sensors (with UVA_{254} the most common) is currently more widespread compared to those for fluorescence (e.g. Wittmer et al.[114]) and will therefore be the main surrogate under investigation in this chapter.

Correlation models using ΔUVA_{254} were first introduced by Bahr. et al.[63] but further elaborated and/or extended by several others.[40,64,82,100,103,113,114,227] They have proven their applicability for lab, pilot- and full-scale ozonation processes (see section 3.2 of Chapter 1). Additional measurements to compensate for variations in NO_2^--N concentrations or the reactivity of the EfOM is not necessary as this will automatically be considered in the measurement of ΔUVA_{254}. The use of online spectral sensors also gives (technical) implications which might influence the correspondence between the desired and actual performance of the ozonation process in terms of ΔTrOC. Correlation models are mostly constructed in a controlled (laboratory) environment which does not account for technical application issues such as drift and fouling of sensors and the associated need for technical interventions (e.g. cleaning the sensors). After all, large amounts of technical interventions can make the process more expensive and less reliable. The empirical model developed in Chapter 4 (and used in this work) has been validated extensively (see Chapter 5) which makes the focus of the current work on the difference in ΔTrOC prediction using different spectral sensors.

The objectives of this study were: (i) to assess practical issues (i.e. sensor cleaning, fouling, off-set with lab measurements) to ensure reliable UVA_{254} measurements as controller input and comparing, to the best of the author's knowledge, two different spectral UV-VIS sensors for the first time in this type of control framework, (ii) to understand the importance of UVA_{254}

deviations for a reliable TrOC abatement control, (iii) to increase the current knowledge of differential control operating over several months (and varying weather conditions) on pilot-scale (currently limited available), and, (iv) to balance potential operational cost savings while efficiently reaching desired TrOC abatement (i.e. long term reliabilty), extrapolating the findings of this study using information of commercially available ozone generators to an actual full-scale WRRF. Recently developed correlation models (in Chapter 4 and Chapter 5) are applied in a real environment as a proof-of-concept at pilot-scale, and investigates and evaluates the behavior when real-scale events and/or effluent variations occur, in comparison to alternative control strategies (i.e. flow or load proportional ozone dosing). From a technical point-of-view, this will lead to important guidelines influencing current and future full-scale installations in view of micropollutant control.

2 Materials and Methods

2.1 Experimental set-up and procedure

2.1.1 Set-up of the pilot reactor and online measurement principles

A modular pilot-scale reactor was installed at the municipal WRRF of Aartselaar, Belgium, which has a treatment capacity of 54 000 inhabitant equivalents and is operated by Aquafin NV. The complete set-up of this reactor is described in section 2.2 of Chapter 5.

Conductivity (EC), Oxidation-Reduction potential (ORP), temperature (T) and pH were monitored online (SC1000, Hach-Lange GmbH, Germany) as conventional water quality characteristics. UV-VIS spectral sensors were used from S::CAN (spectro::lyser™, Austria, 1 mm path length) and WTW (NiCaVis® 705 IQ, Germany, 5 mm path length), further referred to as respectively spectral sensor A and B. This group of sensors were vertically mounted as schematically given in Figure 5.1. Flow-through cells have been used for both spectral sensors. Air cleaning was not used to avoid air blockages in the piping networks and to prevent interference on the other sensors. Spectral sensor B was equipped with an ultrasonic cleaning working more or less continuously, and automatically turned off during the (short) measurement time intervals. Manual cleaning of both spectral sensors was done at least once a week according to the specific procedures described by both manufactures to remove both organic and inorganic scaling. Blank checks (with demineralized water) were performed before and after cleaning of

each sensor. The UVA_{254} off-set between both blank checks is considered as an indicator to quantify the amount of fouling. All data signals going from and to sensors, flow meters, valves, etc. were automatically stored and controlled by a PLC (Nextys, Switzerland) combined with Tview software (Texas, USA).

One set of sensors was used for both effluent quality monitoring, and for controlling the applied ozone dose, by switching every 15 minutes between the effluent before and after ozonation. Preliminary monitoring of the municipal wastewater effluent only showed minor fluctuations in effluent characteristics within this time interval. Bahr et al.[63] even observed practical steady-state behavior of DOC and UVA_{254} during one day. As only one set of sensors was used to monitor both the effluent before and after ozonation, potential measurement errors (e.g. due to scaling or calibration off-sets) of the spectral sensors were expected to have a minor effect (Δ relates to a difference, not absolute values). Additionally, the time-delay inherent to the HRT of the system was more or less equal to this switching interval.

2.1.2 Operation and sampling

Continuous experiments have been conducted in a time frame of three months during summer, preceded by five months of preliminary testing. Only the UVA_{254} signal from sensor A was used to control the ozone generator based on its ΔUVA_{254} set-point (see eq. 6.1).

$$\Delta UVA_{254} = (UVA_{254,eff} - UVA_{254,O3}) / UVA_{254,eff} \quad \text{eq. 6.1}$$

The ΔUVA_{254} value was partially renewed every 15 minutes based on the UVA_{254} value before ($UVA_{254,eff}$) and after ($UVA_{254,O3}$) ozonation (allowing some stabilization after switching water streams). The capacity of the generator was adjusted by a PI-controller. Operation was done in different experimental periods in which the set-point was either 25 or 40% ΔUVA_{254}. Both set-points were specifically chosen based on previous research in Chapter 4 and Chapter 5 relating ΔUVA_{254} and ΔTrOCs. The results elaborated in Chapter 4 indicate a removal below detection limit of TrOCs with good ozone reactivity ($k_{O3,TrOC} > 5\times10^4$ M^{-1} s^{-1}) at a ΔUVA_{254} of 25%, while TrOCs with medium or low reactivity could still be detected. Based on the same research, a set-

point of 40% ΔUVA_{254} brings in almost complete removal of all TrOCs with the exception of the most recalcitrant TrOCs ($k_{O3,TrOC} < 10\ M^{-1}\ s^{-1}$). Similarly to Chapter 5 the correspondence of ΔTrOC based on the online or lab determined ΔUVA_{254} is evaluated with the experimentally measured ΔTrOC based on t-tests or the Theil's inequality coefficient (TIC).

Samples (grab and composite (1h and 24h)) were taken to verify the online measurements but also for measuring parameters that can only be determined offline (e.g. instantaneous ozone demand, alkalinity, etc.). More information is given in section 2.2 of Chapter 5. Details related to TrOC analysis, determination of general parameters (e.g. alkalinity, NO_2^--N, COD, EC, pH, etc.), spectral measurements (UV-VIS) and IOD, defining the rapid ozone consumption within 5 seconds after dosing, is given in sections 2.2 to 2.4 of Chapter 3.

2.2 Data handling

The online logged data related to the water (i.e. flow rate, UV-VIS, pH, EC, ORP) and gas phases (i.e. O_2 flow rate, O_3 concentration and generator capacity) were synchronized in time intervals of 15 minutes, similar to the ΔUVA_{254} measurement interval explained earlier. After and before switching the sensor system between the non-ozonated and ozonated effluent, no data was considered for 5 and 3 minutes respectively, to allow all readings to stabilize. Similarly, faulty readings due to non-stabilized control (i.e. not meeting the set-point) or fouled sensors were removed from the data set. Signal and data processing was performed using Matlab® R2015a.

The ozone dose transferred to the secondary effluent based on the ΔUVA_{254} control strategy was calculated from the supplied ozone (accounting for the generator capacity, O_2 flow and effluent flow) and the transfer efficiency. Preliminary experiments indicated a 95% gas-liquid transfer efficiency (not shown). The ozone dose signal was slightly smoothed based on LOcal regrESSion (LOESS function)[228,229] to account for outlier measurements and aid visual representation.

Although the ozone dose was controlled based on a ΔUVA_{254} set-point, the comparison was made with two other established control strategies: flow proportional (i.e. a fixed absolute ozone dose in mg $O_3\ L^{-1}$) and load proportional (i.e. g $O_3\ g^{-1}\ DOC_{eq}$, only accounting for the load before ozonation, equivalent to the dissolved organic carbon). An ozone dose of respectively 10 mg L^{-1} and 1.2 g $O_3\ g^{-1}\ DOC_{eq}$ was considered, equal to the 75th percentile (arbitrary selected) ozone

dose that was applied using the ΔUVA_{254} strategy. The online DOC_{eq} signal was based on the UVA_{254} signal from sensor B, linearly calibrated with offline DOC data ($R^2 = 0.80$).

3 Results and Discussion

3.1 Comparison of online and laboratory UVA_{254} measurements

The comparison of online measured $UVA_{254,eff}$ and $UVA_{254,O3}$ with lab measured UVA_{254} revealed clear differences between both spectral sensors (Figure 6.1). Also a two tailed t-test (as a manner to determine if two sets of data are significantly different from each other) rejecting the hypothesis of being equal by $p < 0.05$, resulted in a p-value $< 10^{-13}$ comparing both sensors. A systematic offset of 1.5 m^{-1} for UVA_{254} by spectral sensor B (Figure 6.1b, equipped with ultrasonic cleaning) resulted in a good agreement in contrast to the systematic offset of 6.7 m^{-1} for spectral sensor A (Figure 6.1a, no automatic cleaning), supporting the previous t-test. The offset between online and lab measurements of UVA_{254} probably originated from the presence of particles and turbidity. As these sensors were continuously used during operation, the effect of fouling on the sensors also occurred which potentially explains the almost 5 times larger offset of spectral sensor A. Moreover, the online UVA_{254} of sensor A was characterized with sudden larger outliers compared to the stable offline UVA_{254}, due to significant fouling requiring manual cleaning. Similarly, the fouling on spectral sensor A was more than 6 times larger than for spectral sensor B during the 3 months of pilot experimentation. A drift of 2.2 m^{-1} day^{-1} (sensor A) and 0.35 m^{-1} day^{-1} (sensor B) on average was noticed due to fouling of the sensors, with peak fouling rates up to 14 and 2.2 m^{-1} day^{-1} respectively. These results clearly demonstrate the need for a good cleaning and maintenance schedule, and procedure for the online sensors. Although both spectral sensors were manually cleaned on a regular basis (minimum 1 to 2 times a week), additional measures should be taken to provide stable and trustworthy UVA_{254} measurements. Sensor B was equipped with an ultrasonic cleaning which clearly made it less prone to fouling. Although not used in the current study, other cleaning alternatives are the use of pressurized air, automated brushes or filters preventing particles to reach the measurement windows of the spectral sensors.[114]

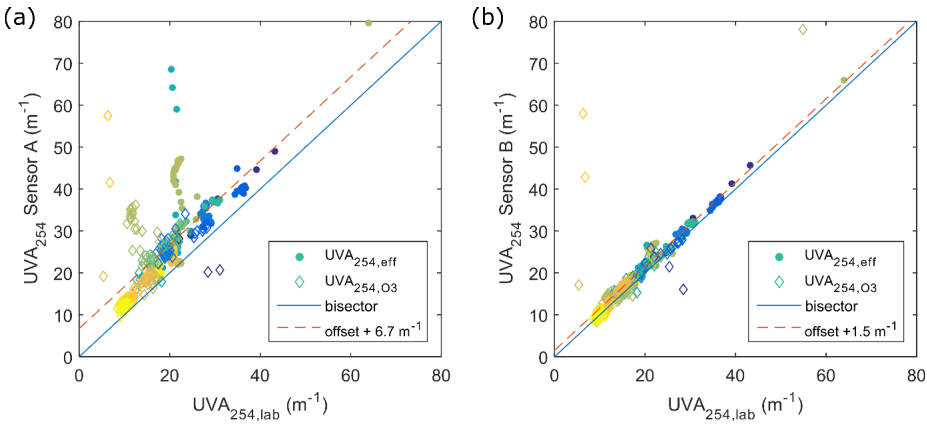

Figure 6.1: Agreement between online (left: spectral sensor A; right: spectral sensor B) and offline (lab) measured UVA_{254} during three months of pilot-scale experiments. Data is presented for measurements both before (●, effluent n = 184) and after (◊, ozonated n = 171) ozonation. All filling of the markers is color-coded according to their date and time of measurements, ranging from dark blue to yellow. Sensor B was equipped with ultrasonic cleaning.

3.2 Operational considerations using ΔUVA_{254}

The ozone dose was controlled by a desired set-point for ΔUVA_{254}, related to specific ΔTrOCs according to the correlation model developed in Chapter 4. The offset in the online $UVA_{254,eff}$ and $UVA_{254,O3}$, as direct input for the control of ΔTrOCs directly impacts the successful operation of the ozonation pilot as this offset is only partially removed when calculating a percentage difference. The achieved $\Delta UVA_{254,lab}$ (lab measurements) revealed a deviation of 6.2% and 3.3% (absolute difference from the median) with the applied set-point of respectively 25% and 40% ΔUVA_{254}. Sensor A was used to determine and control ΔUVA_{254} during normal operation (for practical reasons at the start of the experiments), hence its small differences (-0.8% and -2.1%, absolute difference from median) attributed to irregularities of the PI controller (i.e. not reacting sufficiently/quickly enough). The increased $\Delta UVA_{254,lab}$ in comparison to ΔUVA_{254} from sensor A (the latter is lower because of fouling, Figure 6.2a) indicates an over-dosing of ozone at certain times which relates to additional economical costs and an off-set with the desired ΔTrOC (i.e. more removal). It is noteworthy that the sudden large discrepancies as noticed in Figure 6.1a are less pronounced when calculating the ΔUVA_{254} (Figure 6.2a), although a general off-set is still noticeable. This supports the early mentioned statement and benefit of using only one sensor for measurements before and after ozonation as the offset on both

measurements is partially eliminated. The need for only one sensor instead of two results in a 50% reduction of the investment cost and necessary cleaning compared to the conventional approach of separate sensors before and after treatment. This is of interest given the cost of these commercially available spectral sensors (i.e. capital cost up to € 15 000 or more). Cleaning of the spectral sensors(s) as previously discussed will, however, still be of paramount importance for successful ozone dose. As an example, the difference between $\Delta UVA_{254,lab}$ and ΔUVA_{254} from spectral sensor B (Figure 6.2b) is a good evaluation for its reliability, even if this sensor (with additional ultrasonic cleaning) was only used for monitoring. An absolute difference (between both medians) of -0.9% (25% set-point) and 1.4% (40% set-point) indicates a very good correspondence. Considering the ΔUVA_{254} correlation model, a maximal absolute difference of 4% should be maintained at all times to keep the absolute error on ΔTrOC below 10% at set-points of 25% or 40% ΔUVA_{254}.

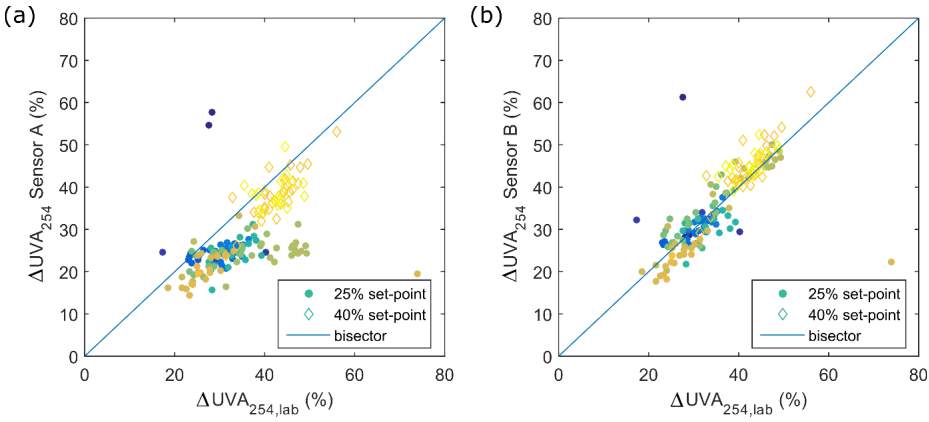

Figure 6.2: Agreement between online (left: spectral sensor A; right: spectral sensor B) and offline (lab) measured ΔUVA_{254} during three months of pilot-scale experiments. Data is presented operating at a set-point of 25 (○, n = 119; lab n = 118) and 40% (◊, n = 53; lab n = 52) ΔUVA_{254}. All filling of the markers is color coded according to their date and time of measurements, ranging from dark blue to yellow. Sensor B was equipped with ultrasonic cleaning.

3.3 Operational influences on ΔTrOC

Correlation models using ΔUVA_{254} in relation with ΔTrOCs have shown to result in a good prediction of ΔTrOC, as exemplified by e.g. Bahr et al.[63] and Chys et al.[227] (and also stressed in

Chapter 4). The levels of achieved ΔTrOCs (laboratory measurements) during operation of the pilot were comparable to other studies.[33,98,120,158] The focus is directed towards medium and low ozone reactive TrOCs ($k_{O3,TrOC} < 5\times10^4$ M^{-1} s^{-1}) as most difficult to remove. TrOCs with $k_{O3,TrOC} > 5\times10^4$ M^{-1} s^{-1} are easily removed by ozone and, of lesser importance, will certainly be removed at high percentages at the applied set-points. The predicted range of ΔTrOC for both spectral sensors and using lab determined ΔUVA_{254} is given in Figure 6.3. No large differences are noticed between the predicted ΔTrOCs from lab or sensor B measurements. Based on t-tests (p-values > 0.05) and the TIC (< 0.3), all TrOCs with $k_{O3,TrOC} < 5\times10^4$ M^{-1} s^{-1} showed a good correspondence between predicted and experimentally measured ΔTrOCs. The use of sensor A, however, results in an under-prediction indicated by the lower median-values in Figure 6.3, and an off-set of the ΔTrOCs. As a result, good correspondence with measured ΔTrOCs was achieved for only 2 of the 6 TrOCs with $k_{O3,TrOC} < 5\times10^4$ M^{-1} s^{-1}. The details concerning the statistical t-tests and TIC calculations can be found in Table 6.1.

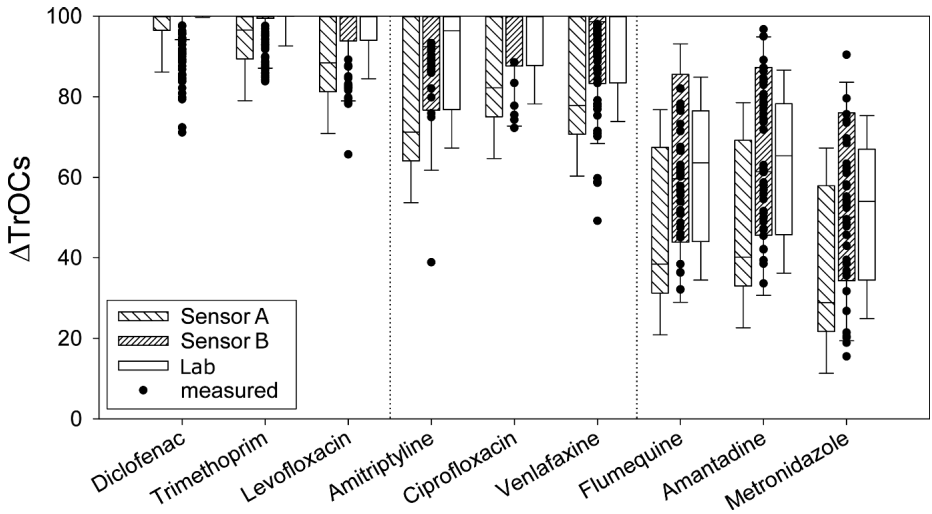

Figure 6.3: Predicted range of ΔTrOC based on ΔUVA_{254} measured with both spectral sensors and by lab analysis, indicated by the bars. The black dots (●) indicate the experimentally measured ΔTrOC values, combined during operation at a 25% and 40% set-point. The 'cutted' bars near 100% ΔTrOC are due to already high ΔUVA_{254} values, and therefore, high predicted TrOC abatement.

Table 6.1: Correspondence between measured and predicted ΔTrOCs (for compounds having a $k_{O3,TrOC}$ < 5×10^4 M^{-1} s^{-1}) by pilot-scale ozonation, using the inflected model from Chapter 4 and ΔUVA_{254} measurements from both online spectral sensors and laboratory analysis. The p-values (< 0.05, t-test) or TICs (> 0.30) indicating a poor correspondence are grey shaded.

TrOCs	Number of data points	t-test (p-values)			TIC		
		Sensor A	Sensor B	Lab.	Sensor A	Sensor B	Lab.
Amitriptyline	34	0.000	0.284	0.856	0.16	0.14	0.08
Ciprofloxacin	7	0.433	0.566	0.546	0.10	0.20	0.09
Venlafaxine	41	0.217	0.620	0.059	0.08	0.09	0.05
Flumequine	31	0.000	0.456	0.367	0.22	0.12	0.10
Amantadine	43	0.000	0.870	0.464	0.18	0.09	0.08
Metronidazole	43	0.008	0.400	0.735	0.23	0.17	0.16

3.4 Effect of dynamic effluent behaviour on applied control strategies

The physical and chemical water characteristics measured during the three month period of pilot experiments showed distinct differences, as depicted in Figure 6.4a. Large variations (up to a factor of 17 within the 5th and 95th percentile values) were seen especially for alkalinity, EC, COD, IOD and UVA_{254}. All these parameters were considered to influence the ongoing reactions during ozonation or to have a direct influence on the correlation models applied for online control.[165] Four distinct periods could be distinguished based on the water quality characteristics, the effluent flow rate through the full WRRF, the amount of rain fall, and the applied ΔUVA_{254} control set-point. Figure 6.5 exemplifies the four different periods concerning the variation of the $UVA_{254,eff}$ signal (sensor B) in relation to the rain fall and the flow through the WRRF. Three of those periods, further referred to as period I, II and III, occurred during the application of a 25% ΔUVA_{254} set-point and are characterized with respectively little rain fall and high variations in $UVA_{254,eff}$ (period I, 27.4-47.5 m^{-1}, Figure 6.5a), sudden rain fall after a long dry period with associated increase of $UVA_{254,eff}$ and consecutive decrease on the long-term (period II, from 32.4

to 23.1 m^{-1}, Figure 6.5b) and rain events resulting in highly increased flow through the WRRF with only small variations in $UVA_{254,eff}$ (period III, $\Delta < 1.7$ m^{-1}, Figure 6.5c).

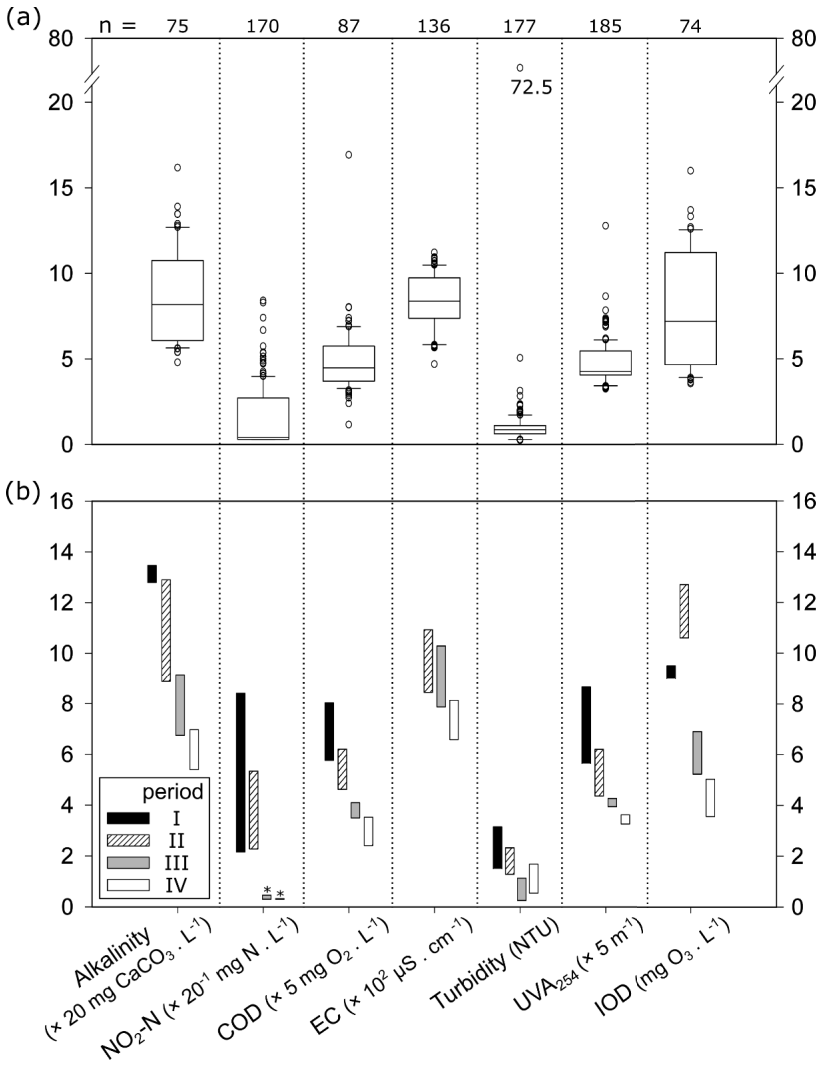

Figure 6.4: Physical-chemical water quality characteristics of the effluent during (a) three months pilot-scale experimentation (laboratory measurements) and (b) four defined periods with varying water characteristics. The whiskers of the boxplots indicate the 10 and 90% percentile of the distribution, while the white dots are the outliers considering all measured data. The bars in part b indicate the minimum and maximum values measured during those periods. An asterisks (*) indicates if the minimal measured values were below detection limits.

During the 4th (IV) period, a 40% ΔUVA_{254} set-point was used. This period is characterized with specific occurrences of high WRRF flow (and high rain fall) and variations (15.0-20.3 m^{-1}) in the $UVA_{254,eff}$ signal (Figure 6.5d). Figure 6.4b furthermore indicates the minimal and maximal measured physical-chemical water quality characteristics values during each period. This variation clearly influenced the required ozone dose (Figure 6.6) to meet the ΔUVA_{254} set-point. Depicted in the lower charts of Figure 6.6, the effluent matrix reactivity is established as the ratio of UVA_{254} removed ($UVA_{254,eff}$ - $UVA_{254,O3}$) per mg O_3 L^{-1} consumed. The 'standard value' seems to be near 1 m^{-1} mg^{-1} L but significant lower reactivity is noticed during periods II and III (down to 0.3 m^{-1} mg^{-1} L), following variations in the water quality characteristics. More details are given in the following paragraphs.

Relatively dry weather conditions (= period I), and therefore low flow rate through the WRRF (see Figure 6.5a), clearly results in a more concentrated effluent with $UVA_{254,eff}$, alkalinity, COD and IOD up to 43.3 m^{-1}, 269 mg $CaCO_3$ L^{-1}, 40.2 mg O_2 L^{-1} and 9.5 mg O_3 L^{-1} (Figure 6.4b). In perspective, the median concentration during the full three month of pilot experimentation was 21.4 m^{-1}, 164 mg $CaCO_3$ L^{-1}, 22.4 mg O_2 L^{-1} and 7.2 mg O_3 L^{-1}. A load proportional control strategy during this type of period logically results in a very high ozone dose as exemplified in Figure 6.6a (between 15-30 mg O_3 L^{-1}). This in contrast to the control by ΔUVA_{254} at the fixed set-point of 25%, showing an ozone dose between 6.7-12 mg O_3 L^{-1}, gradually decreasing in time similar to the $UVA_{254,eff}$ signal. The matrix reactivity is clearly high (1.2 m^{-1} mg^{-1} L on average, Figure 6.5a) during this period which minimized the ozone demand to meet the 25% ΔUVA_{254} set-point, although high effluent loadings (i.e. $UVA_{254,eff}$, DOC_{eq}, …) were detected. It is therefore not completely illogic to apply other O_3:DOC ratios during periods in which the effluent composition is significantly different. Manual or semi-automatic mechanisms might be in place at full-scale based on operator's judgement or based on a long-term evaluation (i.e. several days or weeks of measurement of flow rate, rain events, water quality characteristics, etc.) resulting in a heuristic control approach. In the current situation, an ozone dose of 0.58 g O_3 g^{-1} $DOC_{eq.}$ (= 75th percentile of the ΔUVA_{254} based ozone dose during period I) would be more suited and can be also applied during other periods with dry weather conditions (little rain events and no large WRRF effluent flow for longer periods). Adjusting the O_3:DOC ratio during period I to 0.58 g O_3 g^{-1} $DOC_{eq.}$ would result in a more appropriate dosing (7.2-15 mg O_3 L^{-1}) compared to the ΔUVA_{254} control, both in terms of costs (i.e. less ozone dosing) and ΔTrOC (as a result of the ozone reactivity, see Figure 6.6). This lower O_3:DOC ratio can however not be continuously applied as higher doses are need during periods II to IV.

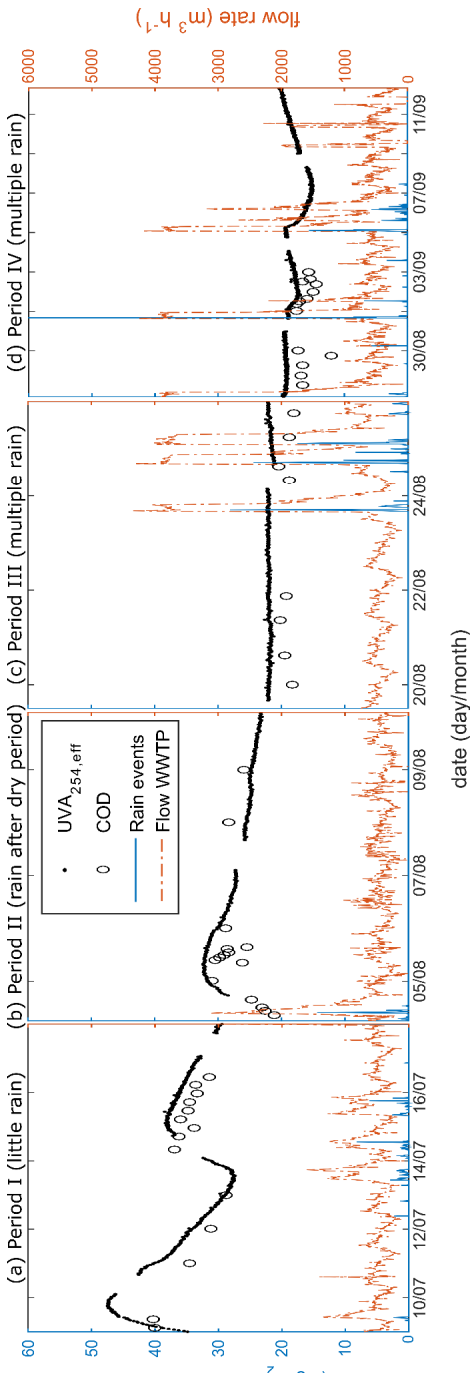

Figure 6.5: Time profile of measured $UVA_{254,eff}$ (black dots), WRRF flow rate (orange line), and rain events (blue line, www.wateninfo.be) during the four selected periods of pilot-scale operation. COD samples (white dots) are obtained from laboratory measurements and are an additional representation of the organic matter content. Period I to IV includes 9.0, 5.3, 6.3 and 15.7 days, respectively.

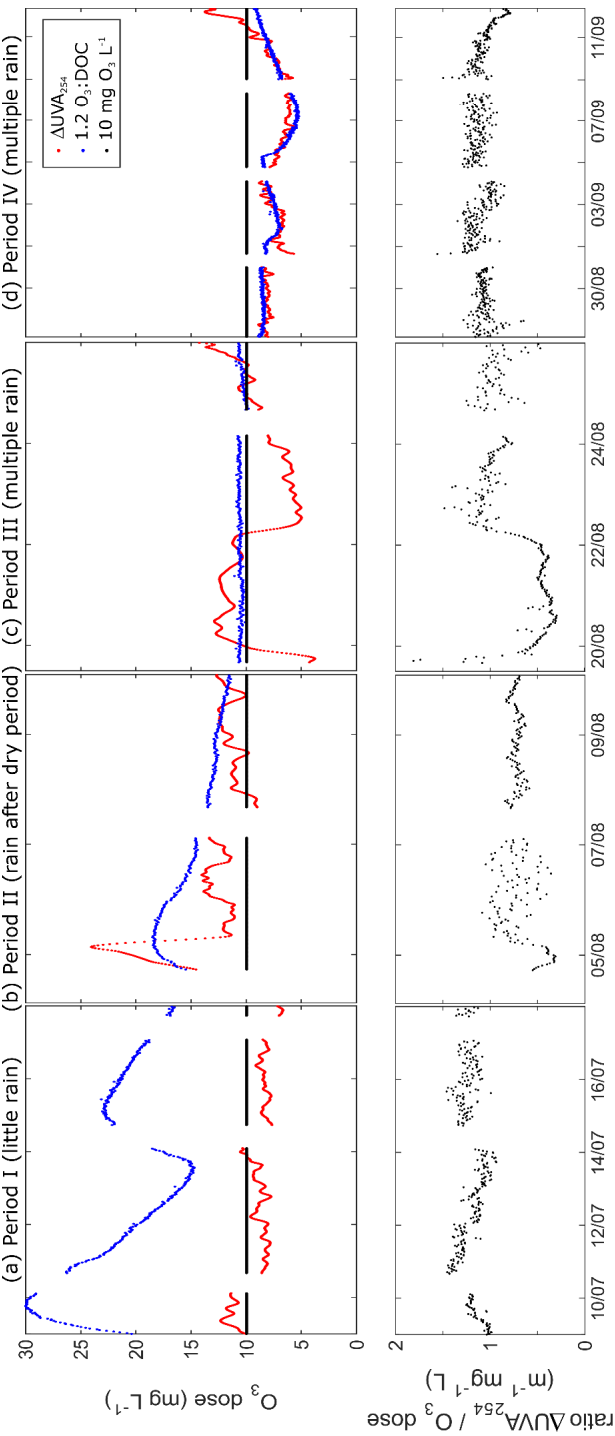

Figure 6.6: Ozone dose (mg O_3 L^{-1}) based on the three control strategies (upper charts) and the ratio of absolute UVA_{254} removal ($UVA_{254,eff}$-$UVA_{254,O3}$) per mg O_3 L^{-1} dosed (bottom charts) during the four selected periods of pilot-scale operation.

The sequence of rain events during periods II to IV resulted in a higher dilution of the received influent at the WRRF. Consequently, less concentrated secondary effluent was observed during the consecutive periods (Figure 6.4), as exemplified by the decreasing trend of the $UVA_{254,eff}$ signal (Figure 6.5). Associated with these weather conditions, a lower matrix reactivity was noticed during period II (0.3-1.1 m^{-1} mg^{-1} L). Period II is characterized with a sudden rain event and therefore a large increase of the flow through the WRRF (Figure 6.5b). Typically associated with this type of event, also known as the "first flush" phenomenon, a temporarily more concentrated effluent can be noticed. This means that this event will have a limited influence on the overall required ozone dose (and costs, discussed in section 3.5) but are important to cope with to ensure reliable TrOC abatement at all times. This event resulted in a very low effluent reactivity (down to 0.3 m^{-1} mg^{-1} L) at the same time the maximal concentrated effluent was noticed, probably due to the presence of more recalcitrant organics or flushed out suspended solids. This is in line with the assumed attribution of dilution and run-off of unconventional components during storm events by El-taliawy et al.,[162] affecting their TrOC abatement at similar O_3:DOC ratios.

The large WRRF size implies a significant buffering of this event, which probably results in a stabilization period of several days in which the $UVA_{254,eff}$ signal is decreasing. The sudden change of the effluent composition led to an increased ozone demand for both the load proportional and differential (i.e. ΔUVA_{254}) control strategy (Figure 6.6b). The flow proportional control (i.e. 10 mg O_3 L^{-1}) did not cope with the altered ozone demand as higher and more variable ozone doses are needed (ranging from 9.0 up to 24.0 mg O_3 L^{-1}) in line with the varying organic load ($UVA_{254,lab}$) from 0.22 to 0.31 m^{-1} and lower effluent reactivity (Figure 6.6).

Period III follows alternating dry and rainy weather conditions and also contains some rain events itself, associated with increased flow through the WRRF (Figure 6.5c). Although this period is characterized with a low variation of the $UVA_{254,eff}$ signal (Δ < 1.7 m^{-1}), especially compared with the other periods, the ozone dose varied between 3.8 and 14 mg O_3 L^{-1} to achieve the required 25% ΔUVA_{254} set-point (Figure 6.6c) and might therefore be the most interesting period to compare a load proportional and differential control strategy with each other. This is clearly associated with the large variations of the effluent composition and ozone demand (between 0.3 and 1.8 m^{-1} mg^{-1} L, Figure 6.6) during this period. As the load proportional control strategy is not capturing any changes in matrix reactivity of the incoming effluent (i.e. no feedback of the effluent after ozonation), the required ozone dose stabilizes between 9.8 and 11 mg O_3 L^{-1}. Although the average ozone dose is similar for all three strategies (all between 9.3-10.5

mg O_3 L^{-1}), temporarily over- or under-dosing will result in a higher potential by-product formation or inefficient TrOC abatement respectively.

The fourth period contains a changing profile of different rain events and some periods of dry weather (Figure 6.5d). Although a higher ΔUVA_{254} set-point was applied, it was chosen to consider the same O_3:DOC ratio for the load proportional control strategy. The effluent concentration in this period was significantly lower as exemplified by its low $UVA_{254,eff}$ signal, potentially due to an increased number of (large) rain events. Also the physical-chemical water quality parameters show low values compared to the other periods (Figure 6.4b), and the 75th percentile of the ΔUVA_{254} based ozone dose during this specific period differed less than 0.1 g O_3 g^{-1} DOC_{eq} from the one defined for periods I to III. Both the ΔUVA_{254} and load proportional control strategy resulted in similarly changing ozone doses (5.6-14 mg O_3 L^{-1} and 5.2-9.3 mg O_3 L^{-1} respectively, Figure 6.6d). Due to a lowering effluent matrix reactivity at the end of this period as a potential result of consecutive rain events, the load proportional control does not detect the increased ozone demand. This resulted in a lower ozone dose than the ΔUVA_{254} strategy.

From all four periods, it becomes clear that both the effluent matrix load and composition (i.e. reactivity) are highly variable (from 0.3 to 1.8 m^{-1} mg^{-1} L, see lower chart of Figure 6.6). This impacts the ozone demand (from 3.8 to 24 mg O_3 L^{-1} (25% ΔUVA_{254}) and from 5.6 to 14 mg O_3 L^{-1} (40% ΔUVA_{254})) and hence the TrOC abatement (and potential by-product formation). It becomes clear that the matrix reactivity is especially variable in periods with rapidly changing events as is the case of period II. Periods with low (i.e. period I) or high rain fall (period IV) seem both to have a similar effluent reactivity, although their clear differences in (organic) loads (Figure 6.4). It should however be noticed that a higher ΔUVA_{254} set-point was applied during period IV. Up to 25% ΔUVA_{254}, UVA_{254} decreases at a fast pace as a function of consumed ozone.[115] At higher ΔUVA_{254}, the slope decreases,[115] hence its lower reactivity (i.e. a lower m^{-1} mg^{-1} L at high ΔUVA_{254}). It also appears that the effluent reactivity (in terms of the ratio ΔUVA_{254} / O_3 dose in m^{-1} mg^{-1} L) is inversely correlated with the ozone dose applied by the ΔUVA_{254} control strategy (Figure 6.7a). This again confirms that the effluent quality (i.e. its reactivity and ozone demand) and not its load or concentration will determine the ozone dose. The practical independent behavior of the effluent reactivity compared to the effluent load (as $UVA_{254,eff}$) again supports this statement (Figure 6.7b).

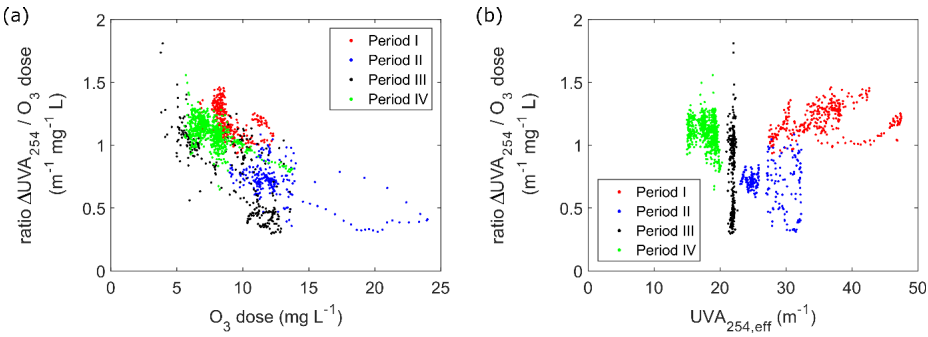

Figure 6.7: Effluent matrix reactivity, depicted as the ratio of absolute ΔUVA_{254} by the consumed ozone (in m^{-1} mg^{-1} L), in relation with (a) the ozone dose (ΔUVA_{254} strategy) and (b) the effluent UVA_{254} signal ($UVA_{254,eff}$) for period I to IV.

3.5 Economical comparison of control strategies for a dynamic effluent

The flow rate of the full-scale WRRF effluent stream, of which only a side-stream was used during pilot-experimentation, was multiplied with the absolute ozone dose (mg O_3 L^{-1}) of the three different control strategies to extrapolate for the required ozone capacity (in kg O_3 h^{-1}) in case of a full-scale application. The required ozone capacity of the generator (i.e. kg O_3 h^{-1}) for all four periods is given in Figure 6.8, with indication of the minimum and maximal applicable generator capacity. The operational expenditure (OPEX) was determined accounting for energy (€ 0.10 kWh^{-1})[230] and (liquid) oxygen (€ 0.10 kg^{-1} O_2, 0.05-0.15 kg O_3 kg^{-1} O_2 depending on the used ozone generator and capacity)[231] consumption. Oxygen and energy consumption rates account for the generation of ozone, cooling, off-gas destruction and other small costs (e.g. PLC control). Four different full-scale applicable ozone generators (10-15 wt%, Wedeco, Germany) were considered having a maximum capacity of 27.5 kg O_3 h^{-1} and minimally operated at 5% of its maximum capacity. The minimal or maximal generator capacity (and associated OPEX) was considered when the required ozone dose (kg O_3 h^{-1}) exceeded these limits. The capital expenditure (CAPEX) of each generator contains standard parts (e.g. ozone gas analyser, ozone diffuser system, ambient ozone monitor, system start-up, on-site training, etc.), using 20 °C cooling water (WRRF effluent), and determined accounting for a depreciation time of 10 years and 5% annual interest rate. Civil works and interconnecting piping with preceding treatment steps at the WRRF are not included.

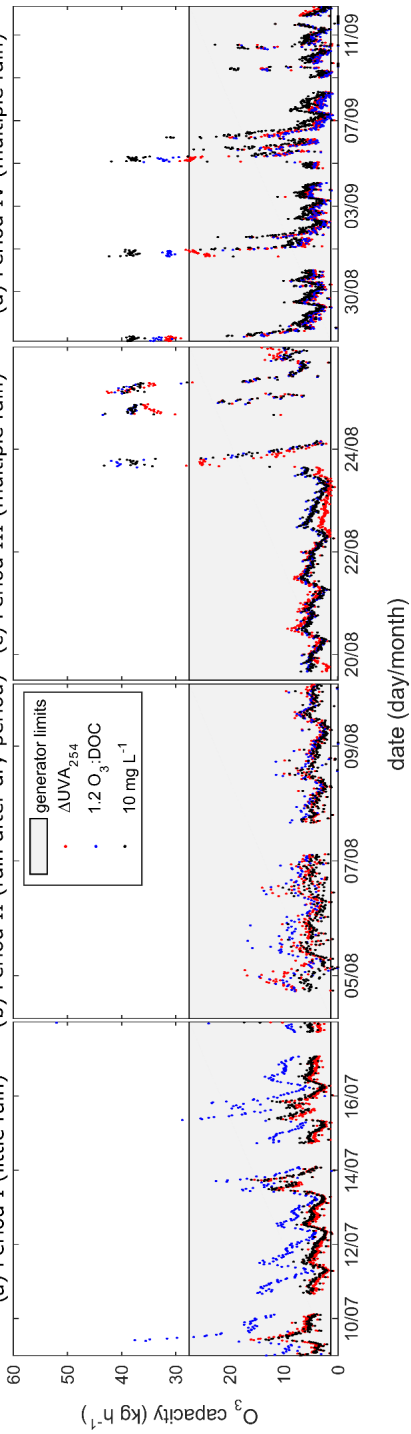

Figure 6.8: Ozone capacity required (kg O_3 h^{-1}) based on the three control strategies during the four selected periods of pilot-scale operation.

Concerning the four periods individually, the OPEX are logically in line with the ozone doses depicted in Figure 6.6 and observations discussed in the previous sections. An overview of the individual OPEX per m^3 is given Figure 6.9. Briefly stated, the large over-dosing during period I of the load proportional control resulted in twice as much OPEX compared to the ΔUVA_{254} control strategy. A corrected O_3:DOC ratio (0.58 instead of 1.2) already results in a reduction of the average OPEX from 0.041 to 0.023 € m^{-3}, already closer to the ΔUVA_{254} control strategy (0.020 € m^{-3}). During period II, the flow proportional strategy was not able to fulfill the variable ozone demand, hence its lower costs compared to the ΔUVA_{254} control strategy (0.023 compared to 0.028 € m^{-3}). Similar results were noted for the load proportional strategy (0.031 € m^{-3}). Period III resulted in more or less similar ozone doses for all three control strategy despite the variable effluent reactivity. Small differences are consequently noticed for the average OPEX (€ m^{-3}): 0.018 (ΔUVA_{254}), 0.018 (flow proportional) and 0.019 (load proportional). The application of the load and flow proportional control strategy during period IV resulted in an OPEX of 0.016 and 0.019 € m^{-3} respectively, differing slightly when using the ΔUVA_{254} strategy (-1% and 18% respectively).

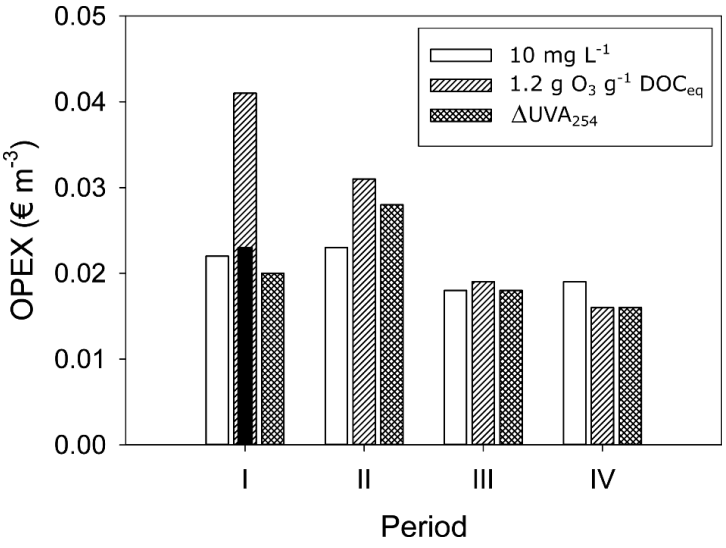

Figure 6.9: OPEX for each control strategy during the four defined periods of pilot-scale operation (in average € m^{-3}). The OPEX applying 0.58 g O_3 g^{-1} DOC_{eq} in period I is indicated by a filled black bar.

In general, during the full three month period of pilot experiments, the average OPEX equaled to 0.018 € m^{-3} and varied between 0.017-0.019 € m^{-3} depending on the considered full-scale ozone generator during the calculations. In the same year of experimentation, the WRRF of Aartselaar discharged on average 28 542 m^3 day^{-1} secondary effluent (www.VMM.be). Consequently, tertiary ozonation for TrOC abatement applying the ΔUVA_{254} control strategy in a similar way as during the pilot scale experiments would result in an OPEX of 186 549 € $year^{-1}$ (on average, between 175 384 – 202 722 € $year^{-1}$ depending on the ozone generator). In comparison with the application of the flow (196 662 – 228 004 € $year^{-1}$, 0.019-0.022 € m^{-3}) or load proportional (224 024 – 259 200 € $year^{-1}$, 0.022-0.025 € m^{-3}) control strategy, a respective OPEX reduction of 11% and 22% was obtained. Also accounting for the CAPEX (ranging from approxiametly 85 000 to 105 000 € $year^{-1}$) of the different generators, the total expenditure (TOTEX) of the ozonation process is between 300 627 – 312 829 € $year^{-1}$ (flow proportional), 328 480 – 344 025 € $year^{-1}$ (load proportional) or 278 905 – 287 547 € $year^{-1}$ (ΔUVA_{254} control). A ΔUVA_{254} control strategy (0.027-0.028 € m^{-3}) is capable to reduce the total cost by 7-8% or 15-16%, in comparison to flow (0.029-0.030 € m^{-3}) or load (0.032-0.033 € m^{-3}) proportional dosing respectively.

3.6 Applicability and considerations for the control of tertiary ozonation

To ensure the desired TrOC abatement at the most favorable cost, a reliable online UV-VIS sensor equipped with an online cleaning mechanism is needed. Additionally, a structured manual cleaning and maintenance schedule is required to ensure correct UVA_{254} measurements as input for the ozone dose control strategy. Cleaning of the sensors was proposed minimal once a week. However, this might have its practical impact. Interrupting the online UVA_{254} measurement during manual cleaning removes the most important input parameter for a correct ozone dose control. Consequently, interruption intervals should be minimized as much as possible, while the ozone dose determined before interruption can be maintained until the sensor is back to normal operation. Cleaning of one sensor typically takes less than one hour and variation of the secondary effluent is seen minimal during this time interval.

All three control strategies clearly result in different ozone dosing, having their implications for the overall ozone consumption and OPEX. From an economical point-of-view, the ΔUVA_{254} strategy resulted in clear cost savings over the full three month experimental period, although some selected periods showed similar or even lower costs by applying load or flow proportional

control (Figure 6.9). Nevertheless, next to the fact that the most economical option is preferred, the most important issue is that utilities need to operate the system (i.e. the ozone dose) in a way to achieve the treatment target at any time. The current application represents the desired TrOC abatement in the most effective way, supported by different other applications,[63,64,158] preventing as much as possible any unwanted by-products (e.g. bromate, NDMA or other harmful organics). Additionally, changes in the effluent composition affecting the overall reactivity are captured by applying this control strategy. For example, Figure 6.4b shows a varying NO_2^--N concentration in the effluent from 0.42 mg N L^{-1} to below detection limit (< 0.015 mg N L^{-1}), responsible for a varying instant ozone demand up to 1.4 mg O_3 L^{-1}, while still reaching the imposed ΔUVA_{254} set-point. Stapf et al.[158] also observed an increased ozone demand because of elevated NO_2^--N concentrations applying a ΔUVA_{254} control, although the used generator was not able to cope with the increased demand at that time. This all makes the differential (i.e. ΔUVA_{254}) applied control strategy superior to the others as those are ignorant for these alterations in ozone reactivity.

The application of a load proportional control strategy showed clear differences in ozone dose compared to the ΔUVA_{254} control. The application of an O_3:DOC ratio considers the secondary effluent load entering the ozonation reactor, and will not account for anything occurring during the ozonation process, for example keeping the NO_2^--N issue in mind or the variable effluent matrix reactivity (Figure 6.6). Logically, the flow proportional ozone control strategy is not suitable for online control as it is only accounting for the flow rate and not at all for the varying composition of the effluent. In practice, this control strategy should solely be used as fallback option in case of spectral measurements failure. It must be kept in mind however that models correlating ΔUVA_{254} and ΔTrOCs contain a certain error (expressed by confidence intervals, see Chapter 4 and Chapter 5).

Although it is advantageous of having a feedback loop to ensure good ozone dosing control, the major drawback of the proposed ΔUVA_{254} control strategy using only one UV-VIS sensor is the increased response time. The required maximal response time will depend on the overall variability of the effluent and the discharge regulation that is in place (e.g. are temporary exceedings allowed?). The response time is mainly depending on (i) the switching interval between the measurement before and after ozonation (i.e. 15 minutes in the current research) and (ii) the HRT of the ozone reactor (i.e. around 12 minutes, depending on the effluent flow rate). Fine tuning both intervals to each other minimizes the impact but additional adjustment time is still needed compared to a load proportional control strategy which is constantly able to adjust

the ozone dose (i.e. DOC_{eq}). It can therefore be hypothesized that the ΔUVA_{254} control strategy can be extended with an additional safety control signal based on the DOC_{eq}, resulting in one combined feedback-feedforward (i.e. master-slave). The ΔUVA_{254} control will ensure the desired ΔTrOC abatement while the DOC_{eq} measurement has the potential of increasing the reaction speed of the control if periods with rapid and highly varying effluent flow rate and composition occur. In this way, an even more accurate control is potentially guaranteed and both the ΔUVA_{254} and DOC_{eq} measurements can be done using one and the same sensor.

4 Conclusion

UVA_{254} based control of ozone dosing for the abatement of TrOCs in secondary WRRF effluent is a reliable and effective control mechanism. The use of one sensor to measure the effluent characteristics both before and after ozonation results in a reliable system and can slightly reduce the effect of fouling on the measurements. Nevertheless, the need for cleaning is clearly indicated and the use of ultrasonic cleaning results in significantly less fouling. Manual interventions are necessary at an estimated rate of once a week.

Feedback control of ozone dosing (i.e. ΔUVA_{254} based control) also results in significant cost savings compared to feedforward control approaches (i.e. flow or load proportional control). Additionally, and maybe of even higher importance, the use of ΔUVA_{254} as control parameter ensures the supply of the required ozone doses during varying water quality and weather conditions. This ensures the desired TrOC abatement, but also minimizes ozone overdosing and the potential of by-product formation. However, the additional response time of using ΔUVA_{254} might be a disadvantage, which opens perspectives for the combination with load-based approaches (i.e. O_3:DOC ratio based control) and the construction of a combined feedback-feedforward system. Testing can now be done on full-scale installations to establish this new control concept.

Chapter 7

Comparing (biological) filtration and ozonation in view of micropollutant removal, unselective effluent toxicity, and the potential for combined real-time control

This chapter has been redrafted from:

Chys, M., Demeestere, K., Ingabire, A.S., Dries, J., Van Langenhove, H. & Van Hulle, S.W.H. Enhanced treatment of secondary municipal wastewater effluent: comparing (biological) filtration and ozonation in view of micropollutant removal, unselective effluent toxicity, and the potential for real-time control, *Water Sci. Technol.* **2017**, *76* (1), 236-246.

1 Introduction

Pending (European) legislation and the dedication to protect the aquatic ecosystem and drinking water resources are driving municipal wastewater treatment plants to upgrade their current treatment installations.[22,23] Several tertiary treatment steps are being put forward of which ozonation and activated carbon (AC) are the most preferred.[33–35] A Swiss study[36] emphasized that in general, AC induces a higher cost compared to ozonation. The application of a tertiary ozonation step has been defined as one of the major solutions to reduce the discharge level of trace organic contaminants (TrOCs) in receiving water bodies.[28,32] Ozonation has shown very fast reactions in the presence of effluent organic matter (EfOM) with the removal of a broad range of TrOCs due to the generation of unselective hydroxyl radicals (HO•). Although most TrOCs are degraded by ozonation, oxidation products are formed not only due to reaction with TrOCs but mainly by reaction with the bulk organic matter or other constituents present in the water matrix. Ozonation has consequently been associated with the potential of by-product formation depending on the ozone dose and water matrix composition. Most by-products, originating from the reaction of ozone with different chemical moieties, have a higher biodegradability compared to their parent compounds. Consequently, a polishing step following ozonation is favorable as an additional barrier to prevent the discharge of potential toxic products. With the adaption of the Swiss water protection act in March 2014, ozonation was put forward together with powdered activated carbon to reduce the discharge of TrOCs, either followed by a polishing step (e.g. sand filtration) to eliminate bioavailable oxidation products.[28] Lim et al.[42] stressed the potential for biological filtration processes to cope with NDMA formation as an alternative for the more energy intensive UV photolysis.

Mostly the use of (powder or granular) activated carbon (AC) or the combination of ozonation and slow sand filtration (SSF) is investigated, while the use of different other types and combinations of biological filtration steps is scarcely examined. Therefore, three different (biological) filtration technologies are put forward in the current study of which their main principle is clearly different: trickling filtration (TF), slow sand filtration (SSF) and biological activated carbon filtration (BAC). Both SSF and BAC are filtration types in which the filter material is fully submerged resulting in anoxic or anaerobic conditions (lower in the filter bed) for the ongoing biological processes. BAC has the additional benefit of adsorbing components present in the effluent on active sites of the carbon surface. Potential adsorption onto filter sand of a SSF can be seen as negligible compared to BAC. TF is studied as a potential alternative. To

the best of the author's knowledge, TF has never been applied as a polishing technology for ozonation. TF is a relatively simple and highly reliable technology that produces effluent of consistent quality. In contrast to SSF or BAC, the TF contains non-submerged bed material (mostly small rocks or plastics) on which a biological slime can develop,[211] which is exposed to the air making oxygen more easily diffusing through the filter bed. Reungoat et al.[35] could identify the oxygen concentration in the effluent as a limiting factor, even more than the EBCT (empty-bed contact time), for the performance of biological filters. Combining non-submerged with a part of submerged material, both aerobic and anaerobic organisms can develop, leading to a broader spectrum of organisms available to enhance the degradation of components present in secondary effluent.

A possible barrier for the implementation of these additional treatment technologies is the operator's concern about monitoring and controlling the performance. Several monitoring and control strategies, mostly uniformly applicable, have been developed to optimize the ozone dosage to reduce operational costs but still reaching the desired removal of TrOCs. One of the most recent correlation models has been developed in this dissertation based on UVA_{254} measurements to control the ozone dose during ozonation of secondary effluents from municipal WRRFs, applied for the abatement of TrOCs. A generical framework is presented relating different surrogates and ongoing chemical kinetics to construct correlations for any compound with known apparent second order reaction rate constants towards ozone ($k_{O3,TrOC}$) and HO• ($k_{HO•,TrOC}$). Mainly, two different reaction phases are defined for which a separate linear correlation is obtained. Although this framework has been developed for a single ozonation step, it has not been investigated yet whether these correlation models are more widely applicable also taking into account additional treatment steps following the ozonation. Studies relating UVA_{254} and AC adsorption are already available.[232,233] Considering potential synergistic effects between ozonation and a post-treatment, an even more optimal ozone dosing can be pursued.

Given the discussion above, an optimal tertiary treatment is needed that is aiming for a high TrOC removal and a decrease of the unselective toxicity. In this study, biological filtration technologies are investigated with different governing main mechanisms (i.e. adsorption, aerobic, anoxic and/or anaerobic conditions). The intrinsic value of these filtration technologies is investigated in comparison with ozonation, as stand-alone tertiary treatment. The applicability of correlation models developed in Chapter 4 for ozonation in combination with TF, SSF or BAC is statistically investigated, keeping in mind the different reactivity of the studied TrOCs with

ozone. As such (follow-up of) TrOC removal by the combination of ozonation and suitable (biological) post-treatment (i.e. polishing) technologies is investigated.

2 Materials and methods

2.1 Experimental procedures

Secondary effluent of the municipal WRRF in Harelbeke, Belgium (116 100 I.E., Aquafin NV) was weekly collected after conventional activated sludge treatment within a period of two months. A graphical representation of the complete lab-scale set-up is given in Figure 7.1. All sampled effluent was first fed to a rapid sand filter with a height of 0.60 m and a diameter of 0.065 m, containing sand with a grain size of 0.4 to 0.8 mm to remove any larger particles (e.g. sludge flocs). A filtration rate of 5.4 m h^{-1} (or 300 mL min^{-1}) was maintained.

In the next step, half of the effluent was ozonated in a reactor containing 11 L of effluent operated in semi-batch mode with a constant flow of an ozone/oxygen-gas mixture through a porous diffusion plate. An Anseros ozone generator was used (COM-AD-02) while the oxygen flow rate was set at 600 mL min^{-1}. On average, 4.2 ± 0.6 mg O_3 per liter of effluent was added which is considered as a commonly applied ozone dosage for the removal of TrOCs in pilot- and full-scale applications.[22] Both the inlet and outlet gaseous ozone concentrations were monitored by means of a UV-based gas analyzer (GM-OEM, Anseros) and logged every second using a Cole-Parmer DAQ module (model No. FN-18200-00). Additional details about the ozonation set-up and associated mass balance calculations are given by Audenaert et al.[113] and Chys et al.[110]

Three different post-treatment technologies using biological and physical-chemical filtration were applied to both ozonated and non-ozonated effluent. Six columns contained two replicates of each technology, being a trickling filter using lava stones (TF), a slow sand filter (SSF), and a (biological) activated carbon filter (BAC). Details about the different design characteristics are given in Table 7.1 and Figure 7.1. In literature, a wide range of flow rates (from 0.5 to ± 50 bed volumes per day (BVs day^{-1})) is used although it has been indicated that the fastest removal of dissolved organic carbon (DOC, i.e. a surrogate for the organic matter) occurs near the top of the columns.[35,211] Escolà Casas and Bester[234] obtained high elimination of some TrOCs (e.g. 41% diclofenac, 94% propranolol, 85% iomeprol) in a SSF with a low flow rate (± 1 BV day^{-1}).

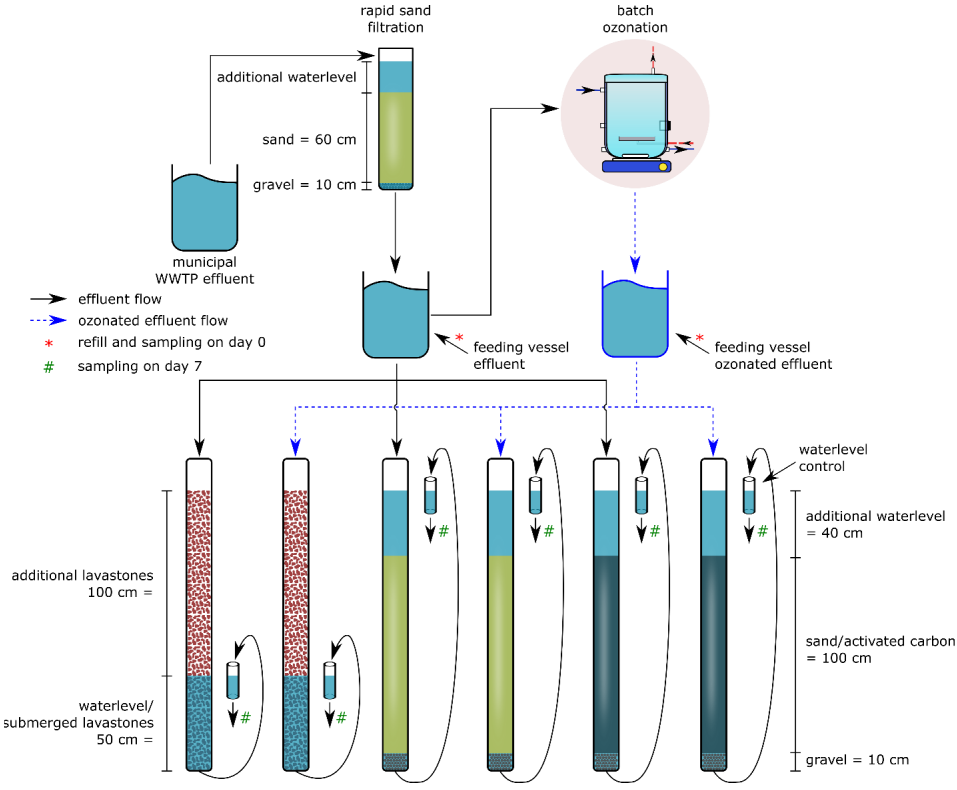

Figure 7.1: Schematic view of the experimental lab-scale set-up with, in chronological order: the sampled municipal WRRF effluent, rapid sand filtration, ozonation of effluent, and the different post-treatment columns (from left to right: trickling filter, slow sand filtration and (biological) activated carbon filtration; each in double of which the left one is fed with effluent and the right one with ozonated effluent). The * and # are respectively indicating the time of sampling for TrOCs and toxicity analysis at day 0 and day 7.

Consequently, flow rates were chosen during experimentation to allow for sufficient residence time but also at a level that makes the experimental procedure practically feasible. At start-up, all columns were filled with the respective materials at the given heights. The water level within the trickling filter was significantly kept below the level of the filling material as this ensured having both aerobic and anoxic zones. All columns were fed from the top and were inoculated with 50 mL of supernatant of sludge (i.e. after 30 minutes settling), obtained from the municipal WRRF, before starting the experiments. Both ozonated and non-ozonated effluent, placed in two separate containers and weekly refilled, were fed to one of the two replicates of each post-

treatment technology. During the experimental period, after initial start-up, the complete set-up was running for 6 consecutive weeks before sampling and measuring TrOCs and toxicity to allow for a certain adaptation period. Effluent was used without spiking of any TrOCs. Additional samples were taken biweekly for COD and nutrient analysis and weekly for BOD_5. The follow-up of pH, conductivity and UV-VIS absorbance was done at least three times a week.

Table 7.1: Design parameters of the three different post-treatment technologies and their set-up

Design parameter	**Trickling filter** TF	**Slow sand filter** SSF	**(Biological) granular activated carbon filter** BAC
Filter material	Lava stones	Fine sand	Granular activated carbon (Organosorb 10®, Desotec, Belgium)
Filter material diameter (mm)	8 - 18	0.4 - 0.8	0.4 - 1.7
Supporting bottom material	n.a.	Gravel	Gravel
Supporting bottom material diameter (mm)	n.a.	1.7 – 2.5	1.7 – 2.5
Bed Volume, BV (L)	0.17[a] 0.52[b]	0.35	0.35
Flow rate (BV d^{-1})	5.1[a] 1.7[b]	2.5	7.1

[a] only considering the volume of submerged filter material

[b] considering the total volume of submerged and non-submerged filter material

n.a. = not applicable

2.2 Analytical methods

Details related to TrOC analysis, determination of general parameters (e.g. alkalinity, NO_2^--N, COD, EC, pH, etc.) and spectral measurements (UV-VIS) were already provided in sections 2.2 to 2.4 of Chapter 3 and are not repeated here.

Toxicity was measured using the BioTox kit (Aboatox Oy, Finland). This kit uses freeze-dried naturally bioluminescent marine bacteria *Vibrio fischeri*.[235,236] Bioanalytical assays for the follow-up of unselective toxicity determining the reduction in luminescence of the *Vibrio fischeri* is widely applied in municipal wastewater effluent and ozonation studies.[237] The test protocol involved combining 500 µL of test samples (with adjusted salinity of 2% sodium chloride) with 500 µL of reconstituted bacteria. After a contact time of 30 min at 15°C, the decrease of light intensity was measured with a portable tube luminometer (Berthold Technologies Junior LB 9509). The inhibitory effect is compared to a negative control (2% sodium chloride) to give the percentage growth (i.e. light) inhibition. Chromate was used to perform a positive control on the used protocol. More details on the usage of the BioTox kit is given in Dries et al.[236]

2.3 Correlation model for process control and data analysis

As a control strategy, the relationship between ΔUVA_{254} and ΔTrOC as proposed by several authors[40,63,64,81,114,227] was evaluated for both ozonation as a stand-alone treatment and for its combination with TF, SSF or BAC. In particular, the correlations experimentally constructed in Chapter 4 for 9 model TrOCs with an ozone reactivity ranging from fast ($k_{O3,TrOC} > 5\times10^4$ M^{-1} s^{-1}) to slow ($k_{O3,TrOC} < 10$ M^{-1} s^{-1}) are investigated: diclofenac, trimethoprim, levofloxacin ($k_{O3,TrOC} > 5\times10^4$ M^{-1} s^{-1}), amitriptyline, ciprofloxacin, venlafaxine (5×10^4 M^{-1} $s^{-1} > k_{O3,TrOC} > 10$ M^{-1} s^{-1}), amantadine, flumequine and metronidazole ($k_{O3,TrOC} < 10$ M^{-1} s^{-1}). The same 9 TrOCs were under investigation within the current study.

Although this correlation model has been constructed for ozonation of municipal effluent, its applicability when also incorporating an additional post-treatment is of interest but not investigated yet. Therefore, the ΔUVA_{254} determined by measurements before and after the entire tertiary treatment (ozone whether or not in combination with TF, SSF or BAC) is used to predict the TrOCs removal. The correspondence between measured, of which TrOC levels could be

quantified before and after treatment, and predicted data is evaluated using (i) an unpaired t-test of which the null-hypothesis (difference is not significant) is rejected by $p < 0.05$ and (ii) the Theil's inequality coefficient (TIC) of which a value below 0.3 is commonly seen as an indicator for a good agreement.[219]

3 Results and Discussion

3.1 Intercomparison of different tertiary treatment technologies: ozonation versus TF, SSF and BAC

3.1.1 Physical-chemical water characteristics

During the experimental period, every week, fresh effluent was collected and supplied to the post-treatment technologies. Daily averages of the effluent flow rate and temperature (at the municipal WRRF, geoloket.VMM.be) showed an opposite behaviour (Figure 7.2). While the effluent flow rate decreased from 97 to 46 m^3 day^{-1} in the 6-weeks period, most probably due to a decrease of rain events, the effluent temperature slightly increased (from 9 to 12 °C). This phenomenon is likely due to a seasonal change as sampling was done in the transition from winter to spring (February – March). Parallel to these variations, although also depending on the treatment performance, conductivity (EC; from 825 to 1242 μS cm^{-1}) and total nitrogen (TN; from 3.21 to 13.4 mg N L^{-1}) might indicate towards a lower dilution of the wastewater (e.g. less rain events) entering the WRRF. It is assumed that meteorological changes can have a significant influence on the biological processes within the WRRF. Consequently, a lower removal during this biological treatment step is temporarily expected (especially related to TN) resulting in higher values of the secondary treated effluent characteristics. Nevertheless, UVA_{254} (13.0 – 16.5 m^{-1}) and COD (15.5 – 18.6 mg O_2 L^{-1}) remained more or less constant within the considered timeframe.

The effect of different tertiary treatment technologies on these physical-chemical water characteristics is given in Figure 7.3. TF or SSF treatment do not induce a statistically significant change on the COD, BOD_5 and UVA_{254} level of the effluent (Figure 7.3a), which are all surrogates related to the organic matter content. BAC treatment yields high removal efficiencies for COD (≥ 67%), BOD_5 (≥ 53%) and UVA_{254} (≥ 93%) for all collected samples. Fresh granular activated carbon has been used at the start-up of the BAC experiments which makes that the

total load of organics on the activated carbon has most likely not exceeded its maximum capacity. Ozonation resulted over all weeks of operation in an average reduction of 42 ± 5% UVA_{254} and only minor, non significant, variations in COD (decrease) and BOD (increase, due to the formation of smaller and more biodegradable oxidation products).

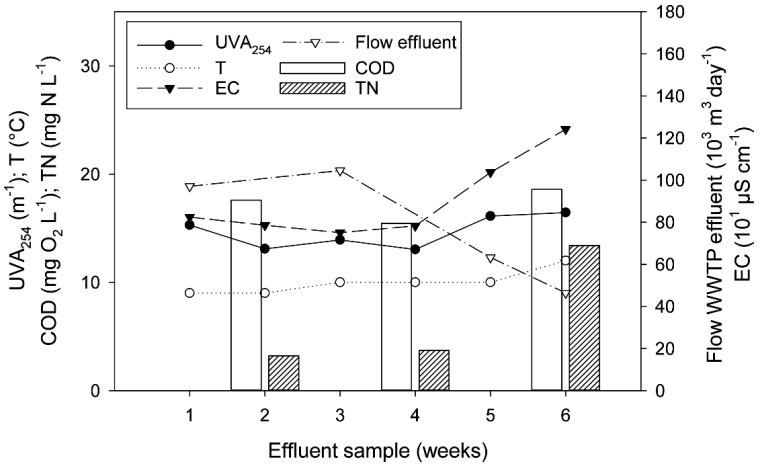

Figure 7.2: Municipal WRRF effluent characteristics before SSF, TF, BAC or ozone treatment during the 6 weeks of experimentation. The effluent flow rate and temperature are a daily average and was obtained through the Flanders Environment Agency (www.VMM.be).

Considering the effect of the different treatments on NO_3^--N, oPO_4^{3-}-P and TN, only some polishing and minor changes are noticed (Figure 7.3b). According to a t-test, oPO_4^{3-}-P was significantly (p-value < 0.05) removed during SSF and BAC (on average 22 and 16% respectively, presumably by ongoing biological processes) but not by TF or ozonation (on average 14 and 9% respectively). Total nitrogen and NO_3^--N did not show any statistically significant alterations during TF, SSF, BAC or ozonation. Nevertheless, a remarkable increase of NO_3^--N after ozonation can be seen. As known, the reaction of ozone in the presence of NO_2^--N or nitrogen containing organic moieties might lead to an increase of NO_3^--N as a final oxidation product. NH_4^+-N was only present at very low concentrations in the effluent (max. 0.03 mg NH_4^+-N L^{-1}) and, therefore, is not taken into further consideration.

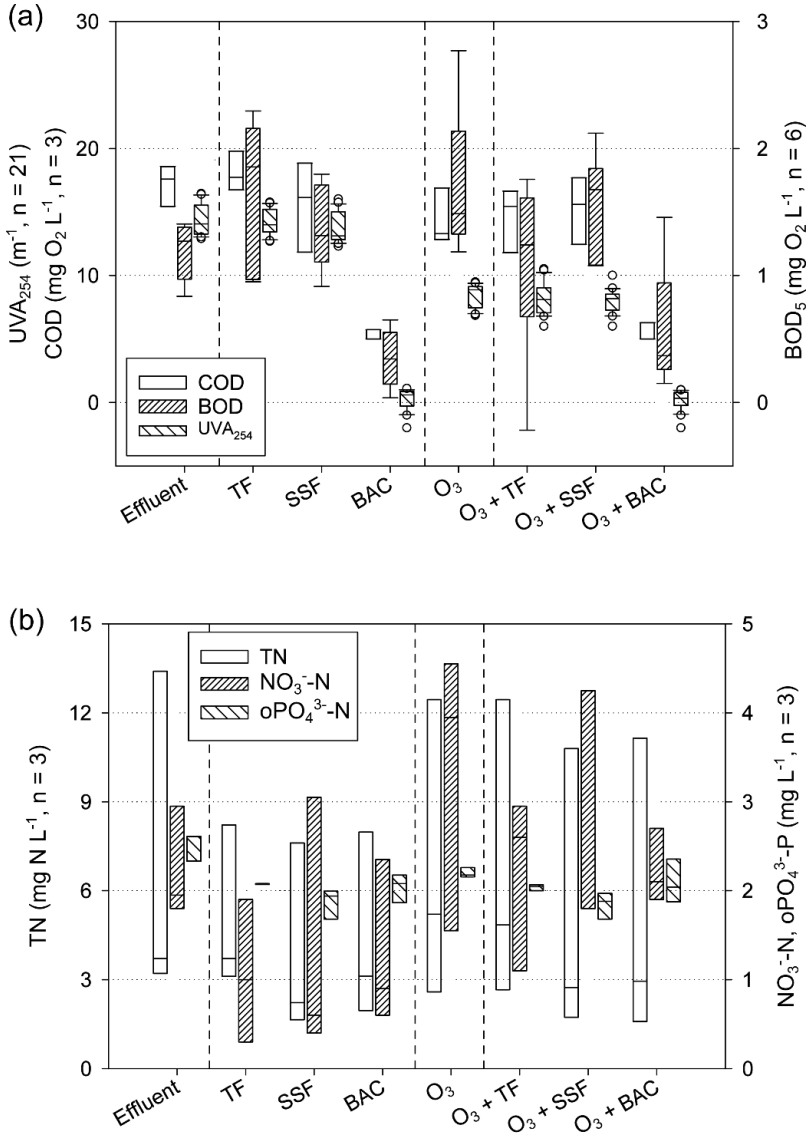

Figure 7.3: Physical-chemical water characteristics before and after (combined) treatment: (a) UVA_{254} (m^{-1}), COD and BOD_5 (mg O_2 L^{-1}) and (b) nutrients TN, NO_3^--N (mg N L^{-1}) and oPO_4^{3-}-P (mg P L^{-1}). The number of samples of each characteristic is indicated on the left or right y-axis.

3.1.2 Pharmaceuticals

The WRRF effluent was analysed for a total of 35 pharmaceuticals of which 18 components could be quantified within a range of 2 to 506 ng L^{-1} (Table 7.2). Large differences are noticed among the studied tertiary treatment technologies. No removal is obtained for 10 and 9 TrOCs by TF and SSF treatment, respectively, and the removal of most other TrOCs is rather similar and limited (< 59%) with both technologies. Ciprofloxacin (> 87 versus 70 %), levofloxacin (83% versus no removal) and metronidazole (76 versus 21%), however, are clearly better removed by SSF. Although these TrOCs are not easily biodegraded (i.e. they are still present after activated sludge treatment), the bacteria present in the slow sand filter might start to adapt to the specific conditions (i.e. limited nutrients, presence of TrOCs). Ciprofloxacin has been shown to be recalcitrant for biodegradation in aqueous systems[238] although some degradation has been reported in soil[238] and in a biofilter[239]. Most likely, the removal of ciprofloxacin, levofloxacin and metronidazole is a result of both enhanced biodegradation and sorption. Based on the log K_{ow} of these TrOCs (respectively 2.3, 0.35 and -0.1), a low tendency for sorption can be expected; although levofloxacin has been found to adsorb on granular media as e.g. sand.[240] Yang et al.[241] observed an averaged removal of 80 and 71% for ciprofloxacin and levofloxacin, respectively, during biological treatment. Sorption onto sludge flocs, as these TrOCs contain charged chemical groups, was seen to be significant compared to biodegradation as the log K_d (representative for the sorption of components on sludge) for ciprofloxacin is reported to be 4.3. Levofloxacin is more polar but no log K_d value is found in literature. Nevertheless, it is assumed by Yang et al.[241] that the high K_d values for other fluoroquinolone antibiotics such as norfloxacin, trovafloxacin, and gemifloxacin suggest that levofloxacin is also strongly adsorbed. Filtration by BAC yields significantly higher removal percentages for all 18 TrOCs. All are removed above 80% or even to concentrations below the detection limit. This clearly indicates the technical applicability of BAC filtration for a wide range of TrOCs. It can be assumed that, although inoculation of bacteria occurred before start-up of the filtration columns, adsorption will be the main removal mechanism as TrOC removal is clearly better compared to TF and SSF, and fresh AC was used at start-up.

Table 7.2: Removal (%) of TrOCs after different (combined) treatments of WRRF effluent.

TrOCs	Effluent ng L^{-1}	TF %	SSF %	BAC %	O_3 %	O_3 + TF %	O_3 + SSF %	O_3 + BAC %
Alprazolam	3	n.r.	n.r.	bdl	42	34	29	bdl
Amantadine	45	n.r.	n.r.	98	59	59	56	98
Amitriptyline	35	51	46	94	96	52	65	94
Carbamazepine	487	n.r.	n.r.	bdl	bdl	bdl	bdl	bdl
Ciprofloxacin	71	70	bdl	bdl	59	bdl	bdl	bdl
Diazepam	2	18	n.r.	bdl	64	35	38	68
Diclofenac	506	n.r.	n.r.	bdl	bdl	bdl	bdl	bdl
Flumequine	5	15	10	bdl	17	n.r.	13	15
Indomethacin	48	bdl	bdl	bdl	bdl	bdl	bdl	bdl
Levofloxacin	30	n.r.	83	bdl	80	78	83	bdl
Metronidazole	24	21	76	82	56	46	76	57
Nalidixic acid	5	n.r.	15	bdl	n.r.	n.r.	n.r.	bdl
Nevirapine	8	n.r.	n.r.	bdl	bdl	bdl	bdl	bdl
Paracetamol	132	59	51	bdl	30	68	bdl	53
Sulfamethoxazole	24	n.r.	n.r.	bdl	95	82	92	bdl
Tetracycline	50	25	32	bdl	bdl	bdl	bdl	bdl
Trimethoprim	74	n.r.	n.r.	85	87	12	81	76
Venlafaxine	367	n.r.	n.r.	98	97	96	97	89

n.r. = removal efficiency < 10%; bdl = concentration after treatment is below detection limit

The performance of ozonation towards TrOCs removal is clearly better than that of TF and SSF, but not as good as that of BAC. For 10 pharmaceuticals, removal efficiencies were higher than 80% (or the compound was not detected anymore in the ozonated effluent). Only nalidixic acid showed to be fully recalcitrant towards ozonation, allthough the concentration was already close to the detection limit (DL = 2 ng L^{-1}, see Vergeynst et al.[189]). For the other TrOCs, removal efficiencies in the range of 17 to 64% are obtained. It should be noted that the measured TrOCs have a wide variety in ozone reactivity, as exemplified by their apparent secondary reaction rate constant with ozone, $k_{O3,TrOC}$. The additional use of TF or SSF after ozonation is in general not able to decrease the TrOC concentrations even more which is in compliance of there stand-alone use. Differences between ozonation only or combined with TF or SSF can be attributed to

analytical measurement errors (i.e. TrOCs removed to low ng L^{-1} concentrations by ozone only) or potential desorption of TrOCs of the filters.

Figure 7.4 shows the total quantified TrOC concentrations before and after tertiary effluent treatment. Whereas TF and SSF do not lead to a reduction in the summed TrOCs concentration, ozonation and BAC treatment enable a decrease of more than 90% and 99%, respectively. This complies the target, i.e. removal of at least 80% of a set of indicator TrOCs during the full treatment train, as recently proposed by the Swiss regulator.[22]

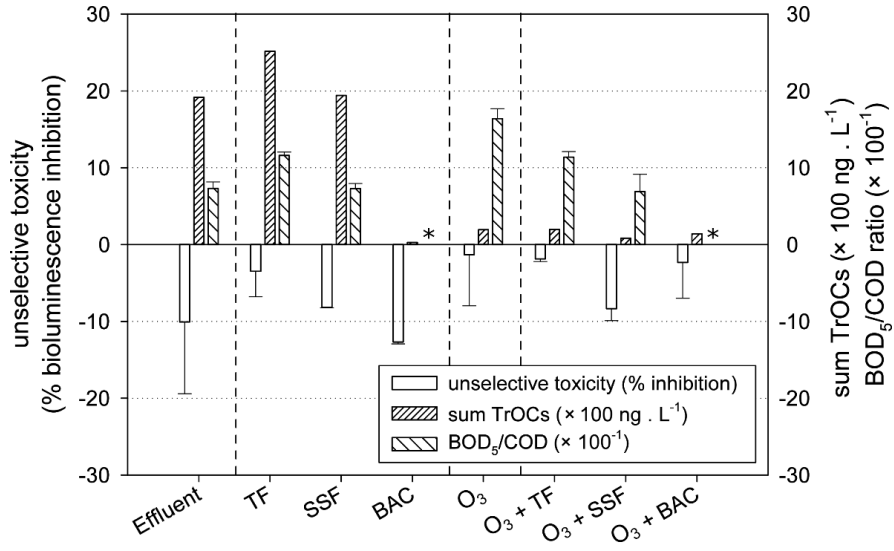

Figure 7.4: Toxicity, sum of quantified TrOCs, and biodegradability in the secondary treated WRRF effluent and after different (combinations of) post-treatments. The negative values for toxicity represent a lower percentage of inhibition (of light intensity by *Vibrio fischeri*) than the control sample (i.e. 2% sodium chloride). The BOD_5/COD ratio after BAC and ozonation + BAC could not be determined as the COD after treatment was below the detection limit (indicated with *).

3.1.3 Toxicity

Considering unselective toxicity (Figure 7.4), the tertiary treatment technologies are showing some differing results compared to TrOC removal. To start, it should be mentioned that the inhibition of the secondary effluent on the luminescent *Vibrio fischeri* of the BioTox kit was

already negative (i.e. a lower toxicity) compared to the control solution (2% sodium chloride). It is likely to consider that the effluent contains more nutrients than the control solution (made in demineralised water) which probably favours the growth rate of the *Vibrio fischeri*. For further comparison of the inhibition after tertiary treatment, this phenomenon is non-essential as all results can be compared to the toxicity of the WRRF effluent. Although rather high deviations are noticed for most replicated measurements (see error bars in Figure 7.4), being inherent to the measuring protocol,[236,237] interesting trends can be observed. Compared to the WRRF effluent, toxicity (percentage bioluminescence inhibition values) increases by a value of 9 and 7 % after ozonation and TF. SSF and BAC treatment do not show an important effect regarding the measured toxicity (i.e. < 3% increase or decrease). Especially for ozonation, an increase of the BOD_5/COD ratio (from 0.07 to 0.16, Figure 7.4) indicates changes in the water matrix with the formation of smaller and more biodegradable moieties, which have been associated to an increased toxicity. The formation of possibly toxic by-products through reactions of ozone with bulk organic matter has already been discussed extensively in literature (see e.g. Knopp et al.[242] and Reungoat et al.[35]). The minor increase of toxicity after TF is most likely associated with the slight decrease in available nutrients (mainly TN and NO_3^--N, Figure 7.3b) and thus hampering the *Vibrio fischeri* growth as a result of the biological activity within the filter. During BAC filtration, the significant decrease of TrOCs and other organics (as indicated by COD and UVA_{254} measurements) may be compensated by a reduction in nutrients, resulting in similar toxicity values before and after BAC.

All in all, only little differences in toxicity are noticed for the different (bio)filtration technologies. Based on Figure 7.4, BAC showes high TrOC removals and a decreased BOD_5/COD ratio but no effect on toxicity. Ozonation clearly shows to remove TrOCs but also increases the toxicity level and BOD_5/COD ratio which requires an additional post-treatment. TF and SSF seem inefficient as stand-alone technologies considering their limited effect on TrOCs and BOD_5/COD.

3.2 Combination of ozonation and (bio)filtration

Among the three different post-treatment technologies, only BAC could improve the removal of BOD_5, COD and UVA_{254} compared to the levels obtained with a preceding ozonation (Figure 7.3a). This in agreement with previous results as also here TF and SSF are not able to result in a

significant added removal of these organic surrogate parameters. In contrast, the latter two technologies could reduce the oPO_4^{3-}-P level, measured after ozonation, by an additional 7 – 15%, up to levels similar as obtained with TF and SSF without preceding ozonation. Total nitrogen and NO_3^--N showed some minor decreases although not statistical significant when adding TF, SSF or BAC as post-ozonation technologies. Although not investigated in detail, the combination of ozonation and BAC might increase the time before break-through.

Regarding TrOCs, the added value of a post-ozonation treatment technology is noticed only for the SSF. Figure 7.4 shows that the total amount of quantified TrOCs decreases from 192 ng L^{-1} (after ozonation) to 82 ng L^{-1} (after ozonation + SSF), showing the potential of SSF as an effective polishing step for the ozonated effluent. Considering the individual components in Table 7.2, the most pronounced improvement is obtained for ciprofloxacin (> 87% removal), metronidazole (76% removal) and paracetamol (> 80% removal), being TrOCs that could also be largely removed by stand-alone SSF (respectively > 87, 76 and 51% removal).

For both TF and BAC, the total concentration of the measured TrOCs could not be further reduced when applying these technologies as post-ozonation treatment. It can even be noticed that BAC as a stand-alone technology yields higher TrOCs removal compared to the combined ozonation + BAC treatment. This might be due to the fact that oxidative treatment during ozonation increases the polarity and hydrophilicity of the TrOCs which might result in less favourable adsorption on the active sites of the activated carbon surface. Schoutteten et al.[243] concluded that when targetting mixtures of TrOCs with ozonation, a trade-off has to be made towards the overall reactivity and behavior of different TrOCs (products) when combined with AC. Although the parent TrOC will keep its original adsorption behavior, reaction products of ozonation were shown to be less adsorbed by AC depending on the transformations for specific TrOCs (e.g. atrazine, carbamazepine, dinoseb).

The increased toxicity of the municipal WRRF effluent after ozonation was lowered by all three post-treatment technologies (Figure 7.4), although the effect of TF and BAC following ozonation is only minor. However, when applying SSF after ozonation, the toxicity is reduced again to the level measured in the secondary effluent. Next to that, the biodegradability (BOD_5/COD) of the treated water decreased to that of the WTTP effluent, supporting the hypothesis that the increased toxicity of the effluent after ozonation has been induced by changes in the matrix composition that also increased the biodegradability, in agreement with what has been previously described in literature.[35,242]

Overall, ozonation in combination with SSF or single BAC filtration are the treatment technologies giving the best technical performance regarding both TrOC removal and toxicity. Economical considerations might be determining in the choice to be made. Moser[36] estimated the cost depending on the WRRF size for ozonation and sand filtration in the range of 4.8 to 36.7 CHF (4.1 to 31.5 €) and 5.9 to 32.2 CHF (5.1 to 27.7 €) i.e.$^{-1}$ y^{-1}. AC costs were higher, between 21.5 and 95 CHF (18.5 to 81.6 €) i.e.$^{-1}$ y^{-1}, mainly because of the replacement of exhausted activated carbon.[35,36] Without replenishment of exhausted carbon, the biological filter will logically exhibit a behavior similar to more inert materials such as e.g. the slow sand filter. Using BAC as a polishing post-ozonation technology clearly becomes too expensive, as also Prasse et al.[34] recently reported. Ozonation, followed by SSF to cope with a potential increase in toxicity and as final polishing step, is thus the preferred treatment chain to reduce TrOCs levels in secondary WRRF effluent.

3.3 Applicability of surrogate measurements for online control of TrOCs removal during combined tertiary treatment

The measured TrOC removal of nine selected pharmaceuticals with a large range in 2nd order reaction rate constants ($k_{O3,TrOC}$ ranging from < 1 to 10^6 M^{-1} s^{-1}) is compared with the predicted TrOC removal, based on the ΔUVA_{254} – ΔTrOC correlations models developed in Chapter 4.

Compared to ozonation, where a good agreement between measured and predicted values was exemplified by both a t-test ($p > 0.05$) and a TIC value of 0.15, a lower predicting power was obtained when considering the data obtained through combined treatments. TIC values of 0.38 (O_3 + TF; $p = 0.026$), 0.22 (O_3 + SSF; $p = 0.047$) and 0.23 (O_3 + BAC; $p = 0.076$) were calculated. Although the t-test and TIC value are indicating a better correspondence for ozonation + SSF than for ozonation + TF, the correlation model can only be used as an indicator. Ozonation + BAC resulted in very high removal efficiencies, as previously described, for both the selected TrOCs and UVA_{254}, which resulted in a 100% predicted removal for all compounds. This makes it hard to draw strong conclusions about the applicabilty of the correlation model for this treatment chain because of the limited measuring range.

Overall, for most TrOCs having a $k_{O3,TrOC}$ > 10 M^{-1} s^{-1} a removal of 100% was predicted by ozonation only at a ΔUVA_{254} of 39%. Especially the slowly reacting TrOCs (and therefore less removed) are of interest for future regulation. For less ozone reactive TrOCs, the model predicts

removal efficiencies of 70% (amantadine and flumequine) and 55% (metronidazole) for ozone only. When considering only these last three instead of nine TrOCs for ozone wether or not in combination with TF, SSF or BAC, the correspondence between predicted and measured removal is statistically significant. The predictive power of the models could not be established considering the TIC values. TIC (and p-)values of 0.28 (O_3; $p = 0.26$), 0.53 (O_3 + TF; $p = 0.19$), 0.36 (O_3 + SSF; $p = 0.18$) and 0.33 (O_3 + BAC; $p = 0.21$) were calculated. This means that, although the correlation models have been developed for ozonation only, the same models can statistically be used to give an indication for the removal of slowly reacting TrOCs considering the complete treatment train, combining ozonation with TF, SSF or BAC.

4 Conclusion

Filtration technologies solely depending on any kind of biodegradation mechanismes (aerobic, anoxic, anaerobic) are inefficient for the removal of TrOCs in the secondary effluent of municipal wastewater treatment plants. In contrast, activated carbon filtration supported by slight biological activity can reduce the TrOCs levels by more than 99% but the replacement of the exhausted carbon makes this technology expensive for full-scale applications. A good alternative showed to be a treatment train consisting of ozonation, reducing the total TrOCs concentration by more than 90%, followed by slow sand filtration as a final polishing also reducing toxicity to the same level as before ozonation.

In terms of monitoring and control of TrOC removal, innovative correlation models based on the online measurement of changes in UVA_{254} were applicable during ozonation. Although the predictive power decreased when TF, SSF or BAC were added as a post-ozonation technology, the same models can still give a good indication of the TrOC removal in secondary WRRF effluent particularly for the most relevant, poorly reactive TrOCs.

Chapter 8

General discussion and perspectives

1 The development, calibration and validation of an online model framework

In this dissertation, a model framework that can be used to monitor or control TrOC abatement during tertiary ozonation of secondary municipal wastewater effluents has been developed, calibrated and validated. In Chapter 4, a surrogate-based correlation model was developed following UVA_{254} or fluorescence reduction (ΔS) during ozonation and correlating to the TrOC abatement (ΔTrOC). Single linear regression models from literature were improved as these were clearly insufficiently representing and explaining physical and chemical phenomena of the oxidation processes. During increasing oxidation, it was hypothesized that mainly two phenomena occur: (i) transformation of the organic matrix leads to products with higher HO• production yields, and (ii) remaining dissolved ozone that is still present after an initial reaction phase with fast direct ozone reactions can react further with hydroxyl ions, forming HO• or other oxidative radicals. Although the generation of HO• depends on complex mechanisms, highly affected by oxidant induced changes of the organic matrix, the correlation between ΔS and ΔTrOCs was clearly affected, resulting in two distinct sections, respectively phase 1 and 2, in their correlation. Transformation of target TrOCs and EfOM is clearly dominated by direct and rapid ozone reactions during phase 1, as a correlation was obtained between the slope and the TrOC specific $k_{O3,TrOC}$. Phase 2 was found less depending on direct ozone reactions, as highly ozone reactive compounds are assumed to be degraded and reactions to be dominated by indirect (and less selective) HO•, exemplified by its independency of the TrOCs specific $k_{O3,TrOC}$.

The given approach is also in line with recently published research by Chon et al.[53] and Park et al.[54] An observed shift in the electron donating capacity of the EfOM was observed by Chon et al.,[53] pointing out an inflected correlation between ΔUVA_{254} and ΔTrOCs. Park et al.[54] developed a kinetic approach using low ozone reactive TrOC indicator compounds, including two empirical parameters representing the O_3/HO• contribution and the effluent water quality (i.e. reactivity) respectively. Some further elaboration was recognized as the influence of a varying water quality was not clear from the research of Chon et al.[53] and Park et al.[54] although this kind of models clearly help to increase the knowledge of the ongoing processes. The developed model in this dissertation was, however, only depending on the TrOC specific $k_{O3,TrOC}$ and the measured decrease of UVA_{254} or fluorescence measurements. Both surrogate types can be measured online which makes the model applicable for any TrOC with a known $k_{O3,TrOC}$. Ozone based degradation has already been investigated intensively in literature resulting in an estimated availability of > 500 compounds in literature with a known $k_{O3,TrOC}$.[39,156,165,244] The $k_{O3,TrOC}$ can be determined

experimentally but recent research also developed QSAR models that reduce the need for extensive experimentation.[225,226] These models were clearly not within the scope of this dissertation but have shown to estimate $k_{O3,TrOC}$ and $k_{HO\bullet,TrOC}$ values with an error within the range of experimentally determined k-values.[226] The exact value of $k_{O3,TrOC}$ for a specific TrOC might thus vary based on the method of determination. Therefore, the developed inflected model considers the variation of experimental regression and the use of varying $k_{O3,TrOC}$. The determination of $k_{O3,TrOC}$ for targeted TrOCs thus allows a straightforward prediction of the abatement pattern within the 95% confidence interval.

Secondary effluent from 15 locations in Belgium has been characterized with different water quality characteristics (Chapter 3), although the differences between different WRRFs was rather low. The highest/lowest values measured were clearly site or event depending, such as varying weather conditions or other events (e.g. malfunctions) during operation of the WRRF. Significant variations were noticed among all plants related to parameters known to influence the ozonation process (e.g. alkalinity, NO_2^--N, pH, etc.). These variations need to be accounted for in a generical and effective control framework, as no direct and reliable measurement is available before ozonation to account for all influencing organic or inorganic constituents (i.e. water quality parameters). Validation of the developed model was therefore performed for different WRRFs and during long-term operation on pilot-scale of which the results are presented in Chapter 5. The new inflected correlation models based on both UVA_{254} or fluorescence measurements showed to predict TrOC abatement at least as good or even better as existing single correlation models from literature.

2 Dealing with effluent dynamics and its influence on the ozone demand

Effluent dynamics played an important role during the pilot-scale investigation of the developed model and when comparing the proposed control framework with two other strategies (Chapter 6). Effluent dynamics in terms of load and different characteristics were outlined in Chapter 3. The control strategies themselves are well explained in Chapter 1 (section 4). The main issue during continuous operation is the variable ozone demand due to a (i) variable load (i.e. concentration) of (in)organic constituents (given in Figure 1.2) in the effluent and/or (ii) an altered effluent composition (i.e. reactivity) of the complete effluent matrix. This observation was clearly in line with previous research showing inconsistencies between the ozone exposure and

achieved TrOC abatement, suggesting a clear water quality dependency.[40,98] Load proportional ozone dosing by e.g. normalizing the ozone dose with the DOC has been indicated as an alternative for flow proportional ozone dosing. However, EfOM variability following storm events due to increased dilution or the run-off of unconventional components resulted in deviations in TrOC abatement.[162,211]

The three control strategies under investigation in Chapter 6, i.e. load proportional, flow proportional and differential control (based on ΔUVA_{254}), all coped in a different way with the variable ozone demand, having their implications for the overall ozone consumption and OPEX. The ΔUVA_{254} clearly led to the most economical favorable solution although an efficient TrOC abatement and minimal potential of by-product formation might even be more important. The ozone dose control applying the model developed in this dissertation was clearly able to meet the imposed target ΔTrOC (see Chapter 5). Changes in the effluent composition, such as a variable ozone demand up to 1.4 mg O_3 L^{-1} due to NO_2^--N fluctuations, unraveled clear differences between the different strategies. The principle of these differences are graphically summarized in Figure 8.1. The application of a load proportional O_3:DOC ratio dosing considers the effluent load entering the ozonation reactor and does not account for its varying composition or effluent reactivity, determined as the ΔUVA_{254} per mg of ozone consumed. It could therefore be stated that a 2nd UVA_{254} measurement is required after the ozonation process. A flow proportional ozone dose is completely lacking in accounting for any variation in load or composition. As already pointed out in Chapter 3, variations in water quality characteristics are rather limited and the matrix reactivity will be the main influencing factor, as confirmed in Chapter 6.

Overall, it became clear that the effluent matrix composition (i.e. reactivity) is highly variable (from 0.3 to 1.8 m^{-1} mg^{-1} L), and impacts the ozone demand from 3.8 to 24 mg O_3 L^{-1} (at a set-point of 25% ΔUVA_{254}) and from 5.6 to 14 mg O_3 L^{-1} (at a set-point of 40% ΔUVA_{254}), and hence the TrOC abatement (and potential by-product formation). The matrix reactivity was mainly variable in periods with rapidly changing events due to e.g. first flush. A 'standard value' of the ozone reactivity was established at around 1 m^{-1} mg^{-1} L. Although the concentration or load of the effluent will influence the ozone demand, it was noticed that the matrix reactivity was correlated with the applied ozone dosing. The practical independent behavior of the effluent reactivity compared to the effluent load (as $UVA_{254,eff}$) confirmed again that the effluent reactivity will mainly determine the needed ozone dose to achieve the ΔUVA_{254} (and thus ΔTrOC) set-point.

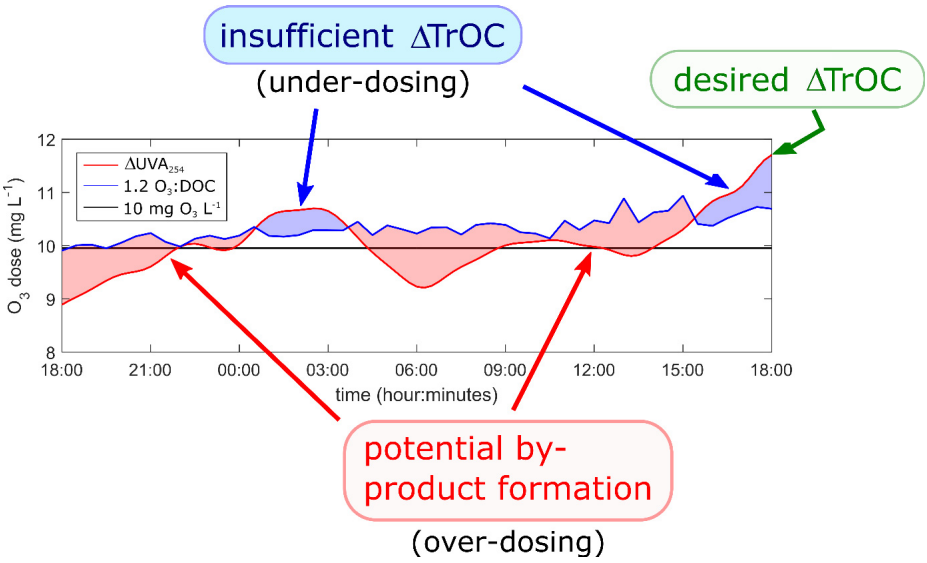

Figure 8.1: Ozone dosing during pilot-scale experimentation using a (i) flow proportional (10 mg O_3 L^{-1}), (ii) load proportional (1.2 g O_3 g^{-1} DOC_{eq}) or (iii) differential UVA_{254} control strategy (obtained during 24 hour of pilot-scale investigation from Chapter 6, 25% ΔUVA_{254} set-point, period III). Over- (red) and under-dosing (blue) regions are indicated by applying the load proportional strategy compared to the differential UVA_{254} strategy.

3 The issue of oxidation transformation products and how to deal with them

The main goal was to achieve (i) a reliable, generically applicable and (cost) efficient TrOC abatement strategy for dynamic conditions and (ii) minimizing the by-product formation potential. Although the latter was not included during model development, it is more than likely to assume that this will be one of the results.

Potential formation of toxic transformation products by ozonation of TrOCs and/or EfOM is a shared concern, hampering the wide application of the technology. The main reason for this is that effects are widely unknown and no optimal ozone dosing strategies are available to limit the potential formation. Different mitigation options exist such as source control (e.g. of NDMA precursors) or post-treatment (e.g. UV-photolysis or biological transformation).[42] Post-treatment of tertiary ozonated effluent has been put forward as a protective barrier against formed by-products. It was for example shown in Chapter 7 that ozonation might lead to an increased

toxicity but that e.g. a biological sand filter is capable to reduce these levels back to those before ozonation. Also e.g. the Swiss legislation is imposing an additional sand filter after ozonation to ensure an efficient barrier for any biologically degradable products. Pre-treatment of effluent by removing (part of) the EfOM by e.g. ion-exchange might be another option in removing precursors although posing an additional investment and treatment cost.[245] Ion-exchange processes are e.g. being used in the production of drinking water for the removal of NOM from surface water.[246] Nevertheless, more investigation needs to be done as reduced presence of EfOM (i.e. in relation to the presence of other constituents) might result in less electron rich moieties (i.e. less direct ozone reactions), and a higher HO• exposure. High HO• exposures have been associated with increased formation of potential toxic transformation products (as discussed in Chapter 1 section 2.3).

Optimal ozone dosing is thus required to lower the extent of by-product formation. The formation of bromate or NDMA, both potentially carcinogenic, has been associated with the ozonation of EfOM although it is often a plant specific issue.[78,95–97] Although the exact precursors are not always known, the formation has been generally associated with high ozone dosages, exceeding effluent specific threshold values, because of reactions with the available EfOM.[42,44,45,78] At these high ozone dosages, ozone will have less competition by electron rich moieties and is therefore more available for reaction with e.g. bromide to form bromate.[53,97] As such, also mixing effects and local occurrence of high ozone concentrations need to be accounted for in the future to limit the formation of toxic by-products as much as possible.

Nevertheless, also here, surrogate-based correlation models are a potential solution. Liu et al.[101] were able to correlate the formation of EfOM originating oxidation products (i.e. aldehydes and carboxylic acids (ACA)) with absorbance and fluorescence surrogates. Also in the formation of potential toxic by-products (e.g. bromate and biological degradable DOC), it appears that two reaction phases can be noticed in the correlations with UV absorbance or fluorescence, similar to the observed phenomena in Chapter 4. This is in accordance with the previous statement that the formation is only occurring at high ozone doses,[99] i.e. less availability of ozone susceptible moieties and mainly indirect ozone reactions are occurring. Further extensions of the model developed in this dissertation need to include the monitoring and control of potential toxic by-products. During the study of Li et al.[99] it could be concluded that the use of O_3:DOC ratio is not sufficient to monitor by-product formation, and the matrix reactivity will need to be accounted for by a differential control strategy.

4 Applicability and practical considerations for the successful implementation at full-scale installations

Practical issues related to the use of online spectral sensors for the control of the ozone dose have been outlined in Chapter 6. It was noticed that cleaning of the sensor will be an important aspect in long-term and reliable control situations. Especially the need for a cleaning utility that can be applied online was pointed out, as the use of ultrasonic cleaning was highly advantageous. It could be concluded that, without any online cleaning, drift of the sensor readings because of fouling was too high to be applicable in full-scale installations. With such online cleaning, manual cleaning could be reduced to once a week which is a feasible interval for operators and maintenance personnel. It should be noted that during such cleaning interval, no online measurements will take place and the ozone dose will need to be fixed representative to the last measured ΔS. As manual cleaning will mostly take less than one hour and effluent variability is seen low during this time interval, no significant implications are assumed and a reliable TrOC abatement can be assured.

Chapter 7 touched the issue of positioning the 2nd reference sensor (i.e. after ozonation) after a post-treatment technology, and briefly assessed its further use as input to the developed correlation model. The UVA_{254} based correlation model was validated for its implementation after a sand filtration step following ozonation although further investigation is needed. This might reduce scaling and the presence of solids in the effluent, influencing the online measurement. The positioning of the 2nd reference sensor has implications on the response time of the dosing control. It not only has to account for the HRT in the ozone reactor but also for the HRT in the sand filter which is easily up to 30 minutes or more if both are combined. Low variability of the effluent can be noticed during this time interval (see Chapter 6) but potential spikes of increased ozone demand will be hard to compensate. This increased lag time to ensure a proper control action was also seen by Stapf et al.[158] as the main reason to place the 2nd reference sensor after the ozonation but before the post-treatment.

During Chapter 6, one of the main advices for further control actions is the use of a combined FB-FF (feedback-feedforward) approach in which the ozone dose is determined by the correlation model developed in Chapter 4 (and validated in Chapter 5). The sensor measuring the effluent before ozonation can be used to react quickly on sudden changes or spikes of the effluent load. This combined FB-FF approach might therefore make it possible to place the 2nd reference sensor after the post-treatment although further investigation to this new control

strategy is needed. The proposed sensor configuration in this dissertation, i.e. one sensor both before and after ozonation, showed great potential and should be further investigated.

5 Potential of UVA and/versus fluorescence surrogate-based models

It was concluded in Chapter 4 that both UVA_{254} and fluorescence have their specific benefits. Further validation during Chapter 5 was supportive to these findings, as UVA_{254} based correlation models showed to work fine for the control of TrOC abatement and the UVA_{254} measurement by online sensors has already been established with commercially available sensors ranging from single wavelength to full spectrum sensors. Also fluorescence sensors exist although some development is still ongoing making them less widely established within the field. Especially some further improvements are needed in accuracy, sensitivity, calibration and the compensation for inner filter effects.[99] Potential benefits of fluorescence measurements are, however, shown as (i) they indicate improved robustness with an increased control range, (ii) they are more sensitive (of potential value for drinking water applications), and (iii) PARAFAC analysis of 3D EEMs enables the simultaneous monitoring of multiple types of organic matter with a different reactive behaviour. Specifically selected wavelengths in Chapter 3 showed distinct reactivity for ozone, providing better understanding of the occurring changes of organic matter during ozonation. In line with these findings, Spiliotopoulou et al.[247] could accurately estimate the low range ozone (0-5 mg O_3 L^{-1}) demand in recirculation aquaculture systems based on frequently used fluorescence peaks within the 3D EEMs (of which some discussed in Figure 1.6 and Figure 1.7 in Chapter 1 section 3.2.3) and a simple correlation with the ozone dose. Monitoring the reactivity of the organic matrix, the aldehydes and carboxylic acids, and the bDOC or bromate formation yield might be better predicted using fluorescence measurements, as indicate by recently published research.[99,101]

Furthermore, spectral surrogate measurements can play a role in a legislative framework. As already mentioned in Chapter 1 (section 2.2), regulation for TrOC abatement before discharge from WRRFs is upcoming in the EU, as examples exist in which regulation is implied (e.g. Switzerland or groundwater replenishment in California, USA). Discharge limits can however be imposed in absolute TrOC concentrations (e.g. in ng L^{-1} or μg L^{-1}) or percentage TrOC abatement (e.g. % or log removal). TrOC concentrations in WRRF effluents have shown to fluctuate, but results in Chapter 3 showed variations mostly within the same orders of magnitude.

A monitoring or control framework for percentage TrOC abatement will thus be of high interest although offline measurements will still be required, although less frequently (i.e. once a month). Imposing discharge limits in form of percentage TrOC abatement thus makes sense, similar to the approach widely used for disinfection purposes (i.e. log removal). Groundwater replenishment systems in California, USA, are subject to a removal of 0.3-0.5 log, depending on the different classes of indicator compounds. In line, the Swiss Water Protection Act also specifies an 80% removal of a five compound set of indicators that need to be removed during wastewater treatment while no absolute concentrations were imposed as discharge limits. This choice was the result of years of thorough research.

It can be finally stated that (i) surrogate-based models are able to reliably control TrOC abatement in tertiary ozonation units at municipal WRRFs, (ii) the use of these models contains much potential with regard to toxicity monitoring, and (iii) researchers and regulation authorities are urged to sit together and combine research and legislation to provide a common framework to protect the aquatic environment while in the same time offering treatment utilities a workable solution to cope with the increased purification objectives.

6 Further recommendations and perspectives

In this dissertation, a novel surrogate-based correlation model framework was developed, calibrated and validated under variable effluent conditions. A better understanding of the effluent dynamics, both in terms of load and composition, was reached which allowed to evaluate potential implications and applicability of different control strategies during continuous operation. The aimed end result of achieving an easily applicable and reliable control framework was obtained, although some recommendations have already been made in previous sections. Furthermore, future research will be needed to facilitate the wide implementation of tertiary ozonation and this control framework for TrOC abatement. An effective solution is available for online control although some issues need to be tackled related to the reactor and process design, knowledge exchange between different parties (e.g. scientists, industrial suppliers and operators), incorporation of toxicological knowledge, etc. Some more details are given below about issues that are seen most valuable to cover during future research:

(i) More data and knowledge on tertiary ozonation should be gathered, applying the developed control strategy preferably at full-scale installations. The effluent dynamics in terms of reactivity should be expanded to understand (regional) differences between plants. Full-scale installations will allow to investigate the influence of different operational settings and weather conditions on the TrOC abatement efficiency and implied costs. With respect to this, spectral UV sensors are already widely used, although mainly for monitoring purposes. Therefore, a lot of data on variability is available in databases, being of high value for scientists, sensor developers, etc. and potentially leading to interesting insights. More data is needed after all on real wastewater environments with presence of e.g. turbidity and solids, known to influence the ozone reactions, where current research is often done in controlled laboratory environments in which a lot of samples and wastewater is filtered before further usage. Scientists and practitioners etc. are therefore urged to work together, share their own specific knowledge and publish data publicly in a complete form, directly usable by others.

(ii) Currently, UVA_{254} received most attention. Although multi-wavelength approaches as displayed for fluorescence spectra showed clear benefits with increased control ranges and sensitivity as main outcome. The potential of these approaches should be investigated in more detail, also for UV-VIS spectra using data reduction methods as PCA to further increase the robustness of current models.

(iii) The current models are effective for control and monitoring purposes although not fully applicable to use during the initial design process of ozonation processes and reactors. Most kinetic approaches rely on the measurement of ozone (and/or HO•) exposures which is difficult during wastewater ozonation.[248] The increased sensitivity of fluorescence measurements and the ability to follow different reactive behavior of the organic matrix is interesting to include in a kinetic modelling framework, even for less concentrated matrices as e.g. drinking water. Different authors also showed the possibility to differentiate (Ef)OM into different organic fractions (e.g. hydrophobic vs. hydrophilic, based on molecular weight, etc.).[113,249,250] The translation of these measurements to kinetic knowledge can be used to improve reactor design.

(iv) The mixing efficiency in ozonation reactors is important although often ignored in most studies. Differences between laboratory experiments (i.e. a controlled environment) and pilot- or full-scale applications are mostly due to an inefficient mixing and/or transfer at the gas-liquid interface. Efficient mixing of the gas and

liquid phase in ozone reactors will avoid local over- (or under-)dosing of ozone which will in return result in a lower formation potential of (toxic) by-products or higher TrOC abatement. Different approaches exist to model reactor configurations, but increased computational knowledge has led to a more wide use of Computation Fluid Dynamics (CFD). Some studies already showed good potential for disinfection purposes, optimizing ozone contactors to reduce the ozone dosage, disinfection costs and by-product formation potential.[251] A combination of CFD and a kinetic model based on spectral surrogate measurements might be able to predict TrOC abatement efficiency, toxic by-product formation potential, etc. and would be extremely valuable for effective reactor design, tailored to the distinct needs of tertiary ozonation.

(v) Additionally to the ozonation process itself, the availability of proper analytical tools will remain of high importance. Investigations in those highly accurate and sensitive measurements technologies, also including different toxicological assessment methods, can therefore not be reduced and should even increase. Offline sampling and detailed molecular characterization of wastewater will remain necessary, new chemical contaminants will emerge during improved (mass spectrometry based) screening approaches, and new challenges related to the accurate and precise measurement of (ultra-)trace levels of these (emerging) TrOCs, their metabolites and transformation products and their effects will necessitate further research on innovative analytical assays.

(vi) A tertiary ozonation step should be considered as treatment step on itself, but also as a part of a complete treatment train from influent wastewater up to the discharge and ecological effects in the surface water. For example, ozonation is often implemented with an additional post-treatment step to reduce the (little) amount of formed biologically degradable products and the associated potential of increased toxicity. Nevertheless, the effect of these easily biologically degradable (and potentially toxic) products ending up in surface waters is not completely known (i.e. toxicity effects), and it is therefore not known if such as treatment step is ecologically beneficial over a direct discharge after ozonation.

(vii) Toxicity of effluents after ozonation is one of the main concerns and needs to be included during (all) further research. It cannot be ignored that the formation of potential toxic by-products should be included in an extended correlation model or during further kinetic investigation of a combined model with surrogate

measurements. In line, not only acute toxicity but also chronic mixture toxicity towards the environment and human health needs continued efforts in future studies.

(viii) In a broader picture, it can be questioned if the current end-of-pipe treatment of municipal wastewater is still efficient in terms of cost and urban resources. Discharge limits are becoming more stringent, as analytical and toxicological knowledge increases, resulting in a better effluent quality. Therefore, a shift to a circular treatment and an increased (direct) reuse should be aimed for. Additionally, in the framework of resource recouvery, the current commen practice of activated sludge treatment might be replaced by an alternative. Nevertheless, the TrOC issue will (presumably) remain. Current knowledge of different treatment processes and how to control them will still be of use although both technological (e.g. new/other interactions between different treatment steps, more stringent effluent quality needs, etc.) as well as societal (e.g. shift from indirect to direct reuse) challenges will arise.

Bibliography

(1) United Nations. *World Urbanization Prospects: The 2014 Revision, Highlights*; New York, 2014.

(2) United Nations. *World Population Prospects: The 2015 Revision, Key Findings and Advance Tables.*; New York, 2015.

(3) WssTP. *WssTP Strategic Innovation and Research Agenda (WssTP SIRA) 2030*; Brussels, 2016.

(4) Tran, Q. K.; Jassby, D.; Schwabe, K. A. The implications of drought and water conservation on the reuse of municipal wastewater: Recognizing impacts and identifying mitigation possibilities. *Water Res.* **2017**, *124*, 472–481.

(5) Yuan, J.; Van Dyke, M. I.; Huck, P. M. Identification of critical contaminants in wastewater effluent for managed aquifer recharge. *Chemosphere* **2017**, *172*, 294–301.

(6) Causanilles, A.; Ruepert, C.; Ibáñez, M.; Emke, E.; Hernández, F.; de Voogt, P. Occurrence and fate of illicit drugs and pharmaceuticals in wastewater from two wastewater treatment plants in Costa Rica. *Sci. Total Environ.* **2017**, *599–600*, 98–107.

(7) Luo, Y.; Guo, W.; Ngo, H. H.; Nghiem, L. D.; Hai, F. I.; Zhang, J.; Liang, S.; Wang, X. C. A review on the occurrence of micropollutants in the aquatic environment and their fate and removal during wastewater treatment. *Sci. Total Environ.* **2014**, *473–474*, 619–641.

(8) Lindholm-Lehto, P. C.; Ahkola, H. S. J.; Knuutinen, J. S.; Herve, S. H. Occurrence of pharmaceuticals in municipal wastewater, in the recipient water, and sedimented particles of northern Lake Päijänne. *Environ. Sci. Pollut. Res.* **2015**, *22* (21), 17209–17223.

(9) Tiedeken, E. J.; Tahar, A.; McHugh, B.; Rowan, N. J. Monitoring, sources, receptors, and control measures for three European Union watch list substances of emerging concern in receiving waters - A 20 year systematic review. *Sci. Total Environ.* **2017**, *574*, 1140–1163.

(10) Gerrity, D.; Snyder, S. Review of Ozone for Water Reuse Applications: Toxicity, Regulations, and Trace Organic Contaminant Oxidation. *Ozone Sci. Eng.* **2011**, *33* (4), 253–266.

(11) Kidd, K. A.; Blanchfield, P. J.; Mills, K. H.; Palace, V. P.; Evans, R. E.; Lazorchak, J. M.; Flick, R. W. Collapse of a fish population after exposure to a synthetic estrogen. *Proc. Natl. Acad. Sci.* **2007**, *104* (21), 8897–8901.

(12) Purdom, C. E.; Hardiman, P. A.; Bye, V. V. J.; Eno, N. C.; Tyler, C. R.; Sumpter, J. P. Estrogenic Effects of Effluents from Sewage Treatment Works. *Chem. Ecol.* **1994**, *8* (4), 275–285.

(13) Gay, F.; Ferrandino, I.; Monaco, A.; Cerulo, M.; Capasso, G.; Capaldo, A. Histological and hormonal changes in the European eel (Anguilla anguilla) after exposure to environmental cocaine concentration. *J. Fish Dis.* **2016**, *39* (3), 295–308.

(14) Thorpe, K. L.; Cummings, R. I.; Hutchinson, T. H.; Scholze, M.; Brighty, G.; Sumpter, J. P.; Tyler, C. R. Relative potencies and combination effects of steroidal estrogens in fish. *Environ. Sci. Technol.* **2003**, *37* (6), 1142–1149.

(15) Pickering, A. D.; Sumpter, J. P. Comprehending Endocrine Disrupters in Aquatic Environments. *Environ. Sci. Technol. A-Pages* **2003**, *37* (17), 331A–336A.

(16) Paltiel, O.; Fedorova, G.; Tadmor, G.; Kleinstern, G.; Maor, Y.; Chefetz, B. Human exposure to wastewater-derived pharmaceuticals in fresh produce: A randomized controlled trial focusing on carbamazepine. *Environ. Sci. Technol.* **2016**, *50* (8), 4476–4482.

(17) Franklin, A. M.; Williams, C. F.; Andrews, D. M.; Woodward, E. E.; Watson, J. E. Uptake of Three Antibiotics and an Antiepileptic Drug by Wheat Crops Spray Irrigated with Wastewater Treatment Plant Effluent. *J. Environ. Qual.* **2016**, *45* (2), 546–554.

(18) Christou, A.; Agüera, A.; Bayona, J. M.; Cytryn, E.; Fotopoulos, V.; Lambropoulou, D.; Manaia, C. M.; Michael, C.; Revitt, M.; Schröder, P.; et al. The potential implications of reclaimed wastewater reuse for irrigation on the agricultural environment: The knowns and unknowns of the fate of antibiotics and antibiotic resistant bacteria and resistance genes – A review. *Water Res.* **2017**, *123*, 448–467.

(19) Rousis, N. I.; Gracia-Lor, E.; Zuccato, E.; Bade, R.; Baz-Lomba, J. A.; Castrignanò, E.; Causanilles, A.; Covaci, A.; de Voogt, P.; Hernàndez, F.; et al. Wastewater-based epidemiology to assess pan-European pesticide exposure. *Water Res.* **2017**, *121*, 270–279.

(20) Moermond, C. T. A.; Smit, C. E.; van Leerdam, R. C.; van der Aa, N. G. F. M.; Montforts, M. H. M. M. *Geneesmiddelen en waterkwaliteit*; 2016.

(21) STOWA. *ZORG: Zoeken naar Oplossingen voor Reductie van Geneesmiddelenemissie uit zorginstellingen. Deel C. Eindrapportage*; 2011.

(22) Audenaert, W. T. M.; Chys, M.; Auvinen, H.; Dumoulin, A.; Rousseau, D.; Van Hulle, S. W. H. (Future) Regulation of Trace Organic Compounds in WWTP Effluents as a Driver for Advanced Wastewater Treatment. *Ozone News* **2014**, *42* (6), 17–22.

(23) Barbosa, M. O.; Moreira, N. F. F.; Ribeiro, A. R.; Pereira, M. F. R.; Silva, A. M. T.

Occurrence and removal of organic micropollutants: An overview of the watch list of EU Decision 2015/495. *Water Res.* **2016**, *94*, 257–279.

(24) VMM. *Pesticiden in oppervlaktewater en RWZI's in 2014*; Aalst, Belgium, 2015.

(25) VMM. *Medicijnen in de waterketen. Resultaten van verkennend onderzoek in de periode 2014-2016*; 2017.

(26) Huber, M. M.; Gbel, A.; Joss, A.; Hermann, N.; Lffler, D.; S, C.; Ried, A.; Siegrist, H.; Ternes, T. a; Gunten, U. Von; et al. Oxidation of Pharmaceuticals during Ozonation of Municipal Wastewater Effluents : A Pilot Study Oxidation of Pharmaceuticals during Ozonation of Municipal Wastewater Effluents : A Pilot Study. *Environ. Sci. Technol.* **2005**, *39* (11), 4290–4299.

(27) Koninklijk Nederlands Waternetwerk. Extra geld voor waterschappen om medicijnresten te verwijderen https://www.h2owaternetwerk.nl/h2o-nieuws/1447-extra-geld-voor-waterschappen-om-medicijnresten-te-verwijderen (accessed Nov 10, 2017).

(28) Eggen, R. I. L.; Hollender, J.; Joss, A.; Schärer, M.; Stamm, C. Reducing the discharge of micropollutants in the aquatic environment: The benefits of upgrading wastewater treatment plants. *Environ. Sci. Technol.* **2014**, *48* (14), 7683–7689.

(29) Baalbaki, Z.; Sultana, T.; Maere, T.; Vanrolleghem, P.; Metcalfe, C. D.; Yargeau, V. Fate and mass balance of contaminants of emerging concern during wastewater treatment determined using the fractionated approach. *Sci. Total Environ.* **2016**, *573*, accepted.

(30) Fairbairn, D. J.; Arnold, W. A.; Barber, B. L.; Kaufenberg, E. F.; Koskinen, W. C.; Novak, P. J.; Rice, P. J.; Swackhamer, D. L. Contaminants of Emerging Concern: Mass Balance and Comparison of Wastewater Effluent and Upstream Sources in a Mixed-Use Watershed. *Environ. Sci. Technol.* **2016**, *50* (1), 36–45.

(31) Drewes, J. E.; Anderson, P.; Denslow, N.; Olivieri, A.; Schlenk, D.; Snyder, S. A.; Maruya, K. A. Designing monitoring programs for chemicals of emerging concern in potable reuse - What to include and what not to include? *Water Sci. Technol.* **2013**, *67* (2), 433–439.

(32) Margot, J.; Kienle, C.; Magnet, A.; Weil, M.; Rossi, L.; de Alencastro, L. F.; Abegglen, C.; Thonney, D.; Chèvre, N.; Schärer, M.; et al. Treatment of micropollutants in municipal wastewater: Ozone or powdered activated carbon? *Sci. Total Environ.* **2013**, *461–462*, 480–498.

(33) Hollender, J.; Zimmermann, S. G.; Koepke, S.; Krauss, M.; Mcardell, C. S.; Ort, C.; Singer, H.; Von Gunten, U.; Siegrist, H. Elimination of organic micropollutants in a municipal wastewater treatment plant upgraded with a full-scale post-ozonation followed by sand filtration. *Environ. Sci. Technol.* **2009**, *43* (20), 7862–7869.

(34) Prasse, C.; Stalter, D.; Schulte-Oehlmann, U.; Oehlmann, J.; Ternes, T. A. Spoilt for choice: A critical review on the chemical and biological assessment of current wastewater treatment technologies. *Water Res.* **2015**, *87*, 237–270.

(35) Reungoat, J.; Escher, B. I.; Macova, M.; Keller, J. Biofiltration of wastewater treatment plant effluent: Effective removal of pharmaceuticals and personal care products and reduction of toxicity. *Water Res.* **2011**, *45* (9), 2751–2762.

(36) Moser, R. *Massnahmen in ARA zur weitergehenden Elimination von Mikroverunreinigungen*; 2008.

(37) Larsen, H. F.; Hansen, P. A.; Boyer-Souchet, F. *Decision support guideline based on LCA and cost/efficiency assessment. (EU FP6 project, deliverable; No. 4.3)*; 2010.

(38) Plósz, B. G.; Benedetti, L.; Daigger, G. T.; Langford, K. H.; Larsen, H. F.; Monteith, H.; Ort, C.; Seth, R.; Steyer, J. P.; Vanrolleghem, P. A. Modelling micro-pollutant fate in wastewater collection and treatment systems: Status and challenges. *Water Sci. Technol.* **2013**, *67* (1), 1–15.

(39) Von Sonntag, C.; von Gunten, U. *Chemistry of Ozone in Water and Wastewater Treatment*; IWA Publishing: London, 2012.

(40) Dickenson, E. R. V. V; Drewes, J. E. J. E.; Sedlak, D. L.; Wert, E. C.; Snyder, S. A. Applying surrogates and indicators to assess removal efficiency of Trace Organic Chemicals during Chemical Oxidation of wastewaters. *Environ. Sci. Technol.* **2009**, *43* (16), 6242–6247.

(41) Ried, A.; Mielcke, J.; Wieland, A. The Potential Use of Ozone in Municipal Wastewater. *Ozone Sci. Eng.* **2009**, *31* (6), 415–421.

(42) Lim, S.; Lee, W.; Na, S.; Shin, J.; Lee, Y. N-nitrosodimethylamine (NDMA) formation during ozonation of N,N-dimethylhydrazine compounds: Reaction kinetics, mechanisms, and implications for NDMA formation control. *Water Res.* **2016**, *105*, 119–128.

(43) WRF. *Removal of Bromate and Perchlorate in Conventional Ozone/GAC Systems (Project nr. 2535).*

(44) Von Gunten, U. Ozonation of drinking water: Part II. Disinfection and by-product

formation in presence of bromide, iodide or chlorine. *Water Res.* **2003**, *37* (7), 1469–1487.

(45) Zimmermann, S. G.; Wittenwiler, M.; Hollender, J.; Krauss, M.; Ort, C.; Siegrist, H.; von Gunten, U. Kinetic assessment and modeling of an ozonation step for full-scale municipal wastewater treatment: micropollutant oxidation, by-product formation and disinfection. *Water Res.* **2011**, *45* (2), 605–617.

(46) Mielcke, J.; Ried, A.-. Removal of micro pollutants from municipal waste water - already "State of the art?" (A review on Europe's activities). In *IOA-EA3G Conference & Exhibition, Toulouse, France, Proceedings*; 2012.

(47) Abegglen, C.; Siegriest, H. *Micropolluants dans les eaux usées urabaines. Etapes de traitement supplémentaire dans les stations d'épuration.*; 2012.

(48) Audenaert, W. T. M. Ozonation and UV/hydrogen peroxide treatment of natural water and secondary wastewater effluent: experimental study and mathematical modelling, Ghent University, Belgium, 2012.

(49) Oneby, M. a.; Bromley, C. O.; Borchardt, J. H.; Harrison, D. S. Ozone Treatment of Secondary Effluent at U.S. Municipal Wastewater Treatment Plants. *Ozone Sci. Eng.* **2010**, *32* (1), 43–55.

(50) Paulouë, J. Le; Langlais, B. State-of-the-Art of Ozonation in France. *Ozone Sci. Eng.* **2008**, *21*, 153–162.

(51) Loeb, B. L.; Thompson, C. M.; Drago, J.; Takahara, H.; Baig, S. Worldwide Ozone Capacity for Treatment of Drinking Water and Wastewater: A Review. *Ozone Sci. Eng.* **2012**, *34* (1), 64–77.

(52) Ried, A. Ozone and its applications. In *International Conference on Ozone and Related Oxidants to Meet Essential Human Needs - Uses for Agri-Food, Industry, Water and Health*; International Ozone Association (IOA): Toulouse, France, 2012; pp 19–20.

(53) Chon, K.; Salhi, E.; von Gunten, U. Combination of UV absorbance and electron donating capacity to assess degradation of micropollutants and formation of bromate during ozonation of wastewater effluents. *Water Res.* **2015**, *81*, 388–397.

(54) Park, M.; Anumol, T.; Daniels, K. D.; Wu, S.; Ziska, A. D.; Snyder, S. A. Predicting trace organic compound attenuation by ozone oxidation: Development of indicator and surrogate models. *Water Res.* **2017**, *119*, 21–32.

(55) Nöthe, T.; Fahlenkamp, H.; Von Sonntag, C. Ozonation of wastewater: Rate of ozone consumption and hydroxyl radical yield. *Environ. Sci. Technol.* **2009**, *43* (15), 5990–5995.

(56) Drewes, J. E.; Fox, P. Fate of natural organic matter (NOM) during ground water recharge using reclaimed water. *Water Sci. Technol.* **1999**, *40* (9).

(57) Goel, S.; Hozalski, R. M.; Bouwer, E. J. Biodegradation of NOM: effect of NOM source and ozone dose. *J. AWWA* **1995**, *87* (1), 90–105.

(58) Fabris, R.; Chow, C. W. K.; Drikas, M.; Eikebrokk, B. Comparison of NOM character in selected Australian and Norwegian drinking waters. *Water Res.* **2008**, *42* (15), 4188–4196.

(59) Liang, Y.; Hong, H. C.; Dong, L. H.; Lan, C. Y.; Han, B. P.; Wong, M. H. Sources and Properties of Natural Organic Matter (NOM) in Water Along the Dongjiang River (the Source of Hong Kong's Drinking Water) and Toxicological Assay of Its Chlorination By-Products. *Arch. Environ. Contam. Toxicol.* **2008**, *54* (4), 597–605.

(60) Maeng, S. K.; Sharma, S. K.; Lekkerkerker-Teunissen, K.; Amy, G. L. Occurrence and fate of bulk organic matter and pharmaceutically active compounds in managed aquifer recharge: A review. *Water Res.* **2011**, *45* (10), 3015–3033.

(61) Nam, S.-N.; Krasner, S. W.; Amy, G. L. Differentiating Effluent Organic Matter (EfOM) from Natural Organic Matter (NOM): Impact of EfOM on Drinking Water Sources. In *Advanced Environmental Monitoring*; Kim, Y. J., Platt, U., Eds.; Springer Netherlands: Dordrecht, 2008; pp 259–270.

(62) Shon, H. K.; Vigneswaran, S.; Snyder, S. A. Effluent Organic Matter (EfOM) in Wastewater: Constituents, Effects, and Treatment. *Crit. Rev. Environ. Sci. Technol.* **2006**, *36* (4), 327–374.

(63) Bahr, C.; Schumacher, J.; Ernst, M.; Luck, F.; Heinzmann, B.; Jekel, M. SUVA as control parameter for the effective ozonation of organic pollutants in secondary effluent. *Water Sci. Technol.* **2007**, *55* (12), 267–274.

(64) Gerrity, D.; Gamage, S.; Jones, D.; Korshin, G. V; Lee, Y.; Pisarenko, A.; Trenholm, R. A.; von Gunten, U.; Wert, E. C.; Snyder, S. A. Development of surrogate correlation models to predict trace organic contaminant oxidation and microbial inactivation during ozonation. *Water Res.* **2012**, *46* (19), 6257–6272.

(65) Lee, Y.; Kovalova, L.; McArdell, C. S.; von Gunten, U. Prediction of micropollutant

elimination during ozonation of a hospital wastewater effluent. *Water Res.* **2014**, *64*, 134–148.

(66) Huber, M. M.; Canonica, S.; Park, G. Y.; Von Gunten, U. Oxidation of pharmaceuticals during ozonation and advanced oxidation processes. *Environ. Sci. Technol.* **2003**, *37* (5), 1016–1024.

(67) Vel Leitner, N. K.; Roshani, B. Kinetic of benzotriazole oxidation by ozone and hydroxyl radical. *Water Res.* **2010**, *44* (6), 2058–2066.

(68) EU. *Proposal COM(2011)876 for a directive of the European Parliament and of the Council amending Directives 2000/60/EC and 2008/105/EC as regards priority substances in the field of water policy*; 2011.

(69) NRWI (National Water Research Institute). *Examining the Criteria for Direct Potable Reuse*; 2013.

(70) CDPH. *Draft Groundwater Replenishment Reuse Regulations*; 2013.

(71) EU. *Directive 2000/60/EC of the European Parliament and of the Council*; 2000.

(72) EU. *Directive 2008/105/EC of the European Parliament and of the Council*; 2008.

(73) EUREAU. *EUREAU initial position paper on amending Directives 2000/60/EC and 2008/105/EC as regards priority substances in the field of water policy*; Brussels; Belgium, 2012.

(74) EU. *Directive 2013/39/EU of the European Parliament and of the Council amending Directives 2000/60/EC and 2008/105/EC as regards priority substances in the field of water policy*; 2013.

(75) Switzerland. *Swiss Federal Law on Water Protection (RS 814.201)*; 2014.

(76) Joss, A.; Schärer, M.; Abegglen, C. Micropollutants: the Swiss strategy www.water2020.eu (accessed May 30, 2017).

(77) OFEV (Office Fédérale de l'Environnement). *Elimination des micropolluants dans les STEP*; 2014.

(78) Wert, E. C.; Rosario-Ortiz, F. L.; Drury, D. D.; Snyder, S. A. Formation of oxidation byproducts from ozonation of wastewater. *Water Res.* **2007**, *41* (7), 1481–1490.

(79) Hammes, F.; Salhi, E.; Köster, O.; Kaiser, H.-P.; Egli, T.; von Gunten, U. Mechanistic and kinetic evaluation of organic disinfection by-product and assimilable organic carbon

(AOC) formation during the ozonation of drinking water. *Water Res.* **2006**, *40* (12), 2275–2286.

(80) Richardson, S. D.; Postigo, C. Drinking Water Disinfection By-products. In *Emerging Organic Contaminants and Human Health*; Barceló, D., Ed.; Springer Berlin Heidelberg: Berlin, Heidelberg, 2012; pp 93–137.

(81) Pisarenko, A. N.; Marti, E. J.; Gerrity, D.; Peller, J. R.; Dickenson, E. R. V. Effects of molecular ozone and hydroxyl radical on formation of N-nitrosamines and perfluoroalkyl acids during ozonation of treated wastewaters. *Environ. Sci. Water Res. Technol.* **2015**, *1* (5), 668–678.

(82) Pisarenko, A. N.; Stanford, B. D.; Yan, D.; Gerrity, D.; Snyder, S. A. Effects of ozone and ozone/peroxide on trace organic contaminants and NDMA in drinking water and water reuse applications. *Water Res.* **2012**, *46* (2), 316–326.

(83) Kosaka, K.; Asami, M.; Konno, Y.; Oya, M.; Kunikane, S. Identification of Antiyellowing Agents as Precursors of N-Nitrosodimethylamine Production on Ozonation from Sewage Treatment Plant Influent. *Environ. Sci. Technol.* **2009**, *43* (14), 5236–5241.

(84) Kosaka, K.; Fukui, K.; Kayanuma, Y.; Asami, M.; Akiba, M. N-Nitrosodimethylamine Formation from Hydrazine Compounds on Ozonation. *Ozone Sci. Eng.* **2014**, *36* (3), 215–220.

(85) Schmidt, C. K.; Brauch, H.-J. N,N -Dimethylsulfamide as Precursor for N -Nitrosodimethylamine (NDMA) Formation upon Ozonation and its Fate During Drinking Water Treatment. *Environ. Sci. Technol.* **2008**, *42* (17), 6340–6346.

(86) Sgroi, M.; Roccaro, P.; Oelker, G. L.; Snyder, S. A. N -Nitrosodimethylamine Formation upon Ozonation and Identification of Precursors Source in a Municipal Wastewater Treatment Plant. *Environ. Sci. Technol.* **2014**, *48* (17), 10308–10315.

(87) Andrzejewski, P.; Kasprzyk-Hordern, B.; Nawrocki, J. N-nitrosodimethylamine (NDMA) formation during ozonation of dimethylamine-containing waters. *Water Res.* **2008**, *42* (4–5), 863–870.

(88) Yang, L.; Chen, Z.; Shen, J.; Xu, Z.; Liang, H.; Tian, J.; Ben, Y.; Zhai, X.; Shi, W.; Li, G. Reinvestigation of the nitrosamine-formation mechanism during ozonation. *Environ. Sci. Technol.* **2009**, *43* (14), 5481–5487.

(89) Padhye, L.; Luzinova, Y.; Cho, M.; Mizaikoff, B.; Kim, J.-H.; Huang, C.-H. PolyDADMAC and dimethylamine as precursors of N-nitrosodimethylamine during ozonation: reaction kinetics and mechanisms. *Environ. Sci. Technol.* **2011**, *45* (10), 4353–4359.

(90) Marti, E. J.; Pisarenko, A. N.; Peller, J. R.; Dickenson, E. R. V. N-nitrosodimethylamine (NDMA) formation from the ozonation of model compounds. *Water Res.* **2015**, *72*, 262–270.

(91) Yoon, S.; Tanaka, H. Formation of N-nitrosamines by chloramination or ozonation of amines listed in Pollutant Release and Transfer Registers (PRTRs). *Chemosphere* **2014**, *95*, 88–95.

(92) Legube, B.; Parinet, B.; Gelinet, K.; Berne, F.; Croue, J. P. Modeling of bromate formation by ozonation of surface waters in drinking water treatment. *Water Res.* **2004**, *38* (8), 2185–2195.

(93) Sorlini, S.; Collivignarelli, C. Trihalomethane formation during chemical oxidation with chlorine, chlorine dioxide and ozone of ten Italian natural waters. *Desalination* **2005**, *176* (1–3), 103–111.

(94) Kim, H. sang; Yamada, H.; Tsuno, H. The removal of estrogenic activity and control of brominated by-products during ozonation of secondary effluents. *Water Res.* **2007**, *41* (7), 1441–1446.

(95) Orlandini, E.; Kruithof, J. C.; VanderHoek, J. P.; Siebel, M. A.; Schippers, J. C. Impact of ozonation on disinfection and formation of biodegradable organic matter and bromate. *J. Water Supply Res. Technol.* **1997**, *46* (1), 20–30.

(96) Nawrocki, J.; Andrzejewski, P. Nitrosamines and water. *J. Hazard. Mater.* **2011**, *189* (1–2), 1–18.

(97) Soltermann, F.; Abegglen, C.; Tschui, M.; Stahel, S.; von Gunten, U. Options and limitations for bromate control during ozonation of wastewater. *Water Res.* **2017**, *116*, 76–85.

(98) Lee, Y.; Gerrity, D.; Lee, M.; Bogeat, A. E.; Salhi, E.; Gamage, S.; Trenholm, R. A.; Wert, E. C.; Snyder, S. A.; von Gunten, U. Prediction of Micropollutant Elimination during Ozonation of Municipal Wastewater Effluents: Use of Kinetic and Water Specific

Information. *Environ. Sci. Technol.* **2013**, *47* (11), 5872–5881.

(99) Li, W. T.; Cao, M. J.; Young, T.; Ruffino, B.; Dodd, M.; Li, A. M.; Korshin, G. Application of UV absorbance and fluorescence indicators to assess the formation of biodegradable dissolved organic carbon and bromate during ozonation. *Water Res.* **2017**, *111*, 154–162.

(100) Nanaboina, V.; Korshin, G. V. Evolution of absorbance spectra of ozonated wastewater and its relationship with the degradation of trace-level organic species. *Environ. Sci. Technol.* **2010**, *44* (16), 6130–6137.

(101) Liu, C.; Tang, X.; Kim, J.; Korshin, G. V. Formation of aldehydes and carboxylic acids in ozonated surface water and wastewater: A clear relationship with fluorescence changes. *Chemosphere* **2015**, *125*, 182–190.

(102) Tripathi, S.; Pathak, V.; Tripathi, D. M.; Tripathi, B. D. Application of ozone based treatments of secondary effluents. *Bioresour. Technol.* **2011**, *102* (3), 2481–2486.

(103) Wert, E. C.; Rosario-Ortiz, F. L.; Snyder, S. A. Using Ultraviolet Absorbance and Color To Assess Pharmaceutical Oxidation during Ozonation of Wastewater. *Environ. Sci. Technol.* **2009**, *43* (13), 4858–4863.

(104) Gamage, S.; Gerrity, D.; Pisarenko, A. N.; Wert, E. C.; Snyder, S. A. Evaluation of Process Control Alternatives for the Inactivation of Escherichia coli , MS2 Bacteriophage, and Bacillus subtilis Spores during Wastewater Ozonation. *Ozone Sci. Eng.* **2013**, *35* (6), 501–513.

(105) Zhang, S.; Gitungo, S.; Axe, L.; Dyksen, J. E.; Raczko, R. F. A pilot plant study using conventional and advanced water treatment processes: Evaluating removal efficiency of indicator compounds representative of pharmaceuticals and personal care products. *Water Res.* **2016**, *105*, 85–96.

(106) Wert, E. C.; Rosario-Ortiz, F. L.; Snyder, S. A. Effect of ozone exposure on the oxidation of trace organic contaminants in wastewater. *Water Res.* **2009**, *43* (4), 1005–1014.

(107) Snyder, S. a.; Wert, E. C.; Rexing, D. J.; Zegers, R. E.; Drury, D. D. Ozone Oxidation of Endocrine Disruptors and Pharmaceuticals in Surface Water and Wastewater. *Ozone Sci. Eng.* **2006**, *28* (6), 445–460.

(108) Leikam, K.; Huber, S. *ABWASSERWERK ROSENBERGSAU Strategie Zukunft - Behandlungsstufe für Mikroverunreinigungen: Pilotierung Ozonung*; 2015.

(109) Singh, S.; Seth, R.; Tabe, S.; Yang, P. Oxidation of Emerging Contaminants during Pilot-Scale Ozonation of Secondary Treated Municipal Effluent. *Ozone Sci. Eng.* **2015**, *37* (4), 323–329.

(110) Chys, M.; Oloibiri, V. A.; Audenaert, W. T. M.; Demeestere, K.; Van Hulle, S. W. H. Ozonation of biologically treated landfill leachate: Efficiency and insights in organic conversions. *Chem. Eng. J.* **2015**, *277*, 104–111.

(111) Dodd, M. C.; Buffle, M. O.; Von Gunten, U. Oxidation of antibacterial molecules by aqueous ozone: Moiety-specific reaction kinetics and application to ozone-based wastewater treatment. *Environ. Sci. Technol.* **2006**, *40* (6), 1969–1977.

(112) Beltran, F. J. *Ozone Reaction Kinetics for Water and Wastewater Systems*; 2004.

(113) Audenaert, W. T. M.; Vandierendonck, D.; Van Hulle, S. W. H.; Nopens, I. Comparison of ozone and HO· induced conversion of effluent organic matter (EfOM) using ozonation and UV/H2O2 treatment. *Water Res.* **2013**, *47* (7), 2387–2398.

(114) Wittmer, A.; Heisele, A.; McArdell, C. S.; Böhler, M.; Longree, P.; Siegrist, H. Decreased UV absorbance as an indicator of micropollutant removal efficiency in wastewater treated with ozone. *Water Sci. Technol.* **2015**, *71* (7), 980–985.

(115) Sharif, F.; Wang, J.; Westerhoff, P. Transformation in Bulk and Trace Organics during Ozonation of Wastewater. *Ozone Sci. Eng.* **2012**, *34* (1), 26–31.

(116) Shon, H. K.; Vigneswaran, S.; Ben Aim, R.; Ngo, H. H.; Kim, I. S.; Cho, J. Influence of flocculation and adsorption as pretreatment on the fouling of ultrafiltration and nanofiltration membranes: Application with biologically treated sewage effluent. *Environ. Sci. Technol.* **2005**, *39* (10), 3864–3871.

(117) Thomas, O.; El Khorassani, H.; Touraud, E.; Bitar, H. TOC versus UV spectrophotometry for wastewater quality monitoring. *Talanta* **1999**, *50* (4), 743–749.

(118) Huebsch, M.; Grimmeisen, F.; Zemann, M.; Fenton, O.; Richards, K. G.; Jordan, P.; Sawarieh, A.; Blum, P.; Goldscheider, N. Technical Note: Field experiences using UV/VIS sensors for high-resolution monitoring of nitrate in groundwater. *Hydrol. Earth Syst. Sci.* **2015**, *19* (4), 1589–1598.

(119) Reungoat, J.; Escher, B. I.; Macova, M.; Argaud, F. X.; Gernjak, W.; Keller, J. Ozonation and biological activated carbon filtration of wastewater treatment plant effluents. *Water*

Res. **2012**, *46* (3), 863–872.

(120) Gerrity, D.; Gamage, S.; Holady, J. C.; Mawhinney, D. B.; Quiñones, O.; Trenholm, R. A.; Snyder, S. A. Pilot-scale evaluation of ozone and biological activated carbon for trace organic contaminant mitigation and disinfection. *Water Res.* **2011**, *45* (5), 2155–2165.

(121) Buffle, M.-O.; Schumacher, J.; Meylan, S.; Jekel, M.; von Gunten, U. Ozonation and Advanced Oxidation of Wastewater: Effect of O 3 Dose, pH, DOM and HO • -Scavengers on Ozone Decomposition and HO • Generation. *Ozone Sci. Eng.* **2006**, *28* (4), 247–259.

(122) Li, W.-T.; Majewsky, M.; Abbt-Braun, G.; Horn, H.; Jin, J.; Li, Q.; Zhou, Q.; Li, A.-M. Application of portable online LED UV fluorescence sensor to predict the degradation of dissolved organic matter and trace organic contaminants during ozonation. *Water Res.* **2016**, *101*, 262–271.

(123) Frimmel, F. H. Photochemical aspects related to humic substances. *Environ. Int.* **1994**, *20* (3), 373–385.

(124) Weishaar, J. L.; Aiken, G. R.; Bergamaschi, B. A.; Fram, M. S.; Fujii, R.; Mopper, K. Evaluation of Specific Ultraviolet Absorbance as an Indicator of the Chemical Composition and Reactivity of Dissolved Organic Carbon. *Environ. Sci. Technol.* **2003**, *37* (20), 4702–4708.

(125) Li, Z.; Sobek, A.; Radke, M. Fate of Pharmaceuticals and Their Transformation Products in Four Small European Rivers Receiving Treated Wastewater. *Environ. Sci. Technol.* **2016**, *50* (11), 5614–5621.

(126) Buffle, M. O.; Von Gunten, U. Phenols and amine induced HO. generation during the initial phase of natural water ozonation. *Environ. Sci. Technol.* **2006**, *40* (9), 3057–3063.

(127) Antoniou, M. G.; Hey, G.; Rodríguez Vega, S.; Spiliotopoulou, A.; Fick, J.; Tysklind, M.; la Cour Jansen, J.; Andersen, H. R. Required ozone doses for removing pharmaceuticals from wastewater effluents. *Sci. Total Environ.* **2013**, *456–457*, 42–49.

(128) Elovitz, M. S.; von Gunten, U. Hydroxyl Radical/Ozone Ratios During Ozonation Processes. I. The Rct Concept. *Ozone Sci. Eng.* **1999**, *21* (3), 239–260.

(129) Henderson, R. K.; Baker, A.; Murphy, K. R.; Hambly, A.; Stuetz, R. M.; Khan, S. J. Fluorescence as a potential monitoring tool for recycled water systems: a review. *Water Res.* **2009**, *43* (4), 863–881.

(130) Hudson, N.; Baker, A.; Ward, D.; Reynolds, D. M.; Brunsdon, C.; Carliell-Marquet, C.; Browning, S. Can fluorescence spectrometry be used as a surrogate for the Biochemical Oxygen Demand (BOD) test in water quality assessment? An example from South West England. *Sci. Total Environ.* **2008**, *391* (1), 149–158.

(131) Birdwell, J. E.; Engel, A. S. Characterization of dissolved organic matter in cave and spring waters using UV–Vis absorbance and fluorescence spectroscopy. *Org. Geochem.* **2010**, *41* (3), 270–280.

(132) Zhang, T.; Lu, J.; Ma, J.; Qiang, Z. Fluorescence spectroscopic characterization of DOM fractions isolated from a filtered river water after ozonation and catalytic ozonation. *Chemosphere* **2008**, *71* (5), 911–921.

(133) Chen, W.; Westerhoff, P.; Leenheer, J. A.; Booksh, K. Fluorescence Excitation−Emission Matrix Regional Integration to Quantify Spectra for Dissolved Organic Matter. *Environ. Sci. Technol.* **2003**, *37* (24), 5701–5710.

(134) Stedmon, C. a.; Markager, S.; Bro, R. Tracing dissolved organic matter in aquatic environments using a new approach to fluorescence spectroscopy. *Mar. Chem.* **2003**, *82* (3–4), 239–254.

(135) TU Wien. *KOMOZAK-Projekt: Weitergehende Reinigung kommunaler Abwässer mit Ozon sowie Aktivkohle für die Entfernung organischer Spurenstoffe*; 2015.

(136) Sgroi, M.; Roccaro, P.; Korshin, G. V.; Greco, V.; Sciuto, S.; Anumol, T.; Snyder, S. A.; Vagliasindi, F. G. A. Use of fluorescence EEM to monitor the removal of emerging contaminants in full scale wastewater treatment plants. *J. Hazard. Mater.* **2017**, *323*, 367–376.

(137) Liu, C.; Li, P.; Tang, X.; Korshin, G. V. Ozonation effects on emerging micropollutants and effluent organic matter in wastewater: characterization using changes of three-dimensional HP-SEC and EEM fluorescence data. *Environ. Sci. Pollut. Res.* **2016**, *23* (20), 20567–20579.

(138) Thompson, C. *Ozone system database (Oral and writen communication)*; 2017.

(139) Verband Schweizer Abwasser- und Gewässerschutzfachleute. Projekte mit Ozon https://www.micropoll.ch/anlagen-projekte/ozon/ (accessed Jul 17, 2017).

(140) Kompetenzzentrum Mikroschadstoffe.NRW. *Ozonung ARA St . Pourçain-sur-Sioule (F)*;

2013.

(141) Takahara, H.; Nakayama, S.; Tsuno, H. Application of Ozone to Municipal Sewage Treatment. *Int. Conf. Ozone UV* **2006**, 3–8.

(142) Yamashita, H.; Kaya, T. Outline and Problem of Reclaimed Water Supply Business in Tokyo. In *WEFTEC, the Water Environment Federation's Annual Technical Exhibition and Conference, Orlando, Florida, USA*; 2009.

(143) Li, W.; Shi, Y.; Gao, L.; Liu, J.; Cai, Y. Occurrence and removal of antibiotics in a municipal wastewater reclamation plant in Beijing, China. *Chemosphere* **2013**, *92* (4), 435–444.

(144) Grünebaum, T. *Elimination von Arzneimitteln und organischen Spurenstoffen: Entwicklung von Konzeptionen und innovativen, kostengünstigen Reinigungsverfahren, Schlussbericht Phase 1: Elimination von Arzneimittelrückständen in kommunalen Kläranlagen, Report to the Minist*; 2011.

(145) Porter, R. Activities at the Gwinnett County F. Wayne Hill WRC to Utilize Less External Energy and Preserve a Watershed's Integriity, POTW workshop. Indiana, USA 2010.

(146) Kompetenzzentrum Mikroschadstoffe.NRW. *Ozonung auf der Kläranlage Bad Sassendorf*; 2013.

(147) Cimbritz, M.; Tumlin, S.; Hagman, M.; Dimitrova, I.; Hey, G.; Mases, M.; Astrand, N.; Jansen, J. la C. *Rening från läkemedelsrester och andra mikroföroreningar - Rapport Nr. 2016-04*; Bromma, Sweden, 2014.

(148) Kompetenzzentrum Mikroschadstoffe.NRW. *Ozonbehandlung Kläranlage Duisburg-Vierlinden*; 2013.

(149) SUEZ. usine des Bouillides https://www.suezwaterhandbook.fr/content/download/5687/91169/version/2/file/Sofia_Antipolis_FR_A4.pdf (accessed Jul 17, 2017).

(150) Schachtler, M.; Hubaux, N. *Die erste Anlage der Schweiz zur Elimination von Mikroverunreinigungen. ARA Neugut- erste grosstechnische Ozonung.*; 2016.

(151) Drury, D. D.; Snyder, S. A. Use of Ozone for Disinfection and EDC Removal at CCWRD http://www.acecindiana.org/content/Presentations/EBC07-O, (accessed Jul 1, 2012).

(152) Baresel, C. Sweden's first purification plant for removal of wastewater pharmaceutical

residues under construction http://www.ivl.se/english/startpage/top-menu/pressroom/news/nyheter---arkiv/2016-11-30-swedens-first-purification-plant-for-removal-of-wastewater-pharmaceutical-residues-under-construction.html (accessed Jul 17, 2017).

(153) Baresel, C.; Malmborg, J.; Ek, M.; Sehlen, R. Removal of pharmaceutical residues using ozonation as intermediate process step at Linkoping WWTP, Sweden. *Water Sci. Technol.* **2016**, *73* (8), 2017–2024.

(154) Hubaux, N.; Schachtler, M. MEHRSTUFIGER OZONEINTRAG - LOD-KONZEPT. *Aqua & Gas N°11*. 2016, pp 50–56.

(155) Schachtler, M.; Hubaux, N. BEAR : INNOVATIVE REGELSTRATEGIE DER OZONUNG. *Aqua & Gas N°5*. 2016, pp 84–93.

(156) Lee, Y.; von Gunten, U. Oxidative transformation of micropollutants during municipal wastewater treatment: Comparison of kinetic aspects of selective (chlorine, chlorine dioxide, ferrateVI, and ozone) and non-selective oxidants (hydroxyl radical). *Water Res.* **2010**, *44* (2), 555–566.

(157) Schaar, H.; Kornfeind, L.; Winkler, S.; Saracevic, E.; Kreuzinger, N. Applying online UV/Vis-spectrometry for process control of an ozonation step for advanced wastewater treatment. *Water Pract. Technol.* **2013**, *8* (2), 151–160.

(158) Stapf, M.; Miehe, U.; Jekel, M. Application of online UV absorption measurements for ozone process control in secondary effluent with variable nitrite concentration. *Water Res.* **2016**, *104* (2), 111–118.

(159) Kompetenzzentrum Mikroschadstoffe.NRW. *Spurenstoffelimination auf dem Gruppenklärwerk Paderborn-Sande*; 2015.

(160) Plattform Mikroverunreinigungen (www.micropoll.ch). *Ozonung ARA Wüeri in Regensdorf*; 2012.

(161) Plattform Mikroverunreinigungen (www.micropoll.ch). *Ozon- und PAK-Behandlung auf der ARA Vidy in Lausanne*; 2012.

(162) El-taliawy, H.; Ekblad, M.; Nilsson, F.; Hagman, M.; Paxeus, N.; Jönsson, K.; Cimbritz, M.; la Cour Jansen, J.; Bester, K. Ozonation efficiency in removing organic micro pollutants from wastewater with respect to hydraulic loading rates and different

wastewaters. *Chem. Eng. J.* **2017**, *325*, 310–321.

(163) Kompetenzzentrum Mikroschadstoffe.NRW. *Vergleichende Untersuchungen zum Einsatz von Aktivkohle im halb- technischen Maßstab am Technikum auf dem KLEM unter besonderer Berücksichtigung der Wirkung auf wesentliche Prozessstufen*; 2016.

(164) Kompetenzzentrum Mikroschadstoffe.NRW. *Demonstrationsanlage Abwasserozonung Kläranlage Aachen Soers (DemO3AC)*; 2015.

(165) Von Gunten, U. Ozonation of drinking water: Part I. Oxidation kinetics and product formation. *Water Res.* **2003**, *37* (7), 1443–1467.

(166) Dobbs, R. A.; Wise, R. H.; Dean, R. B. The use of ultra-violet absorbance for monitoring the total organic carbon content of water and wastewater. *Water Res.* **1972**, *6* (10), 1173–1180.

(167) Eaton, A. Measuring UV absorbing organics: a standard method. *J. AWWA* **1995**, *2* (C), 86–90.

(168) Spencer, R. G. M.; Butler, K. D.; Aiken, G. R. Dissolved organic carbon and chromophoric dissolved organic matter properties of rivers in the USA. *J. Geophys. Res. Biogeosciences* **2012**, *117*, 1–14.

(169) Carter, H. T.; Tipping, E.; Koprivnjak, J. F.; Miller, M. P.; Cookson, B.; Hamilton-Taylor, J. Freshwater DOM quantity and quality from a two-component model of UV absorbance. *Water Res.* **2012**, *46* (14), 4532–4542.

(170) Causse, J.; Thomas, O.; Jung, A. V.; Thomas, M. F. Direct DOC and nitrate determination in water using dual pathlength and second derivative UV spectrophotometry. *Water Res.* **2017**, *108*, 312–319.

(171) Cook, S.; Peacock, M.; Evans, C. D.; Page, S. E.; Whelan, M. J.; Gauci, V.; Kho, L. K. Quantifying tropical peatland dissolved organic carbon (DOC) using UV-visible spectroscopy. *Water Res.* **2017**, *115*, 229–235.

(172) Lee, Y.; von Gunten, U. Advances in predicting organic contaminant abatement during ozonation of municipal wastewater effluent: reaction kinetics, transformation products, and changes of biological effects. *Environ. Sci. Water Res. Technol.* **2016**, *2* (3), 421–442.

(173) Bridgeman, J.; Baker, A.; Brown, D.; Boxall, J. B. Portable LED fluorescence instrumentation for the rapid assessment of potable water quality. *Sci. Total Environ.* **2015**,

524–525, 338–346.

(174) Li, W. T.; Jin, J.; Li, Q.; Wu, C. F.; Lu, H.; Zhou, Q.; Li, A. M. Developing LED UV fluorescence sensors for online monitoring DOM and predicting DBPs formation potential during water treatment. *Water Res.* **2016**, *93*, 1–9.

(175) Tedetti, M.; Joffre, P.; Goutx, M. Development of a field-portable fluorometer based on deep ultraviolet LEDs for the detection of phenanthrene- and tryptophan-like compounds in natural waters. *Sensors Actuators, B Chem.* **2013**, *182*, 416–423.

(176) Schneider, F.; Ruhl, A. S.; Hübner, U.; Jekel, M. Removal of Residual Dissolved Ozone with Manganese Dioxide for Process Control with UV 254. *Ozone Sci. Eng.* **2016**, *38* (2), 79–85.

(177) Song, Y.; Breider, F.; Ma, J.; von Gunten, U. Nitrate formation during ozonation as a surrogate parameter for abatement of micropollutants and the N-nitrosodimethylamine (NDMA) formation potential. *Water Res.* **2017**, *122*, 246–257.

(178) Nakada, N.; Shinohara, H.; Murata, A.; Kiri, K.; Managaki, S.; Sato, N.; Takada, H. Removal of selected pharmaceuticals and personal care products (PPCPs) and endocrine-disrupting chemicals (EDCs) during sand filtration and ozonation at a municipal sewage treatment plant. *Water Res.* **2007**, *41* (19), 4373–4382.

(179) Joss, A.; Carballa, M.; Kreuzinger, N.; Siegrist, H.; Zabczynski, S. Wastewater treatment. In *Human Pharmaceuticals, Hormones and Fragrances: The Challenge of Micropollutants in Urban Water Management*; Ternes, T. A., Joss, A., Eds.; IWA Publishing: London, 2006; pp 243–292.

(180) Guo, J.; Peng, Y.; Guo, J.; Ma, J.; Wang, W.; Wang, B. Dissolved organic matter in biologically treated sewage effluent (BTSE): Characteristics and comparison. *Desalination* **2011**, *278* (1–3), 365–372.

(181) Buxton, G. V; Greenstock, C. L.; Helman, W. P.; Ross, A. B. Critical Review of rate constants for reactions of hydrated electrons, hydrogen atoms and hydroxyl radicals in aqueous solution. *J. Phys. Chem. Ref. Data* **1988**, *17* (2), 513.

(182) Aymerich, I.; Acuña, V.; Ort, C.; Rodríguez-Roda, I.; Corominas, L. Fate of organic microcontaminants in wastewater treatment and river systems: An uncertainty assessment in view of sampling strategy, and compound consumption rate and degradability. *Water*

Res. **2017**, *in press*.

(183) Ort, C.; Lawrence, M. G.; Rieckermann, J.; Joss, A. Sampling for pharmaceuticals and personal care products (PPCPs) and illicit drugs in wastewater systems: are your conclusions valid? A critical review. *Environ. Sci. Technol.* **2010**, *44* (16), 6024–6035.

(184) Ort, C.; Gujer, W. Sampling for representative micropollutant loads in sewer systems. *Water Sci. Technol.* **2006**, *54* (6–7), 169–176.

(185) Eaton, A. D.; Clesceri, L. S.; Rice, E. W.; Greenberg, A. E. *Standard Methods for the Examination of Water and Wastewater, 21st Edition*; Franson, M. A. H., Ed.; APHA American Public Health Association: Washington, DC, 2005.

(186) Hoigné, J.; Bader, H. Characterization Of Water Quality Criteria for Ozonation Processes . Part II : Lifetime of Added Ozone. *Ozone Sci. Eng.* **1994**, *16* (2), 121–134.

(187) Roustan, M.; Debellefontaine, H.; Do-Quang, Z.; Duguet, J.-P. Development of a Method for the Determination of Ozone Demand of a Water. *Ozone Sci. Eng.* **1998**, *20* (6), 513–520.

(188) Bader, H.; Hoigné, J. Determination of ozone in water by the indigo method. *Water Res.* **1981**, *15* (4), 449–456.

(189) Vergeynst, L.; K'oreje, K.; De Wispelaere, P.; Harinck, L.; Van Langenhove, H.; Demeestere, K. Statistical procedures for the determination of linearity, detection limits and measurement uncertainty: A deeper look into SPE-LC-Orbitrap mass spectrometry of pharmaceuticals in wastewater. *J. Hazard. Mater.* **2017**, *323* (part A), 2–10.

(190) Blaen, P. J.; Khamis, K.; Lloyd, C. E. M.; Bradley, C.; Hannah, D.; Krause, S. Real-time monitoring of nutrients and dissolved organic matter in rivers: Capturing event dynamics, technological opportunities and future directions. *Sci. Total Environ.* **2016**, *569*, 647–660.

(191) Audenaert, W. T. M.; Vermeersch, Y.; Van Hulle, S. W. H.; Dejans, P.; Dumoulin, A.; Nopens, I. Application of a mechanistic UV/hydrogen peroxide model at full-scale: Sensitivity analysis, calibration and performance evaluation. *Chem. Eng. J.* **2011**, *171* (1), 113–126.

(192) Murphy, K. R.; Hambly, A.; Singh, S.; Henderson, R. K.; Baker, A.; Stuetz, R.; Khan, S. J. Organic matter fluorescence in municipal water recycling schemes: Toward a unified PARAFAC model. *Environ. Sci. Technol.* **2011**, *45* (7), 2909–2916.

(193) Li, W.-T.; Chen, S.-Y.; Xu, Z.-X.; Li, Y.; Shuang, C.-D.; Li, A.-M. Characterization of dissolved organic matter in municipal wastewater using fluorescence PARAFAC analysis and chromatography multi-excitation/emission scan: a comparative study. *Environ. Sci. Technol.* **2014**, *48* (5), 2603–2609.

(194) Ohno T. Fluorescence Inner - Filtering Correction for Determining the Humification Index of Dissolved Organic Matter. *Environ. Sci. Technol.* **2002**, *36* (4), 742–746.

(195) Murphy, K. R.; Stedmon, C. A.; Graeber, D.; Bro, R. Fluorescence spectroscopy and multi-way techniques. PARAFAC. *Anal. Methods* **2013**, *5* (23), 6557–6566.

(196) Shutova, Y.; Baker, A.; Bridgeman, J.; Henderson, R. K. Spectroscopic characterisation of dissolved organic matter changes in drinking water treatment: From PARAFAC analysis to online monitoring wavelengths. *Water Res.* **2014**, *54*, 159–169.

(197) Van Hulle, S. W. H.; Ciocci, M. C. Statistical evaluation and comparison of the chemical quality of bottled water and flemish tap water. *Desalin. Water Treat.* **2012**, *40* (1–3), 183–193.

(198) Brereton, R. G. *Chemometrics: Data Analysis for the Laboratory and Chemical Plant*; 2003.

(199) Kaiser, H. F. The application of electronic computers to factor analysis. *Educ. Psychol. Meas.* **1960**, *20*, 141–151.

(200) Wu, J.; Ma, L.; Chen, Y.; Cheng, Y.; Liu, Y.; Zha, X. Catalytic ozonation of organic pollutants from bio-treated dyeing and finishing wastewater using recycled waste iron shavings as a catalyst: Removal and pathways. *Water Res.* **2016**, *92*, 140–148.

(201) Chu, W.; Ma, C. W. Quantitative prediction of direct and indirect dye ozonation kinetics. *Water Res.* **2000**, *34* (12), 3153–3160.

(202) National Center for Biotechnology USA. PubChem - Open Chemistry Database https://pubchem.ncbi.nlm.nih.gov/ (accessed Aug 5, 2017).

(203) Real, F. J.; Benitez, J. F.; Acero, J. L.; Casas, F. Comparison between chlorination and ozonation treatments for the elimination of the emerging contaminants amitriptyline hydrochloride, methyl salicylate and 2-phenoxyethanol in surface waters and secondary effluents. *J. Chem. Technol. Biotechnol.* **2015**, *90* (8), 1400–1407.

(204) Real, F. J.; Benitez, F. J.; Acero, J. L.; Roldan, G.; Casas, F. Elimination of the emerging contaminants amitriptyline hydrochloride, methyl salicylate, and 2-phenoxyethanol in

ultrapure water and secondary effluents by photolytic and radicalary pathways. *Ind. Eng. Chem. Res.* **2012**, *51* (50), 16209–16215.

(205) Vieno, N. M.; Härkki, H.; Tuhkanen, T.; Kronberg, L. Occurence of pharmaceuticals in river water and their elimination in a pilot-scale drinking water treatment plant. *Environ. Sci. Technol.* **2007**, *41*, 5077–5084.

(206) Santoke, H.; Song, W.; Cooper, W. J.; Greaves, J.; Miller, G. E. Free-radical-induced oxidative and reductive degradation of fluoroquinolone pharmaceuticals: Kinetic studies and degradation mechanism. *J. Phys. Chem. A* **2009**, *113* (27), 7846–7851.

(207) Hamdi El Najjar, N.; Touffet, A.; Deborde, M.; Journel, R.; Leitner, N. K. V. Levofloxacin oxidation by ozone and hydroxyl radicals: Kinetic study, transformation products and toxicity. *Chemosphere* **2013**, *93* (4), 604–611.

(208) Dodd, M. C.; Zuleeg, S.; Von Gunten, U.; Pronk, W. Ozonation of source-separated urine for resource recovery and waste minimization: Process modeling, reaction chemistry, and operational considerations. *Environ. Sci. Technol.* **2008**, *42* (24), 9329–9337.

(209) Santoke, H.; Song, W.; Cooper, W. J.; Peake, B. M. Advanced oxidation treatment and photochemical fate of selected antidepressant pharmaceuticals in solutions of Suwannee River humic acid. *J. Hazard. Mater.* **2012**, *217–218*, 382–390.

(210) Henze, M.; van Loosdrecht, M. C. M.; Ekama, G. A.; Brdjanovic, D. *Biological Wastewater treatment: Principle, Modelling and Design*; IWA Publishing: London, 2008.

(211) Tchobanoglous, G.; Burton, F. L.; Stensel, H. D. *Wastewater engineering : treatment and reuse*; Metcalf and Eddy, I., Ed.; McGraw-Hill (Boston), 2003.

(212) Westerhoff, P.; Aiken, G.; Amy, G.; Debroux, J. Relationships between the structure of natural organic matter and its reactivity towards molecular ozone and hydroxyl radicals. *Water Res* **1999**, *33* (10), 2265–2276.

(213) Smeti, E. M.; Thanasoulias, N. C.; Lytras, E. S.; Tzoumerkas, P. C.; Golfinopoulos, S. K. Treated water quality assurance and description of distribution networks by multivariate chemometrics. *Water Res.* **2009**, *43* (18), 4676–4684.

(214) Ishii, S. K. L.; Boyer, T. H. Behavior of reoccurring parafac components in fluorescent dissolved organic matter in natural and engineered systems: A critical review. *Environ. Sci. Technol.* **2012**, *46* (4), 2006–2017.

(215) Anumol, T.; Sgroi, M.; Park, M.; Roccaro, P.; Snyder, S. A. Predicting trace organic compound breakthrough in granular activated carbon using fluorescence and UV absorbance as surrogates. *Water Res.* **2015**, *76*, 76–87.

(216) Rosenfeldt, E. J.; Linden, K. G. The ROH,UV concept to characterize and model UV/H2O2 process in natual waters. *Environ. Scieence Technol.* **2007**, *41* (7), 2548–2553.

(217) York, D.; Evensen, N. M.; Martinez, M. L.; De Basabe Delgado, J. Unified equations for the slope, intercept, and standard errors of the best straight line. *Am. J. Phys.* **2004**, *72* (3), 367–375.

(218) Mortier, S. T. F. C.; Van Hoey, S.; Cierkens, K.; Gernaey, K. V.; Seuntjens, P.; De Baets, B.; De Beer, T.; Nopens, I. A GLUE uncertainty analysis of a drying model of pharmaceutical granules. *Eur. J. Pharm. Biopharm.* **2013**, *85* (3 PART B), 984–995.

(219) Audenaert, W. T. M.; Callewaert, M.; Nopens, I.; Cromphout, J.; Vanhoucke, R.; Dumoulin, A.; Dejans, P.; Van Hulle, S. W. H. Full-scale modelling of an ozone reactor for drinking water treatment. *Chem. Eng. J.* **2010**, *157* (2–3), 551–557.

(220) Zucker, I.; Lester, Y.; Avisar, D.; Hübner, U.; Jekel, M.; Weinberger, Y.; Mamane, H. Influence of wastewater particles on ozone degradation of trace organic contaminants. *Environ. Sci. Technol.* **2015**, *49* (1), 301–308.

(221) van der Helm, A. W. C. *Integrated modeling of ozonation for optimization of drinking water treatment (PhD thesis)*; Water Management Academic press: Delft; The Netherlands, 2007.

(222) Korshin, G. V; Kumke, M. U.; Li, C.-W.; Frimmel, F. H. Influence of chlorination on chromophoress and fluorophores in humic substances. *Environ. Sci. Technol.* **1999**, *33*, 1207–1212.

(223) Korshin, G. V.; Benjamin, M. M.; Chang, H. S.; Gallard, H. Examination of NOM chlorination reactions by conventional and stop-flow differential absorbance spectroscopy. *Environ. Sci. Technol.* **2007**, *41* (8), 2776–2781.

(224) Swietlik, J.; Dabrowska, A.; Raczyk-Stanisławiak, U.; Nawrocki, J. Reactivity of natural organic matter fractions with chlorine dioxide and ozone. *Water Res.* **2004**, *38* (3), 547–558.

(225) Sudhakaran, S.; Amy, G. L. QSAR models for oxidation of organic micropollutants in water based on ozone and hydroxyl radical rate constants and their chemical classification. *Water Res.* **2013**, *47* (3), 1111–1122.

(226) Lee, Y.; von Gunten, U. Quantitative structure-activity relationships (QSARs) for the transformation of organic micropollutants during oxidative water treatment. *Water Res.* **2012**, *46* (19), 6177–6195.

(227) Chys, M.; Audenaert, W. T. M.; Deniere, E.; Mortier, S. T. F. C.; Langenhove, H. Van; Nopens, I.; Demeestere, K.; Van Hulle, S. W. H. Surrogate-based correlation models in view of real-time control of ozonation of secondary treated municipal wastewater - model development and validation. *Environ. Sci. Technol.* **2017**.

(228) Cleveland, W. S. Robust Locally Weighted Regression and Smoothing Scatterplots. *J. Am. Stat. Assoc.* **1979**, *74* (368), 829–836.

(229) Cleveland, W. S.; Devlin, S. J. Locally Weighted Regression: An Approach to Regression Analysis by Local Fitting. *J. Am. Stat. Assoc.* **1988**, *83* (403), 596–610.

(230) Severyns, J. *Personal Communication*; 2016.

(231) Lamond, R. *Personal Communication*; 2016.

(232) Altmann, J.; Massa, L.; Sperlich, A.; Gnirss, R.; Jekel, M. UV254 absorbance as real-time monitoring and control parameter for micropollutant removal in advanced wastewater treatment with powdered activated carbon. *Water Res.* **2016**, *94*, 240–245.

(233) Zietzschmann, F.; Altmann, J.; Ruhl, A. S.; Dünnbier, U.; Dommisch, I.; Sperlich, A.; Meinel, F.; Jekel, M. Estimating organic micro-pollutant removal potential of activated carbons using UV absorption and carbon characteristics. *Water Res.* **2014**, *56*, 48–55.

(234) Escolà Casas, M.; Bester, K. Can those organic micro-pollutants that are recalcitrant in activated sludge treatment be removed from wastewater by biofilm reactors (slow sand filters)? *Sci. Total Environ.* **2015**, *506–507*, 315–322.

(235) Dries, J.; De Schepper, W.; Geuens, L.; Blust, R. Removal of ecotoxicity and COD from tank truck cleaning wastewater. *Water Sci. Technol.* **2013**, *68* (10), 2202–2207.

(236) Dries, J.; Daens, D.; Geuens, L.; Blust, R. Evaluation of acute ecotoxicity removal from industrial wastewater using a battery of rapid bioassays. *Water Sci. Technol.* **2014**, *70* (12), 2056–2061.

(237) Macova, M.; Escher, B. I.; Reungoat, J.; Carswell, S.; Chue, K. L.; Keller, J.; Mueller, J. F. Monitoring the biological activity of micropollutants during advanced wastewater treatment with ozonation and activated carbon filtration. *Water Res.* **2010**, *44* (2), 477–492.

(238) Girardi, C.; Greve, J.; Lamshöft, M.; Fetzer, I.; Miltner, A.; Schäffer, A.; Kästner, M. Biodegradation of ciprofloxacin in water and soil and its effects on the microbial communities. *J. Hazard. Mater.* **2011**, *198*, 22–30.

(239) Liao, X.; Li, B.; Zou, R.; Dai, Y.; Xie, S.; Yuan, B. Biodegradation of antibiotic ciprofloxacin: pathways, influential factors, and bacterial community structure. *Environ. Sci. Pollut. Res.* **2016**, *23* (8), 7911–7918.

(240) Dong, S.; Gao, B.; Sun, Y.; Shi, X.; Xu, H.; Wu, J.; Wu, J. Transport of sulfacetamide and levofloxacin in granular porous media under various conditions: Experimental observations and model simulations. *Sci. Total Environ.* **2016**, *573*, 1630–1637.

(241) Yang, X.; Flowers, R. C.; Weinberg, H. S.; Singer, P. C. Occurrence and removal of pharmaceuticals and personal care products (PPCPs) in an advanced wastewater reclamation plant. *Water Res.* **2011**, *45* (16), 5218–5228.

(242) Knopp, G.; Prasse, C.; Ternes, T.; Cornel, P. Elimination of micropollutants and transformation products from a wastewater treatment plant effluent through pilot scale ozonation followed by various activated carbon and biological filters. *Water Res.* **2016**, *100*, 580–592.

(243) Schoutteten, K. V. K. M.; Hennebel, T.; Dheere, E.; Bertelkamp, C.; De Ridder, D. J.; Maes, S.; Chys, M.; Van Hulle, S. W. H.; Vanden Bussche, J.; Vanhaecke, L.; et al. Effect of oxidation and catalytic reduction of trace organic contaminants on their activated carbon adsorption. *Chemosphere* **2016**, *165*, 191–201.

(244) Neta, P.; Huie, R. E.; Ross, A. B. Rate Constants for Reactions of Inorganic Radicals in Aqueous Solution. *J. Phys. Chem. Ref. Data* **1988**, *17* (3), 1027–1284.

(245) Hofman-Caris, C. H. M.; Siegers, W. G.; van de Merlen, K.; de Man, A. W. A.; Hofman, J. A. M. H. Removal of pharmaceuticals from WWTP effluent: Removal of EfOM followed by advanced oxidation. *Chem. Eng. J.* **2017**, *327*, 514–521.

(246) Koreman, E.; Galjaard, G. NOM-removal at SWTP Andijk (Netherlands) with a New Anion Exchange. In *GEWÄSSERSCHUTZ . WASSER . ABWASSER*; Aachen, 2016; p 50.1-50.13.

(247) Spiliotopoulou, A.; Martin, R.; Pedersen, L. F.; Andersen, H. R. Use of fluorescence spectroscopy to control ozone dosage in recirculating aquaculture systems. *Water Res.*

2017, *111*, 357–365.

(248) Buffle, M. O.; Schumacher, J.; Salhi, E.; Jekel, M.; von Gunten, U. Measurement of the initial phase of ozone decomposition in water and wastewater by means of a continuous quench-flow system: Application to disinfection and pharmaceutical oxidation. *Water Res.* **2006**, *40* (9), 1884–1894.

(249) Gonzales, S.; Peña, A.; Rosario-Ortiz, F. L. Examining the Role of Effluent Organic Matter Components on the Decomposition of Ozone and Formation of Hydroxyl Radicals in Wastewater. *Ozone Sci. Eng.* **2012**, *34* (1), 42–48.

(250) González, O.; Justo, A.; Bacardit, J.; Ferrero, E.; Malfeito, J. J.; Sans, C. Characterization and fate of effluent organic matter treated with UV/H2O2 and ozonation. *Chem. Eng. J.* **2013**, *226*, 402–408.

(251) Zhang, J.; Tejada-Martinez, A. E.; Lei, H.; Zhang, Q. Indicators for technological, environmental and economic sustainability of ozone contactors. *Water Res.* **2016**, *101*, 606–616.

Appendices

Appendix A

Split-half analysis validation results

(Supporting information to Chapter 4)

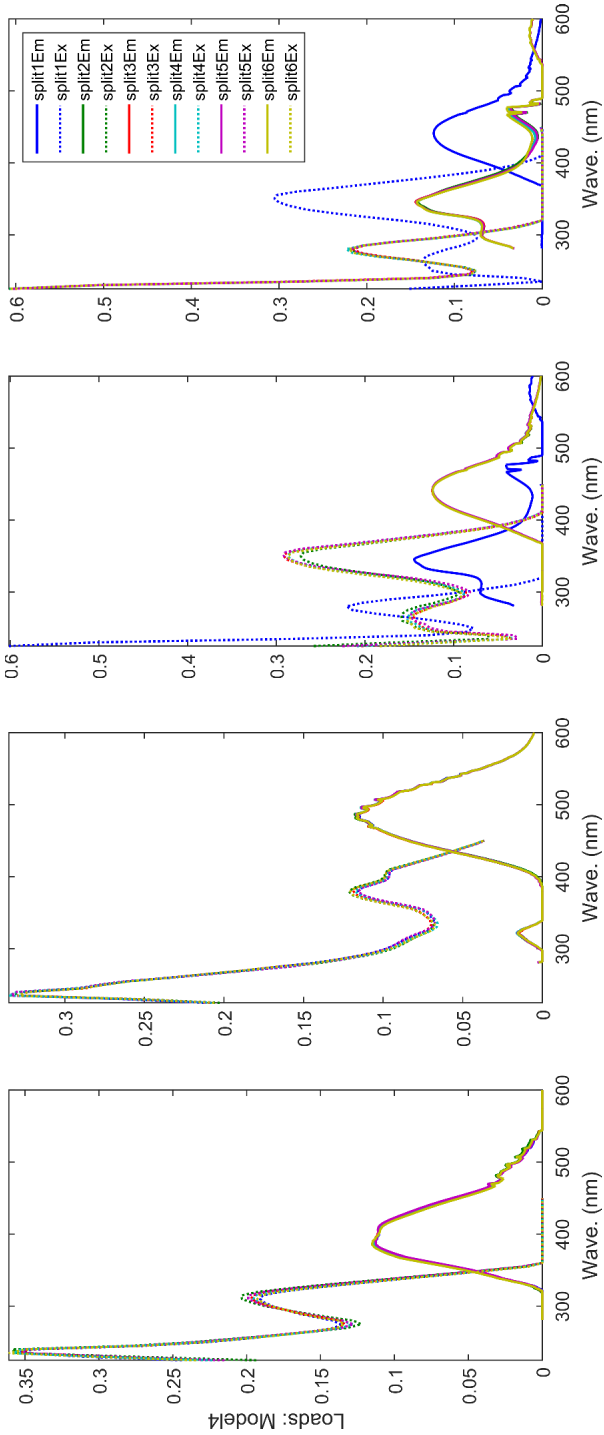

Figure A.1: Spectral loadings after split-half analysis in order to validate the developed PARAFAC model, presented in Chapter 4.

Appendix B

Abatement patterns for (individual) TrOCs in relation to different surrogates

(Supporting information to Chapter 4)

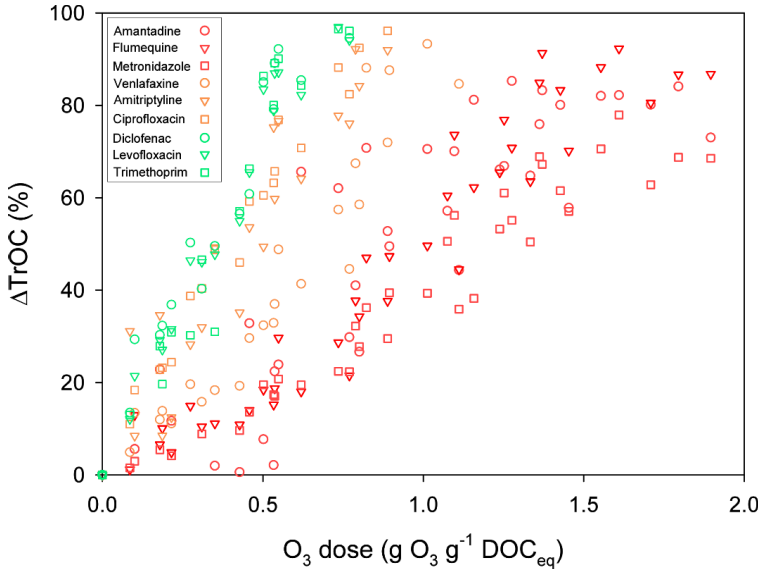

Figure B.1: Abatement pattern of TrOCs in relation to the ozone dose (g O_3 g^{-1} DOC_{eq}) as used for the development of the inflected correlation model given in Figure 4.2 to Figure 4.6.

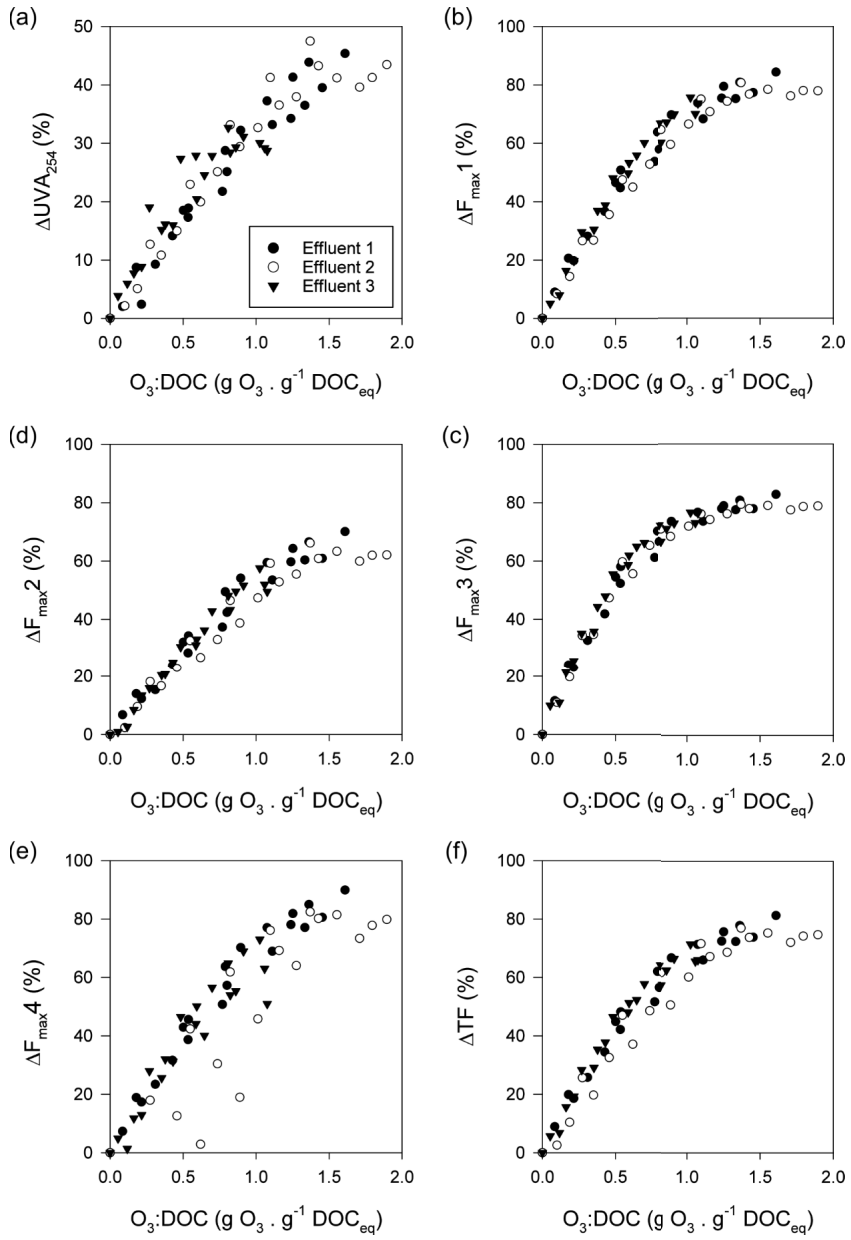

Figure B.2: Decrease of surrogate parameters in relation to the ozone dose (g O_3 g^{-1} DOC_{eq}) for (a) ΔUVA_{254}, (b-e) ΔF_{max}1-4 and (f) ΔTF

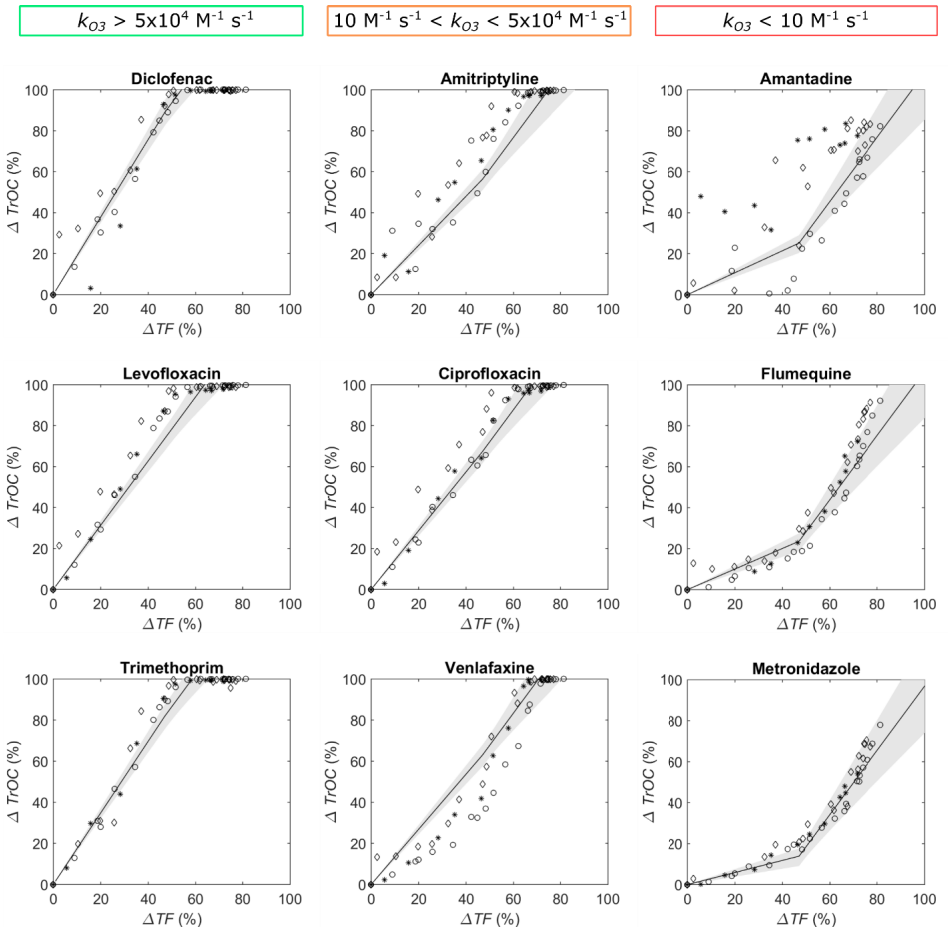

Figure B.3: Abatement pattern for each individual TrOC in relation with ΔTF. Data are obtained from measurements on effluent 1 (○), 2 (◊) and 3 (*). Correlations are drawn based on the developed model and the $k_{O3,TrOC}$ given in Table 3.3. The grey areas are indicating the 95% confidence interval of the calculated correlation.

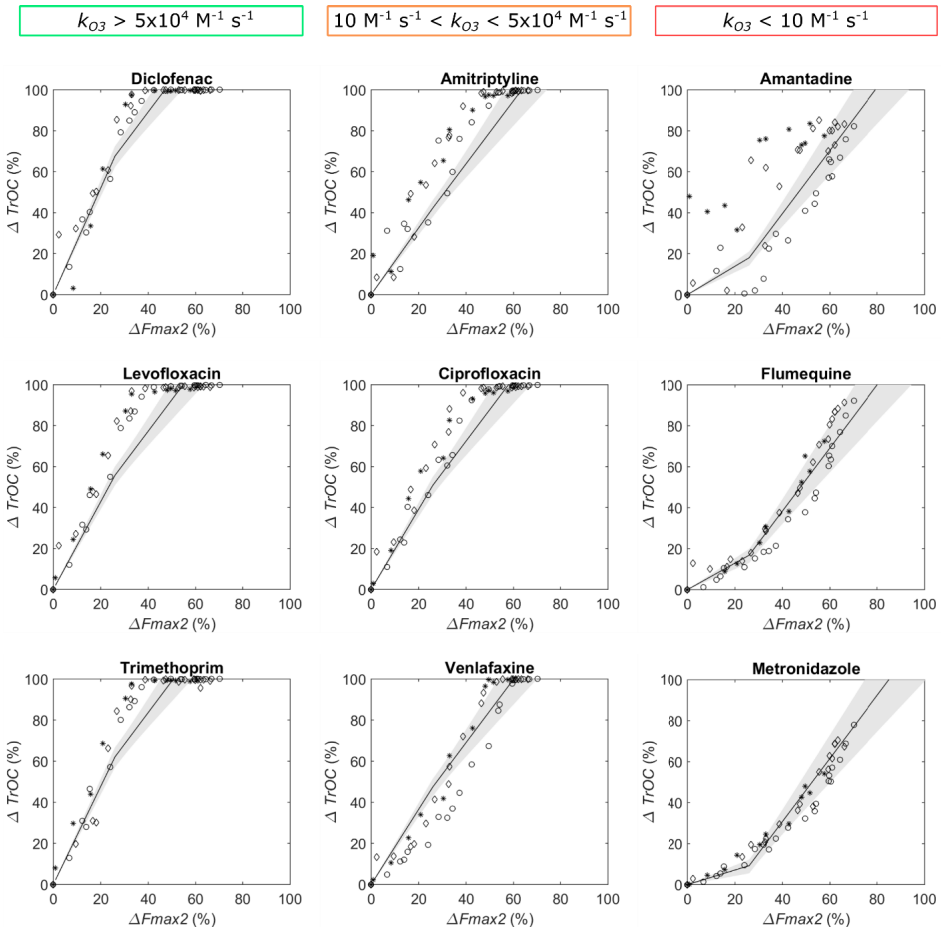

Figure B.4: Abatement pattern for each individual TrOC in relation with $\Delta F_{max}2$. Data are obtained from measurements on effluent 1 (○), 2 (◊) and 3 (*). Correlations are drawn based on the developed model and the $k_{O3,TrOC}$ given in Table 3.3. The grey areas are indicating the 95% confidence interval of the calculated correlation.

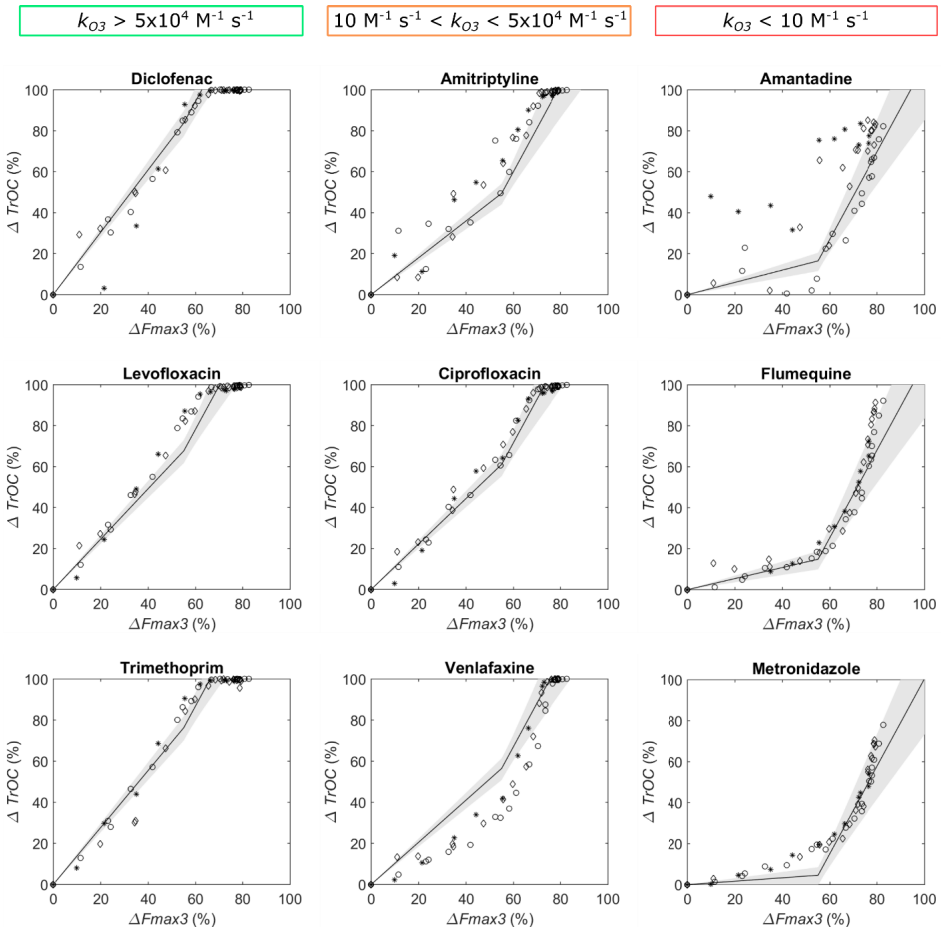

Figure B.5: Abatement pattern for each individual TrOC in relation with $\Delta F_{max}3$. Data are obtained from measurements on effluent (○), 2 (◊) and 3 (*). Correlations are drawn based on the developed model and the $k_{O3,TrOC}$ given in Table 3.3. The grey areas are indicating the 95% confidence interval of the calculated correlation.

Appendix C

Details of single correlation models obtained (1) from literature or (2) constructed with the data from Chapter 4

(Supporting information to Chapter 5)

The abatement of TrOCs (ΔTrOC) using a single correlation model can be estimated using eq. C.1 as extensively described by several authors.[40,63,64,82,100,103,113,114] Slopes (a_s) and intercepts (b_s) for ΔpCBA in relation to ΔUVA_{254}, as reported in literature, are summarized in Table C.2.

Based on the data used for the development of the inflected correlation model in Chapter 4, also a single correlation model was constructed for ΔUVA_{254}, ΔF_{max}1-3 and ΔTF. In accordance to the inflected model, the apparent 2nd order $k_{O3,TrOC}$ is used as main input to construct single correlation models for any TrOC with known $k_{O3,TrOC}$. The slope (a_s) and intercept (b_s) can be calculated using eq. C.2 and C.3 of which the surrogate specific parameters (m_1, m_2, b_1 and b_2) are given in Table C.2. All these parameters (and the uncertainty thereon) have been determined similarly as done for the inflected model of which most explanation is given in Chapter 4.

$$\Delta TrOC = as \times \Delta S + bs \quad \text{(eq. C.1)}$$

$$a_s = m_1 \times \log(k_{O3,TrOC}) + b_1 \quad \text{(eq. C.2)}$$

$$b_s = m_2 \times \log(k_{O3,TrOC}) + b_2 \quad \text{(eq. C.3)}$$

Table C.1: Slopes and intercepts of single correlation models between ΔpCBA and ΔUVA_{254}, as obtained from literature and this work.

Source	**a_s (slope)**	**b_s (intercept)**
Audenaert et al.[113]	1.58	-6.46
Wert et al.[103]	1.95	-30.2
Gerrity et al.[64]	1.31	3.0
Sharif et al.[115]	1.57	0
This work[a] (single correlation)	1.55	-8.00

[a] determined for pCBA using a single correlation model constructed from the same data as used for the development of the inflected model in Chapter 4

Table C.2: Detailed parameters to determine the slope and intercept of the single correlation models developed based on the data from Chapter 4 (i.e. the relation between the abatement of TrOCs and decrease in surrogate measurements based on their apparent 2nd order $k_{O3,TrOC}$)

Surrogate	$a_s = m_1 \times \log(k_{O3,TrOC}) + b_1$			$b_s = m_2 \times \log(k_{O3,TrOC}) + b_2$		
	m_1	b_1	R^2 (n = 7)	m_2	b_2	R^2 (n = 7)
UVA_{254}	0.17 ± 0.01	1.55 ± 0.10	0.88	1.12 ± 0.25	-8.00 ± 2.29	0.60
$F_{max}1$	0.07 ± 0.01	0.87 ± 0.07	0.84	1.00 ± 0.32	-13.32 ± 3.40	0.55
$F_{max}2$	0.12 ± 0.01	1.05 ± 0.07	0.82	0.88 ± 0.26	-9.42 ± 2.51	0.42
$F_{max}3$	0.05 ± 0.01	0.84 ± 0.08	0.84	0.98 ± 0.40	-14.08 ± 4.40	0.58
TF	0.07 ± 0.01	0.89 ± 0.07	0.81	1.10 ± 0.33	-11.88 ± 3.41	0.56

Appendix D

Statistical information supporting the validation of the inflected and single correlation models, and their predictive power

(Supporting information to Chapter 5)

Table D.1: Correspondence between measured and predicted pCBA removal by lab-scale ozonation for the different sampling locations (separately and combined) based on the inflected model from Chapter 4. The values indicating a poor correspondence (t-test: p-value < 0.05; TIC > 0.30) are indicated with grey shading. The MAE (mean absolute error) is added for all locations combined.

Sampling location	**Number of data points**	**t-test (p-value)**					**TIC**				
		UVA_{254}	$F_{max}1$	$F_{max}2$	$F_{max}3$	TF	UVA_{254}	$F_{max}1$	$F_{max}2$	$F_{max}3$	TF
KS1	12	0.800	0.732	0.362	0.026	0.016	0.11	0.09	0.16	0.39	0.46
KS2	12	0.486	0.638	0.765	0.062	0.066	0.15	0.10	0.07	0.32	0.33
KS 1+2	*24*	*0.476*	*0.553*	*0.410*	*0.003*	*0.002*	*0.13*	*0.10*	*0.11*	*0.35*	*0.38*
HL	12	0.825	0.957	0.406	0.229	0.630	0.14	0.12	0.18	0.26	0.15
CW	12	0.965	0.860	0.340	0.987	0.915	0.06	0.07	0.14	0.11	0.08
WRG1	6	0.280	0.921	0.880	0.553	0.426	0.24	0.13	0.46	0.77	0.17
WRG2	6	0.364	0.139	0.036	0.043	0.062	0.21	0.43	0.91	0.95	0.62
WRG 1+2	*12*	*0.149*	*0.236*	*0.064*	*0.0495*	*0.035*	*0.22*	*0.30*	*0.75*	*0.88*	*0.43*
All (1-6)	**60**	**0.407**	**0.443**	**0.574**	**0.002**	**0.004**	**0.13**	**0.14**	**0.31**	**0.52**	**0.28**
MAE (%)	**60**	**9.2**	**8.3**	**17.4**	**29.2**	**15.8**					

Table D.2: Correspondence between measured and predicted pCBA removal by lab-scale ozonation for the different sampling locations (separately and combined) based on the single correlation model based on the data from Chapter 4. The values indicating a poor correspondence (t-test: p-value < 0.05; TIC > 0.30) are indicated with grey shading. The MAE (mean absolute error) is added for all locations combined.

Sampling location (nr.)	**Number of data points**	**t-test (p-value)**					**TIC**				
		UVA_{254}	$F_{max}1$	$F_{max}2$	$F_{max}3$	TF	UVA_{254}	$F_{max}1$	$F_{max}2$	$F_{max}3$	TF
KS1	12	0.659	0.599	0.316	0.258	0.105	0.14	0.09	0.17	0.20	0.28
KS2	12	0.311	0.396	0.518	0.207	0.152	0.17	0.14	0.12	0.22	0.25
KS 1+2	*24*	*0.278*	*0.313*	*0.244*	*0.082*	*0.028*	*0.16*	*0.12*	*0.14*	*0.21*	*0.26*
HL	12	0.969	0.883	0.521	0.649	0.858	0.12	0.13	0.17	0.17	0.14
CW	12	0.720	0.747	0.701	0.805	0.849	0.09	0.14	0.13	0.19	0.15
WRG1	6	0.368	0.797	0.828	0.625	0.609	0.20	0.10	0.41	0.58	0.13
WRG2	6	0.374	0.254	0.093	0.084	0.114	0.22	0.32	0.68	0.71	0.50
WRG 1+2	*12*	*0.187*	*0.280*	*0.129*	*0.100*	*0.101*	*0.21*	*0.24*	*0.55*	*0.63*	*0.35*
All (1-6)	**60**	**0.174**	**0.191**	**0.397**	**0.033**	**0.029**	**0.14**	**0.15**	**0.24**	**0.31**	**0.23**
MAE (%)	**60**	**9.8**	**9.1**	**14.2**	**18.2**	**13.1**					

Table D.3: Correspondence between measured and predicted pCBA removal by lab-scale ozonation for the different sampling locations (separately and combined) based on the single correlation models from literature (only UVA_{254}). The values indicating a poor correspondence (t-test: p-value < 0.05; TIC > 0.30) are indicated with grey shading. The MAE (mean absolute error) is added for all locations combined.

Sampling location (nr.)	**Number of data points**	**t-test (p-value)**				**TIC**			
		a	b	c	d	a	b	c	d
KS1	12	0.822	0.247	0.929	0.795	0.12	0.20	0.13	0.12
KS2	12	0.410	0.122	0.475	0.696	0.14	0.26	0.15	0.10
KS 1+2	*24*	*0.429*	*0.048*	*0.539*	*0.900*	*0.14*	*0.24*	*0.14*	*0.11*
HL	12	0.824	0.600	0.652	0.508	0.12	0.15	0.13	0.15
CW	12	0.860	0.426	0.863	0.842	0.08	0.13	0.11	0.08
WRG1	6	0.462	0.109	0.641	0.759	0.16	0.39	0.12	0.08
WRG2	6	0.449	0.171	0.544	0.668	0.19	0.34	0.18	0.13
WRG 1+2	*12*	*0.269*	*0.030*	*0.420*	*0.579*	*0.18*	*0.36*	*0.16*	*0.11*
All (1-6)	**60**	**0.363**	**0.006**	**0.556**	**0.907**	**0.13**	**0.22**	**0.13**	**0.11**
MAE (%)	**60**	**8.8**	**14.0**	**9.2**	**7.6**				

[a] Audenaert et al.[113]; [b] Wert et al.[103]; [c] Gerrity et al.[64]; [d] Sharif et al.[115]

Table D.4: Correspondence between measured and predicted TrOC removal by pilot-scale ozonation, using the inflected model from Chapter 4. The p-values (< 0.05, t-test) indicating a poor correspondence are grey shaded.

t-test (p-values)		**Surrogates**				
TrOCs	**Number of data points**	UVA_{254} (online)	$F_{max}1$	$F_{max}2$	$F_{max}3$	TF
Diclofenac	39	0.173	0.000	0.001	0.140	0.060
Trimethoprim	41	0.347	0.014	0.074	0.873	0.010
Levofloxacin	23	0.355	0.042	0.182	0.646	0.260
Amitriptyline	34	0.284	0.298	0.025	0.000	0.000
Ciprofloxacin	7	0.566	0.896	0.770	0.256	0.413
Venlafaxine	41	0.620	0.357	0.915	0.010	0.002
Flumequine	31	0.456	0.182	0.123	0.000	0.000
Amantadine	43	0.870	0.217	0.087	0.000	0.000
Metronidazole	43	0.400	0.927	0.946	0.000	0.000
Alprazolam	25	0.040	0.102	0.121	0.000	0.000
Carbamazepine	43	0.722	0.148	0.475	0.272	0.001
Diazepam	34	0.229	0.120	0.106	0.000	0.000
Sulfamethoxazole	43	0.004	0.000	0.000	0.000	0.864

Table D.5: Correspondence between measured and predicted TrOC removal by pilot-scale ozonation, using the inflected model from Chapter 4. TICs (> 0.30) indicating a poor correspondence are grey shaded.

TIC		**Surrogates**				
TrOCs	**Number of data points**	UVA_{254} (online)	$F_{max}1$	$F_{max}2$	$F_{max}3$	TF
Diclofenac	39	0.13	0.07	0.06	0.05	0.13
Trimethoprim	41	0.10	0.06	0.05	0.06	0.14
Levofloxacin	23	0.12	0.09	0.09	0.09	0.15
Amitriptyline	34	0.14	0.10	0.11	0.17	0.20
Ciprofloxacin	7	0.20	0.11	0.11	0.14	0.12
Venlafaxine	41	0.09	0.04	0.05	0.09	0.16
Flumequine	31	0.12	0.10	0.10	0.33	0.27
Amantadine	43	0.09	0.08	0.08	0.27	0.24
Metronidazole	43	0.17	0.15	0.15	0.33	0.26
Alprazolam	25	0.24	0.25	0.22	0.55	0.40
Carbamazepine	43	0.10	0.04	0.04	0.06	0.14
Diazepam	34	0.28	0.29	0.30	0.52	0.42
Sulfamethoxazole	43	0.17	0.11	0.10	0.09	0.13

Table D.6: Mean absolute error (MAE, in %) between measured and predicted TrOC removal by pilot-scale ozonation, using the inflected model from Chapter 4.

MAE (%)		**Surrogates**				
TrOCs	**Number of data points**	UVA_{254} (online)	$F_{max}1$	$F_{max}2$	$F_{max}3$	TF
Diclofenac	39	13.0	10.0	9.1	8.0	17.5
Trimethoprim	41	10.6	8.9	8.2	8.8	17.7
Levofloxacin	23	14.9	12.5	11.6	11.5	18.3
Amitriptyline	34	14.7	12.9	13.7	20.9	23.8
Ciprofloxacin	7	13.9	10.3	9.3	12.8	11.3
Venlafaxine	41	8.0	5.3	6.0	11.4	16.3
Flumequine	31	10.5	8.0	8.8	27.0	21.0
Amantadine	43	9.0	7.9	7.5	26.5	22.0
Metronidazole	43	13.3	10.0	9.1	23.7	18.4
Alprazolam	25	15.3	16.0	15.2	30.7	23.8
Carbamazepine	43	8.4	6.3	6.3	8.9	17.3
Diazepam	34	17.7	18.4	19.2	39.3	31.8
Sulfamethoxazole	43	19.5	15.9	14.2	12.1	17.2

Table D.7: Correspondence between measured and predicted TrOC removal by pilot-scale ozonation, using the single correlation model based on the data from Chapter 4. The p-values (< 0.05, t-test) indicating a poor correspondence are grey shaded.

t-test (p-values)		**Surrogates**				
TrOCs	**Number of data points**	UVA_{254} (online)	$F_{max}1$	$F_{max}2$	$F_{max}3$	TF
Diclofenac	39	0.109	0.000	0.000	0.057	0.014
Trimethoprim	41	0.221	0.000	0.000	0.632	0.158
Levofloxacin	23	0.235	0.003	0.001	0.752	0.135
Amitriptyline	34	0.689	0.915	0.466	0.000	0.172
Ciprofloxacin	7	0.670	0.679	0.428	0.536	0.896
Venlafaxine	41	0.289	0.035	0.006	0.058	0.984
Flumequine	31	0.345	0.164	0.236	0.000	0.004
Amantadine	43	0.494	0.045	0.162	0.000	0.000
Metronidazole	43	0.624	0.333	0.291	0.005	0.014
Alprazolam	25	0.042	0.139	0.070	0.008	0.018
Carbamazepine	43	0.548	0.010	0.003	0.592	0.644
Diazepam	34	0.072	0.065	0.042	0.006	0.010
Sulfamethoxazole	43	0.001	0.000	0.000	0.000	0.000

Table D.8: Correspondence between measured and predicted TrOC removal by pilot-scale ozonation, using the single correlation model based on the data from Chapter 4. TICs (> 0.30) indicating a poor correspondence are grey shaded.

TIC		**Surrogates**				
TrOCs	**Number of data points**	UVA_{254} (online)	$F_{max}1$	$F_{max}2$	$F_{max}3$	TF
Diclofenac	39	0.12	0.07	0.07	0.05	0.08
Trimethoprim	41	0.10	0.06	0.06	0.05	0.08
Levofloxacin	23	0.12	0.10	0.11	0.07	0.10
Amitriptyline	34	0.14	0.08	0.09	0.12	0.08
Ciprofloxacin	7	0.19	0.09	0.11	0.09	0.08
Venlafaxine	41	0.09	0.05	0.06	0.06	0.08
Flumequine	31	0.11	0.08	0.09	0.16	0.16
Amantadine	43	0.09	0.09	0.07	0.17	0.17
Metronidazole	43	0.18	0.16	0.16	0.21	0.22
Alprazolam	25	0.24	0.22	0.22	0.25	0.27
Carbamazepine	43	0.09	0.04	0.04	0.05	0.06
Diazepam	34	0.31	0.31	0.32	0.36	0.35
Sulfamethoxazole	43	0.16	0.12	0.12	0.09	0.12

Table D.9: Mean absolute error (MAE, in %) between measured and predicted TrOC removal by pilot-scale ozonation, using the single correlation model from Chapter 4.

MAE (%)		**Surrogates**				
TrOCs	**Number of data points**	UVA_{254} (online)	$F_{max}1$	$F_{max}2$	$F_{max}3$	TF
Diclofenac	39	12.7	10.1	10.2	8.1	11.3
Trimethoprim	41	10.7	9.1	9.2	7.1	10.2
Levofloxacin	23	15.4	14.1	15.2	8.4	13.3
Amitriptyline	34	14.0	11.0	11.5	15.2	11.1
Ciprofloxacin	7	13.3	8.4	11.9	8.6	6.9
Venlafaxine	41	9.9	7.3	9.1	7.1	7.7
Flumequine	31	8.0	7.1	7.7	13.2	11.1
Amantadine	43	5.9	8.7	6.8	15.8	13.8
Metronidazole	43	9.4	10.7	10.2	14.8	14.9
Alprazolam	25	15.9	14.5	15.6	17.1	16.8
Carbamazepine	43	8.3	6.3	6.2	7.2	7.6
Diazepam	34	20.1	19.9	21.4	25.2	24.4
Sulfamethoxazole	43	19.4	16.8	16.8	12.8	17.2

Appendix E

3D EEMs and comparison of predicted and measured ΔTrOCs during pilot-scale experimentation

(Supporting information to Chapter 5)

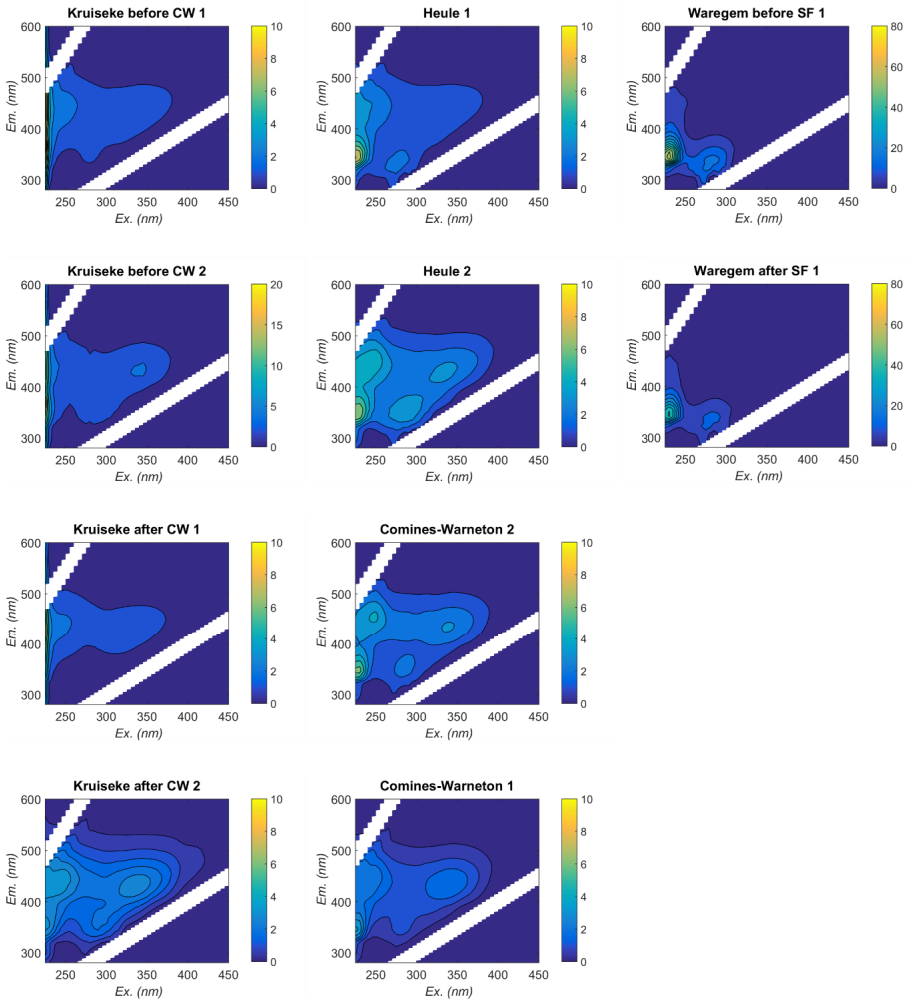

Figure E.1: Visualization of the 3D Excitation Emission Matrices (EEMs) of all effluents used for lab-scale ozonation, with different intensity scales for each effluent sample indicating the RU (Raman Units) values.

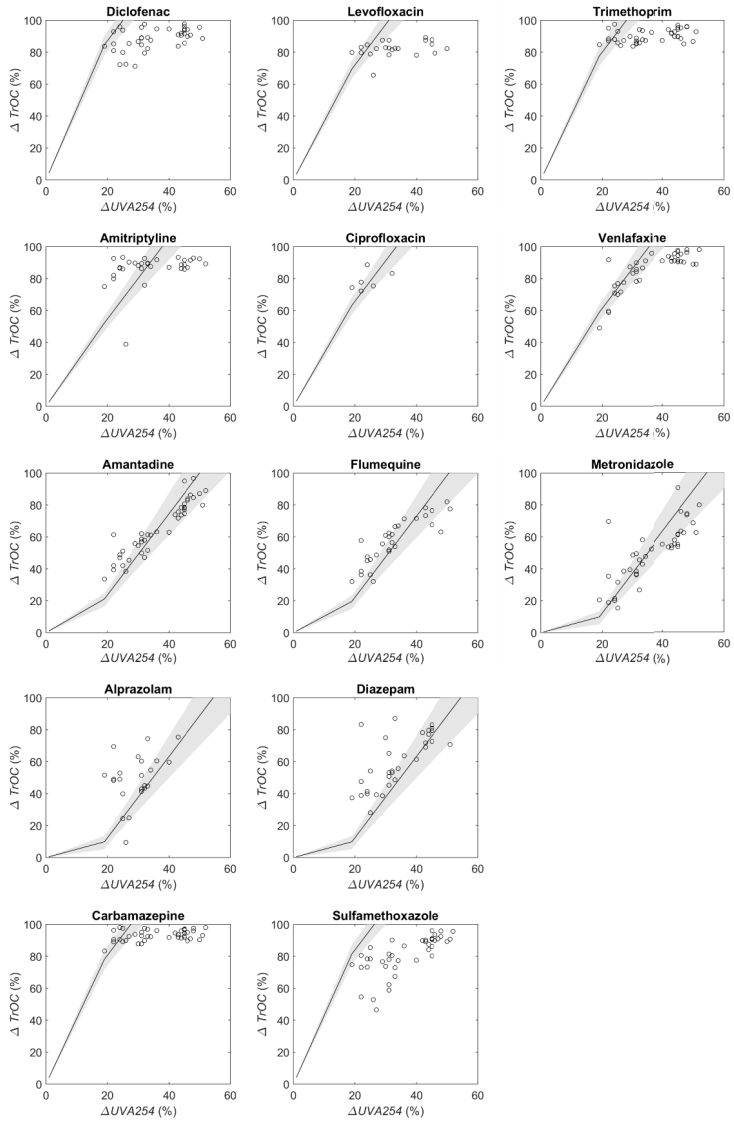

Figure E.2: Abatement patterns of predicted (full lines) and measured ΔTrOCs (dots) in relation to ΔUVA_{254} by applying the inflected model for 13 TrOCs under investigation during pilot-scale experimentation. The shaded grey areas indicate the 95% confidence interval of the model. (negative values of ΔTrOCs not shown if due to an erroneous measurement of TrOCs or ΔUVA_{254})

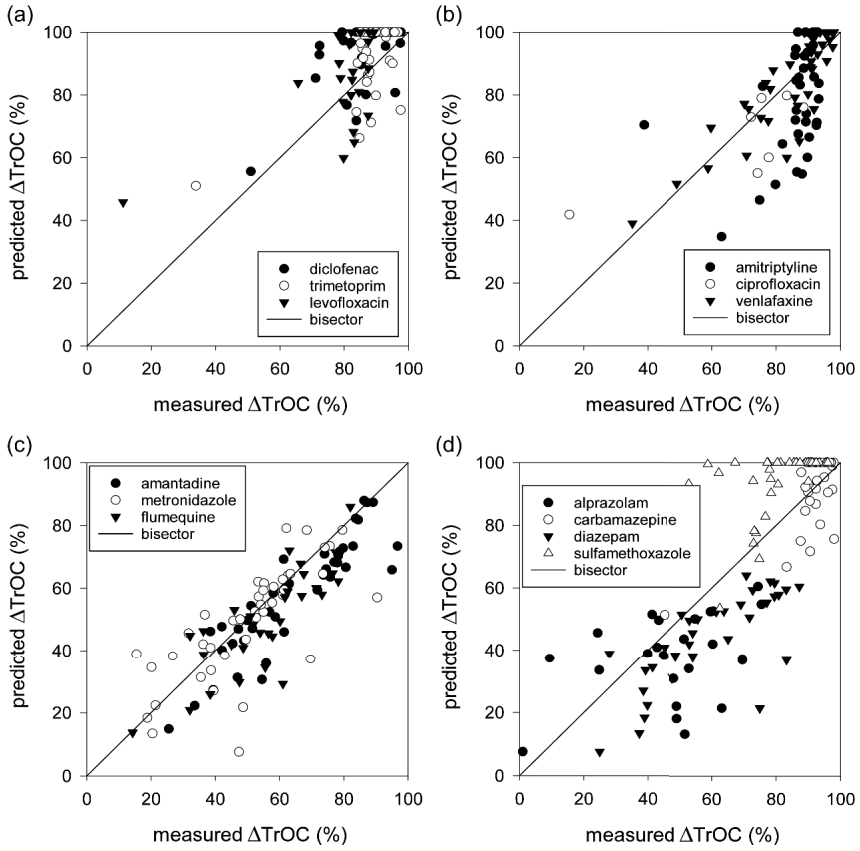

Figure E.3: Measured and predicted ΔTrOC using the inflected correlation model based on the $\Delta F_{max}2$ signal. Data are shown separately for TrOCs that were also used during model development and having different reactivity towards ozone: (a) $k_{O3,TrOC} > 5\times10^4$ M^{-1} s^{-1}, (b) 5×10^4 M^{-1} $s^{-1} > k_{O3,TrOC} > 10$ M^{-1} s^{-1}, (c) $k_{O3,TrOC} < 10$ M^{-1} s^{-1}; and (d) for TrOCs not used during model development. (negative values of ΔTrOCs not shown if due to an erroneous measurement of TrOCs or $\Delta F_{max}2$)

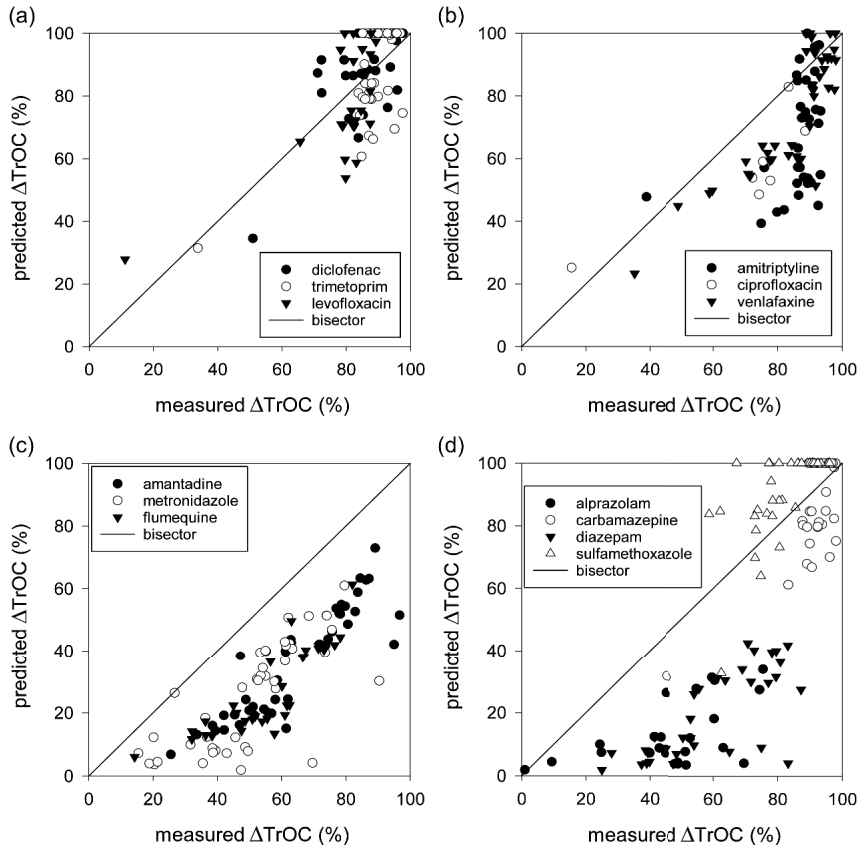

Figure E.4: Measured and predicted ΔTrOC using the inflected correlation model based on the $\Delta F_{max}3$ signal. Data are shown separately for TrOCs that were also used during model development and having different reactivity towards ozone: (a) $k_{O3,TrOC} > 5\times10^4$ M^{-1} s^{-1}, (b) 5×10^4 M^{-1} $s^{-1} > k_{O3,TrOC} > 10$ M^{-1} s^{-1}, (c) $k_{O3,TrOC} < 10$ M^{-1} s^{-1}; and (d) for TrOCs not used during model development. (negative values of ΔTrOCs not shown if due to an erroneous measurement of TrOCs or $\Delta F_{max}3$)

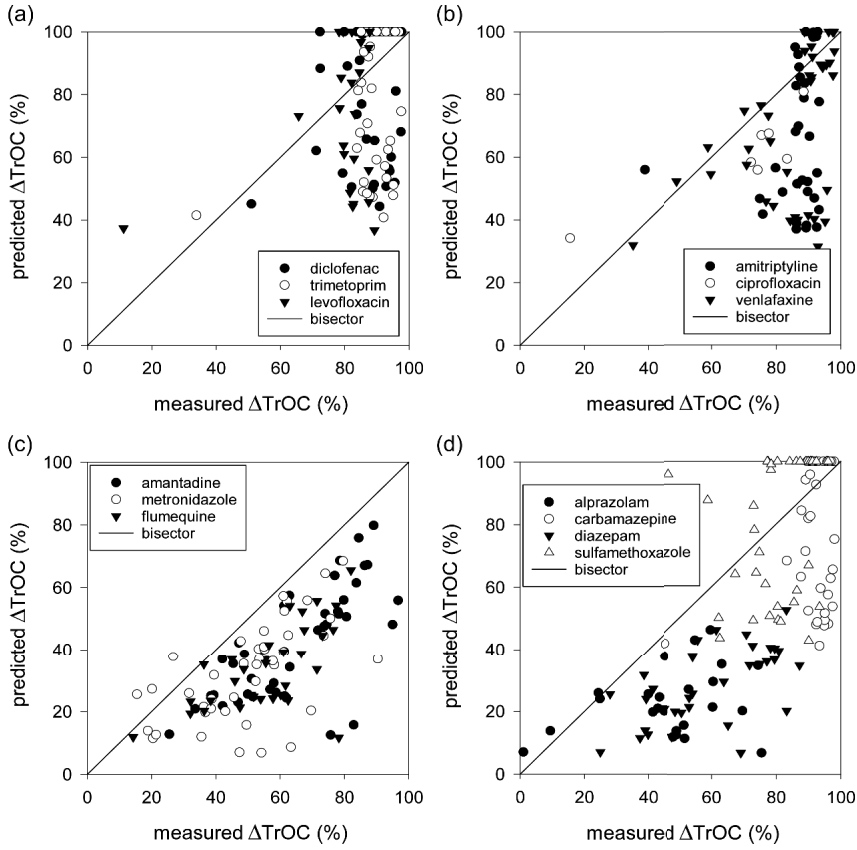

Figure E.5: Measured and predicted ΔTrOC using the inflected correlation model based on the ΔTF signal. Data are shown separately for TrOCs that were also used during model development and having different reactivity towards ozone: (a) $k_{O3,TrOC} > 5\times10^4$ M^{-1} s^{-1}, (b) 5×10^4 M^{-1} $s^{-1} > k_{O3,TrOC} > 10$ M^{-1} s^{-1}, (c) $k_{O3,TrOC} < 10$ M^{-1} s^{-1}; and (d) for TrOCs not used during model development. (negative values of ΔTrOCs not shown if due to an erroneous measurement of TrOCs or ΔTF)

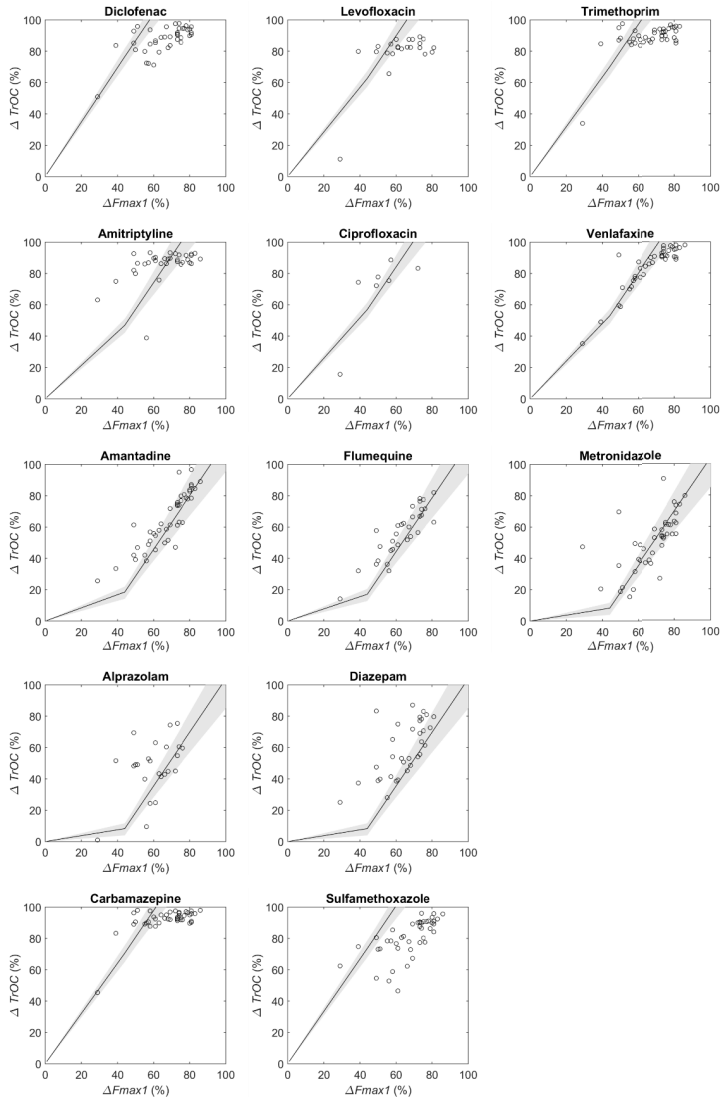

Figure E.6: Abatement patterns of predicted (full lines) and measured ΔTrOCs (dots) in relation to $\Delta F_{max}1$ by applying the inflected model for 13 TrOCs under investigation during pilot-scale experimentation. The shaded grey areas indicate the 95% confidence interval of the model. (negative values of ΔTrOCs not shown if due to an erroneous measurement of TrOCs or $\Delta F_{max}1$)

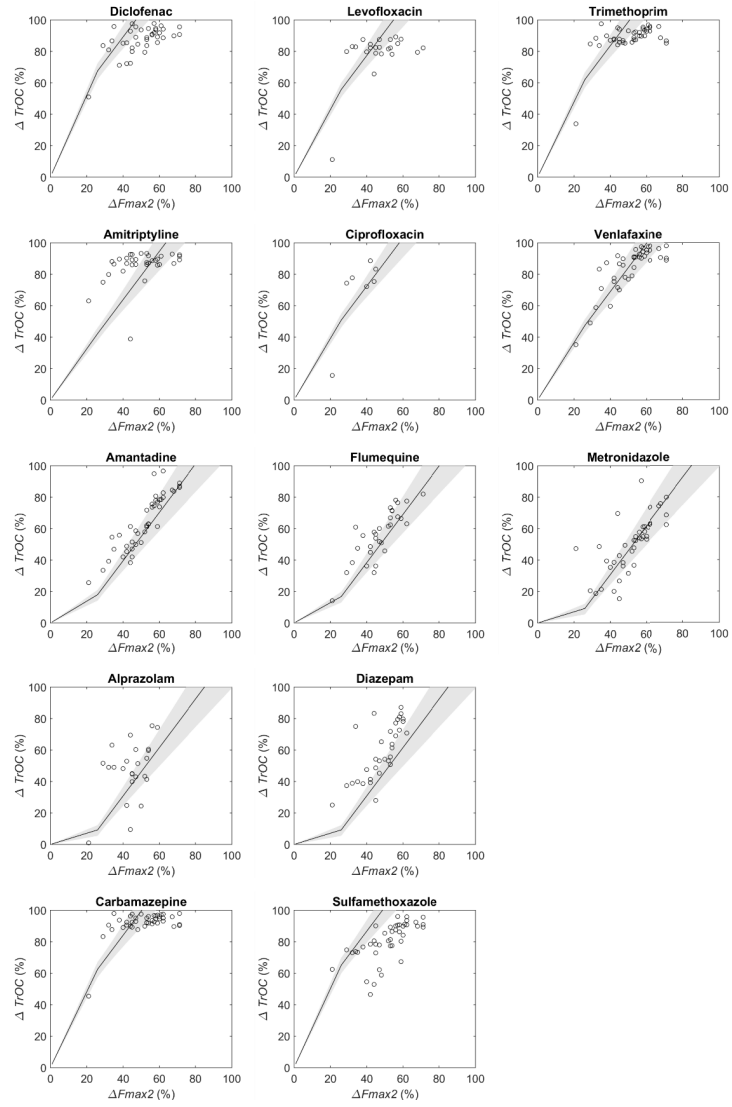

Figure E.7: Abatement patterns of predicted (full lines) and measured ΔTrOCs (dots) in relation to $\Delta F_{max}2$ by applying the inflected model for 13 TrOCs under investigation during pilot-scale experimentation. The shaded grey areas indicate the 95% confidence interval of the model. (negative values of ΔTrOCs not shown if due to an erroneous measurement of TrOCs or $\Delta F_{max}2$)

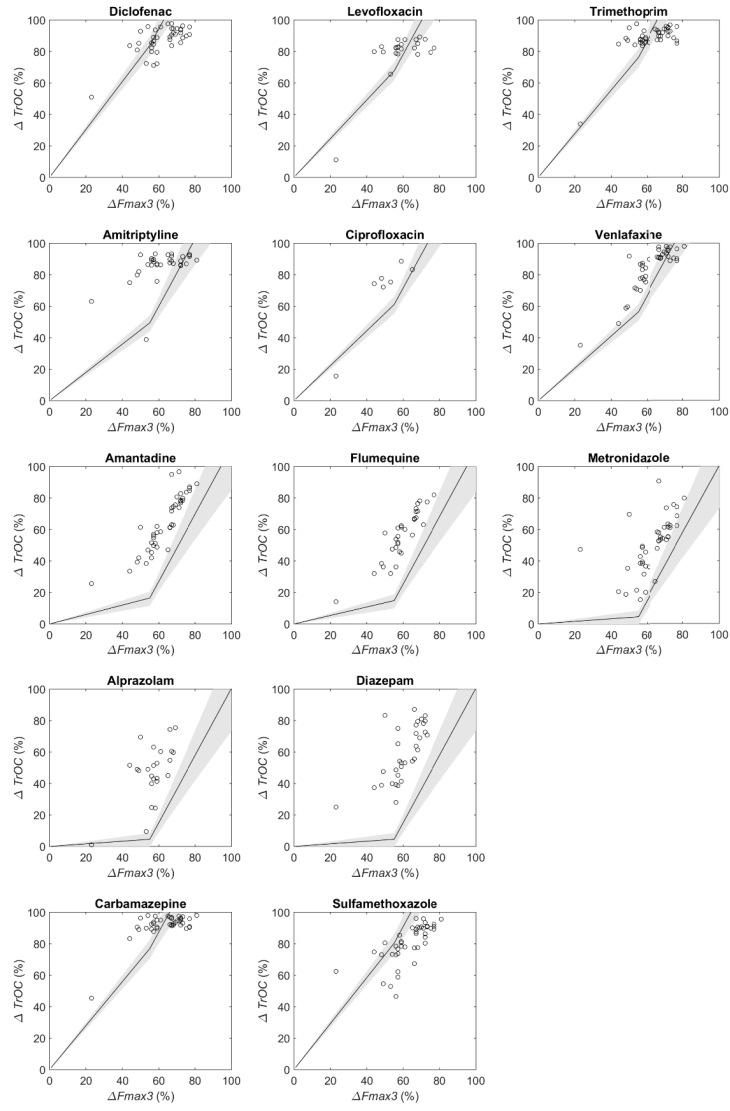

Figure E.8: Abatement patterns of predicted (full lines) and measured ΔTrOCs (dots) in relation to $\Delta F_{max}3$ by applying the inflected model for 13 TrOCs under investigation during pilot-scale experimentation. The shaded grey areas indicate the 95% confidence interval of the model. (negative values of ΔTrOCs not shown if due to an erroneous measurement of TrOCs or $\Delta F_{max}3$)

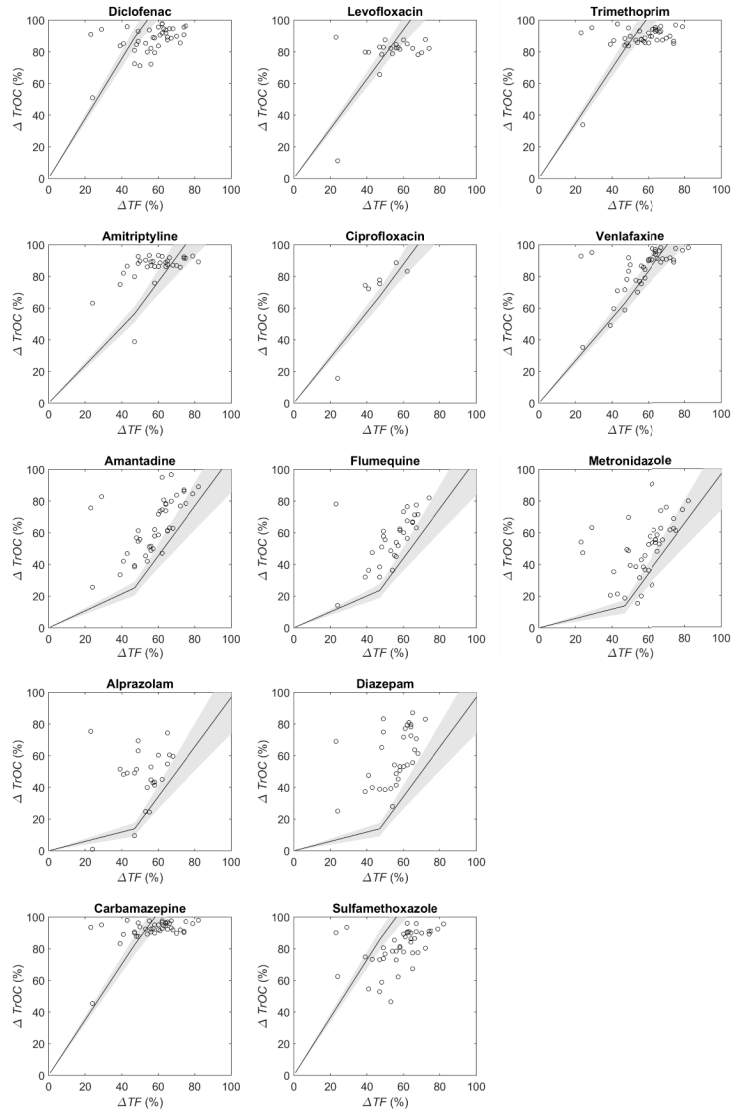

Figure E.9: Abatement patterns of predicted (full lines) and measured ΔTrOCs (dots) in relation to ΔTF by applying the inflected model for 13 TrOCs under investigation during pilot-scale experimentation. The shaded grey areas indicate the 95% confidence interval of the model. (negative values of ΔTrOCs not shown if due to an erroneous measurement of TrOCs or ΔTF)

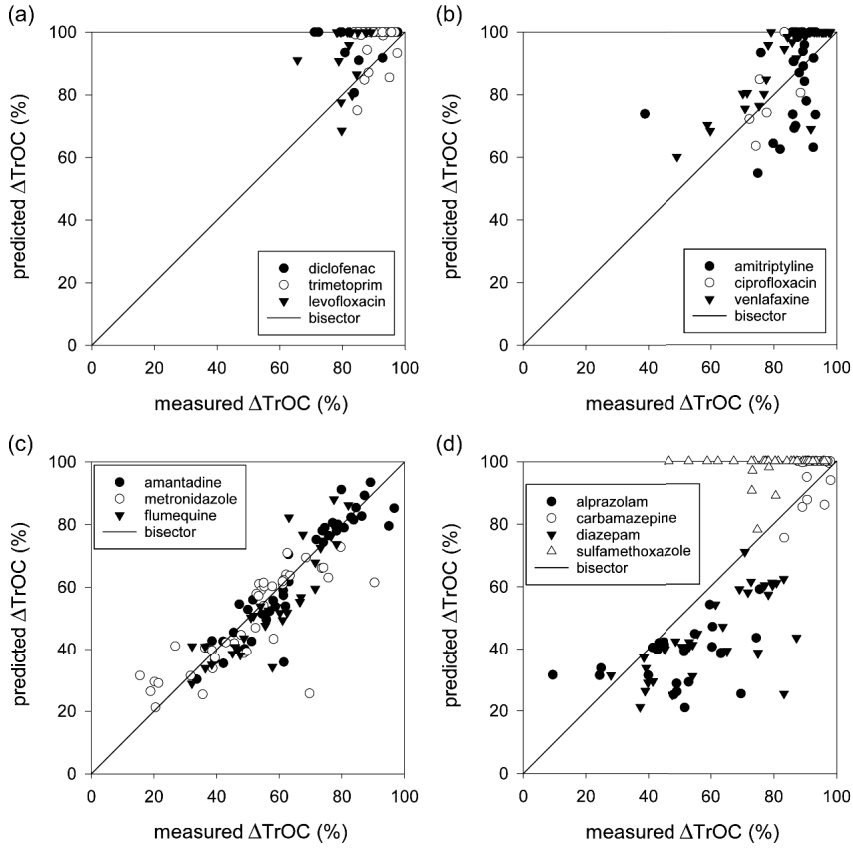

Figure E.10: Measured and predicted ΔTrOC using the single correlation model based on the online ΔUVA_{254} signal. Data are shown separately for TrOCs that were also used during model development and having different reactivity towards ozone: (a) $k_{O3,TrOC} > 5\times10^4$ M^{-1} s^{-1}, (b) 5×10^4 M^{-1} s^{-1} > $k_{O3,TrOC} > 10$ M^{-1} s^{-1}, (c) $k_{O3,TrOC} < 10$ M^{-1} s^{-1}; and (d) for TrOCs not used during model development. (negative values of ΔTrOCs not shown if due to an erroneous measurement of TrOCs or ΔUVA_{254})

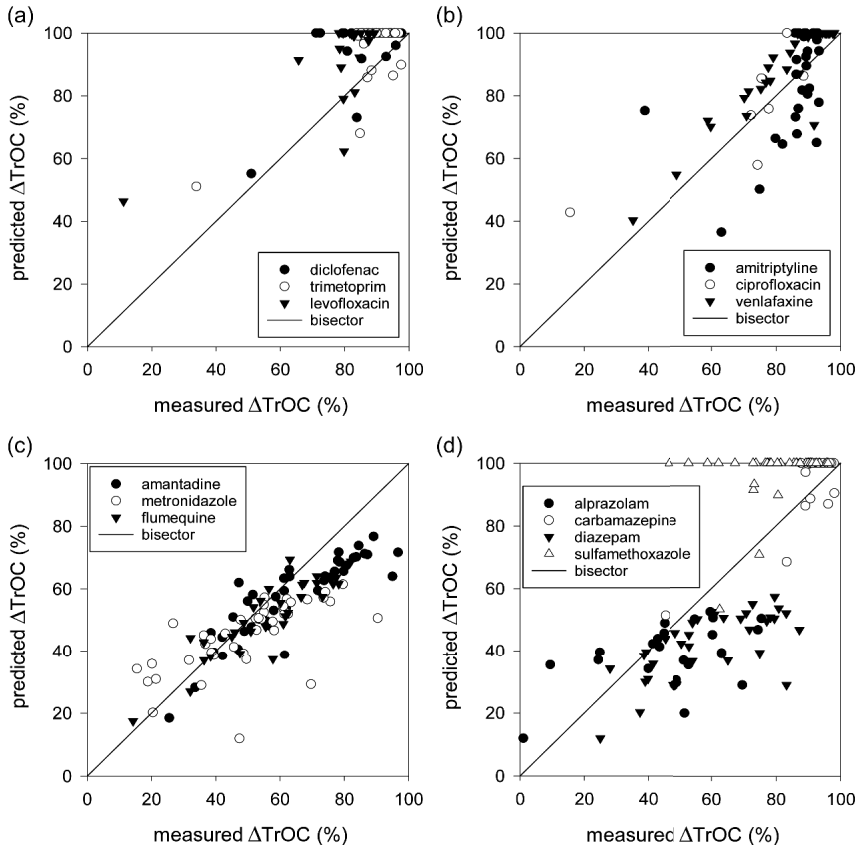

Figure E.11: Measured and predicted ΔTrOC using the single correlation model based on the $\Delta F_{max}1$ signal. Data are shown separately for TrOCs that were also used during model development and having different reactivity towards ozone: (a) $k_{O3,TrOC} > 5\times10^4$ M^{-1} s^{-1}, (b) 5×10^4 M^{-1} $s^{-1} > k_{O3,TrOC} > 10$ M^{-1} s^{-1}, (c) $k_{O3,TrOC} < 10$ M^{-1} s^{-1}; and (d) for TrOCs not used during model development. (negative values of ΔTrOCs not shown if due to an erroneous measurement of TrOCs or $\Delta F_{max}1$)

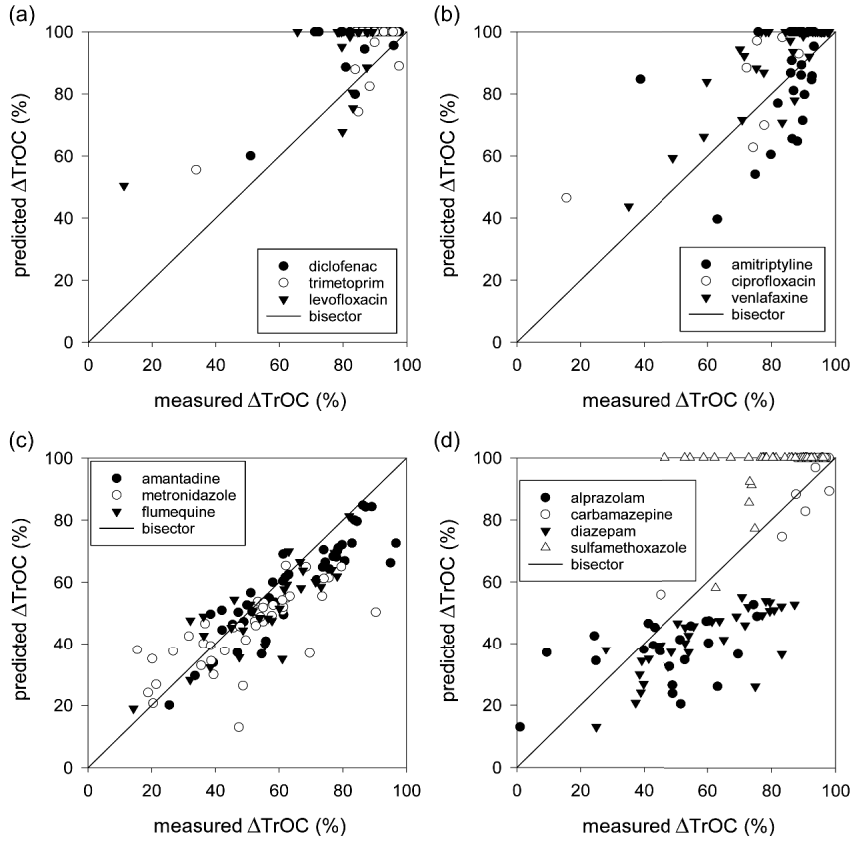

Figure E.12: Measured and predicted ΔTrOC using the single correlation model based on the $\Delta F_{max}2$ signal. Data are shown separately for TrOCs that were also used during model development and having different reactivity towards ozone: (a) $k_{O3,TrOC} > 5\times10^4$ M^{-1} s^{-1}, (b) 5×10^4 M^{-1} $s^{-1} > k_{O3,TrOC} > 10$ M^{-1} s^{-1}, (c) $k_{O3,TrOC} < 10$ M^{-1} s^{-1}; and (d) for TrOCs not used during model development. (negative values of ΔTrOCs not shown if due to an erroneous measurement of TrOCs or $\Delta F_{max}2$)

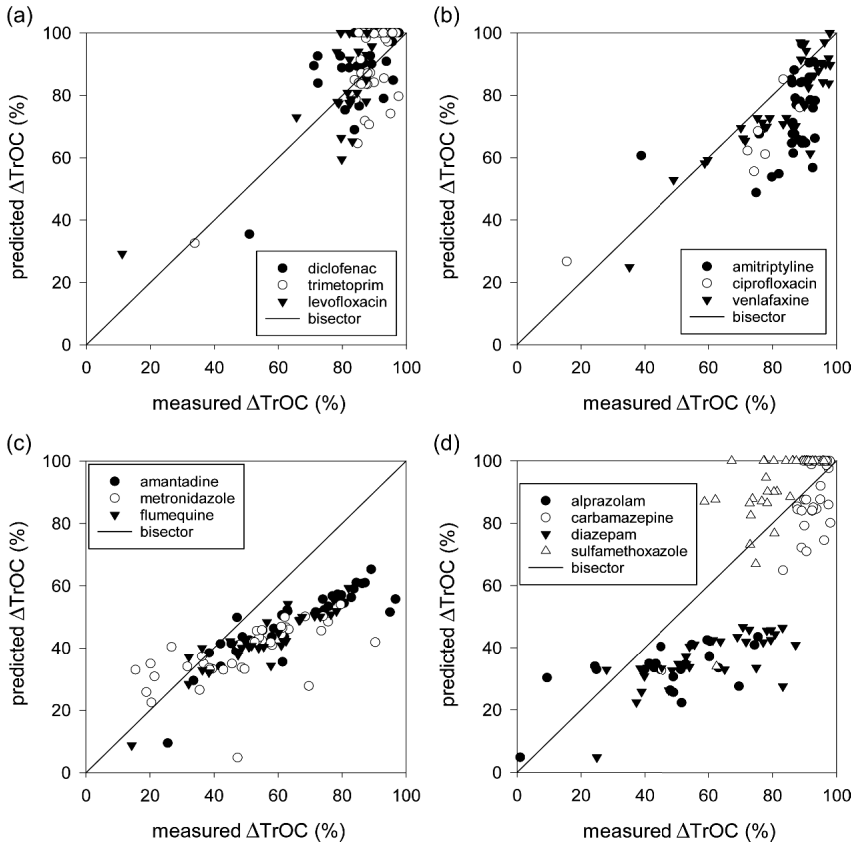

Figure E.13: Measured and predicted ΔTrOC using the single correlation model based on the $\Delta F_{max}3$ signal. Data are shown separately for TrOCs that were also used during model development and having different reactivity towards ozone: (a) $k_{O3,TrOC} > 5\times10^4$ M^{-1} s^{-1}, (b) 5×10^4 M^{-1} s^{-1} > $k_{O3,TrOC} > 10$ M^{-1} s^{-1}, (c) $k_{O3,TrOC} < 10$ M^{-1} s^{-1}; and (d) for TrOCs not used during model development. (negative values of ΔTrOCs not shown if due to an erroneous measurement of TrOCs or $\Delta F_{max}3$)

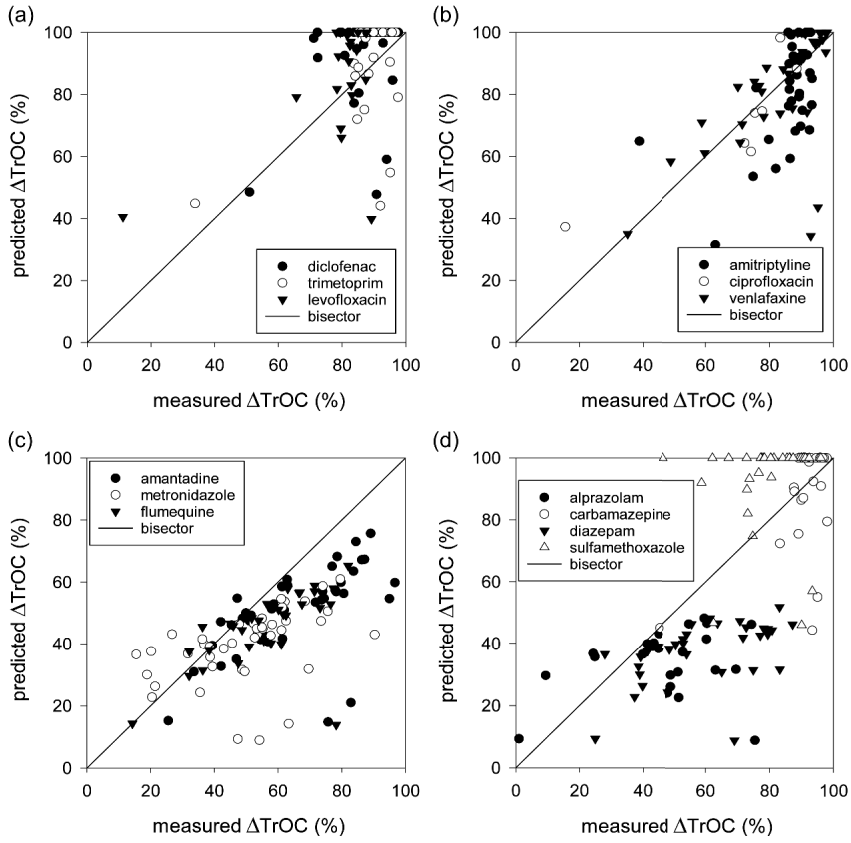

Figure E.14: Measured and predicted ΔTrOC using the single correlation model based on the ΔTF signal. Data are shown separately for TrOCs that were also used during model development and having different reactivity towards ozone: (a) $k_{O3,TrOC} > 5\times10^4$ M^{-1} s^{-1}, (b) 5×10^4 M^{-1} $s^{-1} > k_{O3,TrOC} > 10$ M^{-1} s^{-1}, (c) $k_{O3,TrOC} < 10$ M^{-1} s^{-1}; and (d) for TrOCs not used during model development. (negative values of ΔTrOCs not shown if due to an erroneous measurement of TrOCs or ΔTF)

Curriculum Vitae

Michael Chys
Maalbeekstraat 2 A
8790 Waregem
michael.chys@gmail.be
GSM: +32 499 13 02 20
28 years, married

EDUCATIONAL TRAINING

2013 – 2017 **Doctor (PhD) in Applied Biological Sciences**, Ghent University, Belgium
Dissertation: "Surrogate-based online monitoring and control framework for trace organic contaminant removal during ozonation of secondary wastewater effluent: from lab-scale to practical application"
Promotors: Prof. Stijn Van Hulle, Prof. Ingmar Nopens, Prof. Kristof Demeestere, Dr. Wim Audenaert

2007 – 2011 **Master of Science in industrial sciences: Chemistry**
University College West Flanders, Kortrijk, Belgium
Master Thesis: 'yeast cultivations in microbioreactors' at the Danish Technical University, Kopenhagen, Denmark.
Promotor: Prof. Krist V. Gernaey
Graduated with great distinction and award for best master thesis

PROFESSIONAL EXPERIENCE

2013 – 2017 (Oct. – Dec.) **Doctoral researcher and teaching assistant**: Department of Industrial Biological Sciences (LIWET), Ghent University, Kortrijk, Belgium

2012 – 2013 (Feb.– Sept.) **Research assistant**: ENBICHEM research group
University College West Flanders, Kortrijk, Belgium
Research within the LED H_2O project (low level services for industry and non-profit organizations, funded by the Flanders Knowledge Centre Water

2011 (Oct.-Dec.) **Research assistant**: Thermodynamics research group
University College West Flanders, Kortrijk, Belgium
Research in waste heat recuperation in industry (IWT-TETRA project)

2010 -2011 (Sept. – Jan.) **ERASMUS internship**
Danish Technical University, Copenhagen, Denmark
Master Thesis: 'yeast cultivations in microbioreactors'
Promotor: Prof. Krist V. Gernaey

ADDITIONAL TRAINING

2017	VCA – Basic Elements of Safety
2016	Introduction to Computational Fluid Dynamics
2016	Workshop "Developments in Ozone-Based Treatment for Water Reuse"
2014	Advanced Academic English Writing Skills
2014	Workshop "Ozone Overview and Applications"
2014	Start training PMGE
2013	Training CMS (Content Management System), start training Plone
2013	Basic training 'webredactie en usability'
2012	LED winterschool
2012	Workshop wastewater treatment en analysis (Hach-Lange NV)
2010	IP2010
	(Intensive Programme: 'Green products through a Multicoloured Approach')

ADDITIONAL TEACHING AND PROFESSIONAL EXPERIENCE

2014 – now	Organic Chemistry I & II (teaching assistant)
	(practicum, 2nd Bachelor industrial sciences, Ghent University)
2014	Polymers (teacher) (teaching assistant)
	(practicum, 3rd Bachelor industrial sciences, Ghent University)
2014	Chemical engineering II (teaching assistant)
	(practicum, Master industrial sciences, Ghent University)
2013	Chemical Organic Processes (teaching assistant)
	(theory, 3rd Bachelor industrial Sciences, University college West Flanders)

Others

- (Co-)author of several scientific articles (e.g. **22** A1's, **2** books)
- Tutor or Promotor of **11** master students + technical/scientific support research group
- Board member of BIWA (Belgian committee of the International Water Association)
- Member of the International Ozone Association and International Water Association
- Representative scientific staff (department council) and webmaster department (updates)
- Co-organizer multiple conferences, workshops and symposia
- Frequent reviewer of scientific journals (e.g. Chemical Engineering Journal, Water Science and Technology, etc.)

SCIENTIFIC AWARDS

2012	Best paper in the session 'power plants and cogeneration'
	9th International Conference on Heat transfer, Fluid Mechanics and Thermodynamics, 16 – 18 July 2012, Malta.
2011	Best Master thesis (2010-2011) of the educational program 'Master of Science in industrial sciences: Chemistry'

DETAILED SCIENTIFIC CONTRIBUTIONS

CONFERENCES AND SYMPOSIA ATTENDED

Co-organizer

- 5th IWA BENELUX Regional Young Water Professionals Conference, 5-7 July 2017, Ghent, Belgium. (member of organizing committee)
- 3rd B-IWA Nocturnal, 16 May 2017, Tervuren, Belgium. (member of organizing team)
- 2nd B-IWA Nocturnal, 18 May 2016, Meise, Belgium. (head of organizing team)
- 4th IWA BENELUX Regional Young Water Professionals Conference, 29 October 2015, Leeuwarden, the Netherlands. (member of organizing committee)
- 1st B-IWA Nocturnal, 19 May 2015, Tervuren, Belgium. (member of organizing team)
- 4th IWA/WEF Wastewater Treatment Modelling Seminar, 30 March – 2 April 2014, Spa, Belgium. (member of organizing team)
- 3rd IWA BENELUX Regional Young Water Professionals Conference, 2-4 October 2013, Belval, Luxembourg. (member of organizing committee)

Oral presentations

- 5th IWA BENELUX Regional Young Water Professionals Conference, 5-7 July 2017, Ghent, Belgium.
- Symposium on (in dutch) "Innovaties in de industriële waterzuivering", 27 June 2017, Antwerp (Hoboken), Belgium. (invited speaker)
- 27th SETAC annual meeting, 7-11 May 2017, Brussels, Belgium.
- IOA-PAG Annual conference & expo Proceedings, 28-31 August 2016, Las Vegas, USA.
- EWA IFAT, Munich, Germany: 18th EWA international symposium: Challenges arising from micro-pollutants in wastewater, water and environment, 1-2 June, Munich, Germany.
- 4rd IWA BeNeLux Regional Young Water Professionals Conference, 28-29 September, Leeuwarden, The Netherlands.
- 22nd IOA World Congress & Exhibition Proceedings, 28 June – 3 July, Barcelona, Spain.
- IOA-PAG Annual conference & expo: Ozone : proven solution to emerging challenges, 23-27 August 2014, Montréal, Canada.
- IWA Young Water Professionals pre-conference: Advanced wastewater treatment and water reuse : the future is now, 11 June 2014, Essen, Germany.
- 3rd B-IWA Symposium, 26 May 2014, Brussels, Belgium.
- 19th National Symposium on Applied Biological Sciences (NSABS2014), 7 February 2014, Gembloux, Belgium.
- 2nd European Symposium on Water Technology & Management, 20-21 November 2013, Leuven, Belgium.

- 3rd IWA BENELUX Regional Young Water Professionals Conference, 2-4 October 2013, Belval, Luxembourg.

Other attended conferences (Poster presentation or Participant)

- 10th IWA Leading Edge Conference on Water and Waste Water Technologies, 2-6 June 2013, Bordeaux, France.
- 18th National Symposium on Applied Biological Sciences (NSABS2013), 8 February 2013, Ghent, Belgium.
- IOA International Conference on Ozone and Related Oxidants in Safe Water along its Cycle, 23-24 April 2013, Berlin, Germany.
- IWA International Conference on New Developments in IT & Water, 4-6 November 2012, Amsterdam, The Netherlands.

PUBLICATIONS

Peer-reviewed

1. **Chys, M.**, Audenaert, W., Nopens, I., Demeestere, K. & Van Hulle, S.W.H. Current status and needs for online control of tertiary ozonation, *in preparation*.
2. Rezaei, F., Gorbanev, Y., **Chys, M.**, Nikiforov, A., Van Hulle, S.W.H., Cos, P., Bogaerts, A. & De Geyter, N., Plasma-Treated Organic Solutions for Enhanced Electrospun Nanofibers, *submitted*.
3. Liu, Z., Hosseinzadeh, S., Wardenier, N., Verheust, Y., **Chys, M.** & Van Hulle, S.W.H. Combining ozone with UV and H2O2 for the degradation of micropollutants from different origins: lab-scale analysis and optimization, *submitted*.
4. **Chys, M.**, Audenaert, W.T.M., Nopens, I., Demeestere, K. & Van Hulle, S.W.H. Municipal wastewater effluent characterization and variability analysis in view of tertiary ozonation: the situation in Belgium, *submitted*.
5. **Chys, M.**, Audenaert, W.T.M., Stapel, H., Ried, A., Wieland, A., Weemaes, M., Van Langenhove, H., Nopens, I., Demeestere, K. & Van Hulle, S.W.H. Technical and economical assessment of surrogated-based real-time control and monitoring of secondary effluent ozonation at pilot scale, *submitted*.
6. **Chys, M.**, Audenaert, W.T.M., Deniere, E., Mortier, S.T.F.C, Van Langenhove, H., Nopens, I., Demeestere, K. & Van Hulle, S.W.H. Surrogate-based correlation models in view of real-time control of ozonation of secondary treated municipal wastewater: model development and validation, *Environmental Science & Technology*, accepted. DOI: 10.1021/acs.est.7b04905.
7. Blondeel, E., De Wandel, S., Florin, R., Hugelier, S., **Chys, M.**, Depuydt, V., Folens, K., Du laing, G., Verliefde, A. & Van Hulle, S.W.H. (2017) Physical-chemical treatment of

rainwater runoff in recovery and recycling companies: lab-scale investigation. *Environmental Technology*, in press. DOI: 10.1080/09593330.2017.1354074

8. Oloibiri, V., De Coninck, S., **Chys, M.**, Demeestere, K. & Van Hulle, S.W.H. (2017) Characterisation of landfill leachate by EEM-PARAFAC-SOM during physical-chemical treatment by coagulation-flocculation, activated carbon adsorption and ion exchange. *Chemosphere*, **186**, 873-883.
9. Oloibiri, V., **Chys, M.**, De Wandel, S., Demeestere, K. & Van Hulle, S.W.H. (2017) Removal of organic matter and ammonium from landfill leachate through different scenarios: Operational cost evaluation in a full-scale case study of a Flemish landfill. *Journal of Environmental Management*, **203**, 774-781.
10. **Chys, M.**, Demeestere, K., Ingabire, A.S., Dries, J., Van Langenhove, H. & Van Hulle, S.W.H. (2017) Enhanced treatment of secondary municipal wastewater effluent: comparing (biological) filtration and ozonation in view of micropollutant removal, unselective effluent toxicity, and the potential for real-time control. *Water Science and Technology*, **76(1)**, 236-246.
11. Schoutteten, K.V.K.M., Hennebel, T., Dheere, E., Bertelkamp, C., De Ridder, D.J., Maes, S., **Chys, M.**, Van Hulle, S.W.H., Vanden Bussche, J., Vanhaecke, L. & Verliefde, A.R.D. (2016) Effect of oxidation and catalytic reduction of trace organic contaminants on their activated carbon adsorption. *Chemosphere*, **165**, 191-201.
12. Oloibiri, V., Ufomba, I., **Chys, M.**, Audenaert, W.T.M., Demeestere, K. & Van Hulle, S.W.H. (2015). A comparative study on the efficiency of ozonation and coagulation–flocculation as pretreatment to activated carbon adsorption of biologically stabilized landfill leachate. *Waste Management*, **43**, 335-342.
13. Gao, J., He, Y., **Chys, M.**, Decostere, B., Audenaert, W.T.M. & Van Hulle, S.W.H. (2015). Autotrophic nitrogen removal of landfill leachate at lab-scale and pilot-scale: feasibility and cost evaluation. *Journal of Chemical Technology and Biotechnology*, **90(12)**, 2152-2160.
14. Blondeel, E., Depuydt, V., Cornelis, J., **Chys, M.**, Verliefde, A. & Van Hulle, S.W.H. (2015). Physical-chemical treatment of rainwater runoff in recovery and recycling companies: Pilot-scale optimization. *Journal of Environmental Science and health, Part A*, **50**, 1083-1098.
15. **Chys, M.**, Oloibiri, V.A., Audenaert, W.T.M., Demeestere, K. & Van Hulle, S.W.H. (2015). Ozonation of biologically treated landfill leachate: efficiency and insights in organic conversions. *Chemical Engineering Journal*, **277**, 104-111.
16. Gao, J.L., Oloibiri, V., **Chys, M.**, De Wandel, S., Decostere, B., Audenaert, W.T.M., He, Y.L. & Van Hulle, S.W.H. (2015). Integration of autotrophic nitrogen removal, ozonation and activated carbon filtration for treatment of landfill leachate. *Chemical Engineering Journal*, **275**, 281-287.
17. Gao, J., Oloibiri V., **Chys, M.**, Audenaert, W.T.M., Decostere, B., He, Y., Van Langenhove, H., Demeestere, K. & Van Hulle, S.W.H. (2015). The present status of

landfill leachate treatments and its development trend from a technological point of view. *Reviews in Environmental Science and Bio/Technology*, **14(1)**, 93-122.

18. **Chys, M**., Declerck, W., Audenaert, W.T.M. & Van Hulle, S.W.H. (2015). UV/H2O2, O3 and (photo-) Fenton as treatment prior to granular activated carbon filtration of biologically stabilized landfill leachate. *Journal of Chemical Technology and Biotechnology*, **90(3)**, 525-533.
19. Blondeel, E., **Chys, M.**, Depuydt, V., Folens, K., Du Laing, G., Verliefde, A. & Van Hulle, S.W.H. (2014). Leaching behaviour of different scrap materials at recovery and recycling companies: Full-, pilot- and lab-scale investigation. *Waste Management*, **34**, 2674-2686.
20. Gao, J., **Chys, M**., Audenaert, W.T.M., Van Hulle, S.W.H. & He, Y.L. (2014). Performance and kinetic process analysis of an Anammox reactor in view of application for landfill leachate treatment. *Environmental Technology*, **35(10)**, 1226–1233.
21. **Chys, M**., Depuydt, V., Boeckaert, C. & Van Hulle, S.W.H. (2013). Treatment of rainwater runoff in recovery and recycling companies: lab and pilot scale testing. *Journal of Environmental Science and Health, Part A-Toxic/Hazardous Substances & Environmental Engineering,* **48(8)**, 446-452.
22. **Chys, M**., van den Broek, M., Vanslambrouck, B. & De Paepe, M. (2012). Potential of zeotropic mixtures as working fluids in organic Rankine cycles. *Energy*, **44**, 623-632.

Not listed in the ISA Web of Knowledge

1. Audenaert, W.T.M., **Chys, M.**, Auvinen, H., Dumoulin, A., Rousseau, D. & Van Hulle, S.W.H. (2014) (Future) Regulation of Trace Organic Compounds in WWTP Effluents as a Driver of Advanced Wastewater Treatment. *Ozone News*, **42 (6)**, 17-23.
2. **Chys, M**., Declerck, W., Audenaert, W.T.M. & Van Hulle, S.W.H. (2013). UV/H2O2, O3 en (foto-) Fenton als voorbehandeling voor granulaire actieve kool filtratie van biologisch gestabiliseerd stortplaatspercolaat. *WT-afvalwater*, **13 (5)**, 265-279.
3. Depuydt, V., **Chys, M**., Boeckaert, C., Monballiu, A., Huits, D., Meeschaert, B. & Van Hulle, S.W.H. (2012). Behandelen van afstromend hemelwater bij recuperatie- en recyclagebedrijven: labo- en piloottesten. *WT-afvalwater*, **12 (4)**, 270-281.

Conference contributions

1. De Wandel, S., Gagliano, E., Oloibiri, V., **Chys, M.**, Roccaro, P. & Van Hulle, S.W.H. (2017) Comparison of physicochemical treatment technologies for the treatment of landfill leachate at pilot-scale. *5th IWA BeNeLux Regional Young Water Professionals Conference, Abstracts,* 5-7 July, Ghent, Belgium.
2. Oloibiri, V., Deconinck, S., **Chys, M.**, Demeestere, K. & Van Hulle, S.W.H. (2017) Use of spectral and chemometric methods to understand dissolved organic matter removal during physical chemical treatment of landfill leachate. *5th IWA BeNeLux Regional Young Water Professionals Conference, Abstracts,* 5-7 July, Ghent, Belgium.

3. **Chys, M.**, Audenaert, W.T.M, Marchi, A., Weemaes, M., Van Langenhove, H., Nopens, I., Demeestere, K. & Van Hulle, S.W.H. (2017) Technical and economic assessment of real-time control strategies for micropollutant removal by ozonation at pilot-scale. *5th IWA BeNeLux Regional Young Water Professionals Conference, Abstracts,* 5-7 July, Ghent, Belgium.
4. **Chys, M.**, Audenaert, W.T.M, Marchi, A., Weemaes, M., Van Langenhove, H., Nopens, I., Demeestere, K. & Van Hulle, S.W.H. (2017) Technical and economic assessment of real-time control strategies for micropollutant removal by ozonation at pilot-scale. *SETAC 27th Annual Meeting, Proceedings,* 7-11 May, Brussels, Belgium.
5. **Chys, M.**, Audenaert, W.T.M, Marchi, A., Weemaes, M., Van Langenhove, H., Nopens, I., Demeestere, K. & Van Hulle, S.W.H. (2016) Real-time control of micropollutant removal from secondary effluent by ozonation. *13th IWA Specialized Conference on Small Water and Wastewater Systems & & 5th IWA Specialized Conference on Resources-Oriented Sanitation, Proceedings*, 14-17 September, Athens, Greece.
6. **Chys, M.**, Audenaert, W.T.M, Marchi, A., Weemaes, M., Van Langenhove, H., Nopens, I., Demeestere, K. & Van Hulle, S.W.H. (2016) Real-time control of micropollutant removal by ozonation at pilot-scale. *IOA-PAG Annual conference & expo Proceedings*, 28-31 August 2016, Las Vegas, USA.
7. **Chys, M.**, Audenaert, W.T.M, Marchi, A., Weemaes, M., Van Langenhove, H., Nopens, I., Demeestere, K. & Van Hulle, S.W.H. (2016) Real-time control of micropollutant removal by ozonation at pilot-scale. *18th EWA International Symposium, papers*, 1-2 June, Munich, Germany.
8. **Chys, M.**, Audenaert, W.T.M., Oloibiri, V., Demeestere, K. & Van Hulle, S.W.H. (2015) Ozonation of landfill leachate: cost effectiveness and insights on conversions of organic matter. *22nd IOA World Congress & Exhibition Proceedings*, 28 June – 3 July, Barcelona Spain.
9. **Chys, M.**, Van Hulle, S.W.H., Deniere, E., Vergeynst, L., Van Langenhove, H., Nopens, I., Demeestere, K. & Audenaert, W.T.M. (2015) Robust fluorescence and UV-VIS correlation models for real-time control and assessment of micropollutant removal from secondary effluent using ozonation. *22nd IOA World Congress & Exhibition Proceedings*, 28 June – 3 July, Barcelona Spain.
10. Oloibiri, V., **Chys, M.**, Audenaert, W.T.M., Demeestere, K. & Van Hulle, S.W.H. (2015) Economical and ecological removal and/or recuperation of organic matter and ammonium from landfill leachate: a full scale case study of Flemish landfills. *Industrial Waste & Wastewater Treatment & Valorisation Proceedings*, 21-23 May 2015, Athens, Greece.
11. Oloibiri, V., Ufomba, I., **Chys, M.**, Audenaert, W.T.M., Demeestere, K. & Van Hulle, S.W.H. (2015). Treatment of landfill leachate by coupling coagulation-flocculation or ozonation to granular activated carbon adsorption. *Communications in Agricultural and Applied Biological Sciences, Proceedings 20th PhD Symposium*, 30 January 2015, Leuven, Belgium, **80 (1)**, 57-62.
12. **Chys, M.**, Van Hulle, S.W.H., Deniere, E., Vergeynst, L., Van Langenhove, H., Nopens, I., Demeestere, K. & Audenaert W.T.M. (2015) Robust correlation models for real-time

control of micropollutant removal from wastewater using ozonation. *Micropol & Ecohazard Conference 2015 Abstracts*, 22-26 November, Singapore.

13. Oloibiri, V., Deconinck, S., De Wandel, S., **Chys, M.**, Demeestere, K. & Van Hulle, S.W.H. (2015) Sustainable landfill leachate treatment by resource recovery. *Brussels Sustainable Development Summit, Abstracts*, 19-20 October, Brussels, Belgium.
14. **Chys, M.**, Van Hulle, S.W.H., Deniere, E., Vergeynst, L., Van Langenhove, H., Nopens, I., Demeestere, K. & Audenaert W.T.M. (2015) Developing monitoring and control strategies for emerging contaminant removal from wastewater using ozonation. *4rd IWA BeNeLux Regional Young Water Professionals Conference, abstracts*, 28-29 September, Leeuwarden, The Netherlands.
15. Oloibiri, V., Deconinck, S., De Wandel, S., **Chys, M.**, Demeestere, K. & Van Hulle, S.W.H. (2015) Organic matter and nitrogen recovery from landfill leachate using coagulation flocculation followed by granular activated carbon and ion exchange. *4rd IWA BeNeLux Regional Young Water Professionals Conference, abstracts*, 28-29 September, Leeuwarden, The Netherlands.
16. Oloibiri, V., Deconinck, S., De Wandel, S., **Chys, M.**, Demeestere, K. & Van Hulle, S.W.H. (2015) Organic matter and nitrogen recovery from landfill leachate using coagulation flocculation followed by granular activated carbon and ion exchange. *Posters presented at the ISWA15 world congress Antwerp*, 7-9 September, Antwerp, Belgium.
17. **Chys, M.**, Van Hulle, S.W.H., Deniere, E., Vergeynst, L., Van Langenhove, H., Nopens, I., Demeestere, K. & Audenaert W.T.M. (2015) Robust fluorescence and UV-VIS correlation models for real-time control of micropollutant removal from secondary effluent using ozonation. *1st IWA Resource Recovery Conference, abstracts*, 30 August – 2 September, Ghent, Belgium.
18. **Chys, M.**, Van Hulle, S.W.H., Deniere, E., Nopens, I., Vergeynst, L., Demeestere, K., Van Langenhove, H. & Audenaert W.T.M. (2015) Developing monitoring and control strategies for emerging contaminant removal from wastewater using ozonation. *Americana 2015 Proceedings*, 17-19 March 2015, Montréal, Canada.
19. **Chys, M.**, Dutoit, D., Audenaert, W.T.M., Demeestere, K., Nopens, I. & Van Hulle, S.W.H. (2014). UV-VIS spectral analysis as process tool to assess ozone reactivity for secondary effluent. *IOA-PAG Annual conference & expo Proceedings*, 23-27 August 2014, Montréal, Canada.
20. Audenaert, W.T.M., **Chys, M.** & Van Hulle, S.W.H. (2014). (Future) Regulation of Trace Organic Compounds in WWTP Effluents as a Driver of Advanced Wastewater Treatment. *IOA-PAG Annual conference & expo Proceedings*, 23-27 August 2014, Montréal, Canada.
21. **Chys, M.**, Audenaert, W.T.M., Dutoit, D., Nopens, I., Demeestere, K. & Van Hulle, S.W.H. (2014). UV-VIS spectral analysis as a key process tool for removal of pharmaceuticals from secondary effluent by ozonation. *Advanced Wastewater Treatment and Water Reuse : the Future Is Now, IWA Young Water Professionals Pre-conference Proceedings*, 11 June 2014, Essen, Germany, 52-54.
22. **Chys, M.**, Oloibiri, V., Audenaert, W.T.M., Van Langenhove, H., Demeestere K. & Van Hulle, S.W.H. (2014). Parameter study on the efficiency of ozonation for biologically

treated landfill leachate. *Communications in Agricultural and Applied Biological Sciences, Proceedings 19th PhD Symposium*, 7 February 2014, Ghent, Belgium, **79(1)**, 97-101.

23. **Chys, M.**, Oloibiri, V., Audenaert, W.T.M., Van Langenhove, H., Demeestere, K. & Van Hulle, S.W.H. (2014) Parameter study on the efficiency of ozonation for biologically treated landfill leachate. *9th IWA World Water Congress & Exhibition, Abstracts*, 21-26 September 2014, Lisbon, Portugal.
24. Blondeel, E., **Chys, M**., Depuydt, V., Folens, K., Du Laing, G., Verliefde, A. & Van Hulle, S.W.H. (2014). Leaching behaviour of different scrap materials at recovery and recycling companies: pilot-scale investigation. *9th IWA World Water Congress & Exhibition, Abstracts*, 21-26 September 2014, Lisbon, Portugal.
25. **Chys, M**., Declerck, W., Audenaert, W.T.M. & Van Hulle, S.W.H. (2013). UV/H2O2, O3 and (photo-) Fenton as a pre-treatment to granular activated carbon filtration of biologically stabilized landfill leachate. *3rd IWA BeNeLux Regional Young Water Professionals Conference, Abstracts*, 2-4 October 2013, Belval, Luxembourg.
26. **Chys, M**., Depuydt, V., Blondeel, E., Hugelier, S. & Van Hulle, S.W.H. (2013). Treatment of rainwater runoff in recovery and recycling companies: lab and pilot scale testing. *Communications in Agricultural and Applied Biological Sciences, Proceedings 18th PhD Symposium*, 8 February 2013, Ghent, Belgium, **78(1)**, 235-242.
27. **Chys, M**., Declerck, W., Audenaert, W.T.M. & Van Hulle, S.W.H. (2013). UV/H2O2, O3 and (photo-) Fenton as a pre-treatment to GAC filtration of biologically stabilized landfill leachate. *2nd European Symposium on Water Technology and Management, Proceedings*, 20-21 November 2013, Leuven, Belgium.
28. Gao, J.L., **Chys, M**., Audenaert, W.T.M., Van Hulle, S.W.H. & He, Y.L. (2013). Performance and kinetic process analysis of an anammox reactor in view of application for landfill leachate treatment. *3rd IWA BeNeLux Regional Young Water Professionals Conference, Abstracts*, 2-4 October 2013, Belval, Luxembourg.
29. Blondeel, E., **Chys, M**., Depuydt, V., Folens, K., Du Laing, G., Verliefde, A. & Van Hulle, S.W.H. (2013). Leaching behaviour of different scrap materials at recovery and recycling companies: pilot-scale investigation. *3rd IWA BeNeLux Regional Young Water Professionals Conference, Abstracts*, 2-4 October 2013, Luxembourg.
30. **Chys, M.**, Depuydt, V., Blondeel, E., Hugelier, S. & Van Hulle, S.W.H. (2013). Treatment of rainwater runoff in recovery and recycling companies. *Water and Waste Water Technologies, 10th IWA Leading edge conference, Abstracts*, 2-6 June 2013, Bordeaux, France.
31. van den Broek, M., **Chys, M.**, Vanslambrouck, B. & De Paepe, M. (2012). Mixtures as working fluids in organic rankine cycles for low temperature applications. *Heat Powered Cycles Conference Proceedings*, 10-12 September 2012, Alkmaar, The Netherlands.
32. van den Broek, M., **Chys, M**., Vanslambrouck, B. & De Paepe, M. (2012). Increasing the Efficiency and Generated Electricity of Organic Rankine Cycles by Using Zeotropic Mixtures as Working Fluids. *9th International Conference : Heat transfer, Fluid Mechanics and Thermodynamics, Proceedings.* 16-18 July 2012, Malta, 529–534.

Others

1. Blondeel, E., **Chys, M.**, Depuydt, V., & Van Hulle, S.W.H. (2014) Robuuste en Efficiënte zuivering van afvalWAter van REcuperatie en recyclagebedrijven (REWARE). Kortrijk: Universiteit Gent. Faculteit Bio-ingenieurswetenschappen. Laboratorium voor Industriële Water- en Ecotechnologie ; Vlaams Kenniscentrum Water.
2. De Wandel, S., **Chys, M.** & Van Hulle, S.W.H. (2017) Gevorderde FYsico-chemische Behandeling van Biologisch gestabiliseerd Afvalwater afkomstig van Afvalverwerkende en Recyclerende bedrijven (FYBAR). Kortrijk: Universiteit Gent. Faculteit Bio-ingenieurswetenschappen. Laboratorium voor Industriële Water- en Ecotechnologie.
3. **Chys, M**. (2011) Yeast Cultivations in microbioreactors, MSc Thesis, Technical University of Denmark, Denmark.

PARTICIPATED RESEARCH PROJECTS

1. IWA-TETRA 2010 project: waste heat recuperation using ORC (2010-2012).
   Promotor: Ing. Bruno Vanslambrouck
2. Vlakwa-LED project: local and accessible service centre for water technology (2011-2012).
   Promotor: Dr. Ir. Stijn Van Hulle
3. Vlakwa-LED project: local and accessible service centre for water technology (2013).
   Promotor: Dr. Ir. Stijn Van Hulle
4. IWT-Tetra 2012 project: Robust and efficient treatment of waste water of scrap companies REWARE (2012-2014).
   Promotor: Dr. Ir. Stijn Van Hulle
5. Vlakwa-LED project: local and accessible service centre for water technology (2014).
   Promotor: Prof. Dr. Ir. Stijn Van Hulle
6. Vlakwa-LED project: local and accessible service centre for water technology (2015).
   Promotor: Prof. Dr. Ir. Stijn Van Hulle
7. IWT-Tetra 2014 project: Advanced physico-chemical treatment of biologically stabilised waste water coming from recycling companies FYBAR (2014-2016).
   Promotor: Prof. Dr. Ir. Stijn Van Hulle
8. Vlakwa-LED project: local and accessible service centre for water technology (2016).
   Promotor: Prof. Dr. Ir. Stijn Van Hulle
9. INTERREG V: Integrale Mobiele PROceswatervoorziening Voor een Economische Delta (IMPROVED, 2016 - 2018).
   Promotor: Prof. Dr. ir. Arne Verliefde, co-promotor: Prof. Dr. Ir. Stijn Van Hulle
10. INTERREG V: I-QUA (2017 - 2020).
    Co-promotor: Prof. Dr. Ir. Stijn Van Hulle

GUIDED MASTER THESISSES

2015 – 2016	M. Bauwens, 'Ozonisatie van secundair effluent op piloot-schaal: praktische implicaties bij de opvolging en sturing van micropolluentverwijdering', Ghent University, Belgium. J. Vangrinsven, 'Verwijdering van organische micropolluenten in secundair RWZI effluent via piloot-schaal ozonisatie: chemische analyse van geneesmiddelen en on-line opvolging via surrogaatmetingen', Ghent University, Belgium.
2014 – 2015	E. Deniere, 'Ozonisatie van secundair effluent: opvolging en controle van micropolluentverwijdering', Ghent University, Belgium. C. Nikuze, 'Water quality of secondary effluent: measurement of physical-chemical (surrogate) parameters and post-ozonation', Ghent University, Belgium. P.-J. De Buyck, 'Ozonisatie en rietvelden voor de verwijdering van farmaceutica uit afvalwater', Ghent University, Belgium.
2013 – 2014	I.C. Ufomba, 'Treatment chain for biologically stabilized landfill leachate: coagulation/flocculation versus ozonation prior to activated carbon adsorption', Ghent University, Belgium. A.S. Ingabire, 'Post-treatment of municipal wastewater effluent: effect on organic matter and micropollutant removal', Ghent University, Belgium. D. Dutoit, 'Ontwerp en implementatie van een minireactor', Ghent University, Belgium.
2012 – 2013	W. Declerck, 'Behandelen van stortplaatspercolaat via autotrofe stikstofverwijdering en geavanceerde oxidatieprocessen', University College West Flanders/Ghent University, Belgium. S. Hugelier, 'Optimalisatie van de waterzuiveringsinstallatie bij het schrootverwerkend bedrijf Casier Recycling nv', University College West Flanders/Ghent University, Belgium. V.A. Oloibiri, 'Ozonation of biologically treated landfill leachate', Ghent University, Belgium.

Succes is not a trophy you get. It is a story you write constantly.

(N.P.B.)